Key mechanisms regulating synaptic and cell wide forms of homeostatic plasticity

by

Sonya Kee Yun Jakawich

A dissertation submitted in partial fulfillment
of the requirements for the degree of
Doctor of Philosophy
(Neuroscience)
in the University of Michigan
2011

Doctoral Committee:

Assistant Professor Michael Mark Alexander Sutton, Chair
Professor Jack M. Parent
Professor Edward L. Stuenkel
Assistant Professor Catherine A. Collins
Assistant Professor Hisashi Umemori

DEDICATION

To my loving friends and family. Thank you.

ACKNOWLEDGEMENTS

Thank you, Mike for being a great mentor and constantly pushing me to be the best scientist that I can be. This thesis is written in collaboration with all of the past and present members of the Sutton Lab. Thank you for the scientific conversation and technical help. I would also like to thank the members of my thesis committee and my collaborators Gentry Patrick and Steven Djakovic for their continued support and advice.

TABLE OF CONTENTS

DEDICATION ii

ACKNOWLEDGEMENTS iii

LIST OF FIGURES vi

ABSTRACT viii

CHAPTER

I. Introduction 1

II. An Essential Postsynaptic Role for the Ubiquitin Proteasome System in Slow Homeostatic Synaptic Plasticity in Cultured Hippocampal Neurons 27

III. Local presynaptic activity gates homeostatic changes in presynaptic function driven by dendritic BDNF synthesis 75

IV. Activity dependent localization of the proteasome gates state-dependent homeostatic plasticity 141

V. Discussion 179

BIBLIOGRAPHY 194

LIST OF FIGURES

FIGURE

2.1 Scaling of mEPSC amplitude accompanies chronic UPS inhibition……..55

2.2 Similar synaptic changes in AMPAR expression accompany AP and UPS blockade…….57

2.3 Suppression of network activity and UPS inhibition drive similar changes in surface GluA2 expression at synapses……...59

2.4 Chronic changes in neuronal activity induce bidirectional changes in proteasome activity……61

2.5 Postsynaptic UPS inhibition scales excitatory synaptic function in a cell autonomous manner……63

2.6 UPS inhibition occludes slow homeostatic plasticity……..65

2.7 UPS inhibition drives enhancement of synaptic AMPAR expression irrespective of activity levels…….67

2.8 UPS inhibition enhances surface GluA2 expression at synapses irrespective of network activity…….69

2.9 Postsynaptic UPS activity overrides changes in network activity during slow homeostatic plasticity……71

2.10 Phosphorylation of Rpt6 at S120 mimics bidirectional homeostatic plasticity…...73

2.11Working model of slow homeostatic plasticity…….74

3.1 AMPAR blockade induces a state-dependent enhancement of presynaptic function……110

3.2 Postsynaptic changes induced by AMPAR blockade are unaffected by coincident AP blockade……...112

3.3 Activity-dependent uptake of syt-lum at synapses……114

3.4 Presynaptic changes induced by AMPAR blockade are prevented by coincident AP blockade……...116

3.5 Increase in presynaptic function is specific to AMPA receptor blockade……118

3.6 Presynaptic and postsynaptic homeostatic changes are induced by AMPAR blockade in parallel……120

3.7 Local presynaptic activity gates retrograde enhancement of presynaptic function induced by AMPAR blockade……122

3.8 BDNF release and signaling are required for presynaptic, but not postsynaptic, compensation induced by AMPAR blockade……124

3.9 BDNF alters presynaptic function independent of structural synaptic changes or changes in synaptic AMPARs……126

3.10 BDNF enhances presynaptic function in a state-dependent manner…….128

3.11 Local BDNF signaling is necessary and sufficient for homeostatic changes in presynaptic function 130

3.12 BDNF acts downstream of protein synthesis to enhance presynaptic function induced by AMPAR blockade……..132

3.13 AMPAR blockade enhances synthesis and compartment-specific expression of BDNF……134

3.14 Blockade of glutamate miniature synaptic activity does not globally increase BDNF expression……..136

3.15 AMPAR blockade drives dendritic BDNF synthesis……138

3.16 Parallel roles for dendritic protein synthesis in compensatory presynaptic and postsynaptic changes induced by AMPAR blockade……140

4.1 Proteasome function is required for state-dependent increases in mEPSC frequency but not amplitude downstream of AMPAR blockade……166

4.2 State-dependent increases in function require proteasome activity at active presynaptic terminals……..168

4.3 Proteasome function is required downstream of retrograde synaptic signaling by BDNF……..170

4.4 Presynaptic but not postsynaptic polyubiquitination is required for state-dependent increases in presynaptic function……172

4.5 Activity is required for localization of the proteasome to presynaptic terminals…174

4.6 Phosphorylation of Rpt6 at S120 regulates localization of the proteasome to the presynaptic terminal……176

4.7 Working model of state-dependent homeostatic plasticity……..178

ABSTRACT

Key mechanisms regulating synaptic and cell wide forms of homeostatic plasticity

By

Sonya Kee Yun Jakawich

Chair: Michael M.A. Sutton

Sustained alterations in neuron activity elicit compensatory changes in synaptic function, a form of adaptation known as homeostatic plasticity. Homeostatic forms of plasticity are thought to maintain neural circuit activity within a dynamic, yet stable, functional range in the face of potentially destabilizing environmental influences. In recent years, homeostatic plasticity has received considerable attention as its dysregulation may lead to instability of neuronal circuits which, in turn, may contribute to the development of neurological disorders such as epilepsy. Typically, sustained changes in network activity drive a slow form of homeostatic plasticity that emerges over an 18-24 hr period. However, neurons also exhibit homeostatic adaptations that emerge 1-3 hr following direct disruption of synaptic activity, suggesting that separate slow and rapid forms of homeostatic plasticity exist at synapses. Both slow and rapid forms of homeostatic plasticity can emerge as changes in presynaptic neurotransmitter release

(presynaptic compensation) or in the abundance of postsynaptic neurotransmitter receptors (postsynaptic compensation). However, the molecular mechanisms underlying these unique slow and rapid forms of homeostatic plasticity remain largely unknown. Here, key molecular events underlying these homeostatic forms of regulation are elucidated.

Slow homeostatic plasticity requires targeted protein degradation by the postsynaptic ubiquitin proteasome system (UPS). Postsynaptic blockade of the UPS can both mimic and occlude slow homeostatic plasticity expression mechanisms suggesting that network driven changes in activity engage proteasome function to drive slow homeostatic adaptations at synapses. In contrast, rapid homeostatic plasticity requires presynaptic UPS function. Rapid homeostatic plasticity mechanisms require coupling of presynaptic UPS function with postsynaptic protein translation, retrograde synaptic signaling by BDNF/TrkB and the presence of presynaptic action potential activity. Together, these results demonstrate that slow (disruption of network activity) and rapid (disruption of synaptic activity) forms of homeostatic plasticity require unique pre- and post- synaptic mechanisms that additionally work together to coordinate expression of pre- and post- synaptic functional compensation. Understanding key molecular components underlying homeostatic plasticity mechanisms may lead to an advanced understanding of destabilizing neurological disorders, such as epilepsy.

CHAPTER I

Introduction

Maintaining the fixity of the 'milieu interieur': The evolution of homeostatic plasticity

Homeostasis in biological systems: Foundations

Given that our internal environment interacts with the ever changing external world, how does our internal environment remain stable? Constancy of the internal, biological, environment has fascinated philosophers and scientists for centuries (Claude, 1865, 1878; Cannon, 1926, 1929). In 1878, Claude Bernard wrote, "it is the fixity of the 'milieu interieur' which is the condition of free and independent life," suggesting that the ability of biological organisms to command a stable internal environment, in the face of external disruption, is what defines life itself. Achieving an internal 'steady state of flux' (Schoenheimer, 1942), or homeostasis (Cannon, 1926), has become a fundamental theme in modern biology (Henderson and Haggard, 1918; Austin et al., 1922; Perlman, 1977). Early studies of homeostatic mechanisms were primarily concerned with stability of the constituents within blood (Henderson and Haggard, 1918) but in 1884, J. Hughlings Jackson hypothesized that in response to nervous system disruption, a separate, undisrupted element of the nervous system is capable of taking control of the part that

was previously disrupted, suggesting that the nervous system retains the capacity to activate compensatory mechanisms in a stimulus dependent manner (Jackson, 1884). Indeed, deprivation of stimulatory adrenergic fiber input to the smooth dilator muscle of the iris increased dilation of the lesioned pupil compared to the un-lesioned side (Anderson, 1903) and the enhanced dilation was due to a reversible sensitization to adrenaline (Meltzer and Auer, 1904; Eliot, 1905; Simeone, 1938). Increased stimulation of the smooth muscle fibers was hypothesized to be the result of increased excitability of the smooth muscle of the iris (Anderson, 1903). These early studies on adrenergic control of the iris suggest that sensitization of nerve-muscle impulses can occur in a reversible manner and that the sensitization interaction that occurs between nerve and smooth muscle is controlled though an active, rather than a passive, physiological mechanism - a key feature of homeostatic regulation (Cannon, 1926). Sensitization of disrupted nerve-muscle connections was later defined as 'the law of denervation' (Cannon, 1929) and came to represent a family of phenomena known as denervation supersensitivity (Cannon and Rosenblueth, 1949). In addition to adrenergic control of the smooth muscles in the iris (Anderson, 1903), denervation supersensitivity has been observed in deafferented frog muscle (Harris and Nicholls, 1956) as well as cat gastrocnemius (Brown, 1937). Of particular relevance to homeostasis in the central nervous system Axelson and Thessleff (1959) hypothesized that the observed increase in muscle excitability observed during denervation supersensitivity was due to an increase in the total number of receptors located on the muscle (Axelsson and Thesleff, 1959); While proposed to account for excitability changes in muscle, this key hypothesis that synaptic protein can be

homeostatically regulated further suggested that synapses in the central nervous system could undergo homoestatic plasticity.

Although denervation supersensitivity of neuromuscular synapses was widely studied in the 1960s, 1970s, and 1980s, the first indication that central synapses exhibit similar homeostatic regulation was provided in 1998. In a now classic paper, Turrigiano and colleagues (1998) found that networks of cortical neurons exhibited bidirectional, synaptic adaptations in response to long-term changes in activity. They showed that chronic (48 hr) inhibition of voltage gated Na^+ channels with tetrodotoxin (TTX) produced an increase in miniature excitatory postsynaptic current (mEPSC) amplitude, a measure of basal synaptic function (Katz and Miledi, 1963; Colomo and Erulkar, 1968; Brown et al., 1979). Conversely, chronic (48 hr) hyperactivation of neuron firing rate (through inhibition of GABAA receptors) resulted in the opposite effect - an overall decrease in mEPSC amplitude (Turrigiano et al., 1998). The changes in mEPSC amplitude reported by Turrigiano et al. (1998) were further found to be multiplicative in nature owing to the fact that the entire distribution of mEPSC amplitudes was shifted by a common "scaling" factor. Collectively, this bidirectional central nervous system homeostatic-like mechanism was termed "synaptic scaling" to reflect the multiplicative and presumptive cell wide nature of homeostatic compensation. More generally, however, "homeostatic plasticity" is used regardless of the multiplicative or non-multiplicative nature of compensation.

Based on early studies of synaptic scaling (O'Brien et al., 1998; Turrigiano et al., 1998), it was proposed that neurons are capable of adjusting synaptic properties to stabilize individual neuron firing rate through a mechanism that is characterized by three

main traits: 1) Global neuronal compensation - adaptation occurs in a cell wide, multiplicative manner that serves to retain synapse-specific information that has been previously stored through other, primarily Hebbian forms of plasticity such as long term potentiation and long term depression (Turrigiano et al., 1998; Turrigiano and Nelson, 2004), see also (Rabinowitch and Segev, 2008), 2) A slow timecourse – synaptic scaling is a process that requires ~24 hr before the first compensatory changes in synapse function become evident (Davis and Goodman, 1998; Turrigiano et al., 1998; Watt et al., 2000) see also (Sutton et al., 2006; Ibata et al., 2008) and, 3) Regulation primarily through postsynaptic mechanisms (Wierenga et al., 2005; Gainey et al., 2009) such as activity dependent regulation of the surface expression of AMPA receptor subunits (Rao and Craig, 1997; Lissin et al., 1998; O'Brien et al., 1998; Turrigiano et al., 1998; Liao et al., 1999) see also (Desai et al., 1999).

Functional Significance of Homeostatic Plasticity

Homeostatic plasticity mechanisms are widely observed at central synapses

Since the early description of synaptic scaling in cultured visual cortical neurons (Turrigiano et al., 1998), synaptic scaling has been demonstrated in neuron populations across the nervous system. More generally, however, "homeostatic plasticity" is used regardless of the multiplicative or non-multiplicative nature of compensation. Homeostatic phenotypes have been described in the spinal cord (Rivera-Arconada and Lopez-Garcia; Chub and O'Donovan, 1998; O'Brien et al., 1998; Galante et al., 2001;

Gonzalez-Islas and Wenner, 2006), the hippocampus (Sutton et al., 2006), the nucleus accumbens (Ishikawa et al., 2009; Sun and Wolf, 2009), , the locus coeruleus (Cao et al., 2010), the striatum (Azdad et al., 2009) and the cerebellum (Iijima et al., 2009). Homeostatic plasticity also occurs across multiple neurotransmitter systems with such compensatory mechanisms documented in glutamate (Turrigiano et al., 1998; Sutton et al., 2006), GABA (Bartley et al., 2008; Saliba et al., 2009), glycine (Ganser and Dallman, 2009), endocannabinoid (Kim and Alger, 2010) and dopamine systems (Azdad et al., 2009; Sun and Wolf, 2009). Given the ubiquitous nature of these compensatory responses, homeostatic plasticity mechanisms are likely important for long term maintenance of neuron function and health throughout the lifespan of an organism.

Homeostatic compensation is also widely observed *in vivo*, particularly in several sensory systems. In the cochlear nucleus, monaural hearing loss promotes an increase in the expression of AMPARs balanced with a decrease in the expression of glycine receptors at auditory nerve to bushy or fusiform cells (Whiting et al., 2009) which is completely reversible one day post re-instatement of hearing (Whiting et al., 2009). During the critical period, 2 days of dark rearing increases mEPSC amplitude in visual cortical neurons in a multiplicative manner (Goel and Lee, 2007) as well as the firing rate of layer 4 star pyramidal neurons in acute slices from the visual cortex of rats (Maffei et al., 2004) suggesting that global, synaptic scaling mechanisms are regulating homeostatic responses due to changes in visual stimuli (Maffei et al., 2004; Goel and Lee, 2007). Dark rearing also increases the amplitude of AMPAR mEPSCs in layer 2/3 of the visual cortex (Desai et al., 2002; Goel and Lee, 2007; Maffei and Turrigiano, 2008). Additionally, the firing rates of star pyramidal neurons and mEPSC amplitude in layer

2/3 were restored to normal levels 48 hr after vision was reinstated (Maffei et al., 2004; Goel and Lee, 2007) suggesting that, *in vivo*, bidirectional homeostatic plasticity mechanisms exist to modulate neuron responses to incoming sensory stimuli. Interestingly, homeostatic compensation has also been observed following *in vivo* blockade of action potentials with TTX in the rodent hippocampus (Echegoyen et al., 2007). Two days following hippocampal implantation of a TTX filled Elvax-polymer pellet, hippocampi from Elvax-implanted animals exhibited increased excitability relative to vehicle treated controls (Echegoyen et al., 2007) suggesting that homeostatic plasticity *in vivo* can occur in response to long term perturbation of neuron network function.

Homeostatic plasticity is also well conserved throughout species and has been documented in *Drosophila* (Davis and Murphey, 1993; Davis and Goodman, 1998; Frank et al., 2006), *Xenopus laevis* (Borodinsky et al., 2004) and chicks (Chub and O'Donovan, 1998; Gonzalez-Islas and Wenner, 2006) in addition to rodents (Turrigiano et al., 1998). Conservation of homeostatic mechanisms across such diverse species suggests that there has been strong evolutionary pressure to maintain homeostatic plasticity mechanisms in diverse neural circuits despite the unique external environments in which these organisms live.

Homeostatic plasticity mechanisms may contribute to neurological disease

Given the long lifespan of the post-mitotic nervous system (Marder and Goaillard, 2006) it is no surprise that a check and balance mechanism exists within the nervous system to maintain stability of neuron networks over long periods of time (Turrigiano,

2008; Pozo and Goda, 2010). Given the role of homeostatic plasticity in promoting neuron network stability, does dysregulation of homeostatic plasticity lead to the development or the progression of neurological disease? Indeed, homeostatic plasticity has been hypothesized to play a role in learning and memory (Miller, 1996; Murthy et al., 2001), epilepsy (Evers et al.; Seeburg et al., 2008; Seeburg and Sheng, 2008; Doyle et al., 2010; Kim and Ryan, 2010), psychiatric disorders (Dickman and Davis, 2009) and addiction (Dani and Heinemann, 1996; Ishikawa et al., 2009; Sun and Wolf, 2009). However, a direct link between altered homeostatic plasticity and abnormal neuron function during disease states has been difficult to make, largely because the molecular mechanisms underlying homeostatic plasticity have remained poorly defined. Therefore, it would be of further interest to pursue studies aimed at understanding the molecular pathways underlying homeostatic plasticity and by extension the etiology of neurological diseases such as addiction and epilepsy.

A family of plasticity mechanisms underlies homeostatic regulation at synapses

It is becoming increasingly clear that global, synaptic scaling is only one form of compensatory plasticity and that a large group of homeostatic plasticity mechanisms may exist within the nervous system. Additional studies have emerged over the past decade that have expanded the view of the classical synaptic scaling model (Murthy et al., 2001; Burrone et al., 2002; MacLean et al., 2003; Thiagarajan et al., 2005; Frank et al., 2006; Sutton et al., 2006; Echegoyen et al., 2007; Branco et al., 2008; Ibata et al., 2008; Kim

and Tsien, 2008) which, in particular, expand the spatial and temporal properties of homeostatic plasticity.

Local Forms of Homeostatic plasticity

Although the multiplicative nature of synaptic changes was thought to represent a key feature of homeostatic plasticity, recent studies have demonstrated that homeostatic plasticity can occur in a local, spatially restricted manner. For example, under normal, basal conditions, release probability is highly heterogeneous along a branch of dendrite (Branco et al., 2008) but after 2 hr of spatially restricted dendritic stimulation presynaptic release probabilities along the stimulated branch were similar in magnitude suggesting that postsynaptic depolarization is capable of controlling local, presynaptic release probability in a rapid, homeostatic manner (Branco et al., 2008). Additionally, blockade of NMDAR activity along a restricted segment of dendrite selectively increases compensatory surface expression of GluA1 containing AMPARs while having no effect on surface GluA1 expression at sites flanking the perfused region (Sutton et al., 2006) suggesting that spatially restricted blockade of synaptic activity activates homeostatic compensation specifically at synapses where activity has been disrupted. Indeed, a single synapse composed of a presynaptic bouton from a neuron expressing Kir2.1, an inwardly rectifying potassium channel, opposed to a dendritic spine from a normal WT neuron exhibited an increase in the surface amount of GluA1 expression relative to neighboring WT synapses (Hou et al., 2008) demonstrating the ability of neurons to undergo synapse

specific homeostatic plasticity mechanisms and challenging the argument that homeostatic compensation relies on a cell wide compensatory mechanism.

Presynaptic Expression of Homeostatic plasticity

Although a dominant view has been that homeostatic plasticity at excitatory synapses is largely mediated via postsynaptic expression mechanisms, homeostatic regulation of presynaptic function has also been described. For example, inhibition of neuron network activity can increase the size of active zones as well as the number of docked vesicles within the presynaptic terminal (Murthy et al., 2001; Moulder et al., 2006) and can increase presynaptic function as measured by strylyl dye uptake (Bacci et al., 2001; Burrone et al., 2002; Moulder et al., 2006; Han and Stevens, 2009b; Kim and Ryan, 2010) or electrophysiology (Murthy et al., 2010; Jakawich et al., 2010). Additionally, single cell expression of Kir2.1 increases presynaptic input onto Kir2.1 expressing cell and this maintains the firing rate of Kir2.1 expressing cells at a level that is comparable to the firing rate of neighboring cells that are not expressing Kir2.1 (Burrone et al., 2002). Additionally, homeostatic adaptation can manifest as a concurrent increase in both pre- and post- synaptic function in the hippocampus (Bacci et al., 2001; Galante et al., 2001; Thiagarajan et al., 2002; Lauri et al., 2003; Thiagarajan et al., 2005) as well as the cortex (Gong et al., 2007). These studies suggest that functional compensation at synapses can be achieved through multiple homeostatic mechanisms but whether pre- and post- synaptic compensation rely on distinct molecular mechanisms remains to be determined.

Rapid vs. Slow Induction of Homeostatic plasticity

Blocking action potentials in cultured neurons drives a characteristically slow form of homeostatic plasticity that emerges ~18-24 hrs post-treatment (Turrigiano et al., 1998; Sutton et al., 2006). However, direct blockade of synaptic activity rapidly induces synaptic compensation on a much faster time-scale (1-3 hrs; Sutton et al., 2006; Aoto et al., 2008), suggesting that distinct slow and rapid forms of homeostatic plasticity may exist. Indeed, at the *Drosophila* neuromuscular junction (NMJ) blocking a fraction of postsynaptic AMPARs results in an acute homeostatic decrease in both miniature and evoked end plate potential amplitudes (Frank et al., 2006). Curiously, however, homeostatic compensation occurring over the next 10 min was sufficient to restore end plate potential amplitudes to near normal levels (Frank et al., 2006) suggesting that within minutes, blockade of AMPAR initiates homeostatic compensation sufficient to restore evoked neuron function at the *Drosophila* NMJ (Frank et al., 2006). Curiously, it has been reported that TTX-induced homeostatic plasticity can also occur on the order of hours if neurons are cultured on a bed of glia (Ibata et al., 2008) suggesting that a critical interaction between glia and neurons may be responsible for temporal regulation of homeostatic plasticity, possibly through a TNFalpha based mechanism (Stellwagen and Malenka, 2006). Together these studies illustrate that homeostatic plasticity can exhibit multiple spatial and temporal profiles and further suggests that the final compensatory output likely involves the interaction between several, mechanistically distinct forms of homeostatic plasticity.

Synapse driven homeostatic plasticity

Miniature synaptic events are quantal release events that occur independently of action potential evoked neurotransmitter release (Katz and Miledi, 1963; Colomo and Erulkar, 1968; Brown et al., 1979). Contrary to early thoughts that miniature activity contributed little or no synaptic information, miniature activity can directly control local protein translation in dendrites (Sutton et al., 2004) as well as the structure of dendritic spines (McKinney et al., 1999) suggesting that miniature events play a pivotal role in regulating synapse structure and function. Therefore, direct manipulation of synaptic activity could be sufficient to induce expression of homeostatic plasticity at synapses. Indeed, blockade of miniature synaptic activity through AMPA- or NMDA- type glutamate receptors induces robust homeostatic compensation that can manifest as pre- or post- synaptic forms of compensation (O'Brien et al., 1998; Thiagarajan et al., 2005; Sutton et al., 2006; Gong et al., 2007; Aoto et al., 2008). Interestingly, recent evidence suggests that neurotransmitter release triggered by APs and miniature activity may derive from unique presynaptic vesicle populations (Atasoy et al., 2008), which might imply a specific functional role for homeostatic plasticity tuned to miniature synaptic events. Therefore, understanding how neurons respond to direct synaptic disruption, in comparison to AP disruption, is likely to uncover unique aspects of molecular control during homeostatic plasticity.

Regardless of their potential functional role, the quantal nature of mEPSCs have made them long-standing attractive readouts of synaptic function. Since mEPSCs represent postsynaptic responses to a single vesicle filled with neurotransmitter, changes in mEPSC amplitude generally reflect alterations in postsynaptic sensitivity to

neurotransmitter. On the other hand, changes in mEPSC frequency often reflect changes in the rate at which synaptic vesicles are released from axon terminals, that is, alterations in presynaptic release probability. Hence, while changes in specific mEPSC characteristics do not definitively demonstrate a pre- or postsynaptic mechanism, they do provide initial evidence for such changes and yield a strong rationale for testing functional compensation in each synaptic compartment

Is neurotransmitter receptor sensitization or desensitization involved in homeostatic response mechanisms?

Although frank homeostatic plasticity at central synapses has only recently been studied intensely, the related phenomenon of receptor sensitization and desentization has a much longer history. Thus, it has long been known that receptors can rapidly undergo allosteric and post-translation modifications that can alter normal sensitivity to neurotransmitters (Robinson and Berridge, 2003). For example, following chronic cocaine exposure, an acute drug challenge can elicit an increase in extracellular dopamine levels greater than that relative to naïve control animals (Bradberry, 2007). Conversely, prolonged tonic exposure to dopamine can result in a decreased sensitivity of dopamine receptors to an acute dopamine challenge (Barton et al., 1991). Indeed, neurotransmitter receptor sensitization and desensitization may rapidly induce homeostatic plasticity mechanisms (Frank et al., 2006) and may underlie homeostatic alterations in long term changes in AMPAR surface expression (Turrigiano et al., 1998; Sutton et al., 2006; Gainey et al., 2009). Therefore, determining the molecular underpinnings of homeostatic

plasticity may elucidate overlapping roles for receptor sensitization and/or desensitization and homeostatic plasticity.

Developmental regulation of homeostatic control at synapses

Given heterogeneous spatial and temporal expression mechanisms, how is the timing and locus of homeostatic plasticity regulated? Although largely an open question, it has previously been suggested that developmental state is one variable that may control how homeostatic response mechanisms may be implemented at synapses (Wierenga et al., 2006; Echegoyen et al., 2007; Swann et al., 2007; Han and Stevens, 2009a). Specifically, functional synapse formation seems to be a critical regulation point for phenotypic manifestation of homeostatic processes (Burrone et al., 2002; Huupponen et al., 2007) and mature neurons seem to have a higher threshold for the induction of homeostatic processes in response to pharmacological inhibition of neuron activity with TTX (Hupponen et al., 2007). *In vivo* studies further suggest that during the critical period, 2 days of dark rearing increases mEPSC amplitude in a multiplicative manner suggesting that global, synaptic scaling mechanisms are regulating homeostatic responses (Goel and Lee, 2007). In contrast, in 3 month old, mature animals, 2 days of dark rearing increased mEPSC amplitude in a non-multiplicative manner (Goel and Lee 2008) suggesting that within the same subset of neurons. These data suggest that sensory experience can homeostatically modify cortical responses via two distinct mechanisms (uniform and non-uniform respectively) that are a function of development of neuron networks with respect to age. Together, these studies suggest that maturation of neuronal

circuits plays a critical role in sensing and regulating homeostatic expression mechanisms.

Molecular mechanisms contributing to homeostatic adaptations at synapses

Many different synaptic proteins are involved in homeostatic plasticity mechanisms

Several proteins have been well characterized as mediators of homeostatic function. Among those proteins are the immediate early gene Arc/Arg3.1 (Shepherd et al., 2006), brain derived neurotrophic factor (Rutherford et al., 1997; Rutherford et al., 1998), retinoic acid (RA; Aoto et al., 2008), various cell adhesion molecules (Okuda et al., 2007; Cingolani and Goda, 2008; Cingolani et al., 2008) as well as glial derived TNFalpha (Steinmetz and Turrigiano; Stellwagen and Malenka, 2006; Cingolani et al., 2008; Kaneko et al., 2008). In addition to the group of well characterized homeostatic signaling molecules, a host of other proteins have been implicated in regulating homeostatic plasticity including adenylyl cyclase 1 (Gong et al., 2007), voltage gated sodium channels (Aptowicz et al., 2004), vesicular pumps (De Gois et al., 2005; Iijima et al., 2009; Doyle et al., 2010), CREB (Cao et al., 2010), 2010), various calcium signaling proteins (Pawlak et al., 2005; Ibata et al., 2008; Djakovic et al., 2009; Jensen et al., 2009; Saliba et al., 2009), Narp (Doyle et al., 2010) and Cbln1 (Iijima et al., 2009). Together these studies highlight that molecular mechanisms underlying homeostatic plasticity are likely to involve a complicated interaction between many cellular signaling components.

A major challenge moving forward will be for studies to integrate these molecules into a cohesive mechanistic framework.

The role of cell trans-synaptic proteins in homeostatic plasticity

Cell adhesion molecules are required for the spatial alignment of cellular components, such as pre- and post- synaptic compartments (Sudhof, 2008). Interestingly, C-terminal function of β3 integrin is required for homeostatic plasticity in both dissociated and organotypic slice cultures (Cingolani et al., 2008; Cingolani and Goda 2008). Disruption of C-terminal integrin binding to postsynaptic scaffolding proteins decreases mEPSC amplitude through increased GluA2 endocytosis (Cingoliani et al., 2008). Additionally, postsynaptic expression of β 3 integrin increases mEPSC amplitude and in contrast, expression of a truncated C-terminal tail of β 3 integrin, that does not contain β 3 integrin cell adhesion properties, decreases mEPSC amplitude (Cingoliani et al., 2008). Moreover, loss of beta catenin expression or expression of a dominant negative form of N-cadherin reduces mEPSC amplitude (Okuda et al., 2007) and cells lacking beta catenin fail to undergo bidirectional homeostatic plasticity during network quiescence/hyperactivity with TTX and bicuculline, respectively (Okuda et al., 2007). Together, these data suggest that cell adhesion molecules play an important role in homeostatic plasticity and raise the possibility that transsynaptic mechanisms are required for proper homeostatic functioning.

The role of intracellular proteins in homeostatic plasticity

Arc/Arg3.1 is an immediate early gene whose mRNA and protein is regulated by neuron activity *in vivo* (Steward et al., 1998; Steward and Worley, 2001). Arc is required for the maintenance of LTP and LTD as well as the consolidation of long term memories (Plath et al., 2006). Interestingly, Arc/Arg3.1 expression is regulated by neuron activity in both cultured hippocampal as well as cortical neurons. Chronic silencing of neuron networks with TTX decreases the amount of Arc/Arg3.1 protein expression whereas hyperactivation of neuron networks increases the total amount of Arc/Arg3.1 as measured by immunofluorescence (Shepherd et al., 2006). Overexpression of Arc/Arg3.1 prevents the ability of neurons to homeostatically increase the strength of synapses during long term activity blockade with TTX (Shepherd et al., 2006) and Arc knockout animals show enhanced basal synaptic function as measured by an increase in mEPSC amplitude as well as frequency relative to the WT littermate control mice (Shepherd et al., 2006). Furthermore, knockout of Arc/Arg3.1 expression occludes network induced bidirectional homeostatic plasticity (Shepherd et al., 2006) suggesting that rapid regulation of synaptic signaling by immediate early genes could contribute to the underlying mechanisms of homeostatic plasticity.

Exogenous RA or pharmacological induction of RARalpha synthesis is sufficient to increase mEPSC amplitude in both organotypic slice culture as well dissociated primary hippocampal cultures (Aoto et al., 2008) and occludes TTX/APV induced homeostatic plasticity (Aoto et al., 2008). Furthermore, blockade of RA synthesis or knockdown of RA expression using shRNA prevents TTX/APV induced increases in mEPSC amplitude (Aoto et al., 2008) suggesting that RA synaptic signaling is required

for homeostatic plasticity. Indeed, TTX/APV application induces RA synthesis in neurons (Aoto et al., 2008) and exogenous application of RA is sufficient to increase the surface expression of GluA1 by increasing the local dendritic synthesis of GluA1 (Aoto et al., 2008; Maghsoodi et al., 2008). Interestingly, TTX application on its own is insufficient to alter RA synthesis in neurons (Aoto et al., 2008), which could explain why TTX treatment is not sufficient to drive the rapid postsynaptic compensation driven by blockade of NMDAR-mediated miniature neurotransmission (TTX/APV; Sutton et al., 2006). RA induced synthesis of GluA1 further occludes GluA1 synthesis during TTX/APV induced homeostatic plasticity (Aoto et al., 2008; Maghsoodi et al., 2008) in dendritic RNA granules (Maghsoodi et al., 2008) suggesting that RA serves as an essential intermediate between activity blockade and local synthesis of new AMPARs.

Ca^{2+}/Calmodulin dependent protein kinase 2 (CAMKII) is a member of a serine/threonine family of kinases that are important for Hebbian forms of synaptic plasticity as well as learning and memory (Lisman et al., 2002). Inhibition of postsynaptic CAMKII at the *Drosophila* NMJ increases end junction potentials through an increase in synaptic cluster size of GluAII containing receptors (Morimoto et al., 2009). Interestingly, expression of CAMKII T286D, a CAMKII phospho-mimetic, increases both EPSC and mEPSC amplitude in cultured visual cortical neurons by increasing quantal content and decreasing the density of synaptic contacts on CAMKII T286D-expressing neurons (Pratt et al., 2003). Conversely, inhibition of endogenous CAMKII with an autoinhibitory peptide, decreased mEPSC amplitude while increasing synapse density (Pratt et al., 2003). Interestingly, manipulation of neuron firing rate inversely alters the expression levels of alpha and beta CAMKII proteins (Thiagarajan et al., 2002).

As activity levels raise the amount of alpha CAMKII also raises but the total amount of beta CAMKII decreases (Thiagarajan et al., 2002) suggesting that as network activity rises, the sensitivity of CAMKII signaling decreases and when network activity is low, calcium sensitivity through CAMKII signaling increases (Thiagarajan et al., 2002). Curiously, however, when synaptic activity is inhibited alpha CAMKII expression levels are preferentially increased when NMDA receptor signaling is blocked and beta CAMKII expression levels are preferentially increased when AMPA receptor signaling is blocked suggesting that AMPAR and NMDAR blockade could mediate different downstream signaling events through differential regulation of CAMKII expression levels (Thiagarajan et al., 2002).

Polo like kinase 2 (Plk2) is a member of the polo family of serine/threonine kinases whose expression is rapidly induced during seizure like activity (Kauselmann et al., 1999; Seeburg and Sheng, 2008) or prolonged blockade of GABAA receptors with pictrotoxin (Seeburg et al., 2008) suggesting that Plk2 may play a role in regulating activity dependent increases in synaptic function during conditions of high neuron activity. Indeed, knockdown of Plk2 expression with either a Plk2 dominant negative or a Plk2 targted RNAi prevented picrotoxin induced synaptic scaling in cultured hippocampal neurons (Seeburg et al., 2008). Interestingly, Plk2 activity requires coordinated phosphorylation of target proteins with CDK5, a neuronal kinase whose activity is induced by AB peptides (Alvarez et al., 2001; Town et al., 2002). Coordinated priming by CDK5 and subsequent phosphorylation by Plk2 is required for homeostatic decreases in function (Seeburg et al., 2008). Furthermore, knockdown of CDK5 expression prevents picrotoxin induced scaling down of synapses (Seeburg et al., 2008)

and unmasks the presence of previously silent terminals (Kim and Ryan, 2010). Silencing of neuron activity with TTX decreases presynaptic expression of CDK5 and mimics the effect of unsilencing presynaptic terminals with downregulation of CDK5 expression (Kim and Ryan 2010). Together these studies suggest that rapid activity dependent phosphorylation is important for the expression of homeostatic plasticity, particularly during homeostatic decreases in neuron function.

The role of secreted molecules in homeostatic plasticity

Tumor necrosis factor alpha (TNFalpha) is an inflammatory cytokine largely thought to regulate apoptotic function and inflammation (Beutler et al., 1985; Dayer et al., 1985). Curiously, however, TNFalpha is emerging as a key signaling molecule during induction of homeostatic plasticity. Scavenging TNFalpha prevents quiescence induced homeostatic increases in function (Stellwagen and Malenka 2006) but TNFalpha does not seem to be required for hyperactivity induced homeostatic decreases in function (Stellwagen and Malenka 2006). Interestingly, glial derived TNFalpha is required for homeostatic plasticity (Stellwagen and Malenka 2006) suggesting that homeostatic plasticity may involve a tripartate synpase mechanhism (Stellwagen and Malenka 2006). These studies suggest that acute immune response mechanisms may have overlapping molecular bases with homeostatic plasticity and it would be interesting to understand if homeostatic plasticity is indeed a part of a cellular survival/death network or if homeostatic plasticity purely utilizes TNFalpha as a glial derived activity dependent synaptic signal.

Brain derived neurotrophic factor (BDNF; Barde et al., 1982) is a member of the nerve growth factor family of neurotrophic factors (Leibrock et al., 1989) and has multiple roles in neuron survival (Barde et al., 1982; Johnson et al., 1986; Hofer and Barde, 1988). BDNF predominately signals through the interaction with its high affinity receptor TrkB (Klein et al., 1991; Soppet et al., 1991; Squinto et al., 1991) where binding of BDNF to TrkB initiates downstream signaling via activation of TrkB through autophosphorylation of TrkB receptors (Zirrgiebel et al., 1995). BDNF and its receptor, TrkB, are highly expressed in the nervous system (Liebrock et al., 1989) where BDNF expression has been shown to be regulated by changes in activity such as high K^+ (Zafra et al., 1990; Elliott et al., 1994), long term potentiation (Castren et al., 1993; Gartner and Staiger, 2002), exogenous application of glutamate receptor agonists (Zafra et al., 1990; Lindefors et al., 1992) as well as seizure-like phenotypes (Ballarin et al., 1991; Ernfors et al., 1991; Isackson et al., 1991; Dugich-Djordjevic et al., 1995). BDNF additionally modulates synaptic strength (Lohof et al., 1993; Korte et al., 1995) as well as plasticity (Korte et al., 1995; Figurov et al., 1996; Kang and Schuman, 1996; Patterson et al., 1996; Pozzo-Miller et al., 1999; Xu et al., 2000) and is thought be an activity dependent, local, retrograde synaptic signaling messenger (Magby et al., 2006). Interestingly, BDNF protein expression is bidirectionally regulated during network quiescence and hyperactivation (Jia et al., 2008) and during periods of prolonged (6 hr) deloparization (Iijima et al., 2009). BDNF can prevent TTX-induced postsynaptic scaling (Rutherford et al., 1998, Rutherford 1999) suggesting that BDNF expression as well as function may be highly regulated during homeostatic plasticity.

Homeostatic signaling molecules mediate homeostatic responses in vivo

Three proteins required for expression of homeostatic plasticity *in vitro*, BDNF, Arc and TNFalpha, are also critical for homeostatic plasticity *in vivo*. BDNF expression is rapidly regulated by exposure to light (Castren et al., 1992) BDNF mRNA expression levels are significantly lower in dark reared rats compared to normal light/dark control animals (Castren et al., 1992) and the deficit in BDNF mRNA expression is rescued upon light exposure (Castren et al., 1992). In addition, BDNF can potentiate synaptic transmission in the visual cortex from both acute slices (Carmignoto et al., 1997) as well as synaptosomes (Simsek-Duran and Lonart, 2008) suggesting that light can homeostatically alter neuron function by regulating relative amounts of BDNF expression. Arc knockout (KO) mice fail to undergo activity dependent shifts in ocular dominance following monocular depravation or open-eye potentiation, post-dark rearing (McCurry et al., 2010) despite having normal visual acuity (McCurry et al., 2010) and developmental progression (Gao et al., 2010). Additionally, dark reared Arc KO animals failed to undergo potentiation of mEPSC amplitude (Gao et al., 2010) that is normally observed with dark rearing (Goel and Lee et al., 2010) and specifically, deficits in excitatory synaptic scaling are observed in the Arc KO animals (Gao et al., 2010). Furthermore, following 5 d of monocular deprivation, TNFalpha knockout mice have a decreased capacity for visual plasticity (Kaneko et al., 2008).

These findings draw attention to the fact that the list of proteins thought to be involved in homeostatic plasticity is growing exponentially but the manner in which these

diverse molecular players interact is still largely unknown. A more detailed mechanistic framework is necessary before it will be possible to fully integrate the existing findings.

Homeostatic compensation is a lasting form of neuron plasticity - how are enduring changes in neuron function induced?

Memories are hypothesized to arise through the modification of existing neuronal connections (Cajal, 1984) through the strengthening or weakening of individual synaptic connections (Hebb, 1949) by a mechanism that has long been attributed to protein synthesis dependent mechanisms. Recently, however, the importance of protein degradation to the fidelity of enduring neuron plasticities, as well as learning and memory, is beginning to be elucidated.

A role for protein synthesis in neuron plasticity

Enduring changes in brain function, such as long term memory formation (Agranoff and Klinger, 1964; Agranoff et al., 1965; Davis et al., 1965; Brink et al., 1966) and long term potentiation (Stanton and Starvey, 1985; Frey et al., 1988) require activity dependent protein synthesis. Protein synthesis is also required for denervation supersensitivty (Fambrough 1970; Grampp et al., 1972) Goold et al., 2010 as well as for the expression of both NMDAR and retinoic acid induced homeostatic plasticity (Sutton et al., 2006; Aoto et al., 2008). Protein synthesis is further required for homeostatically

induced redistribution of surface GluA1 containing AMPARs (Ito and Schuman, 2009) suggesting that activity dependent protein synthesis is also contributing to enduring changes in function during homeostatic plasticity. Protein synthesis has emerged as a critical regulation point during both Hebbian and homeostatic forms of neuron plasticity. What is less clear, however, is the spatial contribution of protein synthesis during activity dependent modulation of neuron function and it would be of interest to understand the contributions of local protein synthetic mechanisms.

A role for protein degradation in regulating neuron plasticity

Two major pathways of protein degradation exist in eukaryotic cells 1) the lysosome (de Vuve et al., 1953) and, 2) degradation by the ubiquitin proteasome system (UPS). Lysosomal mediated protein degradation is achieved largely through bulk endocytotic mechanisms and is therefore, generally regarded as a moderately specific mechanism for the degradation of membrane proteins (Ravikumar et al., 2010). Protein degradation by the ubiquitin proteasome system, however, is a tightly regulated and energy dependent process (Simpson, 1953; Mandelstam, 1958; Hershko and Tomkins, 1971; Hershko et al., 1984; Demartino et al., 1994) (Hoffman and Rechsteiner, 1994) making the UPS an ideal system for activity dependent regulation of synaptic protein levels. Proteasome mediated degradation requires conjugation of the small 76 amino acid protein, ubiquitin (Schlesinger and Goldstein, 1975; Schlesinger et al., 1975) to target substrates (Ciechanover et al., 1980; Hershko et al., 1980). Conjugation of ubiquitin to a target substrate depends on a series of enzymatic reactions that serve to covalently attach

ubiquitin to its target: 1) Ubiquitin is activated (adenylated) by an E1 activating enzyme (Ciechanover et al., 1981; Ciechanover et al., 1982), 2) Ubiquitin is subsequently transferred to an E2 enzyme through transesterification (Hershko and Ciechanover, 1992) and, 3) Associated with an E3 ubiquitin ligase mediates catalysis of isopeptide bond formation between ubiquitin and its target substrate (Hershko and Ciechanover, 1992). Ubiquitination of 4 or more lysine 48 linked ubiquitin moeities, or polyubiquitination, targets proteins for degradation by a large, multiprotein enzymatic complex, the proteasome (Hershko and Ciechanover, 1998).

Proteasome dependent degradation is required for enduring forms of synaptic plasticity. Proteasome inhibitors block the formation of long term facilitation (Hegde et al., 1993) and long term depression (LTD) in *Aplysia* sensiromotor synapses (Fioravante et al., 2008). Proteasome function has also been reported to decrease following chemical LTD induction (Tai et al., 2010) which may be due to the dissociation of the proteasome into individual regulatory and catalytic subunits (Tai et al., 2010). Interestingly, intact protein degradation is required for long term memory formation (Lopez-Salon et al., 2001), working memory (Wood et al., 2005) as well as the destabilization of existing memories during memory retrieval (Lee et al., 2008) suggesting that protein degradation is important for lasting changes in neuron function that may contribute to the underlying cellular mechanisms of learning and memory.

Further evidence indicates that protein degradation by the proteasome may play a role in homeostatic regulation of neuron function. Prolonged quiescence or hyperactivation of neuron function can alter synaptic protein expression in a proteasome dependent manner (Ehlers, 2003). In addition, manipulation of neuron activity can

directly regulate the basal rate of proteasome degradation (Djakovic et al., 2009) and prevent synaptic scaling of $GABA_A$ receptor expression (Saliba et al., 2007). Proteasome function has additionally been linked to activity dependent modulation of presynaptic function (Jiang et al., 2010; Rinetti and Schweizer, 2010); see also (Willeumier et al., 2006) and the expression of the presynaptic proteins DUNC13/MUNC13 (Aravamudan et al., 1999; Aravamudan and Broadie, 2003; Speese et al., 2003) and Rim1alpha (Yao et al., 2007). Taken together, these findings suggest an important role for proteasome function in regulating homeostatic synaptic strength, although it remains unclear how the proteasome may be regulating both pre- and post- synaptic homeostatic plasticity.

How is homeostatic plasticity mediated?

The overall goals of this study are to: 1) To define the role(s) of proteasome function during homeostatic plasticity, 2) to determine the role(s) of protein synthesis during homeostatic plasticity, 3) to determine the spatial specificity (pre- or post-synaptic) of both protein synthesis and protein degradation during homeostatic plasticity, 4) to determine the molecular nature of synaptic communication during homeostatic plasticity and 5) to understand the interaction between blockade of action potentials and blockade of miniature synaptic activity during homeostatic synaptic plasticity. Described here are three molecularly distinct forms of homeostatic plasticity that differ in spatial as well as temporal expression patterns. Each form of homeostatic plasticity further requires a unique activity dependent protein regulatory mechanism. Prolonged (days) inhibition of proteasome function induces a form of homeostatic plasticity that both mimics and

occludes classical synaptic scaling mechanisms and suggests that activity dependent modulation of the rate of postsynaptic proteasome degradation may mediate the functional compensation observed during slow, postsynaptic homeostatic plasticity. In contrast, rapid (3 hr) inhibition of AMPAR activity induces two distinct forms of homeostatic plasticity: 1) A rapid, postsynaptic form of compensation that relies on the protein synthesis dependent insertion of GluA1 homomeric AMPARs and, 2) A rapid presynaptic form of compensation that requires postsynaptic local protein synthesis of a retrograde synaptic signal, BDNF, as well as spatially distinct presynaptic action potential activity and presynaptic protein degradation by the ubiquitin proteasome system. These three distinct forms of homeostatic plasticity highlight the presence of an intricate synaptic signaling network and the importance of spatially restricted protein localization and expression during activity induced homeostatic plasticity. Therefore, homeostatic plasticity may result from of the interaction multiple signaling networks within a single neuron and ultimately, regulate the balance between long term synapse, intrinsic, and neuron function.

CHAPTER II

An essential postsynaptic role for the ubiquitin proteasome system in slow homeostatic synaptic plasticity in cultured hippocampal neurons

Introduction

Homeostatic forms of synaptic plasticity are thought to buffer otherwise debilitating changes in neural circuit activity through compensatory synaptic adaptations that drive network activity back towards a stable range (Marder and Prinz, 2002; Davis, 2006; Rich and Wenner, 2007; Nelson and Turrigiano, 2008; Rabinowitch and Segev, 2008). At central synapses, this homeostatic control of synapse function has been best characterized through chronic perturbations of activity in cultured neuron networks, where compensatory synaptic modifications emerge in a characteristically slow manner over a period of roughly 24-72 hrs (Rao and Craig, 1997; O'Brien et al., 1998; Turrigiano et al., 1998; Murthy et al., 2001). Recent studies have also demonstrated that more rapid forms of homeostatic plasticity are expressed in the nervous system, where compensatory synaptic modifications are evident in minutes to hours following activity challenges (Sutton et al., 2006; Frank et al., 2006). Although the molecular mechanisms underlying slower forms of homeostatic control are still largely unknown, several findings suggest

that these mechanisms may be qualitatively distinct from more rapid homeostatic mechanisms. For example, whereas blocking both action potential (AP)-driven and spontaneous neurotransmission induces synaptic insertion of GluA1 homomeric receptors that requires dendritic protein synthesis (Ju et al., 2004; Thiagarajan et al., 2005; Sutton et al., 2006; Aoto et al., 2008), AP blockade on its own drives a slower form of compensation associated with an increase in AMPAR half-life (O'Brien et al., 1998), enhanced expression of GluA2-containing AMPARs at synapses (Wierenga et al., 2005), 2005), as well as accumulation of GFP-tagged GluA2 subunits at synapses (Ibata et al., 2008). These findings suggest that de novo synthesis and degradation of existing proteins may differentially contribute to temporally distinct forms of homeostatic plasticity.

Neurons use two major protein degradation pathways – 1) endocytic retrieval and degradation of integral membrane proteins by the lysosome and, 2) regulated degradation of soluble proteins by the ubiquitin proteasome system (UPS). Degradation by the UPS requires covalent attachment of polyubiquitin chains to the target substrate, catalyzed by the sequential action of E1-E3 ubiquitin-conjugating enzymes (Hershko, 2005). Ubiquitin contains 7 lysine residues that can contribute to the polyubiquitination of target substrates, but it is polyubiquitination of a target substrate via lysine 48 (K48) that serves as the cellular marker for targeted protein degradation by the proteasome (Patterson and Lippincott-Schwartz, 2002; Schwartz and Ciechanover, 2009). Given that proteasome function in neurons is bi-directionally regulated by activity (Djakovic et al., 2009), the UPS is poised to play an active role in regulating protein dynamics at the synapse. Indeed, Ehlers (2003) demonstrated that AP blockade and disinhibition of cortical cultures resulted in bi-directional changes in the protein composition of the postsynaptic

density (PSD) that emerge slowly (24-48 hrs) and are UPS-dependent. These observations suggest that the UPS may play a critical role in slow homeostatic plasticity, but it is currently unknown whether homeostatic changes in synapse function similarly require the UPS. Moreover, other studies have recently demonstrated that UPS activity is necessary for homeostatic silencing of presynaptic terminals in response to excessive depolarization (Jiang et al., 2010) and may play other homeostatic roles presynaptically (Willeumier et al., 2006; Rinetti and Schweizer, 2010). Furthermore, astrocytes can play an active role in homeostatic plasticity during chronic changes in activity (Stellwagen and Malenka, 2006). These latter results raise questions about whether the changes in PSD composition observed by Ehlers (2003) reflect a requirement for the UPS postsynaptically, or whether UPS inhibition alters PSD composition indirectly via changes in astrocyte-driven signaling or presynaptic function. Here, we investigate whether activity-dependent regulation of proteasome function in the postsynaptic neuron drives slow homeostatic synaptic plasticity.

Experimental Procedures

Cell Culture

Hippocampi from Sprague-Dawley rat pups (P1-P3) were dissected in cold dissociation media (DM; 82 mM Na_2SO_4, 30 mM K_2SO_4, 5.8 mM $MgCl_2$-$6H_2O$, 252 µM $CaCl_2$-$2H_2O$, 1 mM HEPES, 200 mM glucose, 0.001% w/v phenol red), and transferred to a 15 ml conical tube. The DM was gently removed (leaving ~500 µl of DM remaining

to keep the tissue covered) and replaced with 5 ml of pre-warmed (37ºC) cysteine-activated papain solution (3.2 mg L-cysteine (Sigma-Aldrich; Saint Louis, MO) with 500 µl papain (Sigma-Aldrich; Saint Louis, MO) in 10 ml DM, pH ~ 7.2), and incubated for 15 min at 37ºC to allow for tissue digestion; halfway through the incubation, the tube was inverted ~2-3 times. Cells were then washed 2X in ice-cold DM containing 12.5 % v/v fetal bovine serum to inactivate the papain followed by 2 washes in DM alone. The cells were then washed 2X in chilled normal growth medium [NGM; Neurobasal A (Gibco; Grand Island, NY) supplemented with 2% v/v B27 (Invitrogen; Carlsbad, CA) and 1% v/v Glutamax (Invitrogen; Carlsbad, CA)], then titurated ~10-15 times in 5 ml NGM to obtain a single cell suspension and placed on ice for ~3-5 min. 4.5 ml of the cell suspension was removed from the middle of the cell solution to avoid contaminant material and the cells were placed in a new 15 ml tube and centrifuged at 67 x g (0.5 x 1000 rcf) at 4ºC. 50-70K cells (in a volume of 150 µl) were plated onto poly-D-lysine-coated glass-bottom petri dishes (Mattek; Ashland, MA) and maintained at 5% CO2/37ºC. 4 hrs after plating, 2 ml of NGM-GC (NGM supplemented with 15% v/v glial conditioned media and 10% v/v cortical conditioned media) was added to each dish. Cells were fed 24 hr later by replacing 50% of their media with fresh NGM-GC and every 4 days thereafter by replacing 25% of their media with fresh media. Cells were maintained for 14 days in NGM-GC, then fed every 4 days thereafter with NGM alone. All neurons used for experiments developed for $\geq$ 21 DIV, a time at which the majority of synaptogenesis is completed and network activity is stable.

Whole-Cell Patch Clamp Electrophysiology

Pharmacological agents were added to cultured hippocampal neurons (≥21 DIV) in conditioned media at times as indicated for each reagent. Prior to recording, cells were washed 1X and maintained in HEPES-buffered saline (HBS; 119 mM NaCl, 5 mM KCl, 2 mM $CaCl_2$, 2 mM $MgCl_2$, 30 mM glucose, 10 mM HEPES; pH 7.4) containing 1μM TTX (Calbiochem; San Diego, CA) and 10 μM bicuculline (Tocris; Ellisville, MO). Whole cell patch-clamp recordings were performed using glass recording pipettes, with resistances of 4-6 MΩ when filled with internal solution (100 mM cesium gluconate, 0.2 mM EGTA, 5 mM $MgCl_2$, 40 mM HEPES, 2 mM Mg-ATP, 0.3 mM Li-GTP, pH 7.2). Pyramidal-like neurons were identified for recording based on cell morphology (the presence of a large apical dendrite and a large pyramidal-like cell body). Membrane potential was clamped at -70 mV and miniature excitatory postsynaptic currents (mEPSCs) were recorded using an Axopatch 200B amplifier and Clampex 8.0 software (Molecular Devices). mEPSCs were analyzed off-line using MiniAnalysis (Synaptosoft).

Surface GluA1/2 Immunocytochemistry

Following the appropriate treatment, cells were live labeled with primary antibodies against surface epitopes of GluA1 (sGluA1, 1:10, Calbiochem; San Diego, CA) and GluA2 (sGluA2, 1:100, Chemicon; USA) for 15 min at 37ºC. Following the 15 min incubation, the cells were washed 3X in phosphate buffered saline with $Mg2^+$ and $Ca2^+$ (PBS-MC; 137 mM NaCl, 2.7 mM KCl, 10 mM Na_2HPO_4, 2 mM KH_2PO_4, 1 mM $MgCl_2$ and 0.1mM $CaCl_2$) and immediately fixed in PBS-MC containing 2%

paraformaldehyde and 2% sucrose for 20 min at room temperature (RT). The cells were blocked (2% BSA/PBS-MC for 30 min at RT) and incubated with Alexa555-conjugated secondary antibodies (goat anti-rabbit and goat anti-mouse for GluA1 and GluA2, respectively 1:500; Molecular Probes; Eugene, OR) for 60 min at RT in blocking solution. Cells were then permeabalized with PBS-MC containing 0.1% Triton X-100 for 5 min at RT, and stained for PSD95 as above [using a mouse monoclonal anti-PSD95 antibody (1:200; Fisher) for GluA1 co-labeling and a rabbit polyclonal anti-PSD95 antibody for GluA2 co-labeling (1 μg/ml; AbCam; Cambridge, MA)] using Alexa488-conjugated secondary antibodies (goat anti-mouse and goat anti-rabbit for GluA1 and GluA2 co-labeling, respectively, 1:500; Molecular Probes; Eugene, OR).

Neurons stained for sGluA1/PSD95 or sGluA2/PSD95 were imaged on an Olympus FV1000 inverted confocal microscope using a Plan Apochromat 60x/1.4 NA objective and 2X digital zoom. Areas of interest were selected for imaging guided by epifluorescent visualization of the PSD95 channel, to ensure blind sampling of surface GluA1 and GluA2 expression. Acquisition settings were identical for all treatment groups and were determined to ensure: 1) optimization of the dynamic range of signal intensities to limit saturation, 2) the absence of detectable fluorescence in a no GluA1/2 antibody condition included in all experimental runs, and 3) no fluorescence bleed-through between channels. Image analysis was performed with NIH Image J on maximal intensity z-projections. Dendrites were linearized using the straighten plugin for Image J, and extracted from the full-frame image. For analysis, a “synaptic” GluA1/2 particle was defined as a particle that occupied greater than 10% of the area defined by a PSD95

particle, and the integrated fluorescence intensity of synaptic GluA1/2 particles was quantified using custom written analysis routines for Image J.

paGFPu Imaging and Data Analysis

GFPu (in pEGFP-C1 plasmid backbone; Clontech; Mountain View, CA), a fusion of the CL1 degron (degradation signal) on the C terminus of GFP, was kindly provided by Dr. Ron Kopito (Stanford University, Palo Alto, CA). GFPu is ubiquitinated and specifically degraded by the UPS (Bence et al., 2001, 2005). The AgeI–BsrGI fragment from photoactivatable (pa) GFP (a kind gift provided by Jennifer Lippincott-Schwartz, National Institutes of Health, Bethesda, MD) was subcloned into the GFPu plasmid. paGFPu or paGFP was then subcloned into pSinRep5 (Invitrogen; Carlsbad, CA). For production of recombinant Sindbis virions, RNA was transcribed using the SP6 mMessage mMachine Kit (Ambion; Austin, TX) and electroporated into BHK cells using a BTX ECM 600 at 220 V, 129 Ω, and 1050 µF. Virion was collected after 24h and stored at –80°C until use.

Neurons were infected for 14-16 hours with Sindbis viral vectors prior to imaging. Pyramidal-like neurons infected with paGFPu or paGFP (identified by co-expression of mCherry) were then photoactivated for 10s with a 100 W Hg^{2+} lamp and a D405/40x with 440 DCLP dichroic filter set (Chroma). Confocal images were acquired using a Leica DMI6000 inverted microscope outfitted with a Yokogawa spinning disk confocal head, an Orca ER high-resolution black-and-white cooled CCD camera (6.45 µm/pixel at 1x) (Hamamatsu), a Plan Apochromat 63x/1.4 NA objective, and a Melles

Griot argon/krypton 100 mW air-cooled laser for 488/568/647 nm excitations. Exposure times were held constant during acquisition of all images for each experiment. For image analysis, maximum intensity z-projections were used. Dendrites from individual neurons were then straightened and total integrated density (normalized to dendritic length) of reporter fluorescence was quantified.

Data Analysis

Statistical differences between experimental conditions were determined by either unpaired t-tests (2 groups) or by analysis of variance (ANOVA) and post-hoc Fisher's LSD test (> 2 experimental conditions). Differences were deemed significant if $\alpha < 0.05$ (two-tailed).

Results

Chronic, but not acute, proteasome inhibition scales excitatory synaptic strength

Homeostatic changes in synapse function can occur slowly over a period of 24-72 hrs (Rao and Craig, 1997; Turrigiano et al., 1998, O'Brien et al., 1998; Murthy et al., 2001), or more rapidly within minutes to hours (Sutton et al., 2006; Frank et al., 2006; Aoto et al., 2008). While mechanisms underlying rapid homeostatic changes are partially understood, very little is known regarding how activity drives slower homeostatic adaptations at synapses. Chronic changes in activity (> 24 hr) induce bi-directional

changes in synaptic protein composition mediated by the ubiquitin proteasome system (UPS) (Ehlers, 2003), but a role for the UPS in homeostatic changes in synaptic function has not been assessed. To examine if chronic changes in proteasome function mimic aspects of homeostatic plasticity, we treated cultured hippocampal neurons with a selective proteasome inhibitor lactacystin (10μM), and recorded miniature excitatory postsynaptic currents (mEPSCs) 24 hours later (Fig. 2.1A-C). We found that this chronic inhibition of the UPS induced a robust increase in mEPSC amplitude relative to untreated control cells (Fig. 1A-B; $t_{18} = 8.00$, $p < 0.05$). In contrast, there was no difference in mEPSC frequency between cells treated with lactacystin and untreated control cells (Fig. 1C; $t_{18} = 0.37$, NS) suggesting a selective effect of chronic UPS inhibition on scaling of postsynaptic function in hippocampal neurons. To determine when functional synaptic changes first appear in the course of UPS inhibition, we treated neurons with lactacystin (10μM) and recorded mEPSCs 3, 5, 12, and 24 hr later. Similar to the time-course of slow homeostatic plasticity induced by changes in network activity in cortical (see Turrigiano et al., 1998) and hippocampal neurons (see Sutton et al., 2006), UPS inhibition produced a slow, time-dependent increase in mEPSC amplitude ($F_{4,44} = 3.59$, $p < 0.05$; Figure 2.1D-F) with no effect on mEPSC frequency (data not shown; $F_{4,44} = 0.76$, NS). The increase in synaptic function induced by chronic UPS inhibition was associated with a near uniform rightward shift of mEPSC amplitudes (Figure 2.1F), a profile highly similar to the multiplicative scaling of synaptic function observed following chronic TTX treatment (Turrigiano et al., 1998). These results suggest that UPS inhibition mimics slow homeostatic compensation induced by AP blockade.

To confirm that these changes in mEPSCs were due specifically to disruption of proteasome function, we compared the acute (4 hr) and chronic (18 hr) effects of another UPS inhibitor, MG132 (10μM) with acute and chronic (4 and 24 hr, respectively) treatment with leupeptin (10 μM), a potent inhibitor of cellular proteases found in the lysosome. As we observed with lactacystin, UPS inhibition with MG132 produced no change in mEPSC amplitude at the early (4 hr) time-point but induced a robust increase in mEPSC amplitude after chronic (18 hr) treatment relative to untreated control cells ($F_{2,21} = 4.80$, $p < 0.05$; 18 hr vs control, $p < 0.05$ Fisher's LSD; Figure 2.1G-H). Additionally, like lactacystin treatment, MG132 treatment did not significantly alter mEPSC frequency between groups ($F_{2,21} = 0.24$, NS; Figure 2.1I). By contrast, neither brief (4 hr) nor prolonged (24 hr) lysosomal inhibition with leupeptin altered mEPSC amplitude ($F_{2,24} = 0.19$, NS; Figure 2.1H) or frequency ($F_{2,24} = 0.77$, NS; Figure 2.1I). These results thus demonstrate that proteasome inhibition, but not inhibition of lysosomal-mediated degradation, mimics slow homeostatic changes in synapse function induced by suppression of network activity.

AP blockade and UPS inhibition drive similar changes in synaptic AMPAR expression

Rapid forms of homeostatic plasticity are associated with an increase in GluA1 homomeric receptor expression at synapses (Sutton et al., 2006; Aoto et al., 2008; see also, Ju et al., 2004; Thiagarajan et al., 2005), which is a mechanism that is likely distinct from that underlying slow homeostatic adaptations (e.g., see Sutton et al., 2006; Aoto et

al., 2008). For example, in cortical neuron cultures, chronic AP blockade with TTX induces a coordinate increase in both GluA1 and GluA2 AMPAR subunit expression at synapses (Wierenga et al., 2005; see also, Ibata et al., 2008). Likewise, in hippocampal neurons, scaled mEPSCs following chronic TTX treatment are insensitive to polyamine toxins (Sutton et al., 2006), suggesting an increase in GluA2-containing AMPARs in these neurons during slow homeostatic compensation. To examine changes in surface expression of AMPAR subunits at synapses following changes in activity or UPS inhibition, we live-labeled neurons with antibodies recognizing extracellular epitopes of the GluA1 or GluA2 subunits, then fixed and stained for PSD95 to identify excitatory synapses. The integrated fluorescence intensity of GluA1/A2 particles that colocalized with PSD95 was used to measure relative changes in surface expression of these subunits at synaptic sites. We found that 24 hr TTX treatment induced a significant increase in surface expression of both GluA1 ($F_{3,352} = 9.45$, $p < 0.05$; TTX vs control, $p < 0.05$ Fisher's LSD) and GluA2 ($F_{3,262} = 7.33$, $p < 0.05$; TTX vs control, $p < 0.05$ Fisher's LSD) at PSD95-labeled excitatory synapses (Figure 2.2; see also, Figure 2.3). These changes in AMPAR subunits were largely accounted for by an increase in GluA1/2 content at synapses (as reflected in integrated fluorescence intensity per particle) and to a lesser extent, an increase in density of GluA1 ($F_{3,352} = 3.03$, $p < 0.05$; TTX vs control, $p < 0.05$ Fisher's LSD) and GluA2 particles ($F_{3,262} = 3.26$, $p < 0.05$; TTX vs control, $p < 0.05$ Fisher's LSD). It is likely that this latter measure reflects enhanced detection of particles owing to their increased intensity rather than insertion of receptors at previously AMPAR-silent synapses, since chronic TTX treatment selectively enhances mEPSC amplitude without changes in mEPSC frequency (Turrigiano et al., 1998; Sutton et al.,

2006; see also, Figure 2.7B-C). In contrast to the changes in GluA1/2 expression, the density ($F_{3,352} = 0.36$, NS) and intensity ($F_{3,352} = 0.29$, NS) of PSD95 particles from the same dendrites was unchanged by chronic TTX treatment (Figure 2.2). These observations thus suggest that slow homeostatic increases in synaptic strength are associated with enhanced expression of GluA2-containing AMPARS at existing synapses.

We next examined expression of GluA1 and GluA2 after chronic UPS inhibition to determine if a similar or distinct profile in synaptic AMPAR expression was apparent. Similar to chronic TTX treatment, we found that UPS inhibition with both lactacystin and MG132 induced a coordinate increase in surface GluA1 and GluA2 expression at synapses (both $p < 0.05$ vs control, Fisher's LSD). Also similar to chronic AP blockade, these changes in synaptic AMPAR content following UPS inhibition were not associated with changes in the density or intensity of PSD95 particles. Therefore, in addition to parallel effects on mEPSC amplitude, UPS inhibition and AP blockade induce similar changes in synaptic AMPAR expression at synapses.

Chronic changes in neuronal activity drive bi-directional changes in proteasome function

The observed proteasome-dependent changes in neuronal strength occur on the same slow timescale as those induced by chronic AP blockade, suggesting that slow activity-dependent homeostatic compensation may arise via sustained bi-directional changes in proteasome function. Indeed, a recent study found that AP blockade (with

TTX) induced an acute decrease in neuronal UPS activity, whereas network hyperactivity (via disinhibition with bicuculline) induced acute enhancement of proteasome function (Djakovic et al., 2009). To test if these bi-directional changes in UPS activity are sustained during chronic changes in activity, we imaged a photoactivatable GFP fluorescent UPS reporter (paGFPu), in which paGFP (Patterson and Lippincott-Schwartz, 2002) is fused with a 16 amino acid degron (CL1) that is constitutively poly-ubiquitinated and degraded by the proteasome; it is well established that this reporter is selectively degraded by the proteasome (Bence et al., 2001; Bence et al., 2005; Djakovic et al., 2009). As a control for changes in paGFPu fluorescence independent of UPS activity, we also examined expression of paGFP lacking the proteasome-sensitive degron. Both the UPS reporter (paGFPu) and the UPS-insensitive control reporter (paGFP) were co-expressed with mCherry via an internal ribosomal entry site (IRES) and expressed in neurons using Sindbis viral vectors. We found that chronic activity suppression (2 μM TTX, 10 hrs) significantly diminished paGFPu degradation by the proteasome compared to untreated control neurons, whereas chronic network hyperactivation (40 μM bicuculline) significantly enhanced paGFPu degradation (Fig 2.4A-B; $F_{2,258} = 56.25$, $p < 0.05$; TTX and Bic vs Control; each $p < 0.05$ Fisher's LSD). By contrast, mCherry expression was similar among groups (data not shown), as was expression of paGFP lacking the UPS-sensitive degron (Figure 2.4C-D). These data demonstrate that sustained bi-directional changes in UPS activity accompany chronic changes in activity that induce opposing slow homeostatic synaptic adaptations.

Postsynaptic UPS activity drives cell autonomous scaling of mEPSC amplitude

The results described above indicate that chronic UPS inhibition is sufficient to scale mEPSC amplitude and that postsynaptic UPS activity is regulated by changes in activity that normally drive slow homeostatic scaling of synaptic strength. We next examined whether manipulations of UPS function restricted to the postsynaptic cell are sufficient to drive slow homeostatic changes in synaptic strength. To examine this question, we used Sindbis viral vectors to express a dominant-negative ubiquitin chain elongation mutant (UbK48R) in which lysine 48 (K48) is mutated to an arganine. Ub48R retards the growth of polyubiquitination chains at lysine 48 necessary for proteasome-dependent degradation, without depleting the free ubiqutin pool. As controls, we examined the effects of expressing wild-type ubiquitin (wtUb) or GFP alone in sister cultures. Importantly, the low infection efficiency of Sindbis vectors allowed us to manipulate UPS function in a small (< 1%) proportion of neurons in the network (Figure 4A), allowing us to test the cell autonomous role of the UPS in a hippocampal network that is otherwise unperturbed. Consistent with the idea that the UPS functions postsynaptically to mediate slow homeostatic plasticity in a cell autonomous manner, we found that 24 hr expression of K48R-IRES-GFP in pyramidal-like hippocampal neurons selectively enhanced mEPSC amplitude (Figure 2.5B-C; $F_{4,51} = 2.324$, $p < 0.05$; $p < 0.05$ vs control, Fisher's LSD) without altering mEPSC frequency (Figure 2.5E; $F_{4,51} = 0.75$, NS), a profile similar to both chronic AP blockade and pharmacological UPS inhibition. Moreover, the cumulative probability distribution of mEPSC amplitudes in UbK48R-expressing neurons exhibited a near uniform shift to the right, similar to the characteristic multiplicative scaling induced by AP blockade (Turrigiano et al., 1998). In contrast to the effects of the chain elongation ubiquitin mutant, expression of wtUb-IRES-GFP or

GFP alone had no effect on mEPSCs (vs. control, Fisher's LSD, NS). Moreover, mEPSCs recorded from un-infected cells in the same dish as those expressing Ub48R were also unchanged, indicating that postsynaptic UbK48R expression enhances mEPSC amplitude in a cell autonomous fashion.

UPS inhibition occludes slow homeostatic plasticity

If bi-directional slow homeostatic changes in synaptic strength require changes in synaptic composition mediated by the proteasome, then UPS inhibition should occlude homeostatic changes in synaptic strength induced both by chronic AP blockade and by chronic hyperactivation. To test this idea, we treated neurons with lactacystin (10 μM) either alone, or 30 min prior to chronic treatment with TTX (2 μM), and assessed excitatory synaptic function 4 or 24 hr later. Consistent with previous results (Turrigiano et al., 1998; Sutton et al., 2006; Figure 2.1), we found that neither AP blockade nor UPS inhibition altered mEPSC amplitude or frequency at the early, 4 hr, time-point (Figure 2.6A-C; NS, Fisher's LSD). Moreover, coincident treatment with TTX and lactacystin also failed to alter mEPSCs at this early time-point (NS, Fisher's LSD), indicating that AP blockade and UPS inhibition does not accelerate the slow enhancement of synaptic strength that accompanies either treatment alone. By contrast, 24 hr AP blockade induced a robust scaling of mEPSC amplitude ($F_{6,49} = 6.85$, $p < 0.05$; 24 hr TTX vs control, $p < 0.05$ Fisher's LSD) without changes in mEPSC frequency ($F_{6,49} = 0.85$, NS). As in earlier experiments, 24 hr lactacystin treatment induced a similar scaling of mEPSC amplitude ($p < 0.05$ vs control, Fisher's LSD), and this effect was not additive with AP

blockade when TTX and lactacystin were co-applied (Figure 2.6B; 24 hr lactacystin vs 24 hr TTX+lactacystin, NS, Fisher's LSD). These results indicate that chronic UPS inhibition induces slow enhancement of synaptic strength that occludes slow homeostatic compensation induced by AP blockade.

We next examined how UPS inhibition interacts with chronic network hyperactivation induced by bicuculline. Acutely (4 hr treatment), no changes in mEPSC frequency or amplitude accompanied either hyperactivity (bicuculline) or UPS inhibition alone; combined hyperactivity/UPS inhibition also failed to alter mEPSCs at the early 4 hr time-point (Figure 2.6E). Chronic (24 hr) hyperactivation, however, lead to a robust decrease in mEPSC amplitude (Figure 2.6D-E; $F_{6,55} = 6.02$, $p < 0.05$; $p < 0.05$ vs control, Fisher's LSD) without altering mEPSC frequency (Figure 2.6F; $F_{6,55} = 0.64$, NS), similar to previous studies (Turrigiano et al., 1998; Leslie et al., 2001; Seeburg et al., 2008). Remarkably, despite the robust weakening of synaptic strength induced by chronic hyperactivity alone, mEPSCs scaled upward in strength with coincident lactacystin treatment ($p < 0.05$ vs control, Fisher's LSD) to a degree similar to UPS inhibition alone (24 hr lactacystin vs 24 hr bic+lactacystin, NS, Fisher's LSD), again revealing a non-additive effect of UPS inhibition and chronic changes in network activity. These results indicate that UPS inhibition occludes both homeostatic strengthening and weakening of synaptic strength, and thus suggest a critical role for the proteasome in driving bi-directional synaptic adaptations underlying homeostatic scaling.

Since chronic AP blockade and UPS inhibition induce similar changes in AMPAR subunit expression at synapses, we next examined if these synaptic modifications themselves are bi-directionally regulated by chronic activity and whether

changes in AMPARs induced by UPS inhibition occludes changes induced by alterations of network activity. We treated hippocampal neurons with TTX or bicuculline for 24 hr alone or in combination with either lactacystin (10 μM) or MG132 (10 μM), prior to live surface GluA1 or GluA2 labeling and subsequent immunocytochemistry against PSD95 to label excitatory synapses. As before, we quantified synaptic GluA1/2 expression by analyzing the intensity of GluA1/2 particles that colocalized with PSD95.

We found that, in the absence of coincident UPS inhibition, TTX and bicuculline induced symmetrically opposite changes in synaptic expression of both GluA1 ($F_{8,466}$ = 11.13, $p < 0.05$) and GluA2 ($F_{8,399}$ = 10.64, $p < 0.05$), with AP blockade significantly enhancing GluA1/GluA2 expression and hyperactivity significantly diminishing GluA1/GluA2 expression (Figure 2.7A-C, black bars; $p < 0.05$ vs control, Fisher's LSD). These bi-directional changes in AMPAR subunit expression at synapses parallel slow homeostatic strengthening and weakening, respectively, with chronic activity suppression and elevation. As before (Figure 2.2), chronic UPS inhibition with either lactacystin or MG132 induced a significant increase in expression of both GluA1 and GluA2 at synapses under control levels of activity (both $p < 0.05$ vs control, Fisher's LSD). As we observed for synaptic currents, the changes in synaptic AMPAR expression induced by UPS inhibition occluded the bi-directional changes in GluA1 and GluA2 expression induced by either chronic activity suppression (24 hr TTX; Fisher's LSD vs TTX alone, NS) or chronic activity elevation (24 hr bic; Lac+bic and MG132+bic, each $p < 0.05$ vs control, Fisher's LSD; Figure 2.7A-C; see also, Figure 2.8). These results thus suggest that UPS inhibition drives coordinate increases in GluA1 and GluA2 expression at

synapses in a manner that both mimics and occludes slow homeostatic compensation induced by chronic changes in network activity.

Postsynaptic UPS activity determines the direction of synaptic compensation

We next examined whether manipulation of postsynaptic UPS function, specifically, is sufficient to drive slow homeostatic changes in synaptic strength that occlude that induced by chronic changes in network activity. To address this issue, we used Sindbis vectors to express UbK48R in a small (< 1%) percentage of neurons present in individual cultures, and examined the effects of network-wide activity suppression or elevation in both these neurons and un-infected neurons in the same culture. Neurons expressing Ub48R (24 hr post-infection) exhibited a significant increase in mEPSC amplitude relative to both non-expressing neurons in the same culture as well as GFP-expressing neurons in sister cultures (Figure 2.9A-B; $F_{4,43} = 4.76$, $p < 0.05$; $p < 0.05$ vs control, Fisher's LSD); by contrast, no significant changes in mEPSC frequency were observed (Figure 7D; $F_{4,43} = 0.73$, NS). Moreover, the increase in mEPSC amplitude induced by UbK48R expression was not additive with suppressing network activity, as 24 hr TTX treatment effectively scaled mEPSCs in uninfected neurons (TTX vs control, $p < 0.05$, Fisher's LSD) but not in UbK48R-expressing neurons (Figure 2.9A-B; K48R vs K48R+TTX, NS, Fisher's LSD). In both UbK8R-expressing and non-expressing neurons following 24 hr TTX treatment, a similar near uniform rightward shift of mEPSC amplitudes was observed relative to untreated controls (Figure 2.9C), again

demonstrating that postsynaptic UPS inhibition occludes slow homeostatic increases in synaptic strength induced by chronic suppression of network activity.

We next examined whether postsynaptic UPS inhibition similarly occluded the changes in synaptic strength induced by chronic network hyperactivation. In uninfected neurons, 24 hr bicuculline treatment induced a decrease in mEPSC amplitude relative to untreated control neurons (Figure 2.9E-G; $F_{4,39} = 4.38$ $p < 0.05$; $p < 0.05$ vs control, Fisher's LSD), but mEPSC frequency was not significantly altered (Figure 2.9H; $F_{4,39} = 0.72$, NS). In neurons expressing UbK8R, bicuculline treatment was completely ineffective in scaling mEPSCs, as these neurons still exhibited a significant increase in mEPSC amplitude relative to controls ($p < 0.05$, Fisher's LSD) that was not significantly different from UbK8R-expressing neurons in the absence of bicuculline treatment (Figure 2.9E-H). Taken together, our results indicate that postsynaptic blockade of UPS-dependent degradation drives slow homeostatic increases in synaptic strength in these neurons irrespective of changes in network activity.

Phosphorylation of Rpt6 at S120 mimics bidirectional homeostatic plasticity.

Recently, it has been shown that phosphorylation of Rpt6 at serine 120 (S120) is required for proteasome function (G. Patrick and S. Djakovic, personal communication). We therefore wanted to test if direct phosphorylation of Rpt6 at S120 is sufficient to induce homeostatic plasticity. We infected neurons with a sindbis viral vector containing either WT Rpt6, a phospho-mutant form of Rpt6 in which S120 was mutated to an alanine (S120A) or a phospho-mimetic form of Rpt6 where S120 was mutated to an arganine (S120D). Each viral vector was also co-expressing GFP through an IRES site to

allow for visualization of infected neurons. 24 hr post infection mEPSC amplitude and frequency were recorded from GFP expressing neurons (Figure 2.10). Neurons expressing WT Rpt6 exhibit similar mEPSC amplitude and frequency compared to GFP control neurons (Fisher's LSD; NS). In contrast, S120A expressing neurons exhibited an increase in mEPSC amplitude relative to WT Rpt6 expressing neurons (* $p < 0.05$; Fisher's LSD; Figure 2.10A-B) while having no effect on frequency (Figure 2.10C). Constitutive phosphorylation of Rpt6 (S120D) homeostatically decreased mEPSC amplitude relative to WT Rpt6 expressing neurons (* $p < 0.05$; Fisher's LSD; Figure 2.10A-B) while having no effect on mEPSC frequency (Figure 2.10C). These data suggest that phosphorylation of Rpt6 at S120 is sufficient to regulate bidirectional homeostatic plasticity and suggest a putative link between a postsynaptic activity sensor and regulation of homeostatic function.

Discussion

Our results reveal a postsynaptic role for the ubiquitin proteasome system (UPS) in slow homeostatic adaptations driven by chronic changes in network activity of hippocampal neurons. Specifically, sustained inhibition of the UPS produces a slow increase in mEPSC amplitude that parallels the slow homeostatic plasticity induced by suppression of network activity with TTX (Turrigiano et al., 1998; Sutton et al., 2006). The increase in synaptic strength induced by UPS inhibition is associated with a coordinate increase in surface GluA1 and GluA2 expression at synapses, similar to that

observed following chronic TTX treatment. These functional changes are consistent with the activity-dependent regulation of proteasome function observed during chronic activity changes – activity suppression induces a sustained decrease in UPS-dependent degradation, whereas network hyperactivation significantly enhances proteasome function (Figure 2.4, see also, Djakovic et al., 2009), suggesting that activity suppression may enhance synaptic function though its effect on the UPS. Additional experiments provide strong evidence for this possibility, as UPS inhibition enhances postsynaptic function and synaptic AMPAR expression in a manner that occludes increases induced by chronic activity suppression. More strikingly, UPS inhibition drives homeostatic increases in postsynaptic function even in the face of network hyperactivation, which normally drives homeostatic weakening of synaptic strength. Cell-restricted expression of the ubiquitin chain elongation mutant UbK48R further revealed that postsynaptic UPS inhibition is sufficient to drive slow homeostatic scaling of synaptic strength, and similarly occludes the effects of chronic suppression and hyperactivation of network activity. Taken together, these results reveal a critical role for postsynaptic proteasome-mediated degradation in slow homeostatic plasticity.

Distinct compartment-specific roles for the proteasome in homeostatic synaptic plasticity

Our results, taken together with earlier observations, suggest that the UPS may play distinct roles in the presynaptic and postsynaptic compartments of the synapse during homeostatic plasticity. More generally, a role for the UPS in synaptic plasticity

was first suggested by work in *Aplysia*, where UPS-mediated degradation of PKA regulatory subunits leads to long-lasting autonomous PKA activity necessary for long-lasting presynaptic facilitation of neurotransmission (Hegde et al., 1997; Chain et al., 1999). A more recent study (Zhao et al., 2003) demonstrated that proteasome inhibition in either presynaptic or postsynaptic neurons is sufficient to increase synaptic efficacy at *Aplysia* sensorimotor synapses. Similarly, in mammalian neurons, the UPS is necessary for forms of LTP (Fonseca et al., 2006; Karpova et al., 2006; Dong et al., 2008), and LTD (Colledge et al., 2003; Patrick et al., 2003; Hou et al., 2006) that are known to be induced and expressed postsynaptically. During homeostatic synaptic plasticity, there may be distinct pre- and postsynaptic roles for the UPS, as well. For example, Ehlers (2003) demonstrated large scale and bidirectional changes in protein composition of postsynaptic densities (PSDs) in response to chronic suppression (with TTX) or elevation (with bicuculline) of neuronal activity. Importantly, these changes in PSD composition emerged gradually over the course of chronic treatment, and were shown to arise via changes in UPS function. On the other hand, UPS activity is necessary for homeostatic silencing of presynaptic terminals in response to excessive depolarization (Jiang et al., 2010) and may play other homeostatic roles presynaptically (Willeumier et al., 2006; Rinetti and Schweizer, 2010). These latter results raise questions about whether the changes in PSD composition observed by Ehlers (2003) reflect a requirement for the UPS postsynaptically, or whether UPS inhibition alters PSD composition indirectly via presynaptic effects. Our results demonstrate that the UPS drives postsynaptic compensation in a cell autonomous fashion, thus supporting the notion that the changes in PSD composition revealed by Ehlers (2003) likely reflect cell intrinsic actions of the

proteasome operating on the postsynaptic compartment. Interestingly, while acute UPS inhibition induces a transient increase in presynaptic function in hippocampal neurons (Rinetti and Schweizer, 2010), we did not observe persistent changes in presynaptic function following chronic UPS inhibition, suggesting that a distinct presynaptic role for the UPS may exist for more rapid forms of homeostatic plasticity.

Multiple homeostatic mechanisms operate in hippocampal neurons

It is becoming increasingly apparent that neurons express multiple homeostatic mechanisms that operate over distinct temporal/spatial domains and are responsive to unique facets of neural activity. For example, the synaptic recruitment of GluA2-lacking AMPARs during rapid homeostatic plasticity requires local dendritic synthesis, likely of GluA1 itself (Sutton et al., 2006; Poon and Chen, 2008) and is independent of gene transcription (Aoto et al., 2008), whereas compensation induced by AP blockade has been shown to require CREB-mediated transcriptional activation (Ibata et al., 2008). These mechanistic differences may also map onto whether the resulting compensation is implemented locally (Sutton et al., 2006; Branco et al., 2008) or globally (Turrigiano et al., 1998; Ibata et al., 2008). Although changes in synapse composition are likely the ultimate locus of expression of slow homeostatic plasticity (Ehlers, 2003), it is presently unclear whether the UPS functions on a global (cell-wide) or more local level to drive these synaptic adaptations. On the one hand, synaptic scaling can be induced by focal application of TTX to the cell body (Ibata et al., 2008), suggesting that global aspects of neuronal activity such as firing rate are sufficient to induce compensatory modifications

at synapses. The fact that AP suppression inhibits UPS function, and UPS inhibition alone drives slow homeostatic adaptations that occlude further plasticity imposed by changes in network activity, suggests that the UPS may be responsive to global features of activity and promote synaptic changes in a cell-wide fashion. On the other hand, recent studies have demonstrated activity-dependent synaptic trafficking of proteasomes in dendrites (Bingol and Schuman, 2006; Bingol et al., 2010) raising the possibility that the UPS could also act locally to alter the composition of a more restricted set of synapses.

While a number of studies have all documented increases in AMPAR content at synapses accompanying homeostatic increases in synaptic function, the population of AMPARs that is regulated appears to differ depending on the mode of activity blockade. For example, Turrigiano et al. (1998) originally reported that mEPSC kinetics were unchanged in visual cortical cultures following chronic TTX treatment, suggesting that the increase in postsynaptic function was mediated by an increase in the number, but not type, of AMPARs. Similarly, a coordinate increase in synaptic expression of GluA1 and GluA2 has been observed in cortical neurons treated chronically with TTX (Wierenga et al.,2005; see also, Ibata et al., 2008) as well as in spines of hippocampal neurons opposed to presynaptic terminals rendered silent by Kir2.1 expression (Hou et al., 2008). On the other hand, multiple laboratories have documented a recruitment of GluA2-lacking (and presumptive GluA1 homomeric) AMPARs to synapses (Ju et al., 2004; Thiagarajan et al., 2005; Sutton et al., 2006; Aoto et al., 2008), although it is notable that each of these studies employed receptor blockade either alone or in conjunction with AP blockade, to suppress activity. Our results suggest that the recruitment of GluA2-lacking AMPARs

may be a mechanism unique to rapid forms of homeostatic plasticity, since we find that slow synaptic compensation in hippocampal neurons driven by AP blockade alone drives coordinate increases in GluA1 and GluA2 expression at synapses, similar to that observed in other studies. Conversely, we find that chronic network hyperactivation (with bicuculline treatment) induces a coordinate loss of GluA1 and GluA2 from synapses. These findings also explain why scaled mEPSCs in hippocampal neurons following blockade of miniature neurotransmission are effectively reversed by agents that block GluA2-lacking AMPARs, but scaled mEPSCs following chronic TTX treatment are insensitive to these agents (Sutton et al., 2006). Similarly, recent evidence indicates that blocking miniature transmission, but not AP blockade alone, drives retinoic acid synthesis in neurons, an essential intermediate for de novo GluA1 synthesis necessary for rapid homeostatic plasticity (Aoto et al., 2008; Poon and Chen, 2008). It is unlikely that the UPS plays a role in the relatively fast recruitment of GluA2-lacking AMPARs (within 1-3 hrs, Sutton et al., 2006) during rapid homeostatic plasticity, since the changes in postsynaptic function accompanying UPS inhibition are intrinsically slow to develop, similar to synaptic scaling induced by AP blockade (Turrigiano et al., 1998). Taken together, these observations suggest that changes in AMPAR subunit composition accompany some forms of compensatory plasticity, but not others, indicating that neurons express multiple forms of homeostatic plasticity that are mechanistically distinct.

Activity-dependent regulation of proteasome function links changes in network activity with alterations of synapse function

A major unresolved issue in activity-dependent homeostatic control is the nature of the activity sensor(s) that read out changes in activity above or below the normal range. Given the extended time-course over which synaptic modifications arise during AP blockade, it has been especially difficult to define an activity sensor for slow homeostatic plasticity. Although definitive evidence that any one protein serves as a bona fide homeostatic activity sensor is still lacking, several activity-responsive enzymes have emerged as attractive candidates, including CAMKII (Thiagarajan et al., 2002), eEF2 kinase (Sutton et al., 2007), and Ca2+-sensitive adenylate cyclases (Gong et al., 2007). Irrespective of the true nature of the slow homeostatic sensor, our results suggest that the UPS, likely through Rpt6 phosphorylation at S120 serves as an important integration point through which such a sensor can engage mechanisms that drive compensatory synaptic modifications. For example, we show that network activity bi-directionally regulates proteasome function (see also, Djakovic et al., 2009) and these effects on proteasome function are sustained during chronic activity changes. Moreover, UPS inhibition dictates changes in synaptic function irrespective of network activity, suggesting that the UPS couples sustained changes in network activity with downstream compensatory synaptic modifications.

While our results indicate that network activity is integrated postsynaptically by the proteasome, the manner by which activity interacts with the proteasome on a molecular level is still unknown. One interesting possibility is that activity engages the UPS via posttranslational modification of the proteasome itself, perhaps through direct phosphorylation by activity-dependent protein kinases. For example, direct activity-dependent phosphorylation of the proteasome has been shown to gate proteasome

function (Zhang et al., 2007; Djakovic et al., 2009). Specifically, CAMKII is capable of directly phosphorylating Rpt6 (Djakovic et al., 2009) an AAA-ATPase subunit located in the 19S regulatory cap of the proteasome and whose phosphorylation is required for proteasome function (Zhang et al., 2007). In so far as CAMKII expression (Thiagarajan et al., 2002) and/or function serves an activity-sensing role, our data suggest that interactions with the proteasome provide an interface for linking the detection of activity levels outside the normal range with the appropriate compensatory response. Likewise, it has been shown that PKA can directly phosphorylate Rpt6 as well (Zhang et al., 2007) which provides a similar platform for linking the actions of a putative activity sensor with changes in proteasome function.

Our results demonstrate that the UPS plays a critical role in slow homeostatic adaptations at synapses in hippocampal neurons. It seems likely that this role reflects a combination of direct changes in proteasome function in response to long term changes in activity as well the targeted degradation of specific synaptic proteins ultimately responsible for regulating AMPAR expression and synaptic function. In recent years, many synaptic proteins have been shown to be regulated by the proteasome (e.g., (Yi and Ehlers, 2007; Ding and Shen, 2008; Segref and Hoppe, 2009), suggesting numerous candidate UPS targets that could contribute to changes in synaptic strength, including Arc/Arg3.1 (Shepherd et al., 2006; Joch et al., 2007; Greer et al., 2010), PICK1 (Joch et al., 2007), ROMK1 (Lin et al., 2005), Shank (Gong et al., 2009), GRIP (Guo and Wang, 2007), and GKAP (Hung et al., 2010). Determining the effectors that operate downstream of proteasome function, and how they act coordinately to drive appropriate homeostatic synaptic adaptations, is an important challenge for future studies.

Figure 2.1 Scaling of mEPSC amplitude accompanies chronic UPS inhibition. Representative recordings (A) and mean (+SEM) mEPSC amplitude (B) and frequency (C) from control hippocampal neurons (n = 11) or neurons treated with lactacystin (10 μM) for 24 hrs (n = 8). Chronic lactacystin induced a significant (*$p < 0.05$) increase in mEPSC amplitude, but no change in mEPSC frequency. Scale Bar = 10 pA, 250 ms in (A). (D-F) Time-course of mEPSC scaling during chronic lactacystin treatment. Representative recordings (D) and mean (+SEM) mEPSC amplitude (E) from control neurons (n = 10) or neurons treated with lactacystin (10 μM) for 3 (n = 9), 5 (n = 8), 12 (n = 9), or 24 hrs (n = 8). Lactacystin induced a significant (* $p < 0.05$) time-dependent increase in mEPSC amplitude that emerges slowly (12 hrs). Scale Bar = 10 pA, 250 ms in (D). (F) Cumulative probability distribution of mEPSC amplitudes for control, 3 hr and 24 hr lactacystin-treated neurons. Whereas the distribution of mEPSC amplitudes after 3 hr lactacystin is similar to controls, a near uniform rightward shift of mEPSC amplitudes is observed after 24 hr proteasome inhibition. (G-I) Representative traces (G) and mean (+SEM) mEPSC amplitude (H) and frequency (I) from control neurons (n = 10) or neurons treated with a different proteasome inhibitor MG132 (10 μM) or the lysosomal inhibitor leupeptin (10 μM). Similar to the effects of lactacystin, chronic (18 hr; n = 8 neurons), but not acute (4 hr; n = 9 neurons) treatment with MG132 produced a significant (*$p < 0.05$, relative to control) increase in mEPSC amplitude without altering mEPSC frequency. Neither chronic (24 hr; n = 9 neurons) nor acute (4 hr, n = 10 neurons) treatment with leupeptin altered mEPSCs.

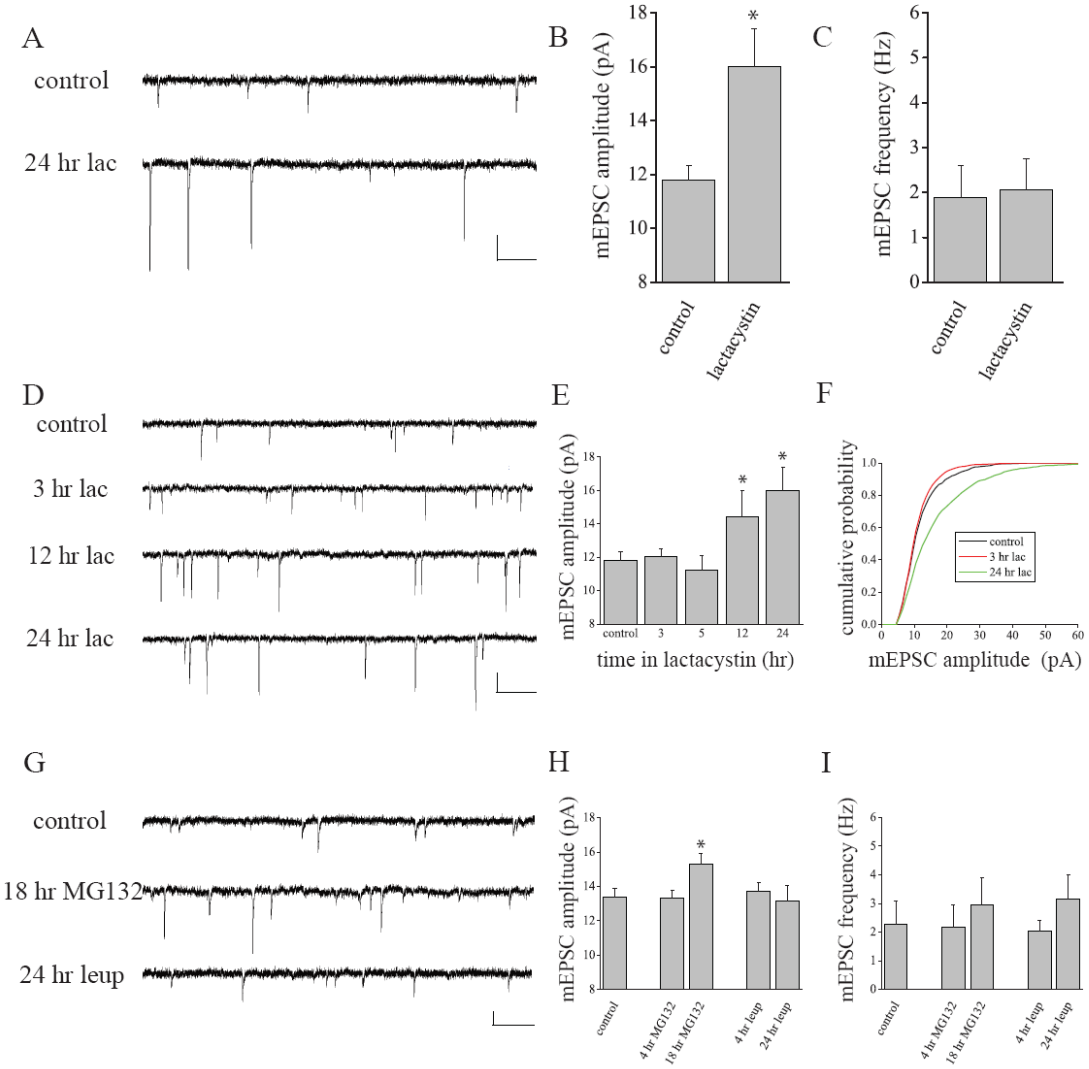
A
control
24 hr lac
B
mEPSC amplitude (pA)
control
lactacystin
C
mEPSC frequency (Hz)
control
lactacystin
D
control
3 hr lac
12 hr lac
24 hr lac
E
mEPSC amplitude (pA)
control
3
5
12
24
time in lactacystin (hr)
F
cumulative probability
control
3 hr lac
24 hr lac
mEPSC amplitude (pA)
G
control
18 hr MG132
24 hr leup
H
mEPSC amplitude (pA)
control
4 hr MG132
18 hr MG132
4 hr leup
24 hr leup
I
mEPSC frequency (Hz)
control
4 hr MG132
18 hr MG132
4 hr leup
24 hr leup

Figure 2.1

Figure 2.2 Similar synaptic changes in AMPAR expression accompany AP and UPS blockade. (A) Representative images of PSD95 (red) and surface GluA1 (sGluA1; green) immunostaining in neurons treated as indicated; merged images are shown in the right panel. Scale Bar = 10 μm. (B, left) Mean (+SEM) normalized (relative to the average control value) intensity of PSD95 particles, and synaptic sGluA1/A2 particles that colocalize with PSD95. (B, right) Mean (+SEM) normalized particle density of PSD95, sGluA1, and sGluA2 in groups, as indicated. AP blockade (2 μM TTX, 24 hr) induced a significant (* $p < 0.05$, Fisher's LSD) increase in sGluA1 (n = 82 neurons) and sGluA2 (n = 61 neurons) intensity at synapses relative to untreated control neurons (n = 89 and 64 neurons, respectively), but did not alter PSD95 particle intensity or density. Similar changes in sGluA1 and sGluA2 expression at synapses were observed following chronic (24 hr) UPS inhibition with lactacystin (10 μM; n = 87 and 66 neurons, respectively) and MG132 (10 μM; n = 98 and 75 neurons, respectively). AP blockade and UPS inhibition also induced a modest, but significant (* $p < 0.05$, Fisher's LSD) increase in sGluA1 and sGluA2 particle density.

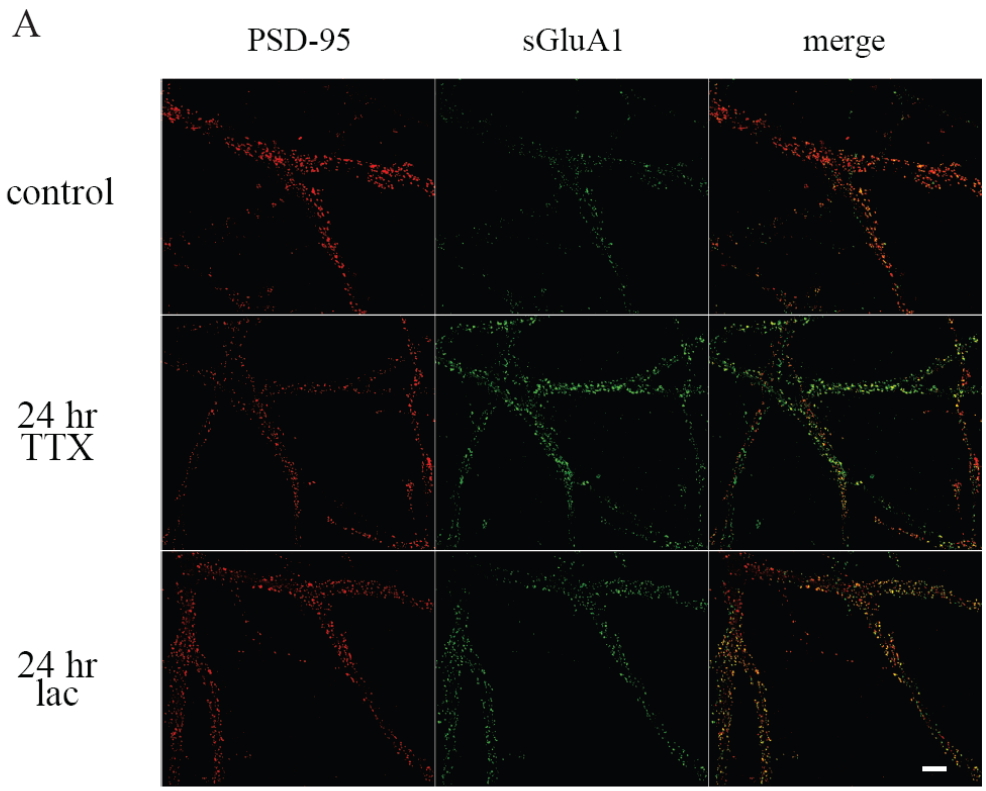
A
PSD-95
sGluA1
merge
control
24 hr
TTX
24 hr
lac

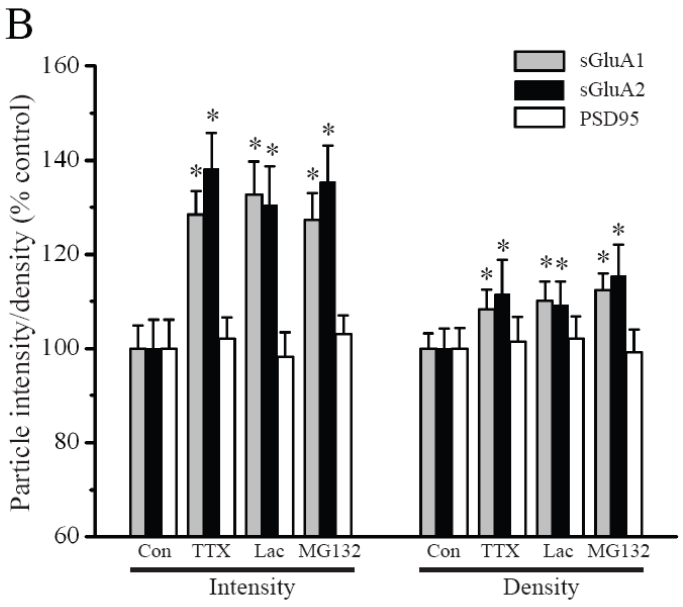
B
sGluA1
sGluA2
PSD95
Particle intensity/density (% control)
160
140
120
100
80
60
Con
TTX
Lac
MG132
Intensity
Con
TTX
Lac
MG132
Density

Figure 2.2

Figure 2.3 Suppression of network activity and UPS inhibition drive similar changes in surface GluA2 expression at synapses. Representative full-frame images of PSD95 (red) and surface GluA2 (sGluA2; green) immunostaining in neurons treated as indicated; merged images are shown in the right panel. Scale Bar = 10 μm. Both AP suppression (24 hr TTX) and UPS inhibition (24 hr lac) induced similar increases in sGluA2 expression at PSD95-labeled synaptic sites.

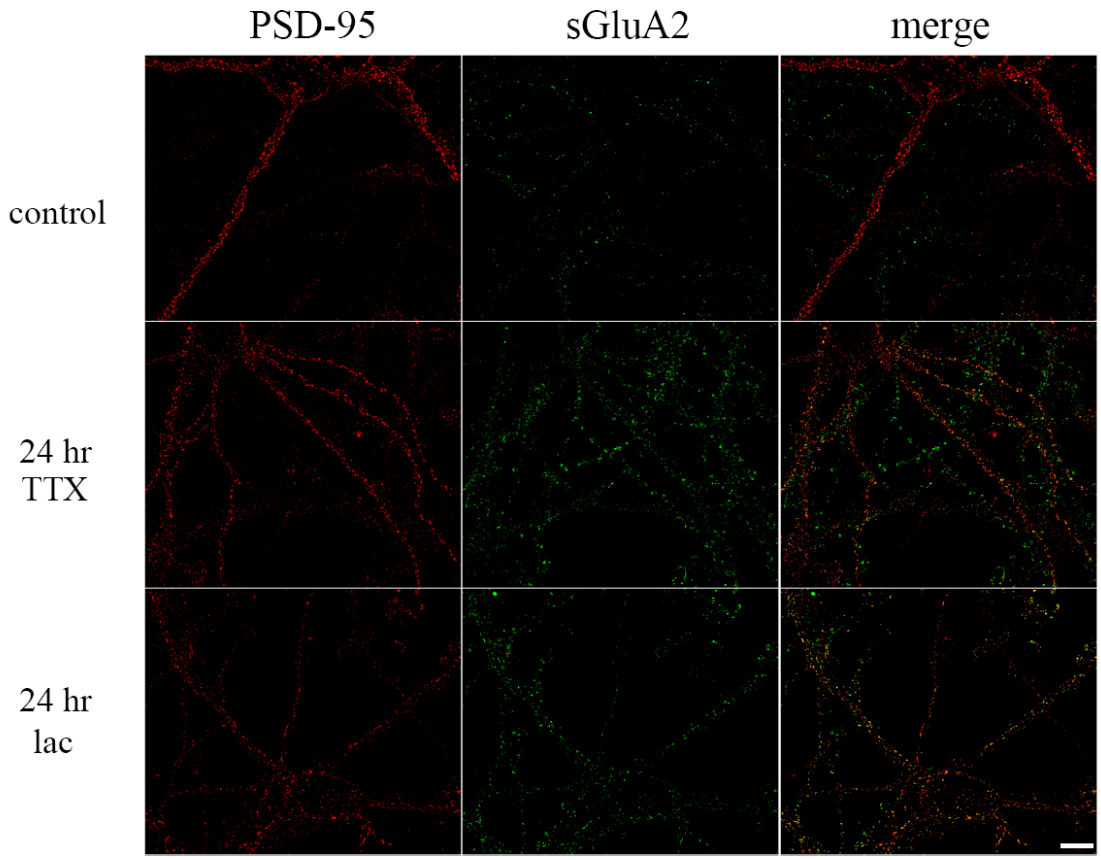

Figure 2.3

Figure 2.4 Chronic changes in neuronal activity induce bidirectional changes in proteasome activity. Neurons were infected with Sindbis viral vectors expressing the 26S proteasome reporter paGFPu-IRES-mCherry or the control (UPS-insensitive) reporter paGFP-IRES-mCherry, and were then treated with 2 μM TTX (n = 92 and 71 neurons, respectively), 50 μM bicuculline (n = 77 and 65 neurons, respectively) or were untreated (control, n = 92 and 70 neurons, respectively) prior to imaging 10 hrs later. Black bar beneath representative images indicates ROI. (A,C) Representative expression of paGFPu (A) and paGFP (C) in neurons treated, as indicated. Fluorescence intensity is indicated by color look-up table; scale bars = 10 μm. (B,D) Mean (+SEM) normalized (relative to the average control value) dendritic paGFPu (B) and paGFP fluorescence intensity in neurons, treated as indicated. Network hyperactivation (bic) induced a significant (* $p < 0.05$, Fisher's LSD) increase in paGFPu degradation (indicated by loss of paGFPu expression), whereas suppression of network activity (TTX) significantly diminished paGFPu degradation relative to controls; fluorescence intensity of the UPS-insensitive paGFP reporter was similar among treatment groups.

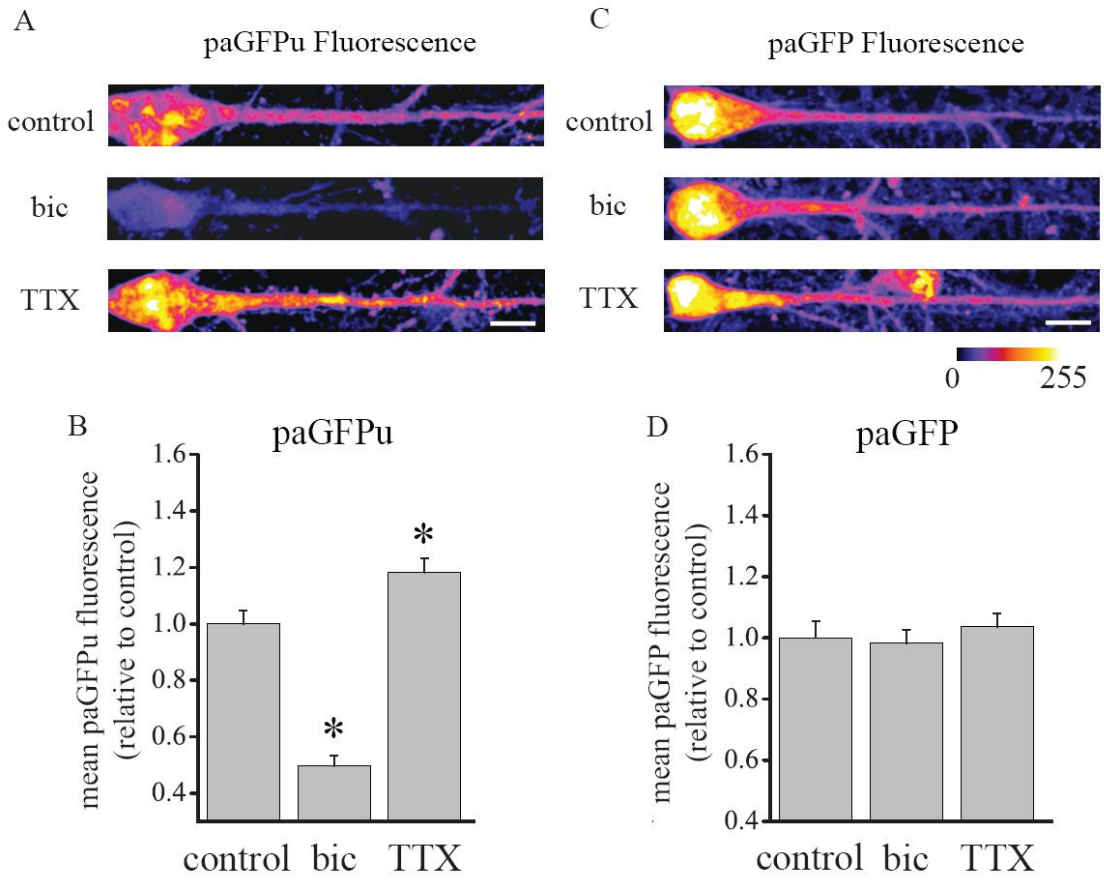
A
paGFPu Fluorescence
control
bic
TTX
C
paGFP Fluorescence
control
bic
TTX
0
255
B
paGFPu
mean paGFPu fluorescence
(relative to control)
1.6
1.4
1.2
1.0
0.8
0.6
0.4
*
*
control
bic
TTX
D
paGFP
mean paGFP fluorescence
(relative to control)
1.6
1.4
1.2
1.0
0.8
0.6
0.4
control
bic
TTX

Figure 2.4

Figure 2.5 Postsynaptic UPS inhibition scales excitatory synaptic function in a cell autonomous manner. (A) Sindbis viral vectors were used to achieve sparse (< 1% of neurons) expression of the ubiquitin chain elongation mutant, UbK48R-IRES-GFP, wild-type ubiquitin (wtUb), or GFP alone. The effects of UbK48R expression were compared with uninfected neurons in the same culture and the expression of wtub-IRES-GFP and GFP alone in sister cultures. (B-E) Representative mEPSC recordings and summary data (C-E) from cells expressing GFP (n = 9), wt ub (n = 13), K48R (n = 14), and uninfected cells present in the K48R-infected dish (n = 8); untreated control neurons (n = 11) from sister cultures were also examined. (C-E) Mean (+ SEM) mEPSC amplitude (C) and frequency (E) from neurons, treated as indicated. UbK48R expression (24 hr) produced a significant (* $p < 0.05$, Fisher's LSD) increase in mEPSC amplitude (but not mEPSC frequency) relative to both untreated control neurons and uninfected neurons present in the K48R dish; no changes in mEPSC amplitude were found in neurons expressing wtUb or GFP alone. (D) Similar to global AP suppression in cultured hippocampal neurons, restricted postsynaptic UbK48R expression induced a rightward shift in the mEPSC amplitude cumulative probability distribution, relative to control neurons (GFP expressing neurons in sister cultures and K48R uninfected neurons recorded from the same culture as K48R-expressing neurons).

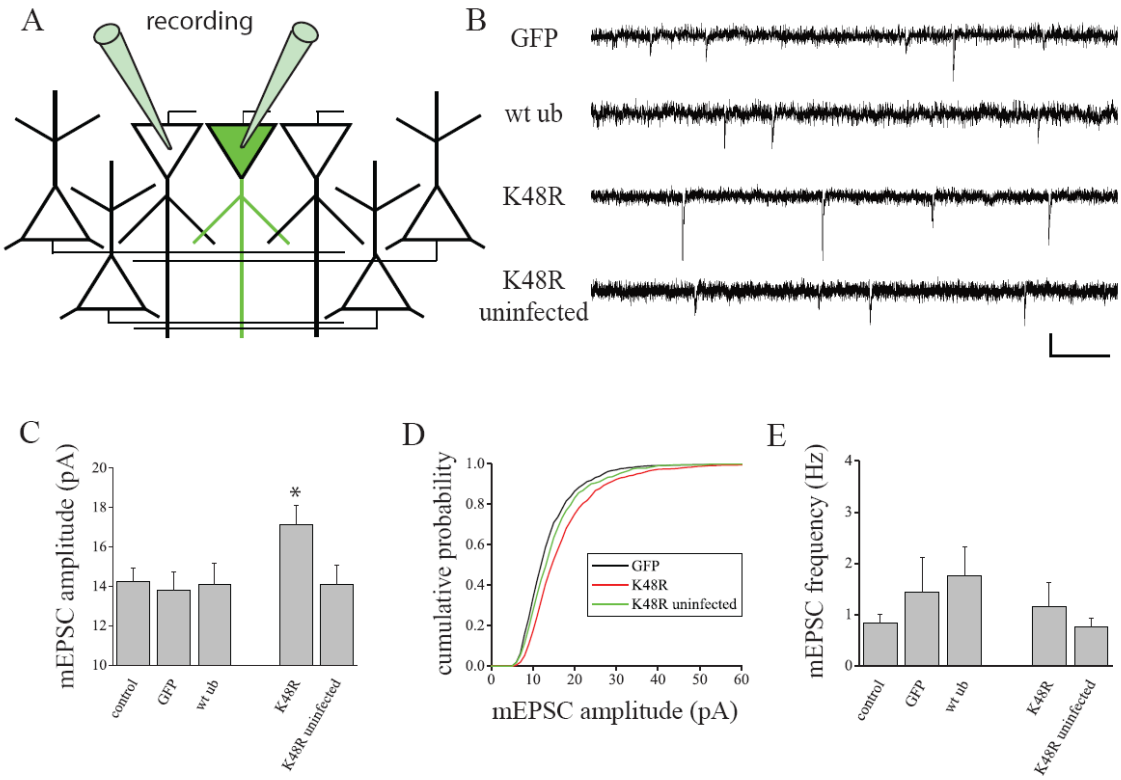
A
recording
B
GFP
wt ub
K48R
K48R
uninfected
C
mEPSC amplitude (pA)
20
18
16
14
12
10
*
control
GFP
wt ub
K48R
K48R uninfected
D
cumulative probability
1.0
0.8
0.6
0.4
0.2
0.0
0
10
20
30
40
50
60
GFP
K48R
K48R uninfected
mEPSC amplitude (pA)
E
mEPSC frequency (Hz)
4
3
2
1
0
control
GFP
wt ub
K48R
K48R uninfected

Figure 2.5

Figure 2.6 UPS inhibition Occludes Slow Homeostatic Plasticity. (A-C) Representative mEPSC recordings (A) and mean (+ SEM) mEPSC amplitude (B) and frequency (C) from neurons, treated with TTX alone (2 μM), lactacystin alone (10 μM), or TTX + lactacystin for 4 or 24 hrs. For the groups shown left to right in (B) and (C), n = 16, 8, 10, 9, 7, 8, and 7 cells, respectively; scale bar in (A) = 10 pA and 250 ms. While neither AP blockade (TTX) nor UPS inhibition (lac) altered synapse function acutely (4 hr, NS), both significantly (* $p < 0.05$, Fisher's LSD) enhanced mEPSC amplitude in response to chronic (24 hr) treatment. Combined TTX+lactacystin treatment for 24 hr, while significantly (* $p < 0.05$, Fisher's LSD) enhancing mEPSC amplitude relative to controls, did not enhance mEPSCs over and above that observed with AP and UPS blockade in isolation. No significant changes in mEPSC frequency were evident. (D-F) Representative mEPSC recordings (D) and mean (+ SEM) mEPSC amplitude (E) and frequency (F) from neurons, treated with bicuculline alone (50 μM), lactacystin alone (10 μM), or bicuculline + lactacystin for 4 or 24 hrs. For the groups shown left to right in (E) and (F), n = 26, 6, 10, 8, 6, 7, and 9 cells, respectively; scale bar in (D) = 10 pA and 250 ms. Whereas chronic (24 hr) hyperactivity imposed by bicuculline alone induces a significant (* $p < 0.05$, Fisher's LSD) decrease in mEPSC amplitude, mEPSC amplitude remains significantly (* $p < 0.05$, Fisher's LSD) enhanced relative to control when hyperactivity is made coincident with UPS inhibition. Network hyperactivation is completely ineffective in reducing the enhanced mEPSCs driven by UPS inhibition (lactacystin vs bic+lactacystin, NS). No significant changes in mEPSC frequency accompany acute or chronic hyperactivity or UPS inhibition.

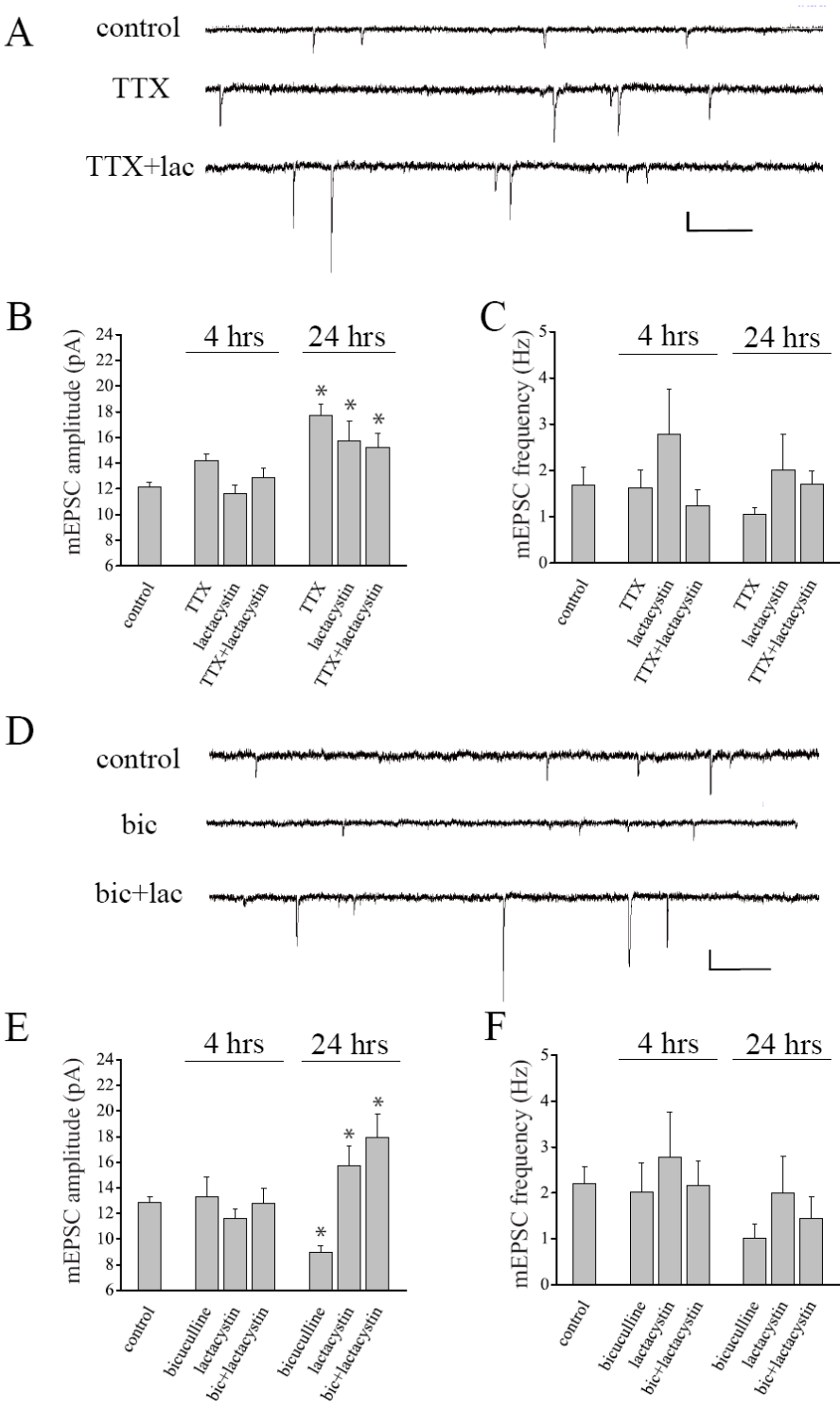
A
control
TTX
TTX+lac
B
4 hrs
24 hrs
mEPSC amplitude (pA)
control
TTX
lactacystin
TTX+lactacystin
C
mEPSC frequency (Hz)
D
bic
bic+lac
E
bicuculline
F

Figure 2.6

Figure 2.7 UPS inhibition drives enhancement of synaptic AMPAR expression irrespective of activity levels. (A) Representative full-frame examples of PSD95 (left, red) and surface GluA1 (middle, green) staining from neurons treated, as indicated; merged PSD95/sGluA1 images are shown in the right panel; scale bar = 10 μm. (B-C) Mean (+SEM) normalized (relative to the average control value) intensity of sGluA1 (B) and sGluA2 (C) particles at synapses (i.e., that overlap with PSD95 particles). Chronic AP blockade (2 μM TTX, 24 hrs) signicantly enhances (*$p < 0.05$), whereas chronic network hyperactivity (50 μM Bic, 24 hrs) significantly diminishes († $p < 0.05$), sGluA1 and sGluA2 expression at synapses relative to control (black bars). UPS inhibition (10 μM lactacystin or 10 μM MG132, 24 hrs) significantly enhances synaptic sGluA1 and sGluA2 expression on its own; this effect is non-additive with chronic AP blockade when UPS inhibitors are applied with TTX and, UPS inhibition still drives increases in sGluA1/2 expression during hyperactivity when UPS inhibitors are applied with bicuculline. For the groups listed from left to right in (B), n's = 64, 75, 62, 45, 46, 38, 44, 52, and 49 neurons. For the groups listed from left to right in (C), n's = 44, 52, 49, 47, 45, 39, 44, 43, and 47 neurons.

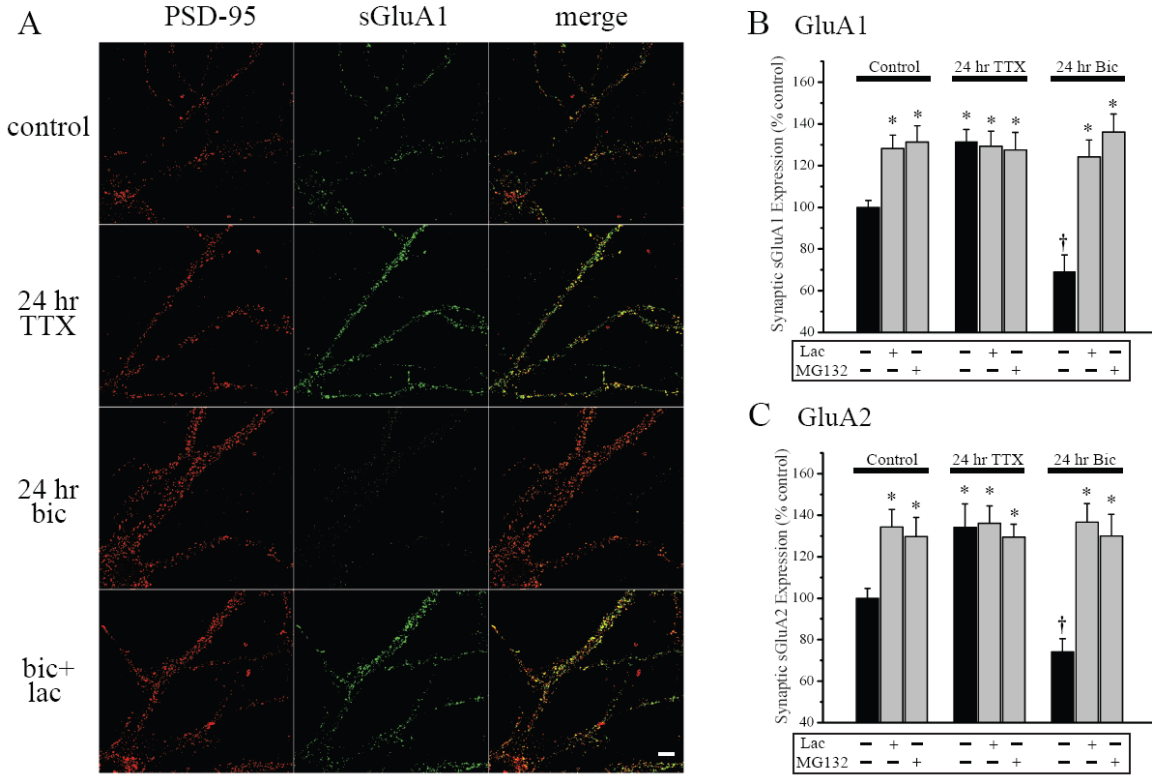
A
PSD-95
sGluA1
merge
control
24 hr TTX
24 hr bic
bic+ lac
B GluA1
Control
24 hr TTX
24 hr Bic
Synaptic sGluA1 Expression (% control)
160
140
120
100
80
60
40
Lac
MG132
C GluA2
Control
24 hr TTX
24 hr Bic
Synaptic sGluA2 Expression (% control)
160
140
120
100
80
60
40
Lac
MG132

Figure 2.7

Figure 2.8 UPS inhibition enhances surface GluA2 expression at synapses irrespective of network activity. Representative full-frame images of PSD95 (red) and surface GluA2 (sGluA2; green) immunostaining in neurons treated as indicated; merged images are shown in the right panel. Scale Bar = 10 μm. Chronic suppression (24 hr TTX) or hyperactivation (24 hr bic) of network activity induces bidirectional changes in surface GluA2 expression at PSD-95 labeled synaptic sites; UPS inhibition enhances synaptic sGluA2 expression even in the face of chronic network hyperactivation.

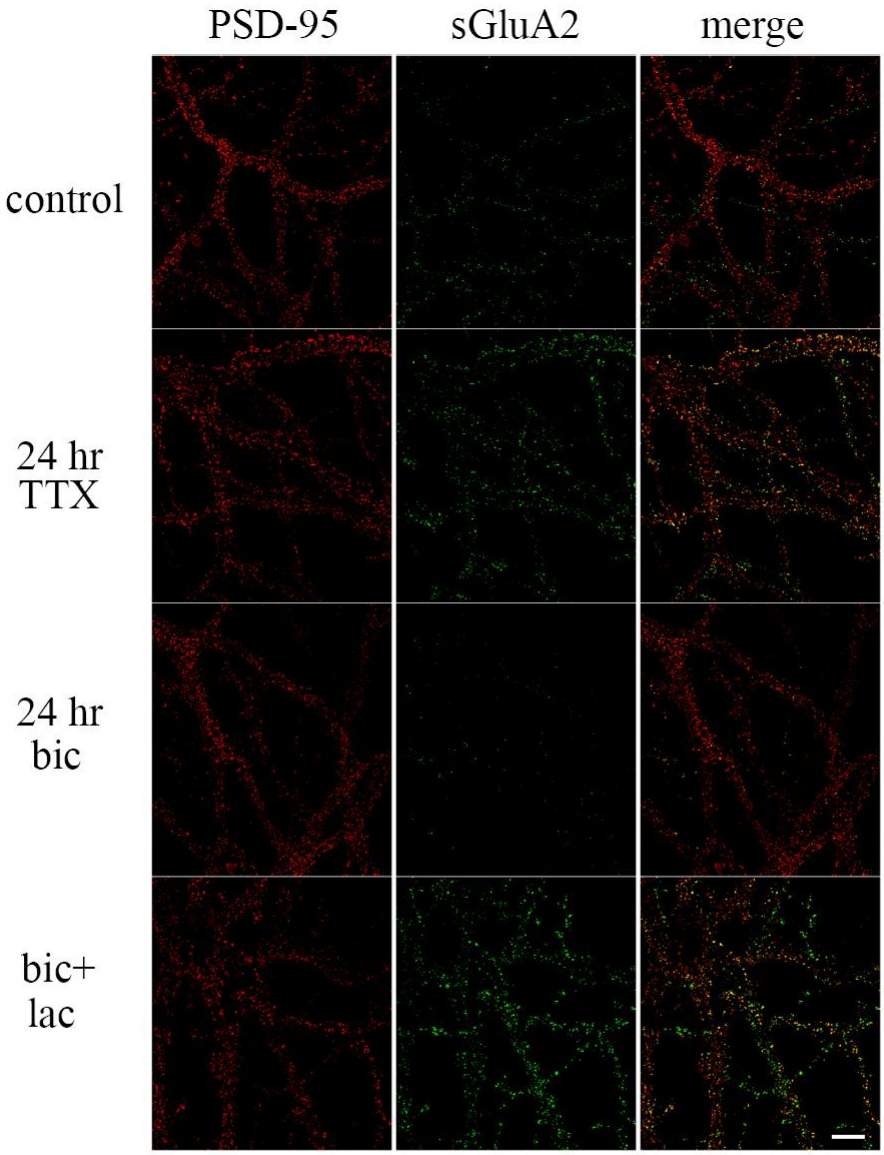

Figure 2.8

Figure 2.9 Postsynaptic UPS activity overrides changes in network activity during slow homeostatic plasticity. (A) Representative mEPSC recordings from untreated controls, K48R-expressing neurons treated with TTX (2μM, 24hr), and uninfected neurons in the same K48R-infected dish (TTX). (B-D) Mean (+ SEM) mEPSC amplitude (B) and frequency (D) from neurons, treated as indicated. For the groups shown left to right in (B) and (D) n = 9, 8, 14, 7 and 9 cells, respectively; the K48R uninfected and K48R groups in the absence of AP blockade are re-plotted from Figure 5 for comparison. Chronic AP blockade induced a significant (* $p < 0.05$, Fisher's LSD) increase in mEPSC amplitude that was similar in Ub48R-expressing neurons and uninfected neurons from the same culture. (C) Cumulative probability distribution of mEPSC amplitudes from the conditions indicated. (E) Representative mEPSC recordings and summary data (F-H) for experiments where postsynaptic UPS inhibition was paired with chronic network hyperactivity (24 hr bic). Shown in (E) are controls and K48R-expressing and non-expressing neurons in the same dish treated with bicuculline (50 μM); scale bar = 10 pA, 250 ms. Mean (+ SEM) mEPSC amplitude (F) and frequency (H) in neurons, treated as indicated. For the groups shown left to right in (F) and (H), n = 9, 8, 14, 7 and 6 cells respectively. Whereas chronic network hyperactivity induced significant (* $p < 0.05$, Fisher's LSD) compensatory decreases in mEPSC amplitude in uninfected neurons, this homeostatic weakening of synaptic strength was completely prevented by postsynaptic expression of UbK48R, as these neurons still exhibit significantly enhanced mEPSC amplitude relative to untreated controls. (G) Opposite shifts of the mEPSC cumulative probability distribution are found in UbK48R-expressing and non-expressing neurons in the same culture exposed to bicuculline for 24 hrs.

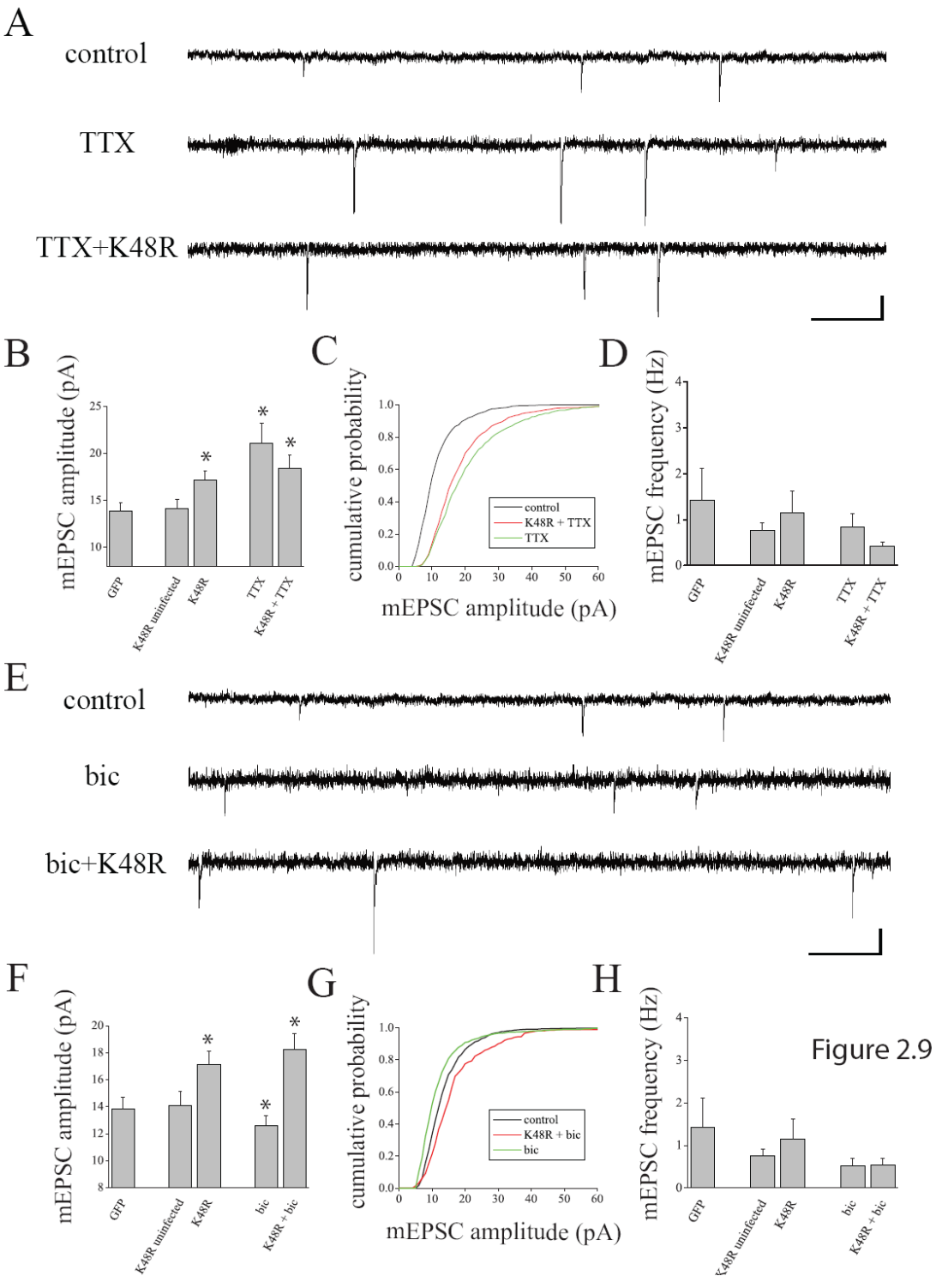
A
control
TTX
TTX+K48R
B
mEPSC amplitude (pA)
GFP
K48R uninfected
K48R
TTX
K48R + TTX
C
cumulative probability
mEPSC amplitude (pA)
control
K48R + TTX
TTX
D
mEPSC frequency (Hz)
E
control
bic
bic+K48R
F
mEPSC amplitude (pA)
bic
K48R + bic
G
cumulative probability
mEPSC amplitude (pA)
control
K48R + bic
bic
H
mEPSC frequency (Hz)

Figure 2.9

Figure 2.10 Phosphorylation of Rpt6 at S120 mimics bidirectional homeostatic plasticity. (A) Example traces of mEPSCs from neurons infected with a Sindbis viral vector containing either GFP alone, WT Rpt6, S120A or S120D respectively. Viral vectors containing WT Rpt6, S120A or S120D co-expressed GFP through an internal ribosomal entry site. 24 hr post infection neurons expressing WT Rpt6 exhibit similar mEPSC amplitude and frequency compared to GFP control neurons. In contrast, expression of S120A homeostatically increases mEPSC amplitude while having no effect on frequency. Constitutive phosphorylation of Rpt6 (S120D) homeostatically decreases mEPSC amplitude relative to control neurons while having no effect on mEPSC frequency. (B-C) Quantification of mEPSC recordings from GFP, WT Rpt6, S120A and S120D expressing neurons. (B) mEPSC amplitude of S120A expressing neurons is increased relative to GFP (control) expressing neurons as well as WT Rpt6 expressing cells whereas the mEPSC amplitude of neurons expressing S120D is decreased relative to WT Rpt6 expressing neurons (* $p < 0.05$; n = 12, 8, 12, 9 left to right; Fisher's LSD). These data suggest that phosphorylation of Rpt6 at S120 is sufficient to regulate bidirectional homeostatic plasticity and suggest a putative link between a postsynaptic activity sensor and regulation of homeostatic function. (C) Quantification of mEPSC frequency. There is no significant difference in mEPSC frequency between groups.

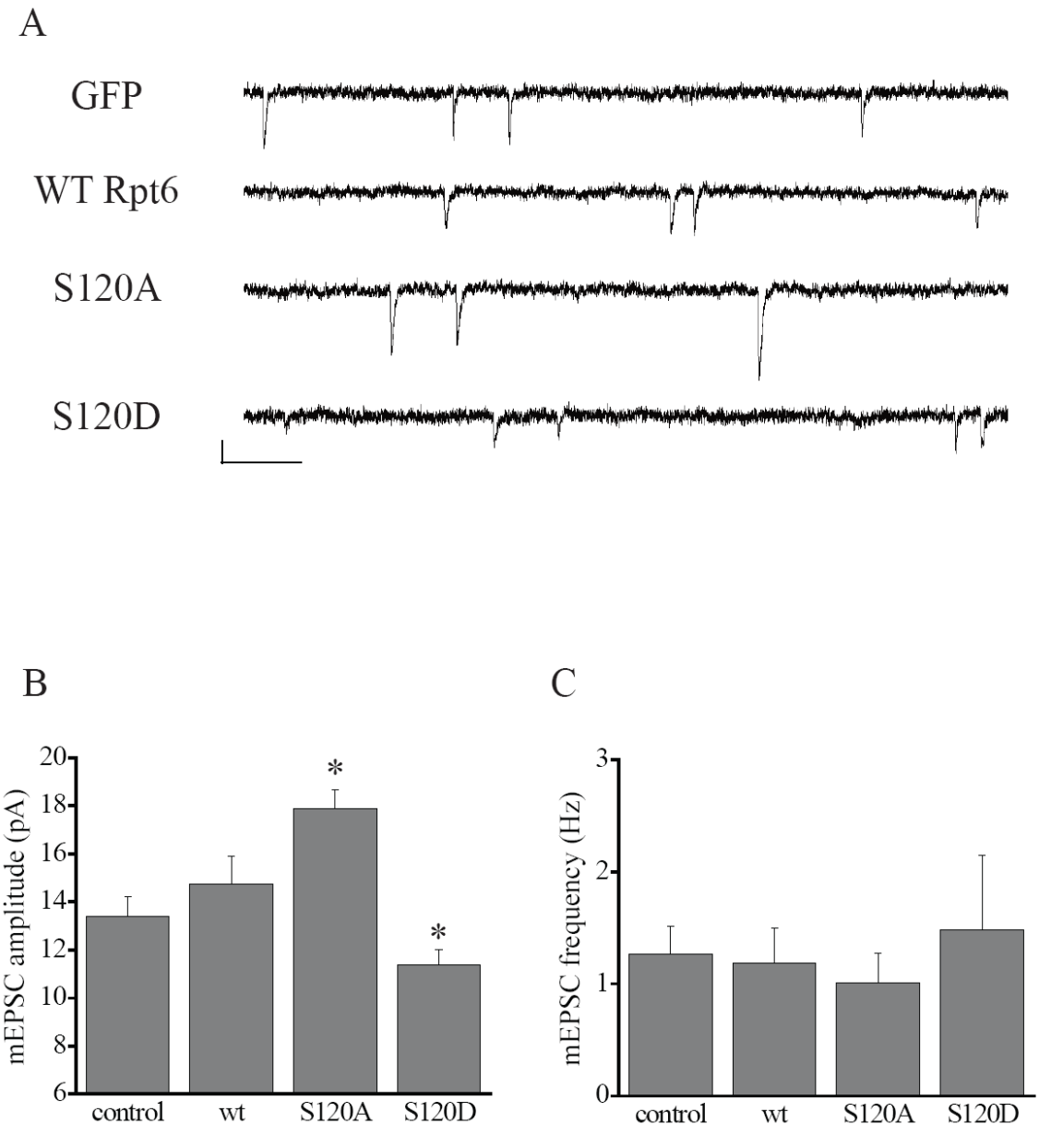
A
GFP
WT Rpt6
S120A
S120D
B
mEPSC amplitude (pA)
20
18
16
14
12
10
8
6
*
*
control
wt
S120A
S120D
C
mEPSC frequency (Hz)
3
2
1
0
control
wt
S120A
S120D

Figure 2.10

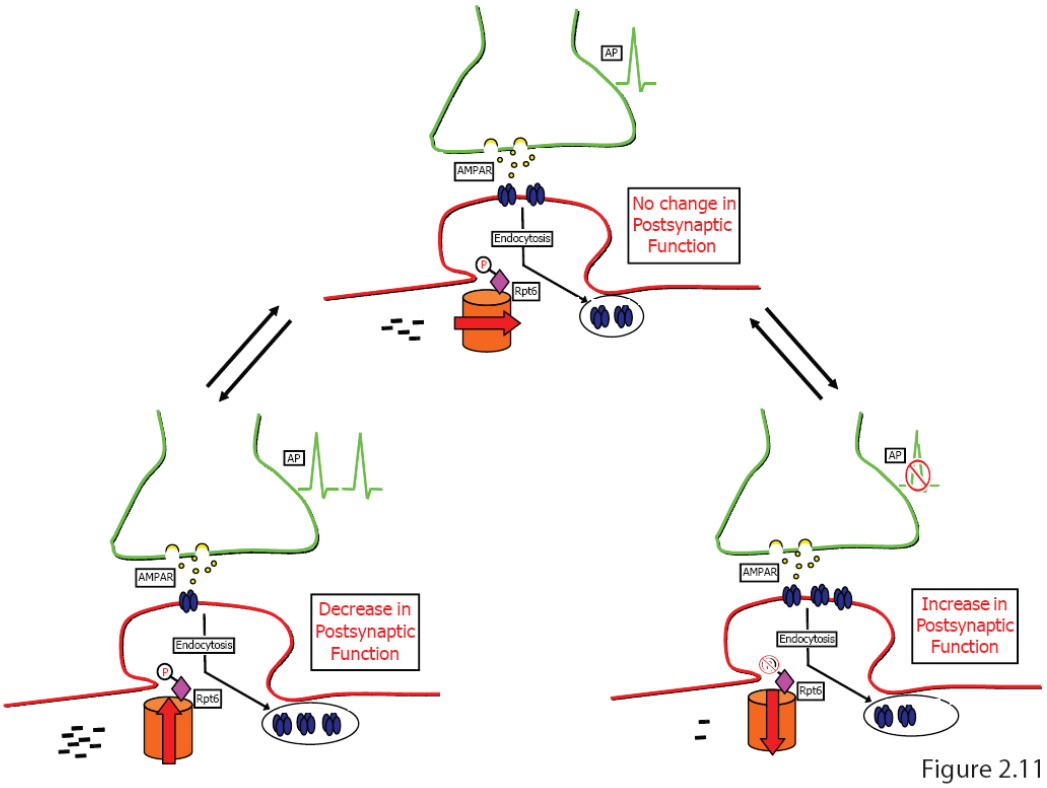

Figure 2.11 Working model of proteasome dependent slow homeostatic plasticity. Under normal conditions, phosphorylation of Rpt6 at S120 remains stable resulting in no net difference in surface expression of AMPARs at the synapse. Under conditions of overexcitation, Rpt6 phosphorylation at S120 is increased leading to a net decrease in surface expression of AMPARs at the synapse and an overall decrease in synaptic function. Conversely, conditions of quiescence lead to an overall decrease in Rpt6 phosphorylation at S120 and a net increase in surface expression of AMPARs and synaptic function.

CHAPTER III

Local presynaptic activity gates homeostatic changes in presynaptic function driven by dendritic BDNF synthesis

Introduction

Activity-dependent forms of synaptic plasticity such as long-term potentiation (LTP) and long-term depression (LTD) have long been considered primary candidates for cellular mechanisms of information storage, but only over the last decade has there been wide interest in understanding how neural circuits maintain stability by offsetting the destabilizing nature of these synaptic modifications (Davis, 2006; Turrigiano, 2008; Pozo and Goda, 2010). It is now known that central neurons have the potential to adapt to changing activity levels by invoking compensatory changes in synaptic function (Turrigiano et al., 1998; O'Brien et al., 1998). In central neurons, such homeostatic forms of synaptic plasticity are typically studied in the context of chronic perturbations of neural activity in networks of cultured neurons, where persistent activity elevation or suppression is met with a gradual weakening or strengthening of synaptic efficacy, respectively (Turrigiano et al., 1998; O'Brien et al., 1998).

Recent studies have revealed that homeostatic synaptic plasticity is associated with heterogeneous expression mechanisms. During activity deprivation, homeostatic

changes at excitatory synapses can manifest as an increase in postsynaptic sensitivity to glutamate (Turrigiano et al., 1998; O'Brien et al., 1998; Wierenga et al., 2005; Sutton et al., 2006), an increase in presynaptic neurotransmitter release (Murthy et al., 2001; Burrone et al., 2002), or some combination of the two (Thiagarajan et al., 2005; Gong et al., 2007). While cell type or developmental age (Wierenga et al., 2006; Echegoyen et al., 2007) may contribute to these differences, recent evidence suggests that the same synapse can exhibit different forms of synaptic compensation tuned to distinct facets of neural activity. Chronic action potential (AP) blockade with tetrodotoxin (TTX) typically induces a slow (> 12 hrs) scaling of postsynaptic function (Turrigiano et al., 1998; Sutton et al., 2006), that is associated with a synaptic accumulation of AMPA-type glutamate receptors (AMPARs) that contain the GluA2 subunit (Wierenga et al., 2005; Sutton et al., 2006; Ibata et al., 2008). By contrast, coincident blockade of APs and miniature synaptic events induces a greatly accelerated homeostatic increase in postsynaptic function (Sutton et al., 2006) mediated by de novo dendritic synthesis of GluA1 and the incorporation of GluA2-lacking AMPARs at synapses (Ju et al., 2004; Sutton et al., 2006; Aoto et al., 2008). Chronic (24 hr) AMPAR blockade (without coincident AP blockade) also induces postsynaptic compensation that requires synaptic incorporation of GluA2-lacking AMPARs, but importantly, an increase in presynaptic release probability is also observed (Thiagarajan et al., 2005; Gong et al., 2007). Furthermore, at the *Drosophila* neuromuscular junction, Frank et al. (2006) also observed a rapid homeostatic adjustment of synaptic efficacy when miniature events were blocked, but these changes were observed in quantal content and were thus reflective of a presynaptic expression mechanism. Hence, while there is convergent support for the role of miniature synaptic

events in homeostatic synaptic plasticity, it is still unclear why direct blockade of excitatory postsynaptic drive can recruit corresponding presynaptic changes in some circumstances, but not others.

A defining feature of synapses in the neocortex and hippocampus is a tight correspondence of pre- and post-synaptic structure indicative of strong functional matching on either side of the synapse. Given that many forms of both homeostatic and Hebbian synaptic plasticity are initially mediated by functional changes that are restricted to the postsynaptic compartment, there must be some mechanism that can recruit corresponding changes in presynaptic function in a retrograde fashion. Indeed, a number of studies have documented such retrograde influences on presynaptic structure and function induced by chronic manipulations of postsynaptic activity and/or function [e.g., (Paradis et al., 2001; Pratt et al., 2003)]. These observations thus raise the question of whether homeostatic adjustment of synapse function is influenced not only by the severity of activity deprivation, but also by the extent to which neurons retain certain activity-dependent signaling capabilities.

Here, we identify a retrograde signaling mechanism in hippocampal neurons that coordinates homeostatic changes in pre- and postsynaptic function. We show that blocking excitatory synaptic drive through AMPARs not only produces faster postsynaptic compensation compared with AP blockade, it also induces retrograde enhancement of presynaptic function that is prevented by coincident AP blockade. This sensitivity to AP blockade reflects state-dependent gating of these presynaptic changes by local activity in presynaptic terminals. Finally, we demonstrate that the local cross-talk between postsynaptic activity and presynaptic function is mediated by local dendritic

release of BDNF as a retrograde messenger, which is required downstream of protein synthesis for the presynaptic changes induced by AMPAR blockade. Our results thus demonstrate a link between local control of protein synthesis in dendrites and activity-dependent transynaptic modulation of presynaptic function.

Experimental Procedues

Cell Culture and Electrophysiology

Dissociated postnatal (P1-2) rat hippocampal neuron cultures, plated at a density of 230-460 mm^2 in poly-D-lysine-coated glass-bottom petri dishes (Mattek), were prepared as previously described (Sutton et al., 2006) and maintained for at least 21 DIV at 37 ºC in growth medium [Neurobasal A supplemented with B27 and Glutamax-1 (Invitrogen)] prior to use. Whole-cell patch-clamp recordings were made with an Axopatch 200B amplifier from cultured hippocampal neurons bathed in HEPES-buffered saline (HBS; containing, in mM: 119 NaCl, 5 KCl, 2 $CaCl_2$, 2 $MgCl_2$, 30 Glucose, 10 HEPES, pH 7.4) plus 1 µM TTX and 10 µM bicuculine. Where indicated, some experiments used HBS containing (in mM) 1 $CaCl_2$ and 2 $MgCl_2$ or 0.5 $CaCl_2$ and 3.5 $MgCl_2$. Whole-cell pipette internal solutions contained, in mM: 100 cesium gluconate, 0.2 EGTA, 5 $MgCl_2$, 2 adenosine triphosphate, 0.3 guanosine triphosphate, 40 HEPES, pH 7.2, and had resistances ranging from 4-6 MΩ. Cultured neurons with a pyramidal-like morphology were voltage-clamped at –70 mV and series resistance was left uncompensated. mEPSCs were recorded in the presence of 1 µM TTX and 10 µM

bicuculine and analyzed off-line using Synaptosoft mini analysis software. For paired-pulse facilitation experiments, HBS contained (in mM) 0.5 $CaCl_2$ and 3.5 $MgCl_2$ and evoked EPSCs were elicited with 0.3 ms pulses delivered by an extracellular bipolar stimulating electrode positioned near the recorded neuron. All PPF experiments were conducted within 15 min of CNQX or CNQX/TTX washout. Statistical differences between experimental conditions were determined by ANOVA and post-hoc Fisher's LSD test.

Immunocytochemisty and Microscopy

All imaging was performed on an inverted Olympus FV1000 laser scanning confocal microscope. Alexa 488 was excited with the 488 line of an argon ion laser and emitted light was typically collected between 500-530 nm with a tunable emission filter. Alexa 555/568 were excited with a 559 nm diode laser and emitted light was typically collected between 570-670 nm. Prior to image collection, the acquisition parameters for each channel were optimized to ensure a dynamic signal range and to ensure no signal bleed-through between detection channels. Identical acquisition parameters were used for each treatment condition, and in each experimental run, we verified that no detectable staining was observed in control samples incubated in the absence of primary antibody (but otherwise processed identically).

For BDNF staining, cells were treated in conditioned media as indicated, then fixed on ice for 30 min with 4% paraformaldehyde (PFA)/4% sucrose in phosphate buffered saline with 1 mM $MgCl_2$ and 0.1 mM $CaCl_2$ (PBS-MC), permeabilized (0.1 %

Triton X in PBS-MC, 5 min), blocked with 2% bovine serum albumin (BSA) in PBS-MC for 30 min, and labeled with a rabbit polyclonal antibody against BDNF (Santa Cruz, 1:100) and a mouse monoclonal antibody against MAP2 (Sigma, 1:5000) for either 60 min at RT or overnight at 4°C. Alexa 488-conjugated goat anti-rabbit (1:250) and Alexa 555-cojugated goat anti-mouse (1: 1000) secondary antibodies (each 60 min at RT) were used to visualize BDNF and MAP2 staining, respectively. In a subset of experiments, Alexa 555-conjugated phalloidin (1:200, Molecular Probes) was used to identify dendritic processes in place of MAP2 staining. For experiments analyzing BDNF expression in axons and astrocytes, the BDNF staining described above was combined with direct Zenon Alexa 568 (Invitrogen) coupling to a Pan-axonal neurofilament mouse monoclonal antibody cocktail (1:8000, clone SMI-312, Covance) or a mouse monoclonal antibody against GFAP (Sigma, 1:1000). Zenon labeling was conducted for 30-min following BDNF immunostaining, after which, the cells were lightly fixed (2% PFA, 5 min) to ensure stability of the signals over time. Neurons with a pyramidal-like morphology were selected for imaging by epifluorescent visualization of MAP2/phalloidin, neurofilament, or GFAP staining, to ensure blind sampling of BDNF expression. Analysis of BDNF expression in astrocytes, or somatic, dendritic, and axonal neuronal compartments was performed on maximal intensity z-compressed image stacks. In each case, BDNF expression was estimated by the average non-zero pixel intensity for each compartment. To analyze BDNF expression processes (axons, dendrites, and astrocytic processes), each process was linearized and extracted from the full-frame image using the straighten plugin for Image J. To combine data across multiple experimental runs of the same experiment, BDNF expression in each image was

normalized against the average non-zero pixel intensity for the respective control group. Statistical differences were assessed by ANOVA, followed by Fisher's LSD post-hoc tests.

For analysis of surface GluA1 expression, neurons were live labeled with a rabbit polyclonal antibody recognizing a surface epitope of GluA1 (10 μg/ml; EMD Biosciences) for 15 min at 37 °C, followed by fixation (2 % PFA in PBS-MC for 15 min at RT), and immunocytochemical labeling with a mouse monoclonal anti-PSD95 antibody (1:1000; Chemicon) as described above. Alexa 488-conjugated goat anti-mouse (1:500) and Alexa 555-conjugated goat anti-rabbit (1:500) secondary antibodies (each 60 min at RT) were used to visualize PSD95 and GluA1 staining, respectively. Neurons were imaged with a Plan-Apochromat 63x/1.4 oil objective with 2x digital zoom and selected based on PSD95 epiflourescence to ensure blind sampling of surface GluA1. For analysis, "synaptic" GluA1 was defined as a particle that occupied greater than 10% of the area defined by a PSD95 particle, and the average integrated intensity (total # of non-zero pixels * intensity) of synaptic GluA1 particles was calculated using custom written analysis routines for Image J. Analysis was performed on both full-frame images as well on dendrites that were straightened and extracted from the full-frame image, where "n" = the number of images or number of dendrites, respectively. Both analysis methods yielded similar results. Statistical differences were assessed by ANOVA, followed by Fisher's LSD post-hoc tests.

To assess presynaptic function directly, we used live-labeling with an Oyster 550-conjugated rabbit polyclonal antibody against the lumenal domain of synaptotagmin 1 (syt-lum; 1:100, Synaptic Systems). Prior to labeling, neurons were treated with 2 μM

TTX for 15 min to isolate spontaneous neurotransmitter release. Neurons were then labeled with anti-syt-lum for 5 min at RT, washed, fixed with 4% PFA/4% sucrose in PBS-MC, permeabilized and blocked as above, then labeled with either a mouse monoclonal antibody against bassoon (1:1000, Stressgen) or a guinea pig polyclonal anti-vglut1 antibody (1: 2500, Chemicon). The intrinsic fluorescent signal of the anti-syt-lum at synaptic sites was amplified by an Alexa 555-cojugated goat anti-rabbit (1:500) secondary antibody, while bassoon or vglut1 staining, respectively was visualized with an Alexa 635-cojugated goat anti-mouse (1:1:000) or Alexa 488-cojugated goat anti-guinea pig (1:250) secondary antibody (each for 60 min at RT). Neurons were imaged with a Plan-Apochromat 63x/1.4 oil objective with 2x digital zoom and selected based on vglut1 epiflourescence to ensure blind sampling of syt-lum expression. For analysis, a "synaptic" syt-lum particule was defined as a particle that occupied greater than 10% of the area defined by a vglut1 particle, and the proportion of vglut particles containing synaptic syt-lum particules was calculated using custom written analysis routines for Image J. Analysis was performed on both full-frame images as well on dendrites that were straightened and extracted from the full-frame image, where "n" = the number of images or number of dendrites, respectively. The results from each analysis method were indistinguishable. Statistical differences were assessed by ANOVA, followed by Fisher's LSD post-hoc tests.

Local Perfusion

All local perfusion experiments were performed on an Olympus FV1000 laser-scanning confocal microscope using Plan-Apochromat 40x/0.95 air (for live imaging) and Plan-Apochromat 40x/1.0 oil (for restrospective imaging) objectives. Stable microperfusion was achieved by use of a dual micropipette delivery system, as described (Sutton et al., 2006). The delivery micropipette was pulled as a typical whole-cell recording pipette with an aperture of ~ 0.5 µm. The area of dendrite targeted for local perfusion was controlled by a suction pipette, which was used to draw the treatment solution across one or more dendrites and to remove the perfusate from the bath. A cell-impermeant fluorescent dye (either Alexa 488 or Alexa 555 hydrazide, 1 µg/ml) was included in the perfusate to visualize the affected area. In all local perfusion experiments, the bath was maintained at 37ºC and continuously perfused at 1.5 ml/min with HBS.

For analysis, the size of the treated area was determined in each linearized dendrite based on Alexa 488/555 fluorescence integrated across all images taken during local perfusion. Adjacent non-overlapping dendritic segments, 25 µm in length, proximal (i.e., towards the cell soma) and distal to the treated area were assigned negative and positive values, respectively. For experiments examining local regulation of BDNF expression, cells were immediately fixed following local perfusion, and processed for immunostaining as described above. Analysis of BDNF expression in local perfusion experiments was performed on maximal intensity z-compressed image stacks. The average non-zero pixel intensity for the entire length of dendrite, excluding the treated area, was used to normalize BDNF intensity and was assigned a value of 1. The intensity of BDNF immunofluorescence was then computed for the treated and all untreated dendritic segments and expressed relative to the average non-treated value. For

experiments examining syt-lum uptake, immediately following local perfusion, 2 μM TTX was bath applied for 10 min to isolate spontaneous neurotransmitter release. Neurons were then live labeled with anti-syt-lum for 5 min at RT, and processed for immunocytochemistry as described above. The density and intensity of vglut particles were calculated for each dendritic segment, and the average value in untreated segments was assigned a value of 1, which was then used to normalize vlgut density and intensity in all segments (including the treated area). The proportion of vglut particles with syt-lum particles was also determined in each segment. Statistical differences in these measurements between segments were assessed by ANOVA and Fisher's LSD post-hoc tests.

BDNF shRNA Transfection

U6 promotor-driven scrambled and BDNF shRNA-expressing plasmids were obtained from OriGene Technologies (Rockville, MD); BDNF shRNA 1: 5'-TGTTCCACCAGGTGAGAAGAGTGATGACC-3, BDNF shRNA 2: 5'-GTGATGCTCAGCAGTCAAGTGCCTTTGGA-3', scrambled: 5'-GCACTACCAGAGCTAACTCAGATAGTACT-3'. Each plasmid additionally contains a tRFP expression cassette driven by a distinct (pCMV) promoter. Neurons were transfected with 0.5 μg of total DNA using the CalPhos Transfection kit (ClonTech; Mountain View, CA) according to the manufacturer's protocol. All experiments were performed 24 hr post transfection.

Western Blotting

Samples were collected in lysis buffer containing, in mM: 100 NaCl, 10 $NaPO_4$, 10 $Na_4P_2O_7$, 10 lysine, 5 EDTA, 5 EGTA, 50 NaF, 1 $NaVO_3$, 1% Triton-X, 0.1% SDS, 1 tablet Complete Mini protease inhibitor cocktail (Roche)/7 ml, pH 7.4. Equal amounts of protein for each sample were loaded and separated on 12% polyacrylamide gels, then transferred to PVDF membranes. Blots were blocked with Tris-buffered saline containing 0.1 % Triton-X (TBST) and 5% non-fat milk for 60 min at RT, and incubated with a rabbit polyclonal primary antibody against BDNF (Santa Cruz, 1: 200) for either 60 min at RT or overnight at 4°C. After washing with TBST, blots were incubated with HRP-conjugated anti-rabbit secondary antibody (1:5000; Jackson Immunoresearch) followed by chemiluminescent detection (ECL, Amersham Biosciences). The same blots were re-probed with a mouse monoclonal antibody against α-tubulin (1:5000, Sigma) to confirm equal loading. Band intensity was quantified with densitometry using NIH image J, and expressed relative to the matched control sample. Statistical differences between treatment conditions and control were assessed by Chi square, whereas comparisons between CNQX and CNQX + anisomycin were assessed with an unpaired t-test (two-tailed).

Results

AMPAR blockade induces state-dependent changes in presynaptic function

We first compared the homeostatic regulation of synapse function induced by chronic (24 hr) AP blockade (2 μM TTX), chronic AMPAR blockade (10 μM NBQX), or a combination of the two (NBQX+TTX). Both AP and AMPAR blockade profoundly decrease excitatory synaptic drive, but each spares a distinct facet of neuronal activity: AP blockade spares miniature neurotransmission, whereas AMPAR blockade spares the capacity for neurons to spontaneously fire APs (as revealed in loose-patch recordings; data not shown). Consistent with previous studies, we found that chronic AP blockade produced a significant increase in mEPSC amplitude, without a corresponding change in mEPSC frequency (Figure 3.1 A-C). Likewise, chronic AMPAR blockade produced a significant increase in mEPSC amplitude, revealed upon NBQX washout, but also a significant increase in mEPSC frequency as reported by others (Thiagarajan et al., 2005; Gong et al., 2007; see also, Murthy et al., 2001). Interestingly, when co-applied over 24 hrs, TTX specifically prevented the increase in mEPSC frequency induced by NBQX, without affecting the increase in mEPSC amplitude (Figure 3.1 A-C). While coincident TTX application prevented the induction of NBQX-dependent changes in mEPSC frequency, it did not prevent the expression of these changes - the increase in mEPSC frequency induced by NBQX alone persisted for at least 60 min with continuous presence of TTX in the recording ringer. These results suggest that chronic AP blockade is effective in establishing compensatory postsynaptic changes it also appears to specifically prevent the development of compensatory presynaptic changes.

As previous studies have demonstrated rapid forms of homeostatic plasticity induced by direct blockade of synaptic activity (Sutton et al., 2006; Frank et al., 2006), we next asked whether the changes in mEPSC amplitude or frequency that accompany

AMPAR blockade develop with different kinetics than the scaling of mEPSC amplitude induced by AP blockade alone. Confirming previous observations (Turrigiano et al., 1998; Sutton et al., 2006), we found that a relatively brief period of AP blockade (2 μM TTX, 3 hrs) was insufficient to alter mEPSC frequency or amplitude (Figure 3.1D-F). However, brief periods of AMPAR blockade (40 μM CNQX, 3 hrs) induced significant increases in both mEPSC amplitude and frequency (Figure 3.1D-F), consistent with an increase in both pre- and post-synaptic function. Again, we found that coincident AP blockade during induction (TTX+CNQX, 3 hrs) specifically prevented the increase in mEPSC frequency without altering the scaling of mEPSC amplitude induced by brief AMPAR blockade (Figure 3.1D-F). These results suggest that AMPAR blockade recruits a "state-dependent" increase in presynaptic release probability – the induction of these presynaptic changes requires that neurons retain the capacity for AP firing.

The state-dependent increase in mEPSC frequency observed after AMPAR blockade could reflect a persistent increase in presynaptic function. Alternatively, it could reflect a postsynaptic unsilencing of AMPAR lacking synapses, since enhanced AMPAR expression at synapses is associated with homeostatic increases in synapse function (O'Brien et al., 1998; Wierenga et al., 2005; Thiagarajan et al., 2005; Sutton et al., 2006). Consistent with the former possibility, we found that AMPAR blockade enhances surface expression of the AMPAR subunit GluA1 at PSD95-labeled excitatory synapses to a similar extent regardless of whether spiking was permitted or prevented with coincident TTX application (Figure 3.1G-H and Figure 3.2). To monitor changes in presynaptic function directly, we examined the activity-dependent uptake of an antibody against the lumenal domain of synaptotagmin 1 (syt-lum) at excitatory synapses marked by

immunoreactivity for the vesicular glutamate transporter (vglut1). Syt-lum uptake is still visible under stringent permeabilization conditions necessary to efficiently co-label synaptic sites in the same cells, and thus provides a direct measure of presynaptic function where overall synaptic density is internally controlled. We first validated the activity-dependent nature of syt-lum uptake at synaptic sites using direct depolarization of synaptic terminals (60 mM K^+), and confirmed that the AP-independent uptake of syt-lum is synaptic (Figure 3.3). We then assessed excitatory presynaptic function after 3 hr AMPAR blockade using synaptic syt-lum uptake as a read-out. Prior to labeling, neurons were exposed to 2 μM TTX for 15 min to isolate spontaneous neurotransmitter release. As a measure of presynaptic function, we quantified the percentage of vglut1-positive excitatory synaptic terminals with accompanying syt-lum staining. We found that 3 hr AMPAR blockade enhanced presynaptic function relative to untreated controls and neurons experiencing a blockade of APs alone with TTX (Figure 3.1I,J and Figure 3.4). Moreover, coincident blockade of both AMPARs and spiking prevented the increase in syt-lum uptake, similar to the state-dependent enhancement of mEPSC frequency revealed by electrophysiology. A similar pattern of results was observed using presynaptic FM4-64X labeling (Figure 3.4). These effects on presynaptic function were not associated with a change in overall density of excitatory synapses (Figure 3.4), illustrating that AMPAR blockade regulates the function of existing excitatory synaptic terminals.

While AMPAR blockade removes excitatory synaptic drive, it does not prevent neurons from spiking spontaneously (data not shown), raising the possibility that state-dependent changes in presynaptic function require presynaptic spiking. To test this

possibility, we used a cocktail of 1 μM ω-conotoxin GVIA and 200 nM ω -agatoxin IVA; CTx/ATx), to block P/Q and N-type $Ca2^{+}$ channels that are localized to presynaptic terminals and normally support AP-mediated neurotransmission (Wheeler et al., 1994). We found that, like TTX treatment, coincident P/Q/N-type $Ca2^{+}$ channel blockade completely prevented the increase in synaptic syt-lum uptake induced by 3 hr AMPAR blockade (Figure 3.1J). In a parallel set of experiments, we similarly found that coincident CTx/ATx treatment specifically prevented the increase in mEPSC frequency induced by AMPAR blockade (Mean ± SEM mEPSC frequency, control = 1.43 ± 0.26 Hz; 3hr CNQX = 3.37 ± 0.58 Hz, $p < 0.05$; CNQX + CTx/ATx = 1.15 ± 0.11 Hz, NS; n = 12, 10, 10; data not shown). Finally, we also examined whether the changes in presynaptic function reflected by spontaneous synaptic vesicle exocytosis extended to changes in evoked release by washing out CNQX (or CNQX+TTX) after 3 hrs and measuring paired-pulse facilitation (PPF). As expected for an increase in evoked release probability, we found that AMPAR blockade significantly inhibited PPF whereas coincident TTX application with CNQX fully restored PPF to control levels (Figure 3.1K-L). Together, these results demonstrate that AMPAR blockade induces two qualitatively distinct compensatory changes at synapses: an increase in postsynaptic function that is induced regardless of spiking activity, and a state-dependent enhancement of presynaptic function that requires coincident presynaptic activity.

NMDAR blockade induces rapid postsynaptic, but not presynaptic, compensation

We next asked whether the homeostatic changes in presynaptic function are driven by AMPAR blockade specifically, or whether they are also evident following NMDAR blockade. We first addressed this issue using mEPSC recordings following 3 hr AMPAR blockade (10 μM NBQX) or 3 hr NMDAR blockade (50 μM APV). We found that whereas both AMPAR and NMDAR blockade induced rapid postsynaptic compensation reflected as an increase in mEPSC amplitude, significant changes in mEPSC frequency emerged after blockade of AMPARs, but not NMDARs (Figure 3.5). Similarly, 3 hr NBQX treatment significantly enhanced syt-lum uptake at synapses, whereas APV treatment did not (Figure 3.5). Since rapid postsynaptic compensation induced by NMDAR blockade is mediated by the synaptic recruitment of GluA1 homomeric receptors (Sutton et al., 2006; Aoto et al., 2008), we also examined the functional role of GluA1 homomers after brief (3 hr) AMPAR blockade. We found that following 3 hr CNQX treatment, addition of 1-Napthylacetylspermine (Naspm; a polyamine toxin that specifically blocks AMPARs that lack the GluA2 subunit) during recording reverses the increase in mEPSC amplitude back to control levels, while having no effect in control neurons (Figure 3.6). Interestingly, while Naspm also decreased mEPSC frequency in a subset of neurons recorded following AMPAR blockade, mEPSC frequency in the presence of Naspm remained significantly elevated relative to control neurons (Figure 3.6). The differential sensitivity of mEPSC frequency and amplitude to both NMDAR blockade and Naspm suggests that the presynaptic and postsynaptic changes are induced in parallel and are at least partially independent. These results suggest that whereas similar postsynaptic adaptations accompany blockade of AMPARs

or NMDARs, the compensatory presynaptic changes are uniquely sensitive to AMPAR activity.

Local activity at presynaptic terminals is required for retrograde modulation of presynaptic function

Does the requirement for either spiking or voltage-gated Ca2+ channels reflect a global network/cell-wide effect or does local activity at presynaptic terminals gate such changes? To distinguish between these possibilities, we examined syt-lum uptake after local microperfusion of either TTX or P/Q/N-type $Ca2^{+}$ channel blockers coupled with global AMPAR blockade (bath application of 20 μM CNQX). Local perfusion was initiated, and 5 min later, CNQX was bath applied for 2 hrs (total local perfusion time of 125 min). Cells were then treated with 2 μM TTX, live-labeled with syt-lum, fixed, and processed for immunostaining against vglut1. As before, we assessed presynaptic function by quantifying the proportion of vglut1-positive excitatory synapses that were also labeled with syt-lum. While local perfusion of vehicle during global AMPAR blockade did not affect the increase in syt-lum uptake, local administration of either TTX or CTx/ATx produced a significant decrease in presynaptic syt uptake in the perfused area relative to apposed terminals on neighboring sections of the same dendrite (Figure 3.7). As an internal control, no differences were observed in vglut1 density (Figure 3.7C) or vglut 1 particle intensity (data not shown) in the perfused area relative to terminals on opposing dendritic segments outside of the perfusion area. The local decrease in presynaptic release probability induced by CTx/ATx required coincident AMPAR

blockade, since no changes in syt-lum uptake were observed in the treated area when bath CNQX was omitted (Figure 3.7D); similar results were found in control experiments using local TTX treatment in the absence of CNQX (Bath Vehicle + local TTX, Mean ± SEM proportion of vglut particles with syt-lum, Untreated areas = 0.31 ± 0.04; Treated area = 0.33 ± 0.06, NS, n = 5 dendrites, 3 neurons). Taken together, these data indicate that AMPAR blockade induces retrograde enhancement of presynaptic function that is gated by local activity in presynaptic terminals.

Postsynaptic BDNF release is required for compensatory presynaptic, but not postsynaptic changes

How does postsynaptic activity blockade lead to sustained increases in presynaptic function? Acute BDNF application can rapidly drive increases in presynaptic function , and extended BDNF exposure can induce structural changes at presynaptic terminals [e.g., (Tyler and Pozzo-Miller, 2001)] suggestive of sustained changes in presynaptic release that may persist when BDNF is no longer present. Consistent with the notion that endogenous BDNF is required for the sustained changes in presynaptic function induced by AMPAR blockade, we found that scavenging endogenous extracellular BDNF (with TrkB-Fc; 1 μg/ml) or blocking downstream receptor tyrosine kinase signaling (with the Trk inhibitor k252a; 100 nM) during AMPAR blockade both specifically block the increase in syt-lum uptake (Figure 3.8A-B), but do not produce changes in overall synapse density (Figure 3.9). Importantly, neither TrkB-Fc nor k252a affected syt-lum uptake in neurons when CNQX and TTX are co-applied, indicating that

these effects are specific for the state-dependent changes in presynaptic function. Interestingly, sequestering BDNF did not affect the enhancement of surface GluA1 expression at synaptic sites during AMPAR blockade (Figure 3.8C-D). Similarly, we found that co-application of TrkB-Fc with CNQX completely prevents the state-dependent increase in mEPSC frequency induced by AMPAR blockade, but does not reduce the increase in mEPSC amplitude (Figure 3.8E-G), suggesting that endogenous BDNF-driven signaling appears to play a specific role in presynaptic compensation. To confirm that postsynaptic BDNF is necessary for the enhancement of presynaptic function induced by AMPAR blockade, we transfected neurons with shRNAs against BDNF or a scrambled control shRNA; transfected neurons were identified by RFP expression, expressed from an independent promoter in each shRNA plasmid. Two distinct BDNF shRNAs effectively knocked-down BDNF expression relative to the scrambled control, as revealed by BDNF immunocytochemistry 24 hrs post-transfection (Figure 3.8H-J) using an antibody with well-established specificity for BDNF. The low transfection efficiency (< 1% of neurons) allowed us to examine selective loss of BDNF from a postsynaptic neuron surrounded by untransfected neurons that are otherwise unperturbed. Hence, mEPSC recordings from transfected neurons revealed that postsynaptic BDNF knockdown (21 hrs prior to AMPAR blockade) did not alter the enhancement of mEPSC amplitude but selectively blocked the increase in mEPSC frequency following brief periods of AMPAR blockade (3 hr CNQX, Figure 3.8K-M). Taken together, these results suggest that BDNF release from the postsynaptic neuron is essential for homeostatic retrograde enhancement of presynaptic function.

BDNF is sufficient to drive state-dependent changes in presynaptic function

We next examined whether BDNF exposure was sufficient to mimic state-dependent enhancement of presynaptic function observed after AMPAR blockade. We treated neurons with varying durations and concentrations of human recombinant BDNF, then washed off BDNF and assayed spontaneous syt-lum uptake. We found that direct BDNF application induces sustained changes in presynaptic function in a time- and concentration-dependent manner, while co-application of TTX or CTx/ATx with BDNF completely prevents this effect (Figure 3.10A-C). These changes in function were not associated with overall changes in synapse density (Figure 3.9), suggesting that like AMPAR blockade, BDNF enhances the function of existing presynaptic terminals. By contrast, BDNF application had no significant effect on surface GluA1 expression at synapses (Figure 3.9), suggesting a selective presynaptic role. Additionally, we found that BDNF application (250 ng/ml, 8 min) enhanced mEPSC frequency within minutes, but these changes rapidly reversed upon BDNF washout (data not shown). By contrast, longer exposure to BDNF (250 ng/ml, 2 hrs) induced a robust and sustained increase in mEPSC frequency, which was prevented by AP or P/Q/N-type $Ca2^{+}$ channel blockade coincident with BDNF exposure (Figure 3.10D,E). Since both AMPAR blockade and BDNF treatment induce sustained increases in mEPSC frequency, we next examined whether these effects were additive. Treating neurons with BDNF for the last 2 hrs of AMPAR blockade produced no greater increase in mEPSC frequency than observed in either condition alone (Figure 3.10F,G), demonstrating that the sustained increase in presynaptic function induced by CNQX treatment occludes such enhancement induced by direct BDNF application. Finally, to examine whether this role of BDNF is local or more

global, we locally scavenged BDNF (via restricted perfusion of TrkB-Fc) during AMPAR blockade (120 min CNQX) and found that the increase in syt-lum uptake was disrupted at presynaptic terminals in the treated area; in the absence of AMPAR blockade (Bath vehicle), local TrkB-Fc had no effect (Figure 3.11). Conversely, direct local application of BDNF (250 ng/ml, 60 min) induced a selective increase in syt-lum uptake at terminals in the treated area, relative to untreated terminals terminating on the same dendrite (Figure 3.11). Taken together, these results suggest a model whereby AMPAR blockade triggers dendritic BDNF release, which drives retrograde enhancement of presynaptic function selectively at active presynaptic terminals.

Retrograde enhancement of presynaptic function requires new BDNF synthesis

Previous studies have demonstrated that rapid postsynaptic compensation at synapses induced by blocking miniature transmission is protein synthesis-dependent (Sutton et al., 2006, Aoto et al., 2008; see also, Ju et al., 2004), so we next examined whether the rapid presynaptic or postsynaptic changes associated with AMPAR blockade require new protein synthesis. As suggested by these earlier studies, we found that the rapid increase in surface GluA1 expression at synapses induced either by AMPAR blockade alone (3 hr CNQX), or AMPAR + AP blockade (CNQX + TTX), is prevented by the protein synthesis inhibitor anisomycin (40 μM, 30 min prior) (Figure 3.12A); a different translation inhibitor emetine (25 μM, 30 min prior) similarly blocked changes in sGluA1 induced by 3 hr CNQX treatment (data not shown). We also found (Figure 3.12B) that the state-dependent increase in syt-uptake induced by AMPAR blockade was

prevented by pre-treatment (30 min prior to CNQX) with either anisomycin (40 uM) or emetine (25 uM). To verify that these changes in surface GluA1 expression and syt-lum uptake are indicative of changes in postsynaptic and presynaptic function, respectively, we examined the effects of anisomycin on mEPSCs (Figure 3.12C,D). In addition to preventing the enhancement of mEPSC amplitude, blocking protein synthesis prevented the state-dependent increase in mEPSC frequency induced by AMPAR blockade, suggesting that rapid homeostatic control of presynaptic function also requires new protein synthesis.

We next asked whether BDNF acts upstream or downstream of translation to persistently alter presynaptic function. BDNF has a well recognized role in enduring forms of synaptic plasticity via its ability to potently regulate protein synthesis in neurons (Kang and Schuman, 1996; Takei et al., 2001; Messaoudi et al., 2002; Tanaka et al., 2008), suggesting that BDNF release might engage the translation machinery to induce sustained changes in presynaptic function. If so, then like AMPAR blockade, the ability of BDNF to drive sustained presynaptic compensation should be prevented by protein synthesis inhibitors. Alternatively, BDNF itself could be a target of new protein synthesis, and could thus act as a translation effector induced by AMPAR blockade [(e.g., (Pang et al., 2004; Bekinschtein et al., 2007)]. If the role of BDNF is downstream of translation, it should recapitulate the enhancement of presynaptic function even in the presence of protein synthesis inhibitors. Indeed, we found that the time-course and magnitude of syt-lum uptake at excitatory synapses after BDNF treatment was virtually identical in the presence or absence of protein synthesis inhibitors (Figure 3.12E-F), despite the fact that these inhibitors completely prevent such increases induced by

AMPAR blockade. These changes again were specific for the presynaptic compartment, since BDNF (250 ng/ml, 2 hrs) failed to alter postsynaptic surface GluA1 expression in the presence of anisomycin (data not shown). Moreover, the increase in mEPSC frequency induced by direct BDNF application was similarly unaffected by blocking protein synthesis with either anisomycin or emetine (Figure 3.12H-I). These results suggest that BDNF acts downstream of protein synthesis to drive state-dependent changes in presynaptic function.

Dendritic synthesis of BDNF accompanies AMPAR blockade

The results described above suggest that BDNF translation is a critical step in establishing state-dependent enhancement of presynaptic function during AMPAR blockade. To explore this idea further, we examined whether AMPAR blockade alters BDNF expression. Western blotting of hippocampal neuron lysates after treatment with CNQX or APV demonstrated that AMPAR, but not NMDAR, blockade induces a time-dependent increase in BDNF expression (Figure 3.13A) that is blocked by anisomycin (Figure 3.13B), indicating that BDNF expression is up-regulated by AMPAR blockade in a protein synthesis-dependent manner. To examine whether BDNF expression after AMPAR blockade was differentially altered in specific sub-cellular compartments, we examined BDNF expression co-localized with specific pre- and postsynaptic markers by immunocytochemistry. We found that the increase in BDNF expression induced by AMPAR blockade was largely accounted for by regulation in dendrites, as MAP2-positive dendrites exhibited a significant increase in BDNF expression in neurons treated

with CNQX (2 hrs), while somatic expression of BDNF from these same cells was unchanged (Figure 3.13C-G). Importantly, both dendritic and somatic MAP2 expression were similar between CNQX treated neurons and controls. These changes in dendritic BDNF expression were again specific to AMPAR blockade, since NMDAR blockade (APV, 2 hrs) failed to alter BDNF expression (Figure 3.14). In a parallel series of experiments, we found that AMPAR blockade failed to alter BDNF expression in neurofilament-positive axons or GFAP-positive astrocytes (Figure 3.13F and 3.14), indicating that AMPAR blockade induces an increase in neuronal BDNF expression that is specific to the dendritic compartment. Moreover, consistent with our biochemical data, the increase in dendritic BDNF expression induced by AMPAR blockade was due to de novo synthesis, since it was prevented by the translation inhibitors anisomycin and emetine (Figure 3.13F,G). Interestingly, blocking background spiking activity with TTX did not prevent the ability of AMPAR blockade to enhance dendritic BDNF expression in a protein synthesis-dependent manner (Figure 3.13H), suggesting that blockade of AP-independent miniature events are sufficient to drive changes in BDNF synthesis. Hence, while the downstream consequences of BDNF synthesis are gated by coincident activity in presynaptic terminals, the synthesis of BDNF appears more tightly linked with excitatory synaptic drive and the postsynaptic impact of miniature synaptic transmission.

Previous studies have documented the importance of local dendritic protein synthesis in forms of homeostatic plasticity induced, in whole or part, by targeting postsynaptic receptors with antagonists (Ju et al., 2004; Sutton et al., 2006; Aoto et al., 2008). Thus, the increase in dendritic BDNF expression could be due to localized dendritic synthesis or alternatively, due to somatic synthesis and subsequent transport

into dendrites. It is well established that BDNF mRNA is localized to dendrites (Tongiorgi et al., 1997; An et al., 2008), and that miniature synaptic events regulate dendritic translation efficiency (Sutton et al., 2004), supporting the possibility that AMPAR blockade induces local BDNF synthesis in dendrites. To examine this possibility, we assessed the effects of locally blocking protein synthesis in dendrites using restricted microperfusion of emetine during global AMPAR blockade. When locally administered 15 min prior to and throughout bath CNQX treatment (40 μM; 60 min), emetine produced a selective decrease in dendritic BDNF expression in the presence of coincident bath CNQX application (Figure 3.15). Again, these local changes in BDNF expression were specific, as local administration of emetine had no effect on MAP2 expression in the same neurons, nor did local emetine have any effect on BDNF expression without coincident CNQX treatment (Figure 3.15D). These results thus indicate that the selective increase in dendritic BDNF expression induced by AMPAR blockade reflects localized dendritic BDNF synthesis. Taken together, our results suggest that AMPAR blockade induces local BDNF synthesis in dendrites which, in turn, selectively drives state-dependent compensatory increases in release probability from active presynaptic terminals.

Discussion

We have shown that different facets of synaptic activity play unique roles in shaping the manner by which neurons homeostatically adjust pre- and postsynaptic

function to compensate for acute loss of activity. In light of both the present findings and prior studies, we propose the following working mechanistic model (Figure 3.16) to explain the compensatory synaptic adaptations that accompany blockade of excitatory synaptic drive. AMPAR blockade induces two rapid and dissociable forms of synaptic compensation: 1) a postsynaptic increase in expression of GluA2-lacking AMPARs and a corresponding enhancement of mEPSC amplitude that is independent of background spiking activity, and 2) a retrograde enhancement of presynaptic function that is driven by the convergence of BDNF-TrkB signaling with AP-triggered $Ca2^{+}$-influx through P/Q/N-type channels. Whereas the postsynaptic changes are sensitive to activity at either AMPARs or NMDARs, the enhancement in presynaptic function is unique to loss of AMPAR activity. Both pre- and postsynaptic changes require new protein synthesis, but appear to depend on distinct dendritically-synthesized protein products - GluA1 synthesis is likely critical for rapid postsynaptic compensation (Ju et al., 2004; Thiagarajan et al., 2005; Sutton et al., 2006; Aoto et al., 2008), while BDNF synthesis is critical for orchestrating retrograde compensatory changes in presynaptic function.

Retrograde Homeostatic Modulation of Presynaptic Function

Many studies have demonstrated postsynaptic forms of homeostatic compensation associated with enhanced expression of AMPARs at synapses (e.g., O'Brien et al., 1998; Wierenga et al., 2005; Sutton et al., 2006). However, clear evidence for homeostatic regulation of presynaptic neurotransmitter release has also been documented (e.g., Bacci et al., 2001; Murthy et al., 2001; Burrone et al., 2002; Thiagarajan et al., 2002; Wierenga

et al., 2006; Branco et al., 2008). While methodological factors can contribute to this heterogeneity in expression (Wierenga et al., 2006), previous examples of retrograde effects of postsynaptic manipulations on presynaptic structure (e.g., Pratt et al., 2003) and function (e.g., Paradis et al., 2001; Burrone et al., 2003; Frank et al., 2006) suggest that intrinsic synaptic properties might also play a role. Indeed, we find that in addition to rapid postsynaptic effects, AMPAR blockade induces rapid (< 3 hr) functional compensation in the presynaptic compartment, an effect that is not observed with either acute (3 hr) or chronic (24 hr) AP blockade [see also, (Bacci et al., 2001)]. Not only was AP blockade insufficient to produce changes in presynaptic function on its own, it also prevented AMPAR blockade from producing those changes. Hence, the compensatory increase in release probability induced by AMPAR blockade is state-dependent, requiring presynaptic spiking and P/Q/N-type $Ca2^{+}$-channel function during the period of AMPAR blockade for its induction.

Our findings complement recent studies regarding retrograde homeostatic regulation of presynaptic neurotransmitter release. Frank and colleagues (2006) found that blocking spontaneous neurotransmission at the *Drosophila* NMJ induced rapid increases in presynaptic release probability, similar to our observations they found that these changes were prevented by mutations in the presynaptic $Ca_v2.1$ channel encoded by the cacophony gene. The similar requirement for presynaptic voltage-gated $Ca2^{+}$ channels in the two studies suggests that the state-dependent regulation of presynaptic function is evolutionarily conserved. Another recent study using hippocampal neurons (Branco et al., 2008) demonstrated that increases in local dendritic activity homeostatically decrease release probability from presynaptic terminals terminating on

that dendrite. Our findings illustrate that the local homeostatic cross-talk between postsynaptic signaling and presynaptic release probability also operates in the opposite direction, where loss of postsynaptic activity selectively enhances release probability from active presynaptic terminals. Finally, whereas our experiments focus on presynaptic changes induced by loss of synaptic input, data from Groth, Lindskog, Tsien and colleagues suggests that restoration of synaptic drive following activity blockade may also rapidly drive retrograde changes in release probability (Groth et al., 2009, Soc. Neurosci. Abs.). Hence, recent work from multiple groups establishes retrograde signaling as an important homeostatic mechanism in neural circuits.

BDNF as a state-dependent retrograde messenger

In our study, scavenging extracellular BDNF, blocking TrkB activation, postsynaptic shRNA-mediated BDNF knockdown, and direct BDNF application all point to BDNF as a retrograde messenger linking postsynaptic consequences of AMPAR blockade with sustained enhancement of presynaptic neurotransmitter release. These results are consistent with previous studies showing that BDNF enhances presynaptic function (e.g., (Lessmann et al., 1994; Li et al., 1998; Schinder et al., 2000; Tyler and Pozzo-Miller, 2001; Groth et al., 2009) via a direct influence of BDNF signaling at the presynaptic terminal (Li et al., 1998; Pereira et al., 2006). In addition to BDNF, recent studies have demonstrated the importance of other releasable factors in homeostatic adjustment of synaptic strength. Stellwagen and Malenka (2006) demonstrated that glial-derived tumor-necrosis factor alpha (TNF-α) can drive postsynaptic compensation in

neurons in response to chronic AP blockade. In our studies, glial cells do not seem to be the source of BDNF responsible for orchestrating presynaptic changes, since AMPAR blockade enhances BDNF synthesis in neuronal dendrites but does not influence BDNF expression in astrocytes. Interestingly, however, the role of TNF-α does seem to complement a more chronic role for BDNF in slow homeostatic adjustment of synaptic strength (Rutherford et al., 1998). In this study, co- treatment with BDNF prevented the gradual scaling of mEPSC amplitude induced by chronic TTX, whereas chronic treatment with a TrkB-IgG BDNF scavenger mimicked the slow scaling induced by TTX. Together with our results, these observations suggest that BDNF may have multiple time-dependent roles in homeostatic synaptic plasticity. Finally, a recent study (Aoto et al., 2008) has implicated the release of retinoic acid (RA) in orchestrating the synaptic incorporation of GluA2-lacking AMPARs to synapses induced by blocking miniature neurotransmission. Interestingly, while Aoto and colleagues (2008) demonstrate that RA mimics mini blockade in driving protein synthesis-dependent postsynaptic recruitment of GluA1 to synapses and enhancing mEPSC amplitude, it had no effect on mEPSC frequency suggesting a selective role in postsynaptic compensation. Together with our findings, these results suggest that distinct releasable factors may be engaged for homeostatic adjustment of pre- and postsynaptic function.

Multiple homeostatic modes control postsynaptic function

For homeostatic forms of plasticity induced by coincident blockade of APs and NMDARs, multiple studies have demonstrated enhanced synthesis of GluA1 in dendrites

(Ju et al., 2004; Sutton et al., 2006) or synaptic fractions (Aoto et al., 2008), and the incorporation of GluA2-lacking receptors at synapses (Ju et al., 2004; Sutton et al., 2006; Aoto et al., 2008). By contrast, blockade of AP's alone induces a slower form of postsynaptic compensation characterized by enhanced expression of GluA2-containing AMPARs at synapses (Turrigiano et al., 1998; Wierenga et al., 2005; Sutton et al., 2006), possibly owing to a decrease in receptor removal and an accumulation of existing synaptic receptors (e.g., O'Brien et al., 1998; Ehlers, 2003; Ibata et al., 2008). These results support the notion that spontaneous and AP-mediated neurotransmission engage unique signaling pathways in neurons (Sutton et al., 2007; Atasoy et al., 2008) and that miniature synaptic events in these neurons play an important role in the acute homeostatic regulation of synaptic strength. Frank et al. (2006) identified a similar role for spontaneous neurotransmission in rapid homeostatic adjustment of synaptic function at the *Drosophila* neuromuscular junction, suggesting that this role for miniature events may be conserved across different synapse classes and species. In a similar vein, Thiagarajan et al. (2005) demonstrated the synaptic recruitment of GluA2-lacking AMPARs in response to chronic (~24 hr) AMPAR blockade, suggesting that loss of AMPAR activity also engages mechanisms that recruit GluA2-lacking AMPARs to synapses. Our results extend these observations by demonstrating that AMPAR blockade induces rapid postsynaptic recruitment of GluA1 that is dependent on new protein synthesis. Moreover, we found that regardless of the presence or absence of background spiking, the increase in synaptic GluA1 and mEPSC amplitude induced by AMPAR blockade is indistinguishable. These results have two important implications. First, they demonstrate that while AP blockade reveals the functional impact of miniature

neurotransmission (see also, Sutton et al., 2006), this role extends to conditions where background spiking is permissive. Second, they suggest that the rapid implementation of these postsynaptic changes is likely determined by changes in excitatory synaptic drive rather than postsynaptic firing rate, since AP blockade alone induces a distinct set of postsynaptic changes (i.e., enhanced expression of GluA2-containing AMPARs) with far slower kinetics (> 12 hr; Turrigiano et al., 1998; Wierenga et al., 2005; Sutton et al., 2006). This notion is further supported by the observation that spatially-restricted blockade of NMDAR miniature events enhances surface GluA1 expression locally (Sutton et al., 2006). While these observations and some theoretical considerations (Rabinowitch and Segev, 2008) argue for a local homeostatic mechanism, there is also strong evidence for more global homeostatic control mechanisms in neurons that may be tuned to firing rate (Turrigiano et al., 1998). There are unique theoretical advantages of global homeostatic mechanisms as well, particularly with regard to preserving information coding capabilities of neurons (Turrigiano, 2008). A recent study directly assessed the impact of blocking postsynaptic firing by confining TTX treatment to the postsynaptic cell body. Ibata et al. (2008) found such somatic AP blockade induced a transcription-dependent accumulation of GFP-tagged GluA2 at multiple sites throughout the dendritic arbor remote from the perfusion site, indicative of a cell-wide homeostatic mechanism. This transcription-dependent connection adds an interesting parallel with other evidence implicating the immediate early gene Arc in global homeostatic control (Shepherd et al., 2006), and also distinguishes this global mechanism with transcription-independent synaptic insertion of GluA2-lacking receptors that accompanies mini blockade (Aoto et al., 2008). Taken together, these observations support the existence of

multiple modes of homeostatic control in neurons that are mediated by separate molecular pathways and implemented over distinct spatial scales.

Dendritic BDNF synthesis drives local changes in presynaptic function

Since the discovery of polyribosomes beneath synaptic sites on dendrites, the hypothesis that dendritic protein synthesis can be engaged to adjust synaptic composition on a local level has received considerable attention. Our results indicate that in addition to allowing for fine spatial control over the postsynaptic element, local dendritic synthesis may also actively participate in controlling the function of apposed presynaptic terminals, through local synthesis of BDNF and perhaps other retrograde messengers. Thus, BDNF is both necessary and sufficient for the state-dependent presynaptic changes induced by AMPAR blockade, but acts downstream of protein synthesis. Furthermore, AMPAR blockade enhances dendritic BDNF expression in a translation-dependent manner, and a local decrease in dendritic BDNF expression accompanies spatially-restricted inhibition of dendritic protein synthesis when performed coincident with AMPAR blockade. This latter result suggests that the mobility of the BDNF pool synthesized in response to AMPAR blockade is restricted, although it is not presently clear what mechanisms are responsible. Future studies examining dynamic BDNF synthesis and trafficking in dendrties will be useful in elucidating mechanisms that are responsible for this restricted mobility. Importantly, preventing spiking in synaptic terminals or the $Ca2^{+}$ influx triggered by spiking completely prevents the sustained presynaptic changes induced by BDNF, but does not appear to affect the synthesis of

BDNF directly. Hence, we conclude that a dendritic source of BDNF participates in enhancing release probability at apposed presynaptic sites, but only at active terminals. It is now of interest to determine how BDNF-driven signaling interacts with signaling driven by AP-triggered $Ca2^{+}$ influx in presynaptic terminals to mediate this state-dependent enhancement of presynaptic function.

BDNF has received considerable attention for its role in long-lasting synaptic plasticity and memory. Much of this interest is driven by the fact that BDNF is known to potently regulate neuronal translation generally (e.g., Takei et al., 2001), and local translation in dendrites in particular [e.g., (Aakalu et al., 2001; Yin et al., 2002)]. Furthermore, there is substantial evidence that one critical role of BDNF in long-term plasticity is for inducing translation, i.e., BDNF acts upstream of protein synthesis for certain forms of LTP (e.g., Kang and Schuman, 1996; Messaoudi et al., 2002; Tanaka et al., 2008). However, evidence has been emerging that BDNF may play distinct roles downstream of protein synthesis, presumably via its own translation (Pang et al., 2004; Bekinschtein et al., 2007). Given that BDNF can act both upstream and downstream of protein synthesis, a critical issue is what unique functional contributions BDNF might make in these different roles. Collectively, our results suggest one important aspect of BDNF's role as a translation effector is to orchestrate presynaptic changes in a state-dependent manner. For homeostatic plasticity, this role of BDNF has the important consequence of coordinating compensatory changes at postsynaptic sites with corresponding increases in presynaptic function. This specific role may well extend beyond homeostatic compensation, and the importance of BDNF as a translation effector in long-term potentiation (Pang et al., 2004) and memory (Bekinschtein et al., 2007)

could relate to its ability to enhance presynaptic function in a state-dependent manner. Although this notion remains speculative, the fact that active presynaptic terminals are uniquely sensitive to BDNF's effects suggests that in other contexts, BDNF could provide feedback to presynaptic terminals in a Hebbian fashion. In other words, our results predict that inputs that are activated in an experience-dependent fashion, as might occur during repetitive training trials, will be selectively strengthened via the state-dependent enhancement of presynaptic function conferred by BDNF. This type of mechanism could, in principle, allow for plasticity mechanisms that are initially confined to the postsynaptic compartment to engage appropriate synaptic contacts and drive coordinate changes in their function so as to effectively match efficacy on both sides of the synapse.

Figure 3.1 AMPAR blockade induces a state-dependent enhancement of presynaptic function (A-C) Representative recordings (A) and mean (+ SEM) mEPSC amplitude (B) and frequency (C) of experiments (27-40 DIV) from the following conditions (24 hr): Control (n = 13), 10 μM NBQX (n = 9), 2 μM TTX (n = 10), TTX+NBQX (n = 8). 24 hr NBQX increases both mEPSC amplitude and frequency (* $p < 0.05$, relative to control); (D-F) Representative recordings (D) and mean (+ SEM) mEPSC amplitude (E) and frequency (F) of experiments (21-38 DIV) from the following conditions (3 hr): Control (n = 10), 40 μM CNQX (n = 12), 2 μM TTX (n = 10), and TTX+CNQX (n = 11). Brief AMPAR blockade induces a significant (*$p < 0.05$, relative to control) increase in both mEPSC amplitude and frequency; AP blockade prevents the increase in mEPSC frequency induced by AMPAR blockade, but not changes in mEPSC amplitude. (G) Representative examples and (H) mean (+SEM) normalized surface GluA1 expression at excitatory synapses (21-40 DIV) from the following conditions (3 hr): Controls (n = 46), CNQX (n = 44), TTX (n = 48), or CNQX+TTX (n = 46). (I-J) Representative examples and mean (+SEM) proportion of vglut1-positive excitatory presynaptic terminals with corresponding syt-lum signal from the indicated treatment groups (DIV 37-40). Left to right n = 54, 49, 52, 50, 64, 68, 64, 67 images. Brief AMPAR blockade significantly (*$p < 0.05$, relative to control) enhances synaptic syt-lum uptake which is prevented by coincident AP (+TTX) or P/Q/N-Ca2+ channel (+CTx/ATx) blockade. (K) Example traces and (L) mean (± SEM) paired-pulse facilitation (PPF). AMPAR blockade (CNQX alone; n = 29 neurons) produced a significant (*$p < 0.05$, relative to control; n = 29 neurons) decrease in PPF; co-application of TTX during AMPAR blockade (n = 29 neurons) restored PPF to control levels. Scale bars = 25 pA, 50 ms.

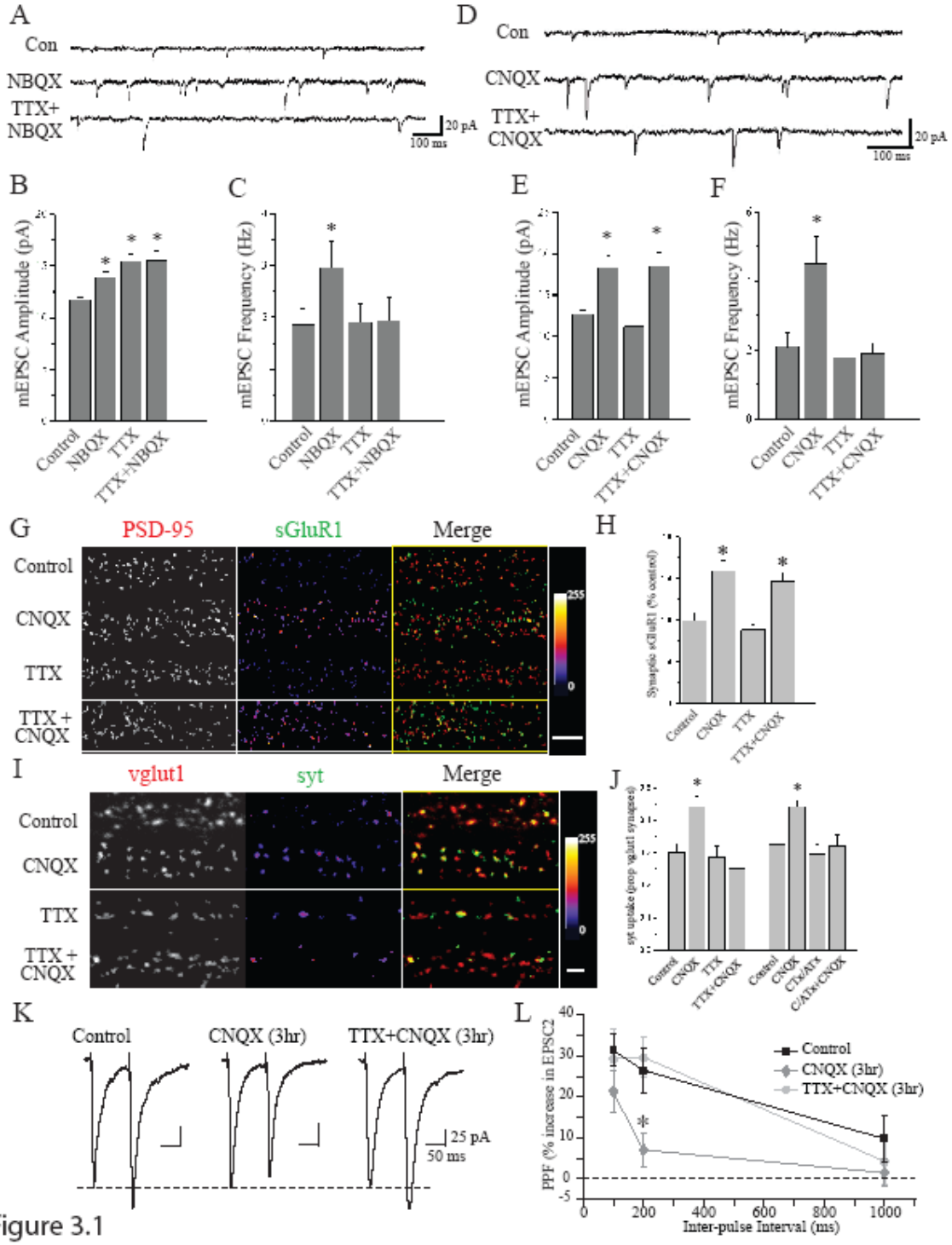
A
Con
NBQX
TTX+
NBQX
20 pA
100 ms
D
Con
CNQX
TTX+
CNQX
20 pA
100 ms
B
mEPSC Amplitude (pA)
Control
NBQX
TTX
TTX+NBQX
C
mEPSC Frequency (Hz)
Control
NBQX
TTX
TTX+NBQX
E
mEPSC Amplitude (pA)
Control
CNQX
TTX
TTX+CNQX
F
mEPSC Frequency (Hz)
Control
CNQX
TTX
TTX+CNQX
G
PSD-95
sGluR1
Merge
Control
CNQX
TTX
TTX +
CNQX
255
0
H
Synaptic sGluR1 (% control)
Control
CNQX
TTX
TTX+CNQX
I
vglut1
syt
Merge
Control
CNQX
TTX
TTX +
CNQX
255
0
J
syt uptake (puncta vglut1 synapses)
Control
CNQX
TTX
TTX+CNQX
Control
CNQX
CTX/ATX
CATX+CNQX
K
Control
CNQX (3hr)
TTX+CNQX (3hr)
25 pA
50 ms
L
PPF (% increase in EPSC2
Control
CNQX (3hr)
TTX+CNQX (3hr)
Inter-pulse Interval (ms)

Figure 3.1

Figure 3.2 Postsynaptic changes induced by AMPAR blockade are unaffected by coincident AP blockade. (A) Full-frame examples of PSD95 (left, red) and surface GluA1 (middle, green) staining from neurons (21-40 DIV) treated, as indicated; merged PSD95/sGluA1 images are shown in the right panel; scale bar = 10 μm. (B) Mean (+SEM) normalized (relative to the average control value) density and intensity of PSD95 particles in the various treatment groups. (C) Mean (+SEM) normalized (relative to the average control value) density and intensity of surface GluA1 particles in the various treatment groups, irrespective of PSD95 colocalization. AMPAR blockade (CNQX) or AMPAR + AP blockade (TTX+CNQX) each produced significant (* $p < 0.05$, relative to control) increases in surface GluA1 expression without accompanying changes in PSD95 expression.

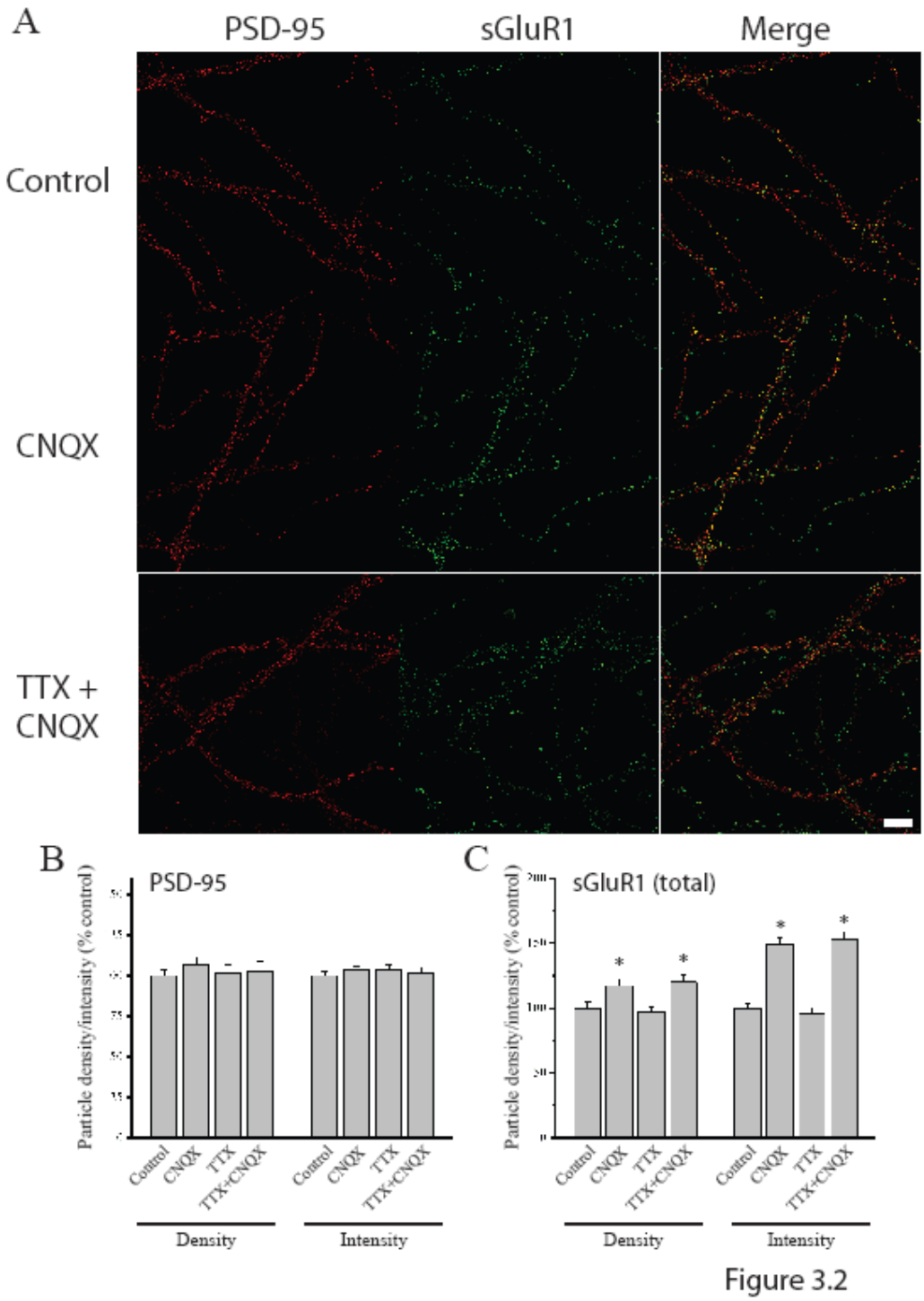
A
PSD-95
sGluR1
Merge
Control
CNQX
TTX +
CNQX
B
PSD-95
Particle density/intensity (% control)
Control
CNQX
TTX
TTX+CNQX
Density
Intensity
C
sGluR1 (total)
Particle density/intensity (% control)
Control
CNQX
TTX
TTX+CNQX
Density
Intensity

Figure 3.2

Figure 3.3 Activity-dependent uptake of syt-lum at synapses. Neurons (21-40 DIV) were live-labeled with a rabbit polyclonal antibody against the lumenal domain of synaptotagmin 1 for 5 min in the presence of 2 μM TTX in either normal HBS or HBS with 60 mM K^+ (equimolar KCl-NaCl substitution), fixed, and processed for immunostaining against bassoon (a structural synaptic marker). (A) Full-frame examples of Bassoon (left, green) and lumenal synaptotagmin (middle, red) staining from neurons treated, as indicated; merged bassoon (green) and syt (red) images are shown in the right panel; fluorescence intensity given by color look-up table; scale bar = 10 μm. Direct depolarization (60 mM K+) of presynaptic terminals markedly enhances syt-lum uptake, demonstrating the activity-dependent nature of syt-lum staining. While weaker, labeling in the presence of TTX and normal K+ is still specific and synaptic. (B). Higher magnification view of the area marked by a dashed box in (A), illustrating strong colocalization (red arrowheads) between syt uptake and bassoon staining; scale bar = 5 μm. (C). Mean (+ SEM) percentage of bassoon-positive synapses with syt-lum labeling in the indicated conditions. Direct terminal depolarization significantly (* $p < 0.05$, relative to TTX alone) enhances syt-lum uptake.

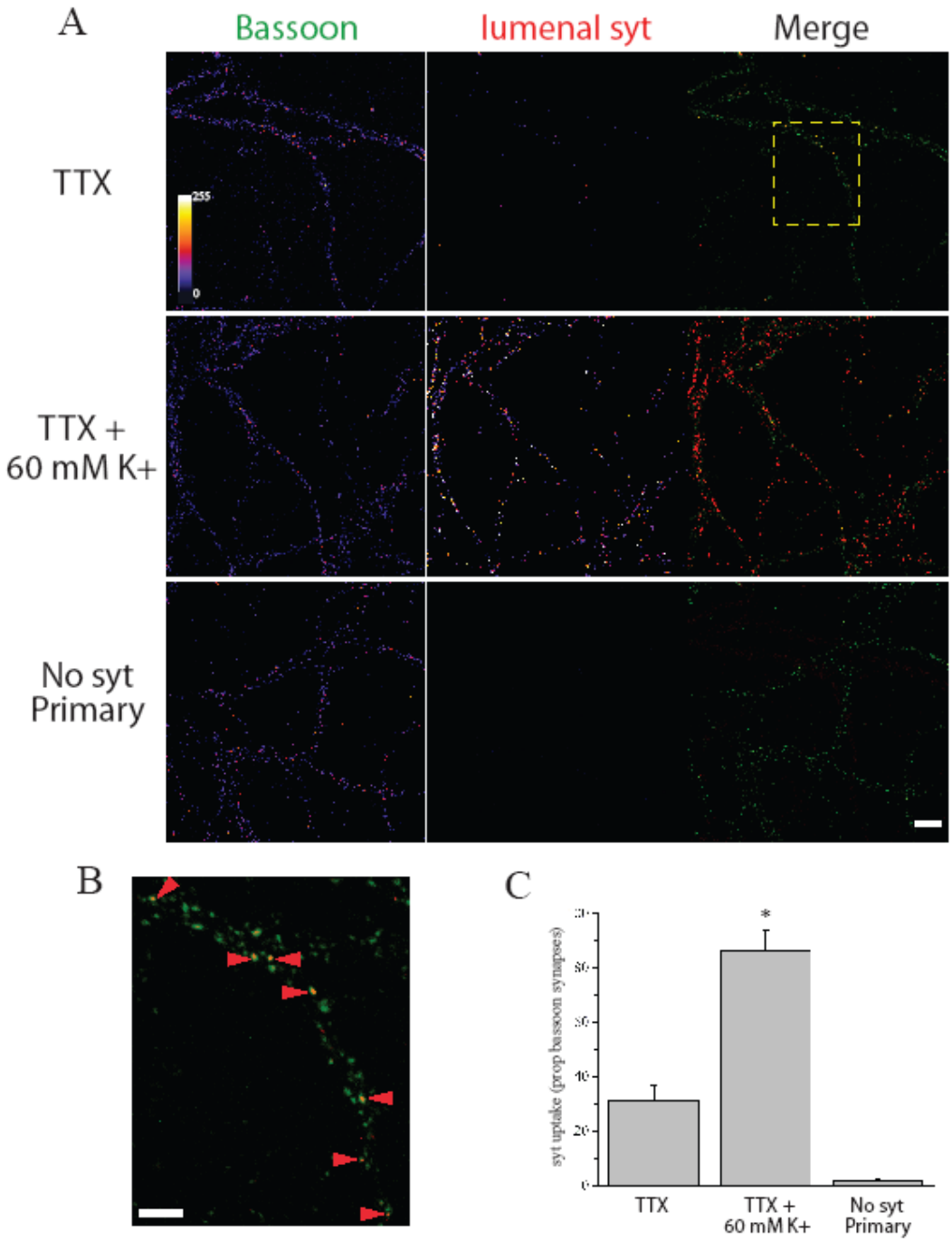
A
Bassoon
lumenal syt
Merge
TTX
255
0
TTX +
60 mM K+
No syt
Primary
B
C
syt uptake (prop bassoon synapses)
*
TTX
TTX +
60 mM K+
No syt
Primary

Figure 3.3

Figure 3.4 Presynaptic changes induced by AMPAR blockade are prevented by coincident AP blockade. (A) Full-frame examples of vglut1 (left, green) and syt-lum (middle, red) staining from neurons (21-40 DIV) treated, as indicated; merged vglut1/syt-lum images are shown in the right panel; scale bar = 10 μm. (B) Mean (+SEM) normalized (relative to the average control value) density and intensity of vglut1 particles in the various treatment groups. (C) Mean (+SEM) normalized (relative to the average control value) density and intensity of syt-lum particles in the various treatment groups, irrespective of vglut1 colocalization. AMPAR blockade (CNQX) significantly (* $p < 0.05$, relative to control) enhanced syt-lum uptake, without changes in overall excitatory synapse density; these changes were prevented by coincident AP blockade (TTX+CNQX). (D) Representative linearized examples of FM4-64FX staining in control neurons or those deprived of activity for 3 hrs via either AMPAR blockade alone (40 μM CNQX), AP blockade alone (2 μM TTX), or both AMPAR + AP blockade (TTX+CNQX); scale bar = 2 μm. (E) Mean (+SEM) normalized (relative to the average control value) density of FM4-64 (black bars) or Bassoon (grey bars) particles in the various treatment groups (21-28 DIV). For the indicated groups (for FM4-64 and Bassoon, respectively): controls (n = 39, 28 neurons), CNQX alone (n =40, 26 neurons), TTX alone (n = 40, 30 neurons), TTX + CNQX (n = 40, 29 neurons). AMPAR blockade (CNQX) produced a significant (*$p < 0.05$, relative to control) increase in FM4-64 uptake that was blocked by coincident AP blockade (TTX+CNQX).

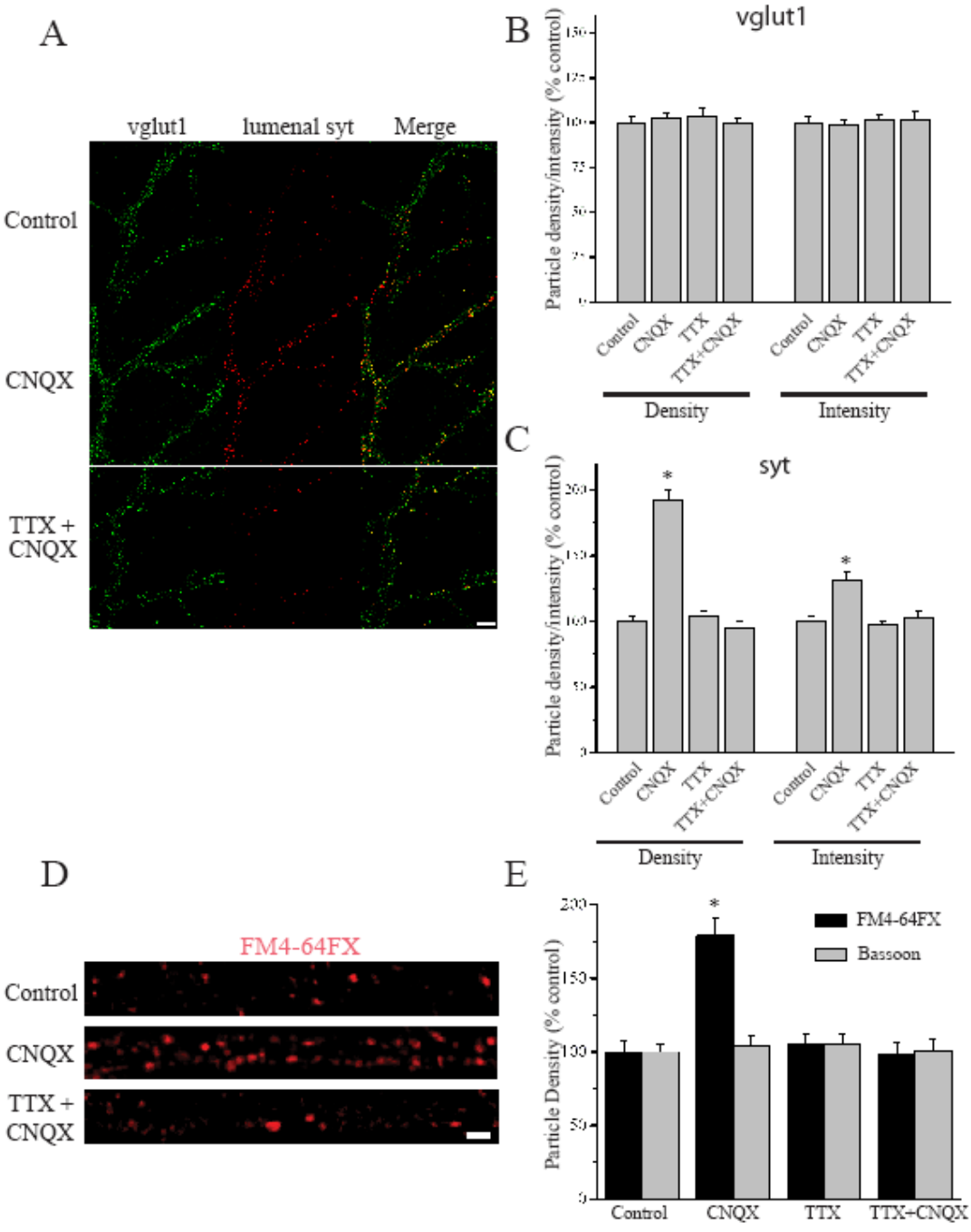
A
vglut1
lumenal syt
Merge
Control
CNQX
TTX + CNQX
B
vglut1
Particle density/intensity (% control)
Control
CNQX
TTX
TTX+CNQX
Density
Intensity
C
syt
Particle density/intensity (% control)
Density
Intensity
D
FM4-64FX
Control
CNQX
TTX + CNQX
E
FM4-64FX
Bassoon
Particle Density (% control)
Control
CNQX
TTX
TTX+CNQX

Figure 3.4

Figure 3.5 Increase in presynaptic function is specific to AMPA receptor blockade. (A) Representative recordings and (B-C) summary of experiments (21-25 DIV) where mEPSCs were recorded under control (untreated) conditions (n = 17), or after short term (3 hr) AMPAR blockade (NBQX; 10 μM; n = 6), or NMDAR blockade (APV; 50 μM; n = 9). Mean (+ SEM) mEPSC amplitude (B) and frequency (C) with treatments as indicated. Both AMPAR and NMDAR blockade produce a significant (* $p < 0.05$, relative to control) increase in mEPSC amplitude, but only AMPAR blockade produces a significant increase in mEPSC frequency. (D-E) Neurons (21 DIV) were treated as indicated then live-labeled with a rabbit polyclonal antibody against the lumenal domain of synaptotagmin 1 for 5 min in the presence of HBS containing 2 μM TTX. (D) Representative examples and (E) mean (+ SEM) syt-lum uptake (DIV 21) in control (untreated; n = 13) neurons and neurons treated for 3 hr with NBQX (10 μM; n = 14; DIV 21) or APV (50 μM; n = 16). AMPAR blockade significantly (* $p < 0.05$, relative to control) enhanced syt-lum uptake, but NMDAR blockade did not, indicating that rapid compensation in presynaptic function is specific for AMPAR blockade.

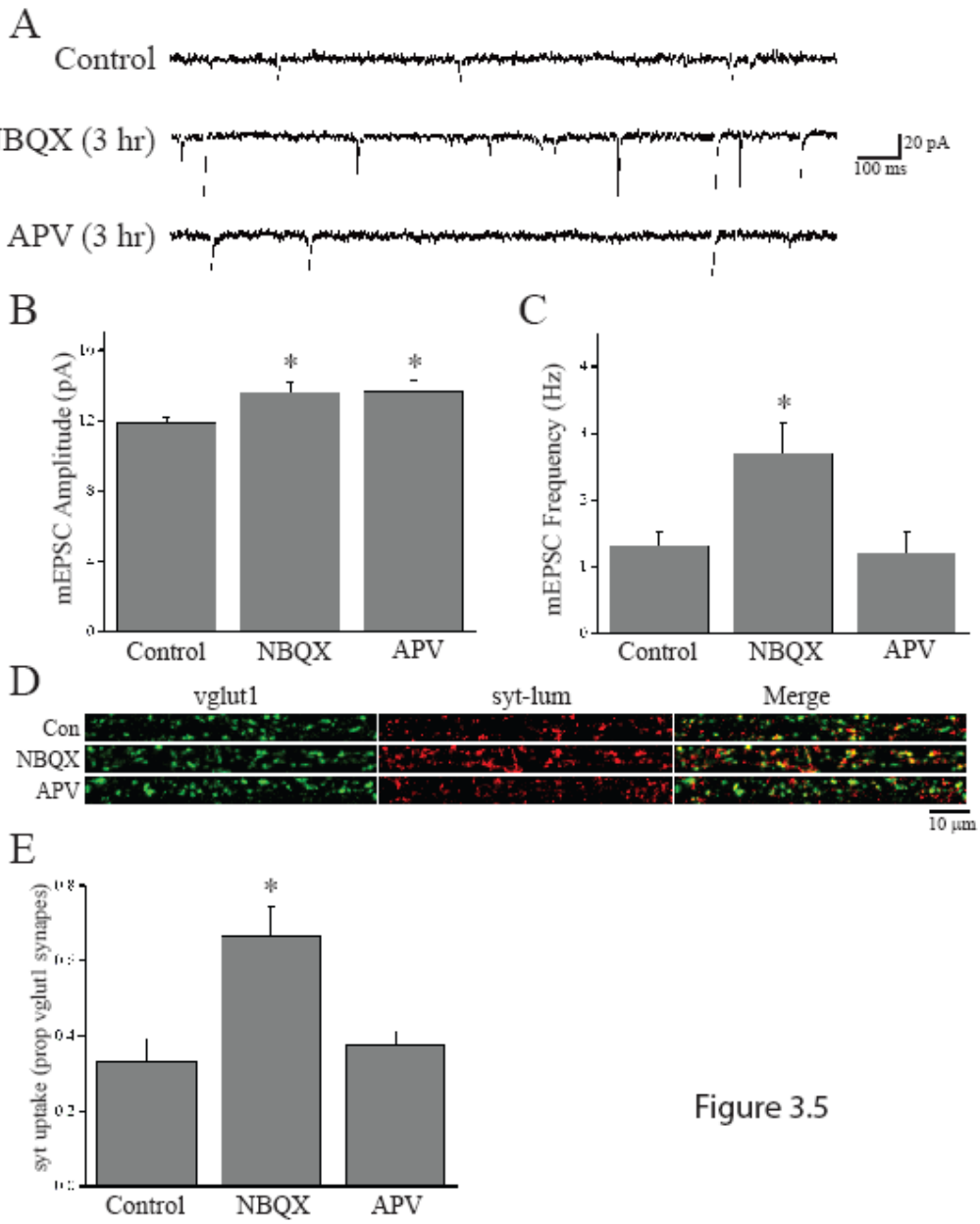
A
Control
NBQX (3 hr)
APV (3 hr)
20 pA
100 ms
B
mEPSC Amplitude (pA)
Control
NBQX
APV
C
mEPSC Frequency (Hz)
Control
NBQX
APV
D
vglut1
syt-lum
Merge
Con
NBQX
APV
10 µm
E
syt uptake (prop vglut1 synapses)
Control
NBQX
APV

Figure 3.5

Figure 3.6 Presynaptic and postsynaptic homeostatic changes are induced by AMPAR blockade in parallel (A-C) Neurons (23-27 DIV) were either untreated (control) or treated with CNQX (40 μM) for 3 hrs prior to washout and subsequent recording of mEPSCs in the presence or absence of 1-Napthylacetylspermine (Naspm; 10 μM) to block activity at GluA1 homomeric receptors (see Sutton et al., 2006). Naspm was applied 15-30 min following CNQX washout. (A) Representative recordings and (B-C) summary data from control neurons (n = 14), neurons treated with CNQX (n = 11), control + Naspm (n = 11), or CNQX-treated cells + Naspm (n = 18). (B) Mean (+ SEM) mEPSC amplitude and (C) frequency for each group as indicated. The increase in mEPSC amplitude induced by CNQX treatment (* $p < 0.05$, relative to control) is abolished by Naspm application. The increase in mEPSC frequency induced by CNQX treatment, however, remains significantly elevated (* $p < 0.05$, relative to control) even in the presence of Naspm. (D) Representative recordings before and after Naspm (10 μM) application from the same neuron previously treated with CNQX (3 hr; 40 μM) (E-F) Summary data of paired recordings (n = 10; 23-27 DIV). (E) Naspm produces a significant decrease in mEPSC amplitude (* $p < 0.05$, paired t-test). (F) A subset of CNQX-treated neurons show a decrease in mEPSC frequency (4/10; left). Mean (+ SEM; right) mEPSC frequency before and after treatment with Naspm; there is a small, but significant (* $p < 0.05$, paired t-test, one tailed) decrease in mEPSC frequency upon the addition of Naspm, but this diminished mEPSC frequency remains significantly elevated relative to untreated neurons. Dashed line in (E) and (F) indicates average mEPSC amplitude and frequency in untreated controls examined in parallel.

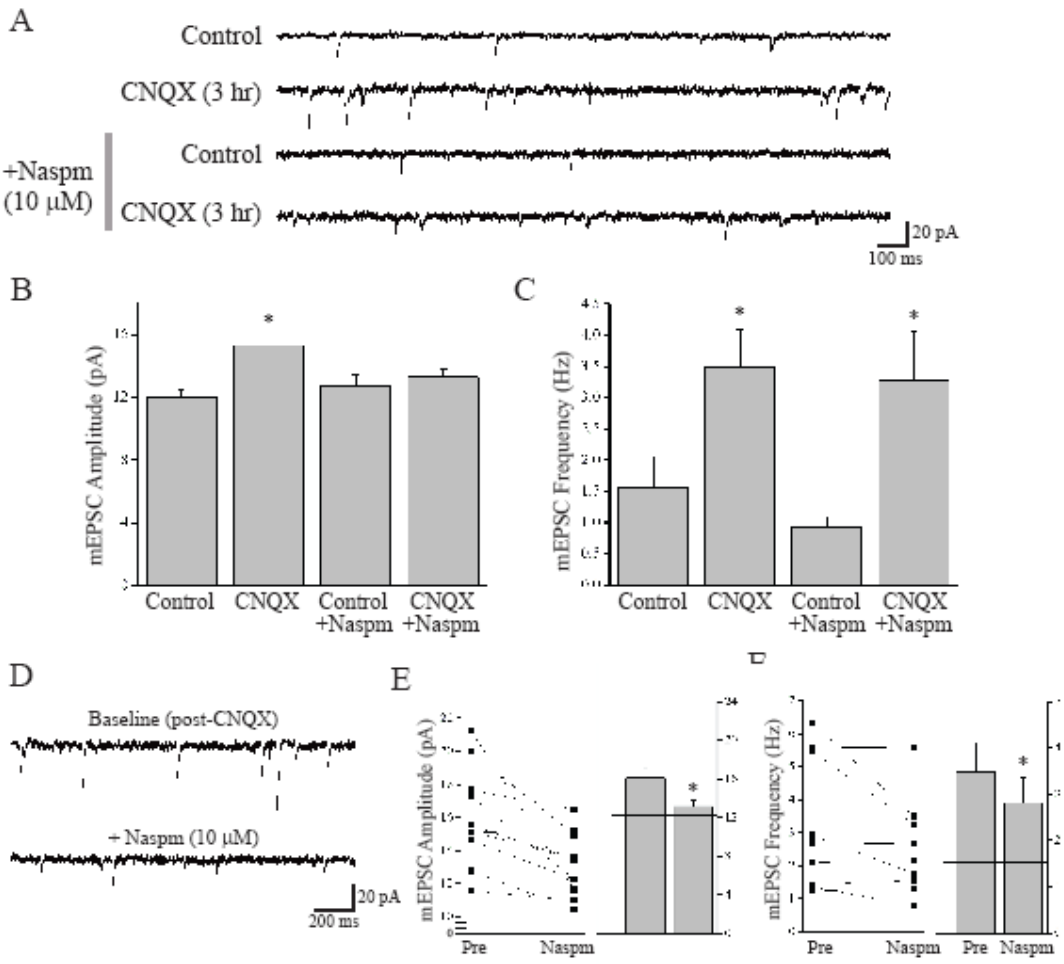
A
Control
CNQX (3 hr)
+Naspm
(10 μM)
Control
CNQX (3 hr)
20 pA
100 ms
B
mEPSC Amplitude (pA)
Control
CNQX
Control
+Naspm
CNQX
+Naspm
C
mEPSC Frequency (Hz)
Control
CNQX
Control
+Naspm
CNQX
+Naspm
D
Baseline (post-CNQX)
+ Naspm (10 μM)
20 pA
200 ms
E
mEPSC Amplitude (pA)
Pre
Naspm
mEPSC Frequency (Hz)
Pre
Naspm
Pre
Naspm

Figure 3.6

Figure 3.7 Local presynaptic activity gates retrograde enhancement of presynaptic function induced by AMPAR blockade (A) Representative DIC image (24 DIV) with superimposed CTx/ATx perfusion spot (red) and syt-lum and vglut1 staining from the same neuron. (B) Linearized dendrite indicated by the arrow shown in (A) with corresponding syt-lum and vglut1 staining registered to the perfusion area (red). Scale bar = 30 μm and 10 μm in (A) and (B), respectively. (C-D) Analysis of group data. On the abscissa, positive and negative values indicate, respectively, segments distal and proximal from the treated area. (C) Mean (± SEM) normalized vglut1 density in treated and untreated dendritic segments; local perfusion did not affect synaptic density. (D) Mean (± SEM) proportion of vglut1-positive synapses with corresponding syt-lum signal in treated and untreated dendritic segments. Coincident AMPAR blockade (20 μM CNQX, 2 hrs) significantly (* $p < 0.05$) increased syt uptake in the treated area in neurons locally treated with vehicle relative to those locally treated with TTX or CTx/ATx. For the groups indicated from top to bottom in (D), n = 10 dendrites from 7 cells; 12 dendrites from 8 cells; 14 dendrites from 10 cells; 11 dendrites from 7 cells (21-35 DIV).

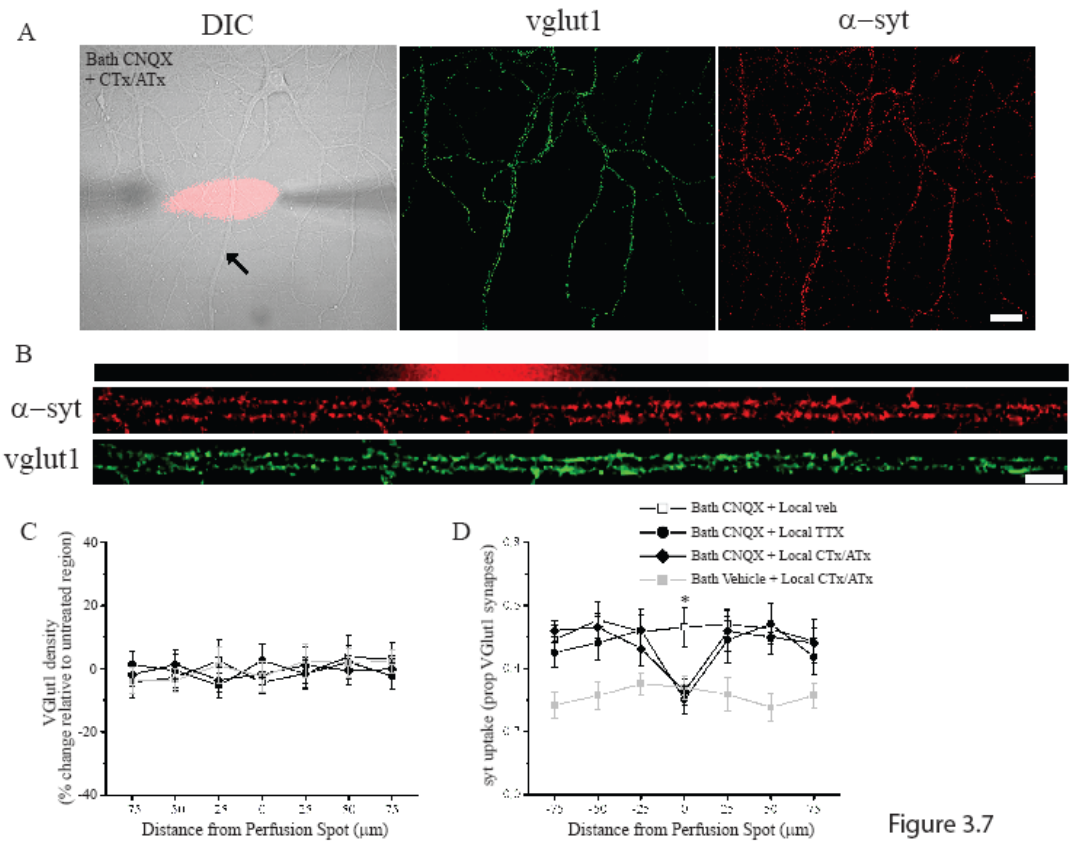
A
DIC
vglut1
α–syt
Bath CNQX
+ CTx/ATx
B
α–syt
vglut1
C
VGlut1 density
(% change relative to untreated region)
Distance from Perfusion Spot (μm)
D
Bath CNQX + Local veh
Bath CNQX + Local TTX
Bath CNQX + Local CTx/ATx
Bath Vehicle + Local CTx/ATx
syt uptake (prop VGlut1 synapses)
Distance from Perfusion Spot (μm)

Figure 3.7

Figure 3.8 BDNF release and signaling are required for presynaptic, but not postsynaptic, compensation induced by AMPAR blockade (A) Representative examples and (B) mean (+ SEM) syt-lum uptake from experiments (25 DIV) where the indicated treatment groups were examined either alone (n = 34 images/group) or co-treated (30 min prior) with trkB-Fc (1 μg/ml; n = 38 images/group) or k252a (100 nM; n = 24 images/group). Scavenging extracellular BDNF (trkB-Fc) or blocking BDNF-induced signaling (k252a) each blocked enhanced syt-lum uptake induced by AMPAR blockade (*$p < 0.05$, relative to control). (C) Representative examples and (D) mean (+ SEM) normalized synaptic sGluA1 expression in the indicated groups (25 DIV). For the groups indicated from left to right, n = 32, 30, 32, 31, 31, 32, 32, 32 images. BDNF is not required for enhanced synaptic GluA1 expression following AMPAR blockade. Scale bars = 5 μm and 10 μm in (A) and (C), respectively. (E) Representative recordings (scale bar = 20 pA, 200 ms) and mean (+ SEM) mEPSC amplitude (F) and frequency (G) in neurons (21-42 DIV) after the indicated treatments either with or without 30 min pre-incubation with 1 μg/ml trkB-Fc. For the indicated groups: control (n = 8, 10), CNQX (n = 11, 12), TTX (n = 8, 8), TTX+CNQX (n = 10, 9). (H-J) Example images (H) and mean (+ SEM) normalized BDNF expression in cell bodies (I) and dendrites (J) of transfected neurons. Scale bar = 10 μm; *$p < 0.05$ vs. scrambled control. (K-M) Representative recordings (K) and mean (+ SEM) mEPSC amplitude (L) and frequency (M) in neurons (21-42 DIV) transfected with either a scrambled control shRNA (Scr) or shRNAs against BDNF. Scale bar = 15 pA, 400 ms. Mean (+ SEM) mEPSC amplitude (L) and frequency (M) in neurons (21-42 DIV) transfected with scrambled shRNA or shRNAs against BDNF.

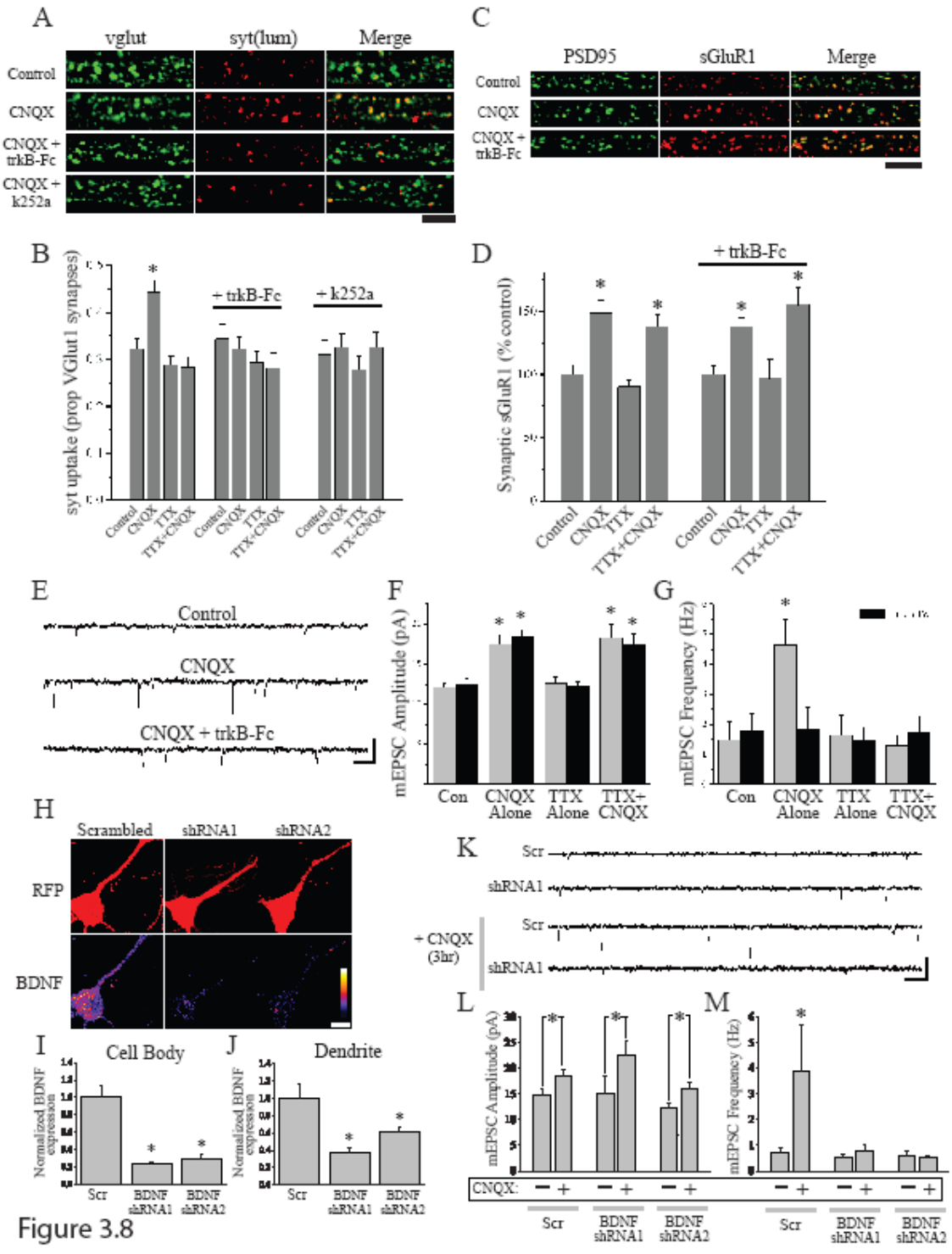
A
vglut
syt(lum)
Merge
Control
CNQX
CNQX + trkB-Fc
CNQX + k252a
C
PSD95
sGluR1
Merge
Control
CNQX
CNQX + trkB-Fc
B
syt uptake (prop VGlut1 synapses)
+ trkB-Fc
+ k252a
Control
CNQX
TTX
TTX+CNQX
D
Synaptic sGluR1 (% control)
+ trkB-Fc
Control
CNQX
TTX
TTX+CNQX
E
Control
CNQX
CNQX + trkB-Fc
F
mEPSC Amplitude (pA)
Con
CNQX Alone
TTX Alone
TTX+ CNQX
G
mEPSC Frequency (Hz)
Con
CNQX Alone
TTX Alone
TTX+ CNQX
H
Scrambled
shRNA1
shRNA2
RFP
BDNF
I
Cell Body
Normalized BDNF expression
Scr
BDNF shRNA1
BDNF shRNA2
J
Dendrite
Normalized BDNF expression
Scr
BDNF shRNA1
BDNF shRNA2
K
Scr
shRNA1
+ CNQX (3hr)
Scr
shRNA1
L
mEPSC Amplitude (pA)
CNQX:
Scr
BDNF shRNA1
BDNF shRNA2
M
mEPSC Frequency (Hz)
Scr
BDNF shRNA1
BDNF shRNA2

Figure 3.8

Figure 3.9 BDNF alters presynaptic function independent of structural synaptic changes or changes in synaptic AMPARs. (A) Neurons (21-28 DIV) were either untreated (controls) or treated for 60 min with BDNF (250 ng/ml) prior to live syt-lum uptake (left) or surface GluA1 labeling (right), followed by fixation and staining for vglut1 or PSD-95, respectively. Left, mean (+SEM) proportion of vglut1-positive excitatory presynaptic terminals with corresponding syt-lum signal in control (n = 15) and BDNF-treated neurons (n = 14). Right, mean (+SEM) normalized (% average control value) surface GluA1 expression at excitatory synapses (colocalized GluA1 and PSD95 particles) in control (n = 16) and BDNF-treated neurons (n = 16). BDNF significantly (* $p < 0.05$, relative to control) enhanced syt-lum uptake at presynaptic terminals, but had no significant effect on surface GluA1 expression at synapses. (B) Mean (+SEM) normalized (relative to 0 min) density and intensity of vglut1 (left) and PSD-95 (right) particles in neurons (25-42 DIV) treated with BDNF (250 ng/ml) for the indicated times. For the groups indicated from left to right in (C), VGLUT1: n = 61, 44, 66, 69 dendrites; PSD-95: n = 17, 16, 15, 18 dendrites. While BDNF produces a significant time-dependent enhancement of presynaptic function (Figure 4), it had no significant effects on the density or intensity of pre- or postsynaptic markers. (C) Mean (+SEM) normalized (relative to untreated control) density and intensity of vglut1 (left) and PSD-95 (right) particles in neurons (DIV 25-28) treated with TrkB-Fc plus the indicated condition; treatments were for 3 hrs. For the groups indicated from left to right in (D), VGLUT1: n = 25, 36, 37, 20 dendrites; PSD-95: n = 21, 20, 23, 30 dendrites. While TrkB-Fc significantly blocks the increase in presynaptic function induced by 3 hr CNQX treatment (Figure 3).

A (Function: + BDNF)

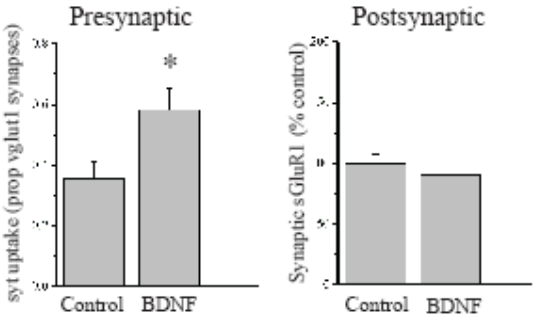

B (Structural: + BDNF)

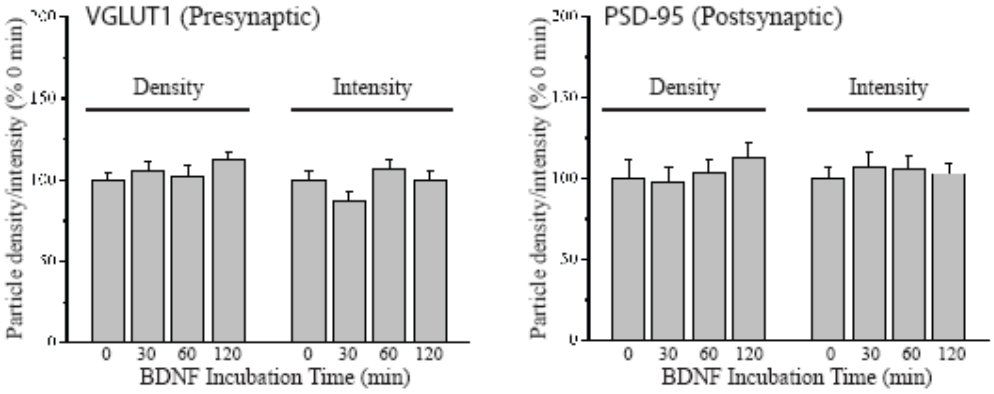

C (Structural: + TrkB-Fc)

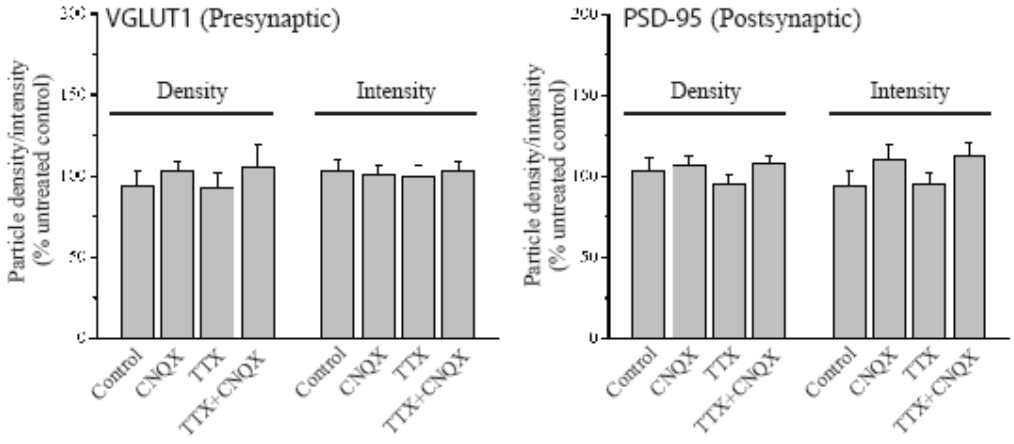

Figure 3.9

Figure 3.10 BDNF enhances presynaptic function in a state-dependent manner (A) Representative examples and (B) mean (± SEM) spontaneous syt-lum uptake from neurons (25-43 DIV) following incubation with BDNF (250 ng/ml) for the indicated times. Color-look up table indicates syt fluorescence intensity; scale bar = 10 μm. BDNF increased spontaneous syt-lum uptake at synapses (* $p < 0.05$, relative to 0 min); coincident treatment with TTX or CTx/ATx completely prevents this effect. (C) Mean (+ SEM) state-depdendent syt-lum uptake as a function of BDNF (2 hr) concentration (* $p < 0.05$ relative control). (D) Representative recordings (scale bar = 20 pA, 200 ms) and (E) mean (+ SEM) mEPSC frequency in neurons (21-51 DIV) treated with BDNF (250 ng/ml, 2 hrs) either alone or coincident with TTX or CTx/ATx. BDNF significantly (* $p < 0.05$ relative control) increases mEPSC frequency which is prevented by AP or P/Q/N-Ca2+ channel blockade. (F) Representative recordings (scale bar = 15 pA, 200 ms) and (G) mean (+ SEM) mEPSC frequency in neurons (21-42 DIV) treated as follows: control (n = 12), BDNF (250 ng/ml, 2 hrs; n = 12), CNQX (40 μM, 3 hrs; n = 12), BDNF+CNQX (n = 8) prior to TTX application and mEPSC recording. Both BDNF and CNQX produce a significant (* $p < 0.05$ relative control) increase in mEPSC frequency, but the combination of the two does not produce a significant additive effect.

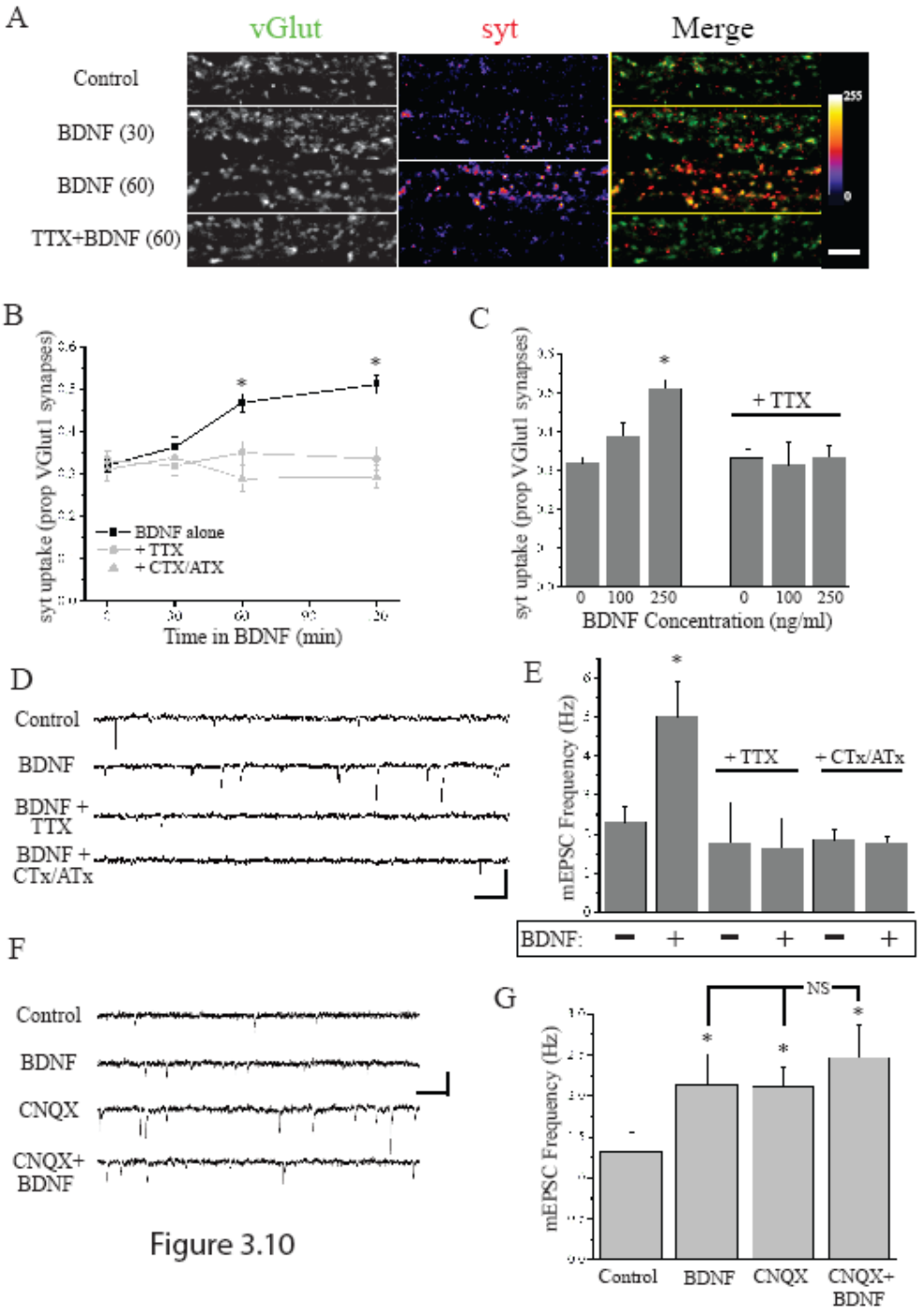
A
vGlut
syt
Merge
Control
BDNF (30)
BDNF (60)
TTX+BDNF (60)
255
0
B
syt uptake (prop VGlut1 synapses)
Time in BDNF (min)
BDNF alone
+ TTX
+ CTX/ATX
C
syt uptake (prop VGlut1 synapses)
+ TTX
0 100 250 0 100 250
BDNF Concentration (ng/ml)
D
Control
BDNF
BDNF + TTX
BDNF + CTx/ATx
E
mEPSC Frequency (Hz)
+ TTX
+ CTx/ATx
BDNF: − + − + − +
F
Control
BDNF
CNQX
CNQX+ BDNF
G
NS
mEPSC Frequency (Hz)
Control
BDNF
CNQX
CNQX+ BDNF

Figure 3.10

Figure 3.11 Local BDNF signaling is necessary and sufficient for homeostatic changes in presynaptic function (A-B) Neurons (21-32 DIV) were perfused with the BDNF scavenger TrkB-Fc (1 μg/ml) for 120 min coincident with either AMPAR blockade (20 μM CNQX to the bath; n = 9 dendrites from 6 neurons) or normal activity (bath vehicle; n = 5 dendrites from 3 neurons). (A) Representative DIC image showing a CNQX-treated neuron with superimposed TrkB-Fc perfusion spot (red) and the same neuron after live-labeling with syt-lum and retrospective vglut1 immunocytochemsitry. (B) Linearized dendrite with corresponding syt-lum and vglut1 staining registered to the perfusion area (red). Scale bar = 20 μm and 10 μm in (A) and (B), respectively. (C-D) Neurons (21-28 DIV) were perfused with BDNF (250 ng/ml) for 60 min in the presence of normal activity (n = 8 dendrites from 5 neurons) prior to live labeling with syt-lum. (C) Representative DIC image with superimposed BDNF perfusion spot (red) and the same neuron after live-labeling with syt-lum and retrospective vglut1 immunocytochemsitry. (D) Linearized dendrite with corresponding syt-lum and vglut1 staining registered to the perfusion area (red). Scale bar = 20 μm and 10 μm in (C) and (D), respectively. (E) Mean (± SEM) normalized vglut1 density in dendritic segments; all data are expressed relative to the average value in untreated segments. (F) Mean (± SEM) proportion of vglut1-positive synapses with corresponding syt-lum signal. Syt-lum uptake was significantly (* $p < 0.05$, relative to untreated segments) diminished in the area treated with TrkB-Fc in CNQX-treated neurons, but not in vehicle-treated neurons. Conversely, local BDNF application significantly (* $p < 0.05$, relative to untreated segments) enhanced syt-lum uptake in the treated area.

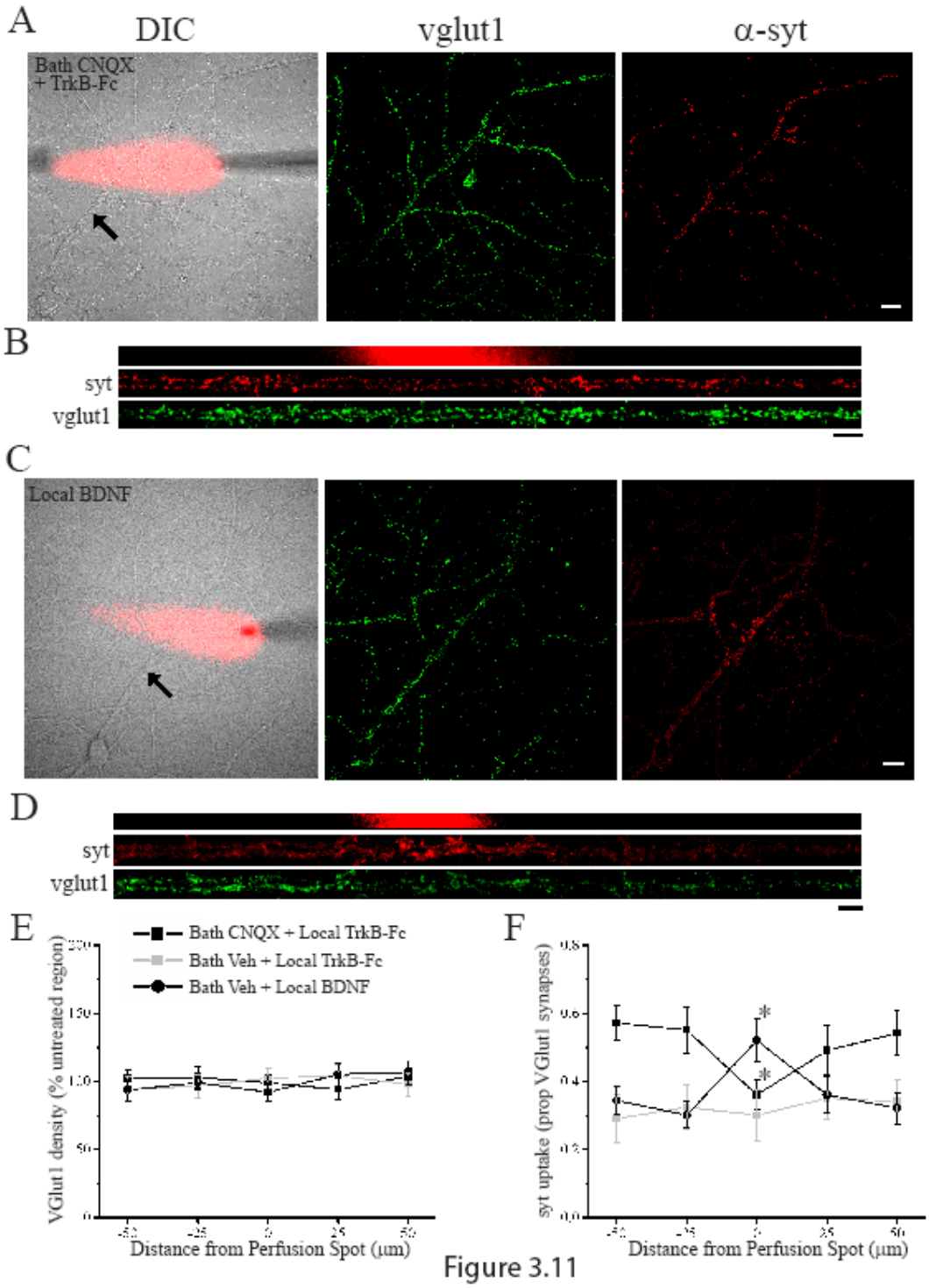
A
DIC
vglut1
α-syt
Bath CNQX
+ TrkB-Fc
B
syt
vglut1
C
Local BDNF
D
syt
vglut1
E
Bath CNQX + Local TrkB-Fc
Bath Veh + Local TrkB-Fc
Bath Veh + Local BDNF
VGlut1 density (% untreated region)
Distance from Perfusion Spot (µm)
F
syt uptake (prop VGlut1 synapses)
Distance from Perfusion Spot (µm)

Figure 3.11

Figure 3.12 BDNF acts downstream of protein synthesis to enhance presynaptic function induced by AMPAR blockade (A) Mean (+ SEM) normalized synaptic sGluA1 expression protein synthesis was blocked with 40 μM anisomycin 30 min prior to and throughout activity blockade. For the groups left to right, n = 38, 38, 38, 34, 40, 44, 48, 48 images (* $p < 0.05$, relative to control). (B) Mean (± SEM) spontaneous syt-lum uptake from neurons following activity blockade in the presence or absence of protein synthesis inhibitors (30 min pretreatment). For the groups left to right, n = 58, 60, 61, 60, 30, 32, 34, 32, 34, 36, 36, 36 images (*$p < 0.05$, relative to control). (C-D) Mean (+ SEM) mEPSC amplitude (C) and frequency (D) in neurons (21-42 DIV) undergoing AP blockade (2 μM TTX, 3 hrs), AMPAR blockade (40 μM CNQX, 3 hrs), or AMPAR + AP blockade (3 hrs). Control (n = 12, 11 cell), CNQX (n = 10, 8), TTX (n = 9, 13), TTX + CNQX (n = 10, 10) (* $p < 0.05$, relative to control). (E) Representative examples and (F) mean (± SEM) spontaneous syt-lum uptake from neurons (24-40 DIV) following incubation with BDNF (250 ng/ml) +/- 40 μM anisomycin or 25 μM emetine (each 30 min prior to BDNF) for the indicated times (* $p < 0.05$, relative to 0 min); the same magnitude and temporal profile of BDNF-induced changes in syt uptake is observed with coincident anisomycin treatment. (G) Mean (+ SEM) syt-lum uptake induced by BDNF in the presence or absence of anisomycin or emetine; (* $p < 0.05$ relative to non-BDNF control). (H) Representative recordings and (I) mean (+ SEM) mEPSC frequency following BDNF application in the presence or absence of protein synthesis inhibitors (neurons 21-34 DIV). For the groups indicated left to right, n = 18, 11, 11, 7, 14, and 17 cells. The significant (* $p < 0.05$) increase in mEPSC frequency induced by BDNF is unaltered by protein synthesis inhibitors.

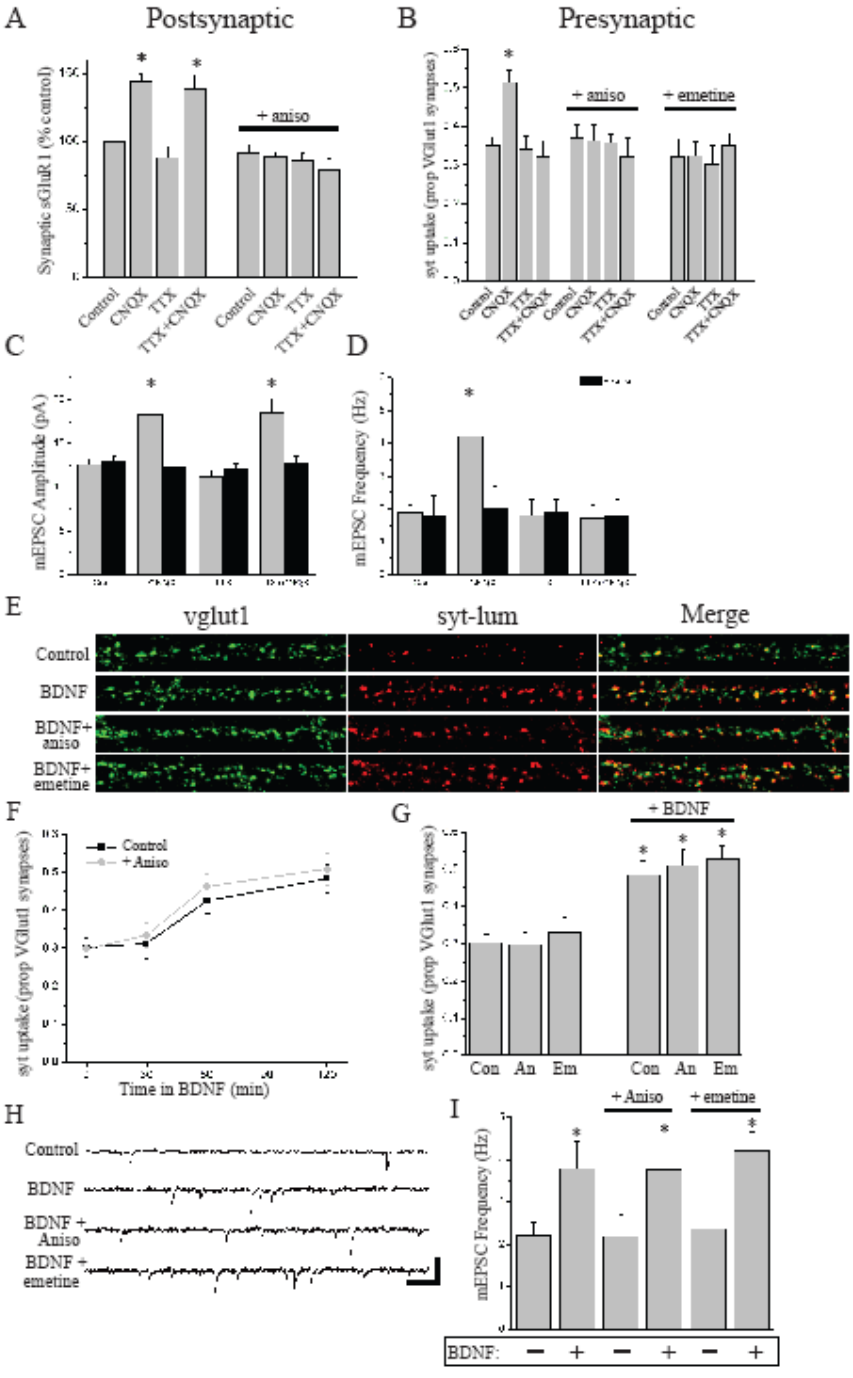
A
Postsynaptic
B
Presynaptic
Synaptic sGluR1 (% control)
syt uptake (prop VGlut1 synapses)
+ aniso
+ emetine
Control
CNQX
TTX
TTX+CNQX
C
D
mEPSC Amplitude (pA)
mEPSC Frequency (Hz)
E
vglut1
syt-lum
Merge
Control
BDNF
BDNF+ aniso
BDNF+ emetine
F
G
Control
+Aniso
Time in BDNF (min)
+ BDNF
Con
An
Em
H
I
BDNF +
Aniso
BDNF +
emetine
BDNF:

Figure 3.12

Figure 3.13 AMPAR blockade enhances synthesis and compartment-specific expression of BDNF (A) Representative Western blots and summary data from experiments with 40 μM CNQX (n = 7) or 50 μM APV (n = 5); * $p < 0.05$ relative to 0 min by chi square. (B) Representative Western blots and summary data in experiments (n = 6) where neurons (DIV 21-32) were treated with CNQX (40 μM, 60 min) +/- anisomycin (40 μM, 30 min before) before harvesting; * $p < 0.05$ relative to CNQX + Aniso (t-test). (C) Representative examples of MAP2 and BDNF staining from a control neuron and one treated with CNQX (40 μM, 2 hrs). (D) BDNF expression in linearized somatic and dendritic segments. (E) 3D plot of relative pixel intensity for the linearized images. Ffluorescence intensity given by color-look table; Scale Bar = 20 μm. (F) Mean (+ SEM) expression of MAP2 and BDNF in somatic and dendritic compartments and BDNF expression in axons, normalized to average control values (*$p < 0.05$, relative to control). Axonal BDNF expression was unaltered by AMPAR blockade (n = 42) relative to untreated controls (n = 41). (G) Mean (+ SEM) dendritic expression of MAP2 and BDNF, normalized to the average control value, in control (untreated) neurons (n = 25) or those treated with CNQX (40 μM, 2 hrs; n = 31), CNQX + emetine (25μM, 30 min prior to CNQX; n =22), or emetine alone (n = 22) (* $p < 0.05$, relative to control). (H) Mean (+ SEM) normalized dendritic expression of BDNF after AMPAR blockade (40 μM CNQX, 2 hrs), AP blockade (2 μM TTX, 2 hrs), or AMPAR + AP blockade (TTX+CNQX); the same conditions were also examined with 30 min anisomycin (40 μM) pre-treatment (28-42 DIV) (* $p < 0.05$, relative to control). Left to right, n = 46, 39, 39, 38, 26, 22, 20, 20 neurons.

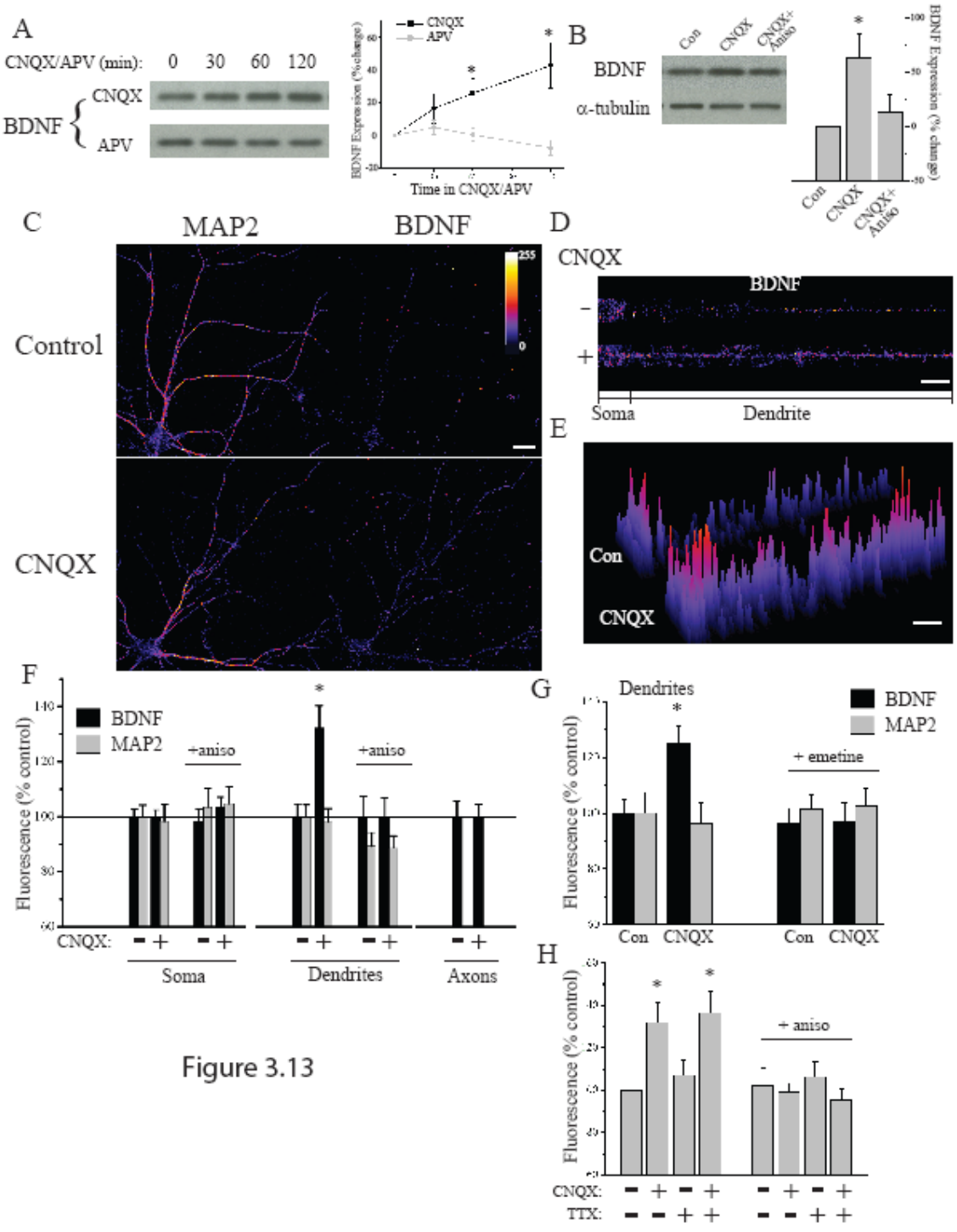
A
CNQX/APV (min): 0 30 60 120
BDNF
CNQX
APV
CNQX
APV
Time in CNQX/APV
B
BDNF
α-tubulin
Con
CNQX
CNQX+ Aniso
BDNF Expression (% change)
C
MAP2
BDNF
Control
CNQX
255
0
D
CNQX
BDNF
Soma
Dendrite
E
Con
CNQX
F
BDNF
MAP2
+aniso
Fluorescence (% control)
CNQX:
Soma
Dendrites
Axons
G
Dendrites
BDNF
MAP2
+ emetine
Con
CNQX
H
+ aniso
CNQX:
TTX:

Figure 3.13

Figure 3.14 Blockade of glutamate miniature synaptic activity does not globally increase BDNF expression (A) Full-frame examples of MAP2 and BDNF staining in untreated (control) neurons (n = 41) or neurons treated for 120 min with 50 μM APV (n = 40); scale bar = 20 μm. (B) Mean (+SEM) normalized (relative to the average control value) BDNF expression in either neuron somata (left) or dendrites (right). In contrast to AMPAR blockade, NMDAR blockade did not significantly alter BDNF expression in either compartment. Experiments were conducted at 21-28 DIV. (C) Full-frame image depicting co-staining for MAP2 (Alexa 488-conjugated goat anti-mouse secondary; green) and neurofilament (NF, using direct Zenon-Alexa 568 conjugation; red), showing non-overlapping dendritic and axonal staining, respectively; scale bar = 20 μm. (D) Representative examples of BDNF staining in axons in both untreated (control) neurons and following 2 hr CNQX treatment; scale bar = 5μm. AMPAR blockade did not alter BDNF expression in axons (see also, Figure 3.15F). (E) Full-frame examples of GFAP (left) and BDNF (right) staining from astrocytes (24-36 DIV), in either control (n = 75 cells) or CNQX (40 μM, 2 hrs; n = 86 cells)-treated cultures; scale bar = 10 μm. (F) Mean (+SEM) normalized (relative to the average control value) BDNF expression in either astrocytic somata (left) or astrocytic processes (right). AMPAR blockade did not significantly alter glial BDNF expression.

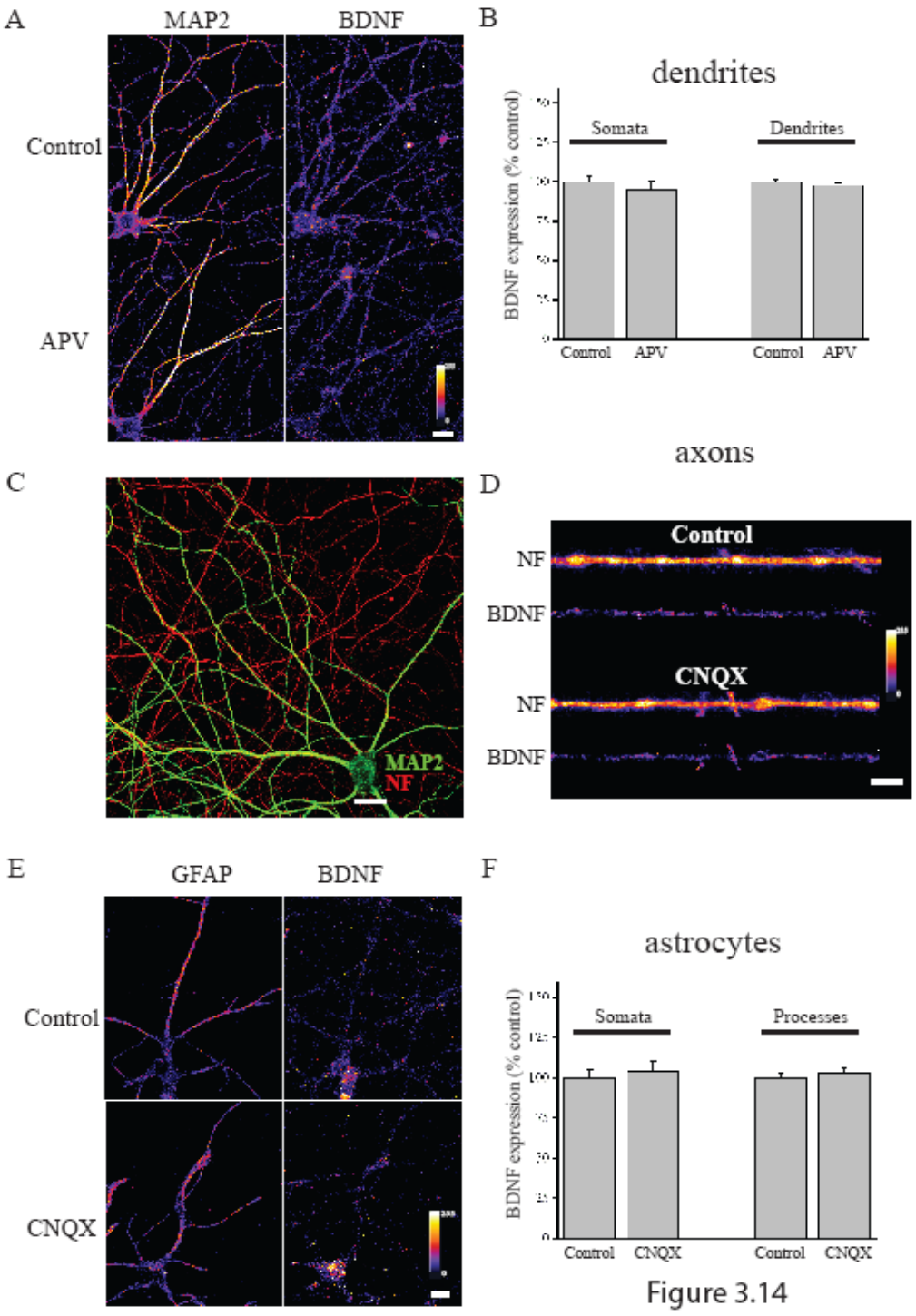
A
MAP2
BDNF
Control
APV
B
dendrites
Somata
Dendrites
BDNF expression (% control)
Control
APV
Control
APV
C
MAP2
NF
D
axons
Control
NF
BDNF
CNQX
NF
BDNF
E
GFAP
BDNF
Control
CNQX
F
astrocytes
Somata
Processes
BDNF expression (% control)
Control
CNQX
Control
CNQX

Figure 3.14

Figure 3.15 AMPAR blockade drives dendritic BDNF synthesis (A) Representative DIC image of a cultured hippocampal neuron (DIV 21) with superimposed emetine (25 μM) perfusion spot (red) and the same neuron after retrospective staining for BDNF and MAP2 from an experiment including coincident AMPAR blockade (bath 40 μM CNQX, 60 min). BDNF/MAP2 fluorescence intensity indicated by color look-up table; scale bar = 20 μm. (B) Linearized dendrite indicated by the arrow cell shown in (A) with corresponding BDNF and MAP2 staining registered to the perfusion area (red). (C) 3D plot of fluorescence intensity for the dendrites shown in (B) relative to the perfusion area; a clear decrease in BDNF expression in the treated area is apparent. (D) Mean (± SEM) normalized BDNF/MAP2 expression in treated and un-treated dendritic segments from the indicated groups (21-31 DIV); all data are expressed relative to the average value in untreated segments. On the abscissa, positive and negative values indicate, respectively, segments distal and proximal from the treated area. Local emetine perfusion significantly (* $p < 0.05$) decreased BDNF expression in the treated area relative to other segments of the same dendrite when CNQX was present (n = 11 dendrites from 7 neurons), but not when vehicle was applied to the bath (n = 9 dendrites from 6 neurons); MAP2 expression in the same neurons was unaltered in the treated area.

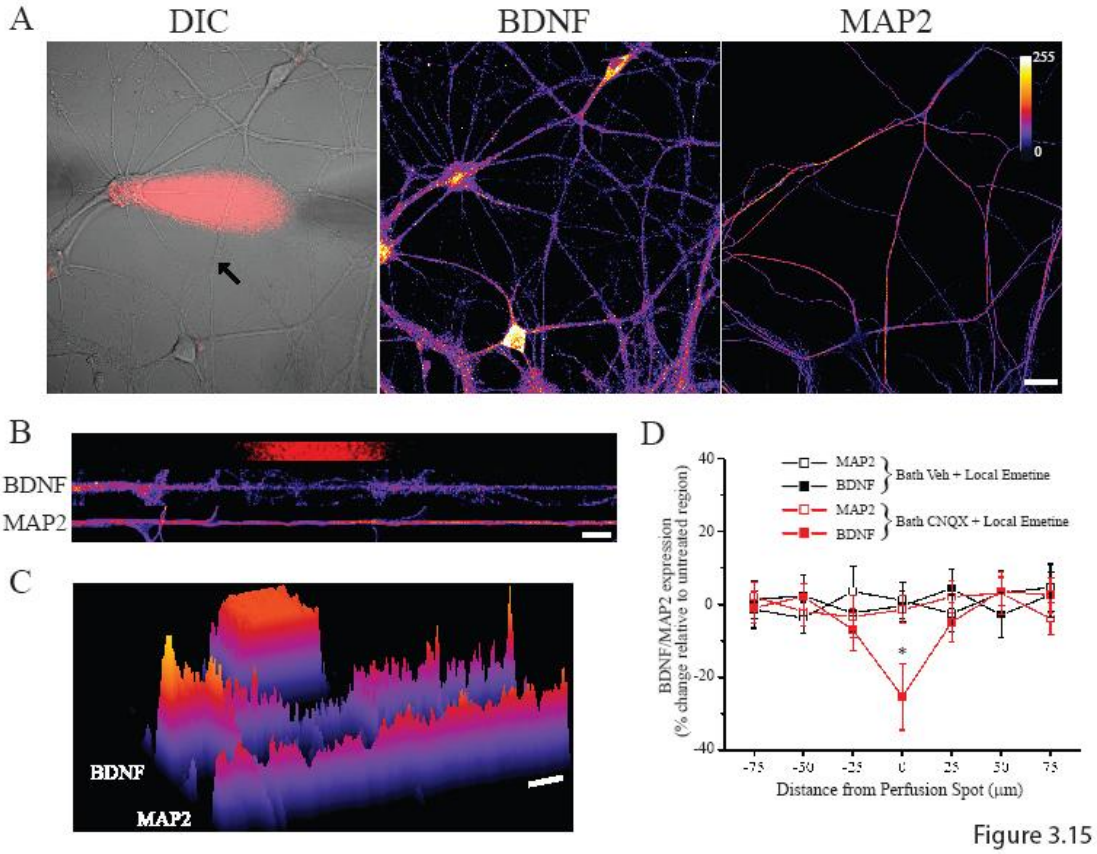
A
DIC
BDNF
MAP2
255
0
B
BDNF
MAP2
C
BDNF
MAP2
D
MAP2
BDNF
Bath Veh + Local Emetine
MAP2
BDNF
Bath CNQX + Local Emetine
BDNF/MAP2 expression
(% change relative to untreated region)
40
20
0
-20
-40
*
-75
-50
-25
0
25
50
75
Distance from Perfusion Spot (µm)

Figure 3.15

Figure 3.16 Parallel roles for dendritic protein synthesis in compensatory presynaptic and postsynaptic changes induced by AMPAR blockade. Model depicting key events underlying rapid homeostatic compensation. AMPAR blockade induces rapid postsynaptic compensation via synaptic incorporation of GluA1 homomeric AMPARs (Thiagarajan et al., 2005) that emerges rapidly (< 3 hrs) and requires new protein synthesis. Studies examining the effects of NMDAR mini blockade have shown that the compensatory synaptic incorporation of GluA1 homomers requires local dendritic synthesis, likely of GluA1 itself (Ju et al., 2004; Sutton et al., 2006; Aoto et al., 2008). These changes in GluA1 are observed equally in the presence and absence of spiking activity (Figure 1). In parallel, AMPAR blockade induces rapid presynaptic compensation that requires coincident activity in presynaptic terminals. The presynaptic changes require the synthesis and release of BDNF, which is locally translated in dendrites in response to AMPAR blockade.

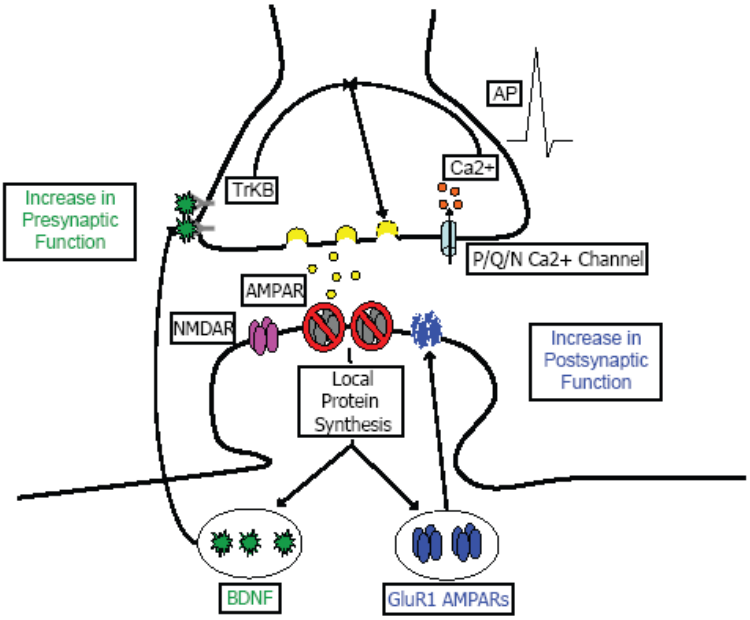
AP
Ca2+
TrKB
Increase in Presynaptic Function
P/Q/N Ca2+ Channel
AMPAR
NMDAR
Increase in Postsynaptic Function
Local Protein Synthesis
BDNF
GluR1 AMPARs

Figure 3.16

CHAPTER IV

Activity dependent localization of the proteasome gates state-dependent homeostatic plasticity

Introduction

Homeostatic plasticity is an ubiquitously expressed form of neuron plasticity that functions to constrain neuron networks within a dynamic, yet stable, functional range (Turrigiano 2008; Pozo and Goda 2010). Diverse mechanisms of homeostatic plasticity exist both at the network (Aptowicz et al., 2004; Maffei et al., 2004; Echegoyen et al., 2007; Swann et al., 2007; Chen et al., 2008; Hartmann et al., 2008; Kim and Tsien, 2008) see also (Murthy et al., 2001; MacLean et al., 2003) as well as at the synaptic level (Rao and Craig 1997; Lissen et al., 1997; O'Brien et al., 1998; Turrigiano et al., 1998; Sutton et al., 2006; Frank et al., 2006; Gong et al., 2007) and recent evidence suggests that homeostatic adaptation is due to robust, yet reversible, changes in protein expression (Ehlers 2003; Aptowicz et al., 2004). Despite progress on understanding how neuron networks respond to activity changes at either the network or synaptic level, little is known about how neurons mediate the interaction between multiple types of activity during homeostatic plasticity. Interestingly, inhibition of more than one facet of activity can alter the temporal and spatial properties of homeostatic plasticity (Sutton et al., 2006;

Jakawich et al., in press; see also Thiagarajan et al., 2005; Gong et al., 2007; Lindskog et al., in press). Previously, we have shown that acute (3 hr) AMPAR blockade with CNQX (40 μM) simultaneously induces two, molecularly distinct forms of homeostatic compensation within the same subset of synapses: 1) a local postsynaptic increase in mEPSC amplitude accompanied by an increase in surface GluA1 (sGluA1) expression and 2) a local presynaptic increase in release probability that requires coincident presynaptic spiking and retrograde synaptic signaling of brain derived neurotrophic factor (BDNF). Presynaptic compensation, downstream of AMPAR blockade, has been termed "state-dependent homeostatic plasticity" to underscore the requirement for presynaptic action potential firing during concomitant synaptic inhibition.

State-dependent homeostatic plasticity is an enduring form of compensatory plasticity lasting ≥ 90 min after the removal of activity blockade (Figure 3.1) and previous work has demonstrated that co-application of a protein synthesis inhibitor, anisomycin, during AMPAR blockade completely prevents functional compensation in both presynaptic and postsynaptic compartments (Figure 3.12). Therefore, it has been proposed that AMPAR blockade induces two, independent mechanisms of activity dependent synapse remodeling (Jakawich et al., in press). Interestingly, protein synthesis is not the sole mechanism responsible for rapid, activity dependent synaptic compensation. State-dependent changes in function, downstream of AMPAR blockade, additionally require retrograde synaptic signaling by BDNF (see also Lindskog et al., in press; Figure 3.8, 9, 10, 11). Curiously, protein synthesis inhibitors fail to block state-dependent homeostatic plasticity induced by direct application of exogenous BDNF (Figure 3.12). These data suggest a mechanism by which state-dependent alterations in

presynaptic protein expression are mediated by a non-protein synthesis dependent mechanism, downstream of both AMPAR blockade and BDNF signaling through its high affinity receptor TrkB.

The ubiquitin proteasome system (UPS) is responsible for degradation of most cytosolic proteins and targets proteins for degradation through covalent modification with a small 76 amino acid protein, ubiquitin (Hershko and Ciechanover, 1992, 1998). It is the subsequent conjugation of 4 or more ubiquitins to a target substrate (polyubiquitination) that initiates degradation of the target protein by a large enzymatic complex, the proteasome (Hershko and Ciechanover, 1992, 1998). Previously, it has been demonstrated that protein degradation by the ubiquitin proteasome system (UPS) is necessary for the maintenance of several forms of enduring neuron plasticity. The UPS is necessary for degradation of the catalytic subunit of PKA during long term facilitation [(LTF; (Hegde et al., 1993)] and Fragile X Mental Retardation protein alpha (FMRFα) induced long term depression (LTD; Fivorante et al., 2008) in *Aplysia*. The UPS if further required for the induction (Dong et al., 2008; Cai et al., 2010) as well as the maintenance (Fonseca et al., 2006) of long term potentiaion (LTP; Karpova et al., 2006; Dong et al., 2008; Cai et al., 2010) and AMPAR endocytosis during LTD (Colledge et al., 2003) in mammals. Proteasome function is further required for consolidation of one-trial inhibitory avoidance learning (Lopez-Salon et al., 2001) as well as the re-entrance of contextual fear memories into a labile state during memory retrieval (Lee et al., 2008) demonstrating that the UPS is necessary for activity-dependent synapse remodeling during several enduring forms of neuron plasticity and memory suggesting, that the

proteasome could be responsible for regulating synaptic composition during state-dependent homeostatic plasticity.

Recently, it has been shown that proteasome function is additionally necessary for homeostatic silencing of presynaptic terminals (Jiang et al., 2010) as well as rapid (min - hr) homeostatic adaptation of presynaptic release probability (Willeumeier et al., 2006 and Rinetti et al., 2010). Proteasome inhibition rapidly and reversibly increases presynaptic function as measured by changes in mEPSC frequency following global application of MG132 (Rinetti et al., 2010). Prolonged depolarization of cultured hippocampal neurons results in homeostatic silencing of presynaptic terminals (Moulder et al., 2004, 2006) but interestingly, the decrease in presynaptic function is blocked by concurrent inhibition of the proteasome, with MG132 (Jiang et al., 2010). Presynaptic silencing is accompanied by a decrease in the expression levels of Munc13-1 and Rim1α, proteins critical for presynaptic vesicle priming, whose expression was restored upon co-application of MG132 (Jiang et al., 2010). These studies suggest that proteasome function is required for rapid, activity dependent modification of basal presynaptic release probability likely due to proteasomal maintenance of synapse number (Jiang et al., 2010). Given the ability of the proteasome to regulate synapse number and function, it seems likely that protein degradation may play a key role in regulating rapid, state-dependent changes in presynaptic function.

Interestingly, further evidence suggests that there is an intimate link between neuron network activity, proteasome localization and synaptic function (Bingol et al., 2006; Willeumeier et al., 2006; Zhang et al., 2007; Djakovic et al., 2009; Bingol et al., 2010) suggesting that proteasome function and/or localization may be gating network

induced changes in presynaptic state-dependent function. Two hour proteasome inhibition with lactacystin or epoxomycin increases the size of the readily releasable pool of synaptic vesicles, in an activity dependent manner (Willeumeir et al., 2006). Co-application of tetrodotoxin (TTX), a voltage gated Na^+ channel blocker, with either lactacystin or epoxymycin completely prevents the increase in the readily releasable pool size (Willeumeier et al., 2006) and suggests that network activity may be poised to directly regulate presynaptic release probability through basal proteasome function (Willeumeier et al., 2006). Indeed, disruption of neuron network activity with either TTX or bicuculline (a $GABA_A$ receptor antagonist) can decrease or increase the basal rate of proteasome function, respectively (Djakovic et al., 2009; Figure 2.4) presumably through activity dependent phosphorylation of the proteasome itself (Djakovic et al., 2009). Furthermore, global depolarization of cultured neuron networks with high K^+ rapidly traffics the proteasome complex into dendritic spines where it remains sequestered during high K^+ treatment (Bingol et al., 2010). Together, these data provide evidence for a model in which network activity may gate state-dependent changes in presynaptic function through activity mediated presynaptic localization of the proteasome.

Here, we demonstrate that protein degradation, by the proteasome, is required for presynaptic state-dependent compensation in cultured hippocampal neurons. Consistent with previous results, blockade of AMPARs (CNQX, 40 μM, 3 hr) increased both pre- and post- synaptic function, as measured by mEPSC amplitude and frequency. Co-application of a proteasome inhibitor, either lactacystin (lac; 10 μM, 30 min pretreatment) or MG132 (10 μM, 30 min pretreatment) did not affect postsynaptic compensation, but selectively blocked the increase in state-dependent presynaptic function, providing

evidence for a specific role for proteasome mediated degradation in the presynaptic compartment. Indeed, BDNF induced state-dependent homeostatic plasticity (which mimics presynaptic state-dependent plasticity induced by CNQX; Figure XX) is also blocked with pretreatment by either lac or MG132. Furthermore, state-dependent increases in presynaptic function specifically require presynaptic but not postsynaptic polyubiquitination as well as the phosphorylation of Rpt6, a critical regulatory subunit of the proteasome. Finally, we demonstrate that localization of the proteasome to presynaptic terminals is mediated by basal levels of action potential activity and that localization of the proteasome is completely independent of AMPAR blockade, which likely reflects the requirement for action potentials during presynaptic state-dependent homeostatic plasticity.

Experimental Procedures

Cell Culture

Hippocampi from Sprague-Dawley rat pups (P1-P3) were rapidly dissected in cold dissociation media (DM; 82 mM Na_2SO_4, 30 mM K_2SO_4, 5.8 mM $MgCl_2$-$6H_2O$, 252 µM $CaCl_2$-$2H_2O$, 1 mM HEPES, 200 mM glucose, 0.001% w/v phenol red), and transferred to a 15 ml conical tube. The DM was gently removed (leaving ~500 µl of DM to keep the tissue covered), and replaced with 5 ml of pre-warmed (37ºC) cysteine-activated papain solution [3.2 mg L-cysteine (Sigma-Aldrich; Saint Louis, MO) with 500 µl papain (Sigma-Aldrich; Saint Louis, MO) in 10 ml DM, pH ~ 7.2], and incubated for 15 min at 37ºC to allow for tissue digestion; halfway through the incubation, the tube was

inverted ~2-3 times. Cells were then washed 2X in ice-cold DM containing 12.5 % v/v fetal bovine serum to inactivate the papain, followed by 2 washes in DM alone. The cells were then washed 2X in chilled normal growth medium [NGM; Neurobasal A (Gibco; Grand Island, NY) supplemented with 2% v/v B27 (Invitrogen; Carlsbad, CA) and 1% v/v Glutamax (Invitrogen; Carlsbad, CA)], triturated ~10-15 times in 5 ml NGM to obtain a single cell suspension and placed on ice for ~3-5 min. 4.5 ml of the cell suspension were removed from the middle of the cell solution to avoid contaminant material and the cells were placed in a new 15 ml tube and centrifuged for 10 min at 67 x g (0.5 x 1000 rcf) at 4ºC. 50-70K cells (in a volume of 150 µl) were plated onto poly-D-lysine-coated glass-bottom petri dishes (Mattek; Ashland, MA) and maintained at 5% CO2/37ºC. 4 hrs after plating, 2 ml of NGM-GC (NGM supplemented with 15% v/v glial conditioned media and 10% v/v cortical conditioned media) were added to each dish. Cells were fed 24 hr later by replacing 50% of their media with fresh NGM-GC and every 4 days thereafter by replacing 25% of their media with fresh media. Cells were maintained for 14 days in NGM-GC, and fed in 4 day intervals thereafter with NGM alone. All neurons used for experiments developed for $\geq$ 21 DIV, a time at which synaptic connections are fully mature and network activity is stable.

Plasmids and calcium phosphate transfections

Synaptophysin-YFP was a kind gift from Hisashi Umemori, and WtUb K48R. WT Rpt6, S120A and S120D were kindly provided by Gentry Patrick (UCSD). Neurons were transfected with 0.5 µg of total DNA using the CalPhos Transfection kit (ClonTech;

Mountain View, CA) according to the manufacturer's protocol. All experiments were performed 24-48 hr post transfection.

Whole-Cell Patch Clamp Electrophysiology

Pharmacological agents were added to cultured hippocampal neurons (≥21 DIV) in conditioned media at times as indicated for each reagent. Prior to recording, cells were washed 1X and maintained in HEPES-buffered saline (HBS; 119 mM NaCl, 5 mM KCl, 2 mM $CaCl_2$, 2 mM $MgCl_2$, 30 mM glucose, 10 mM HEPES; pH 7.4) containing 1μM TTX (Calbiochem; San Diego, CA) and 10 μM bicuculline (Tocris; Ellisville, MO). Whole cell patch-clamp recordings were performed using glass recording pipettes, with resistances of 4-6 MΩ when filled with internal solution (100 mM cesium gluconate, 0.2 mM EGTA, 5 mM $MgCl_2$, 40 mM HEPES, 2 mM Mg-ATP, 0.3 mM Li-GTP, pH 7.2). Pyramidal-like neurons were identified for recording based on cell morphology (the presence of a large apical dendrite and a large pyramidal-like cell body). Membrane potential was clamped at -70 mV and miniature excitatory postsynaptic currents (mEPSCs) were recorded using an Axopatch 200B amplifier and Clampex 8.0 software (Molecular Devices). mEPSCs were analyzed off-line using MiniAnalysis (Synaptosoft).

Total fluorescence HA immunocytochemistry

For fixation, neurons were incubated with warmed (37ºC) 4% PFA/4% sucrose for 20 min at room temperature (RT). The fixed cells were then permeabilized (0.1%

Triton X-100 in PBS-MC, 15 min RT) and blocked (2% BSA in PBS-MC, 30 min RT) prior to staining with a primary antibody for HA (1:500 in 2% BSA, 1 hr RT, Cell Signaling, Danvers, MA). Following the incubation with the primary antibody, cells were washed 3X in PBS-MC and incubated with goat anti mouse Alexa 555 (1:500 in 2% BSA for 60 min at RT, Molecular Probes, Eugene, OR). Neurons stained for HA were imaged on an Olympus FV1000 inverted confocal microscope using a Plan Apochromat 60x/1.4 NA objective and 2X digital zoom. Areas of interest were selected for imaging guided by epifluorescent visualization of syp-YFP expression, to ensure blind sampling of presynaptic HA staining. The parameters were optimized for zero bleedthrough between the 488 and 555 channels and each channel was separately obtained through alternating line scans to ensure that the HA signal was specific to the epitope tagged protein. Image analysis was performed with NIH Image J on maximal intensity z-projections. Dendrites were linearized using the straighten plugin for Image J, and extracted from the full-frame image. For analysis, the integrated fluorescence intensity of HA staining that colocalized with syp-YFP puncta was quantified using custom written analysis routines.

Surface GluA1 Immunocytochemistry

Following the appropriate treatment, cells were live labeled with primary antibodies against surface epitopes of GluA1 (sGluA1, 1:10, Calbiochem; San Diego, CA) for 15 min at 37ºC. Cells were then washed 3X in PBS-MC containing 2% PFA/2% sucrose for 20 min at room temperature (RT), blocked and stained as described above using Alexa 555 goat anti-rabbit secondary antibody (1:500; Molecular Probes; Eugene,

OR). Cells were then permeabilized with PBS-MC containing 0.1% Triton X-100 for 5 min at RT, and stained for PSD95 as above [using a mouse monoclonal anti-PSD95 antibody (1:200; Fisher)] and an Alexa488-conjugated secondary antibody (goat anti-mouse; 1:500; Molecular Probes; Eugene, OR).

Neurons stained for sGluA1/PSD95 or sGluA2/PSD95 were imaged on an Olympus FV1000 inverted confocal microscope using a Plan Apochromat 60x/1.4 NA objective and 2X digital zoom. Areas of interest were selected for imaging guided by epifluorescent visualization of the PSD95 channel, to ensure blind sampling of surface GluA1 expression. Acquisition settings were identical for all treatment groups and were determined to ensure: 1) optimization of the dynamic range of signal intensities to limit saturation, 2) the absence of detectable fluorescence in a no GluA1 antibody condition included in all experimental runs, and 3) no fluorescence bleed-through between channels. Image analysis was performed with NIH Image J on maximal intensity z-projections. Dendrites were linearized using the straighten plugin for Image J, and extracted from the full-frame image. For analysis, a "synaptic" GluA1 particle was defined as a particle that occupied greater than 10% of the area defined by a PSD95 particle, and the integrated fluorescence intensity of synaptic GluA1 particles was quantified using custom written analysis routines for Image J.

Data Analysis

Statistical differences between experimental conditions were determined by either unpaired t-tests (2 groups) or by analysis of variance (ANOVA) and post-hoc Fisher's

LSD test (> 2 experimental conditions). Differences were deemed significant if $\alpha < 0.05$ (two-tailed).

Results

The Ubiquitin Proteasome System is selectively required for presynaptic state-dependent homeostatic plasticity

Acute AMPA receptor blockade (CNQX, 40 μM, 3 hr) induces lasting homeostatic compensation in both pre- and post- synaptic function, both of which rely upon dendritic protein synthesis (Figure 3.12) but enduring changes in state-dependent presynaptic function further require a non-protein synthesis dependent component. While retrograde synaptic signaling of brain derived neurotrophic factor (BDNF) is required for state-dependent compensation (Figure 3.8) co-application of protein synthesis inhibitors fail to block BDNF induced state-dependent changes in presynaptic function induced by direct BDNF application (Figure 3.12). These data suggest that state-dependent homeostatic plasticity requires two different regulatory processes within the same synapse; 1) a protein synthesis-dependent mechanism upstream of BDNF/TrkB signaling and 2) a protein synthesis-independent mechanism downstream of BDNF/TrkB signaling, likely within the presynaptic terminal. Interestingly, presynaptic release probability can be rapidly modified by the ubiquitin proteasome system (UPS) in *Drosophila* (Speese et al., 2003), *Aplysia* (Zhao et al., 2003) and mammals (Willeumeir et al., 2006 and Rinetti et al., 2010). Therefore, proteasome mediated protein degradation could contribute to the increases in presynaptic function during state-dependent homeostatic plasticity. To test

this idea, we treated cultured hippocampal neurons (≥ 21 DIV) with CNQX to block AMPARs (40 μM, 3 hr) with or without lactacystin, an irreversible proteasome inhibitor [10 μM, 30 min pretreatment; (Fenteany et al., 1995)]. Consistent with previous results (Figure 3.1), blockade of AMPARs alone (CNQX) increased both in mEPSC amplitude and frequency (* $p < 0.05$ relative to untreated control neurons; Figure 4.1A-C) revealing parallel pre- and post- synaptic enhancement of homeostatic function. Interestingly, pretreatment with lac had no effect on the increase in mEPSC amplitude (* $p < 0.05$ relative to untreated control neurons; Figure 4.1A-B), but completely prevented the increase in mEPSC frequency (* $p < 0.05$ relative to untreated control neurons; Figure 4.1A, C; n = 15, 16, 12 left to right) induced by AMPAR blockade. These results suggest that protein degradation by the proteasome is selectively required for presynaptic, state-dependent homeostatic plasticity. To confirm that proteasome function is required for state-dependent changes in presynaptic function, we pretreated neurons with a structurally distinct proteasome inhibitor, MG132 (10 μM, 30 min pretreatment). Similar to lac, MG132 selectively and completely blocked the increase in mEPSC frequency (* $p < 0.05$ relative to untreated control neurons; Figure 4.1A, C; N = 5, 7, 6 left to right) that is normally induced downstream of synaptic inhibition (CNQX). Additionally, co-application of MG132 did not affect AMPAR induced increases in mEPSC amplitude (data not shown). Together these data suggest that targeted protein degradation is selectively required for presynaptic state-dependent homeostatic plasticity.

To examine postsynaptic compensation induced by AMPAR blockade, we examined cell-surface expression of the GluA1 (sGluA1) subunit of the AMPA type glutamate receptor. PSD-95 was used as an excitatory postsynaptic marker (Okabe et al.,

1999) and synaptic sGluA1 was quantified as the total integrated intensity of sGluA1 signal at sites of PSD-95 and AMPAR subunit colocalization (> 10% overlap). Consistent with previous observations (Figure 3.2) AMPAR blockade (CNQX; 40 uM; 3 hr) robustly increased postsynaptic sGluA1 expression relative to untreated control cells (data not shown). Consistent with the hypothesis that proteasome function is necessary only for presynaptic compensation, pretreatment with either lactacystin or MG132 did not prevent the CNQX induced increase in synaptic sGluA1 (data not shown). Additionally, neurons treated with lactacystin or MG132 alone had comparable levels of sGluA1 relative to untreated control neurons (data not shown) and the density and intensity of PSD-95 staining did not change between all four groups (data not shown) suggesting that acute proteasome inhibition has no effect on overall synapse number and function. Together, these data suggest that acute modification of proteasome function is not required for postsynaptic compensatory function, downstream of AMPAR blockade.

To confirm that proteasome function is required for a homeostatic enhancement in presynaptic function we first measured presynaptic function using a primary antibody targeted towards the lumenal domain of synaptotagmin (syt), a transmembrane vesicle protein. Live labeling of neurons in the presence of the syt antibody allows for restricted access of the antibody to syt proteins located on synaptic vesicles that are actively exocytosing. Syt labeling was performed in the presence of 1 µM TTX to measure quantal release events as measured at vglut1 positive synapses. Consistent with previous results (Figure 4.2), AMPAR blockade with CNQX (3 hr; 40 uM) increased syt uptake relative to untreated control cells (Figure 4.2; * $p < 0.05$). Pretreatment of neurons with lactacystin or MG132 completely prevented the CNQX induced increase in syt uptake

(Figure 4.2) and importantly, the density and intensity of vlgut positive puncta did not differ between groups (data not shown). Together, these data demonstrate that proteasome function is specifically required for modulation of presynaptic function at existing synapses (Piedras-Renteria et al., 2004) and that basal proteasome function does not regulate the overall synapse number.

BDNF retrograde synaptic signaling is required for state-dependent compensation (Figure 3.8) raising the question, is transsynaptic BDNF signaling required upstream or downstream of proteasome function? If BDNF signaling is required immediately downstream of AMPAR blockade during state-dependent homeostatic plasticity, then presynaptic modification through exogenous BDNF application should also be dependent upon proteasome function. To test this hypothesis, cultured hippocampal neurons were treated with either exogenous BDNF alone (250 ng/mL, 2 hr) or alongside lactacystin (10 μM, 30 min pretreatment) or MG132 (10 μM, 30 min pretreatment) to concurrently inhibit proteasome function. Consistent with previous results, bath application of BDNF increased mEPSC frequency relative to untreated control neurons (* $p < 0.05$ relative to untreated control neurons; Figure 4.3A-B; refs; N = 7, 7, 5, 7, 6, 6 left to right). Pretreatment of neurons with either lactacystin or MG132 completely prevented the increase in mEPSC frequency induced by exogenous BDNF application alone (* $p < 0.05$ relative to untreated control neurons; Figure 4.3A-B) further confirming that BDNF/TrkB is function downstream of AMPAR blockade, during presynaptic homeostatic compensation. Neurons treated with either lactacystin or MG132 alone had no effect on mEPSC frequency (Figure 4.3A-B) or amplitude (data not shown) relative to untreated control neurons (* $p > 0.05$ relative to untreated control neurons). These data suggest that

proteasome function is required for activity dependent modification of protein expression downstream of BDNF retrograde synaptic signaling and that state-dependent proteasome modification of synaptic proteins likely occurs within the presynaptic terminal.

To test if proteasome function is specifically required for the BDNF induced increase in presynaptic function and is not masking a BDNF induced change in synapse number (Tyler and Pozzo-Miller 2001), syt uptake was analyzed in neurons treated with BDNF (250 mg/mL, 2 hr), lactacystin alone (10 μM, 2.5 hr), MG132 alone (10 μM, 2.5 hr) or both BDNF + proteasome inhibitor (either lactacystin or MG132; 30 min pretreatment). Exogenous BDNF treatment significantly increased syt uptake compared to untreated control neurons (* $p < 0.05$ relative to untreated control neurons; Figure 4.3C-D; N= 87, 40, 29, 33, 24, 33 left to right) and as predicted, pretreatment with either lactacystin or MG132 completely blocked the BDNF induced increase in syt uptake (* $p < 0.05$ relative to untreated control neurons; Figure 4.3C-D). Importantly, there was no change in the density or intensity of vglut expression between groups (Figure 4.3C-D) confirming that BDNF enhances presynaptic function independent of changes in synapse number (Tyler and Pozzo-Miller 2001) and suggests that proteasome function is required for BDNF induced increases in presynaptic function at existing synapses.

Presynaptic, but not postsynaptic, polyubiquitination is required for state-dependent homeostatic plasticity

Inhibition of proteasome function with either lactacystin or MG132 during concurrent blockade of AMPARs (Figure 4.1A-C) suggests that targeted protein

degradation is required for state-dependent modification of presynaptic release probability. However, it is known that monoubiquitination through post-translational modification of target proteins can directly affect ion channel activity (Lin et al., 2005) and the regulate surface expression and localization of synaptic proteins such as the AMPAR subunits GluA1 (Burbea et al., 2002; Patrick et al., 2003; Juo and Kaplan, 2004) and GluA2 (Patrick et al., 2003; Yang et al., 2008), ROMK1 (Lin et al., 2009) and GKAP (Hung et al., 2010). To specifically test if polyubiquitination and subsequent protein degradation is the necessary for AMPAR induced compensatory plasticity, we took advantage of a mutant form of ubiquitin in which lysine 48 has been mutated to an arginine (ubK48R). The K48R mutation prevents polyubiquitination of target proteins and therefore ablates the signal necessary for proteasomal degradation. Importantly, however, this mutation still allows for continued monoubiquitination of proteins, preserving post-translational modification, endocytosis and protein trafficking regulated by the ubiquitin proteasome system (Hershko and Ciechanover, 1998).

The data presented above indicate that proteasome function is required for state-dependent compensation in presynaptic function (Figure 4.1) but is proteasome function required within the presynaptic or postsynaptic compartment? To test if postsynaptic polyubiqutination is required for AMPAR induced changes in presynaptic function, we transfected ubK48R along with GFP for visualization of transfected neurons (Figure 4.4A-B). Forty-eight hours post-transfection, mEPSCs were recorded from GFP expressing neurons to determine if there is a specific, postsynaptic requirement for proteasome mediated protein degradation during state-dependent homeostatic plasticity. Consistent with previous reports of AMPAR blockade, GFP transfected neurons treated

with CNQX (3 hr; 40 μM) exhibited an increase in both mEPSC amplitude (data not shown) as well as frequency as compared to GFP transfected control neurons (* $p < 0.05$ relative to untreated GFP expressing control neurons; Figure 4.4A-B; N = 16, 14, 10, 12). Interestingly, in neurons expressing mutant ubK48R, the increase in compensatory function persisted downstream of AMPAR blockade. AMPAR blockade (CNQX; 3 hr; 40 μM) increased mEPSC amplitude (data not shown) as well as frequency relative to GFP expressing control neurons (* $p < 0.05$ relative to untreated GFP expressing control neurons; Figure 4.4C-D) suggesting that postsynaptic polyubiquitination, and subsequent protein degradation, is not necessary for state-dependent changes in presynaptic or postsynaptic function. Importantly, ubK48R expressing cells (non-CNQX treated group) do not exhibit a difference in basal mEPSC frequency relative to the GFP alone expressing control cells (Figure 4.4C-D) suggesting that postsynaptic polyubiquitination does not alter basal synaptic function in cultured hippocampal neurons. Together, these data suggest that postsynaptic protein degradation, mediated by the proteasome, is not necessary for either the pre- or post- synaptic AMPAR induced homeostatic changes in function.

To test if presynaptic polyubiquitation, and subsequent proteasome mediated protein degradation, is necessary for presynaptic state-dependent homeostatic plasticity we co-transfected ubK48R along with synaptophysin-YFP (syp-YFP) to visualize putative presynaptic terminals along a single axon (Figure 4.4E-F). Forty-eight hours post transfection, we live labeled neurons for the lumenal domain of synaptotagmin (syt) and quantified presynaptic function (syt uptake) as the proportion of the syp puncta that also contained syt staining (Figure 4.4E-F). As observed in untransfected control neurons,

AMPAR blockade (CNQX, 40μM, 3 hr) increased syt uptake at syp-YFP expressing terminals relative to control neurons (Figure 4.4E-F; * $p < 0.05$; N = 51, 57, 25 left to right). However, this increase in syt uptake was completely abolished in neurons co-expressing ubK48R (Figure 4.4E-F). Together, these results suggest that the state-dependent increase in presynaptic function induced by AMPAR blockade requires targeted protein degradation by the proteasome within the presynaptic but not the postsynaptic compartment.

Network activity regulates presynaptic localization of the proteasome

State-dependent compensation requires coincident presynaptic action potential firing during AMPAR blockade (Figure 3.1) but it remains unknown how presynaptic action potentials are interacting with local signaling to gate these changes in presynaptic function. Since strong neuronal depolarization, with high K^+, is sufficient to localize and sequester the proteasome into dendritic spines (Bingol et al., 2006 and Bingol et al., 2010) we hypothesized that proteasome localization to the axon terminal may also be modulated in an activity dependent manner. Rpt6 is one of 6 regulatory particle AAA-ATPases (Rpts) located on the regulatory particle of the proteasome (Rubin et al., 1998). Recently, it has been shown that phosphorylation of Rpt6 is necessary for activity dependent dendritic trafficking of the proteasome (Bingol et al., 2010). To test if presynaptic localization of the proteasome is "state-dependent" during AMPAR blockade, we co-transfected an epitope tagged version of WT Rpt6 (WT Rpt6-HA) with synaptophysin-YFP (syp-YFP, Figure 4.5). Since Rpt6 localization has been

demonstrated to be an accurate measure of proteasome localization (Djakovic et al., 2009; Bingol et al., 2010) we estimated proteasome localization using the total integrated fluorescence of WT Rpt6-HA signal, at syp-YFP puncta. Forty-eight hours post-transfection, neurons were treated with CNQX (40 μM; 3 hr) with or without TTX (1 μM ; 5 min pretreatment) to mimic the conditions in which state-dependent compensation is revealed. Curiously, neurons treated with CNQX had a similar level of presynaptic WT Rpt6-HA staining when compared to WT Rpt6-HA untreated control neurons (Figure 4.5A-B; * $p < 0.05$ relative to WT Rpt6 untreated control neurons) suggesting that blockade of AMPARs does not affect presynaptic proteasome localization. Interestingly, however, neurons treated with CNQX + TTX had a significantly decreased amount of total integrated intensity of WT Rpt6-HA staining when compared to the WT Rpt6 untreated control group (Figure 4.5A-B; * $p < 0.05$ relative to WT Rpt6 untreated control group) suggesting that action potential activity is required for the recruitment of the proteasome to presynaptic terminals. Together these data suggest a model where network activity functions to gate local synaptic signaling and ultimately determine if presynaptic compensation will accompany postsynaptic homeostatic compensation, downstream of synaptic inhibition.

Recently, it has been shown that phosphorylation of Rpt6 at serine 120 is required for proteasome function (S120; G. Patrick and S. Djakovic, personal communication) and that the phosphorylation state of the Rpt6 at S120 can mimic bidirectional homeostatic plasticity (Figure 2.10). We therefore wanted to test if direct phosphorylation of Rpt6 at S120 is essential for state-dependent homeostatic plasticity. We utilized a phospho-mutant form of Rpt6 in which S120 was mutated to an alanine (S120A) and asked if the

serine to alanine mutation blocked state-dependent homeostatic plasticity (Figure 4.6A). Cells were transfected with either an empty vector control (prk5) or the Rpt6 S120A phospho-mutant protein along with synaptophysin-YFP (for visualization of axonal processes). As predicted based on previous experiments, prk5 empty vector expressing control neurons exhibited a robust increase in syt uptake (* $p < 0.05$ relative to untreated prk5 expressing control neurons; Figure 4.6A) in response to AMPAR blockade (CNQX; 40 μM; 3 hr). Interestingly, expression of Rpt6 S120A completely prevented the AMPAR induced increase in syt uptake (Figure 4.6A). These data suggest that phosphorylation of Rpt6 S120 is necessary for the expression of state-dependent homeostatic plasticity and suggests that activity may be gating state-dependent homeostatic plasticity through rapid, activity dependent phosphorylation of Rpt6 (Zhang et al., 2007; Djakovic et al., 2009; Bingol et al., 2010).

Phosphorylation of S120 regulates presynaptic proteasome localization

We next asked if phosphorylation of Rpt6 S120 is sufficient to regulate localization of the proteasome to presynaptic terminals. We cotransfected neurons with synaptophysin-YFP (syp-YFP) along with WT Rpt6, Rpt6 S120A or Rpt6 S120D to constitutively prevent phosphorylation (S120A) or mimic phosphorylation (S120D) of Rpt6, respectively (Figure 4.6B). Forty-eight hours post transfection, we immunostained for HA and quantified the amount of presynaptic HA signal (total integrated intensity of HA at syp positive puncta; syt uptake). Strikingly, we found that phosphorylation at Rpt6 S120 is alone sufficient to regulate localization of the proteasome to presynaptic

terminals. Expression of Rpt6 S120A results in lower presynaptic accumulation of the proteasome relative to WT Rpt6 expressing control cells (Figure 4.6B; * $p < 0.05$ relative to WT Rpt6 expressing neurons) and conversely, expression of Rpt6 S120D increases presynaptic expression of the proteasome relative to the WT Rpt6 expressing controls cells (Figure 4.6B; * $p < 0.05$ relative to WT Rpt6 expressing neurons). These results suggest that the state-dependent nature of presynaptic homeostatic plasticity may reflect activity dependent phosphorylation of Rpt6 and subsequent trafficking of the proteasome into and out of presynaptic terminals.

Conclusions and Discussion

Here we describe a novel interaction between presynaptic action potential signaling and the ubiquitin proteasome system (UPS) during presynaptic state-dependent homeostatic plasticity. Presynaptic protein degradation is selectively required for state-dependent increases in presynaptic function and basal network activity regulates presynaptic proteasome localization at synaptic terminals suggesting that activity dependent proteasome trafficking may underlie the state-dependent nature of homeostatic synaptic plasticity. Interestingly, phosphorylation of Rpt6 S120, may serve as a dual regulatory checkpoint during state-dependent homeostatic plasticity. Phosphorylation of Rpt6 S120 is sufficient to bidirectionally regulate presynaptic proteasome localization and is further required for regulation of the basal rate of proteasome function (Djakovic et al., 2009). Together, these results suggest that state-dependent homeostatic plasticity requires coordinated changes in neuron network driven proteasome localization and

function, as well as local changes in AMPAR induced BDNF/TrkB signaling. These data support an overarching model of homeostatic plasticity where the proteasome serves as an integration point between global network driven activity and local synaptic function that leads to stable neuron networks over time.

Our data suggests that activity dependent localization of the proteasome is a consequence of the basal rate of network activity. How is activity regulating the trafficking of the proteasome itself? Neuronal homeostasis is tightly coupled to intracellular calcium concentrations (Chen et al., 2008) and is hypothesized to be important for fidelity of spike encoding (Chen et al., 2008). Additionally, state-dependent homeostatic plasticity requires calcium influx through presynaptic, high voltage activated P/Q- and N- type calcium channels (Figure 3.1). Therefore, it seems likely that the activity dependent signaling pathway necessary during state-dependent proteasome phosphorylation would be tightly linked to voltage activated calcium signals. One interesting possibility is that CAMKII (Djakovic et al., 2009; Bingol et al., 2010) is required for the phosphorylation of Rpt6 during state dependent homeostatic plasticity. CAMKII mediated Rpt6 phosphorylation is required for network driven changes in proteasome function (Djakovic et al., 2009; Figure 2.10) as well as depolarization induced synaptic localization of the proteasome (Bingol et al., 2010). Moreover, network activity can bidirectionally alter the ratio between α and β isoforms of CAMKII within the synapse (Thiagarajan et al., 2002). Fine modifications of CAMKII signaling (Thiagarajan et al., 2002) downstream of changes in neuron network activity nicely poise CAMKII as a rapid, activity dependent modifier of synaptic function during globally

induced forms of homeostatic plasticity. Further studies are needed to address the role of CAMKII during presynaptic activity dependent localization of the proteasome.

Previous work suggests that the proteasome functions to constrain basal levels of presynaptic function (Cline, 2003). Acute (1 hr) blockade of the proteasome, presynaptically at the *Drosophila* NMJ, results in a rapid increase in DUNC13 expression as well as a robust (50%) increase in evoked EJP amplitude (Speese et al., 2003). Additionally, degradation of munc13 by the neuronally restricted, E3 ubiquitin ligase, Fbxo45, is required for maintenance of presynaptic function (Saiga et al., 2009) and siRNA mediated knockdown of Fbxo45 robustly increases mEPSC frequency relative to control neurons (Saiga et al., 2009). Additionally, SCRAPPER knockout (SCRAPPER KO) mice have a proteasome dependent increase in mEPSC frequency relative to WT littermate control mice (Yao et al., 2007) and the increase in mEPSC frequency is phenocopied with overexpression of Rim1alpha (Yao et al., 2007) suggesting that the proteasome dependent balance between SCRAPPER and Rim1alpha can be an active mechanism for regulating basal levels of presynaptic function. Together, these studies suggest that selected components of the ubiquitin proteasome system are required for maintenance of basal presynaptic function.

Conversely, our work suggests that protein degradation by the proteasome is not necessary for basal changes in presynaptic function but is selectively required for activity induced changes in state-dependent homeostatic function. One possibility for why these discrepancies exist is that the above studies manipulate individual components of the ubiquitin proteasome system that directly alther the expression of presynaptic proteins that are known to rapidly modulate presynaptic release probability such as

DUNC13/MUNC13 (Speese et al., 2003) and Rim1α (Yao et al., 2007). In the studies presented here in this manuscript, proteasome function is inhibited in a manner by which the overall stoichiometric ratio of proteins will remain the same, thus not altering the basal rate of presynaptic function and allowing us to isolate deficits in activity driven proteasome function during homeostatic plasticity. Collectively, these studies suggest at least two distinct mechanisms may exist for the proteasome to regulate presynaptic function. One through the regulation of basal presynaptic function through the targeted degradation of presynaptic proteins and two, through the BDNF/TrkB dependent recruitment of the proteasome during state-dependent homeostatic compensation.

Here, we demonstrate a novel role for activity dependent proteasome localization and function during gating of AMPAR induced state-dependent homeostatic plasticity. Interestingly, dysregulation of presynaptic proteasome function has been implicated in several neurological disorders (Gregersen et al., 2005; Cuervo et al., 2010; Rogers et al., 2010) and here we present evidence for an activity dependent link to presynaptic function that could represent a putative integration site for dysregulation neuron network activity and proteasome function that could lead to neurological consequence.

Figure 4.1 Proteasome function is required for state-dependent increases in mEPSC frequency but not amplitude downstream of AMPAR blockade. (A) Representative example traces of mEPSCs from cultured hippocampal neurons (≥ 21 DIV). Neurons were treated with either CNQX (40 μM; 3 hr) to block AMPARs or CNQX + lac (10 μM; 30 min pretreatment) to block both AMPARs and proteasome function. Consistent with previous results (Figure 3.1), blockade of AMPARs induces compensatory increases in both mEPSC amplitude and frequency relative to untreated control neurons, but concurrent inhibition of the proteasome during AMPAR blockade, prevents compensatory increases in mEPSC frequency while having to effect on the AMPAR blockade induced increase in mEPSC amplitude. (B-C) Quantification of mEPSC amplitude (B) and mEPSC frequency (C) from neurons treated with CNQX alone, combined CNQX +l ac, or combined CNQX + MG132 (a reversible proteasome inhibitor; 1 μM; 30 min pretreatment). During AMPAR blockade pretreatment with lac specifically abolishes increases in mEPSC frequency without affecting the increase in mEPSC amplitude (* $p < 0.05$) suggesting that proteasome function is required for homeostatic increases in state-dependent presynaptic function downstream of AMPAR blockade.

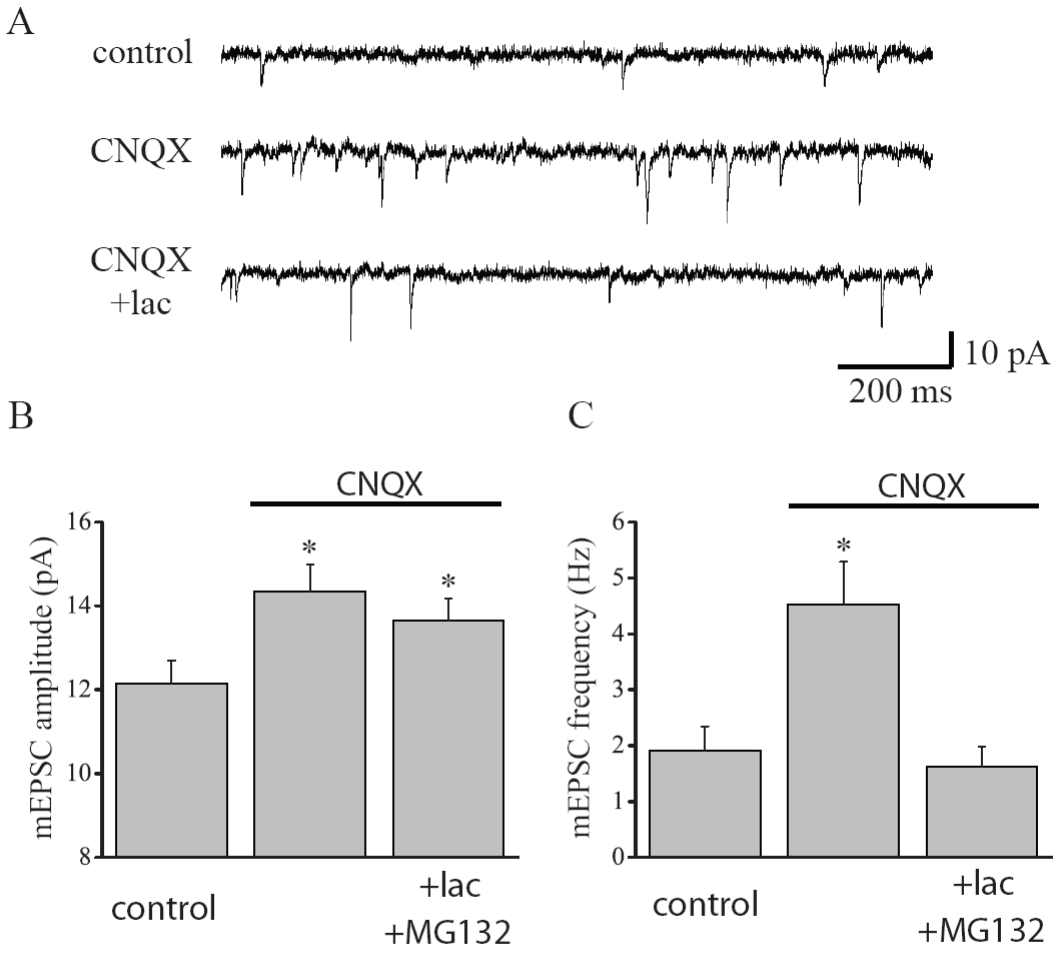
A
control
CNQX
CNQX
+lac
10 pA
200 ms
B
CNQX
mEPSC amplitude (pA)
16
14
12
10
8
*
*
control
+lac
+MG132
C
CNQX
mEPSC frequency (Hz)
6
5
4
3
2
1
0
*
control
+lac
+MG132

Figure 4.1

Figure 4.2 State-dependent increases in function require proteasome activity at active presynaptic terminals. Quantification of the proportion of active, excitatory presynaptic terminals. Neurons were treated, live labeled for syt, and subsequently fixed and processed for vglut immunofluorescence. The proportion of active presynaptic terminals was quantified as the proportion of vglut positive puncta co-expressing synaptotagmin immunofluorescence. Cultured hippocampal neurons treated with CNQX (40 μM; 3 hr) exhibited an increase in the proportion active presynaptic terminals as compared to untreated control neurons (* $p < 0.05$; Fisher's LSD). Pretreatment with either lactacystin or MG132 (10 μM and 1 μM respectively; 30 min pretreatment) prevents the increase in syt uptake normally observed with CNQX treatment alone suggesting that proteasome function is required for homeostatic increases in presynaptic release probability. Importantly, inhibition of proteasome function with either lac or MG132 has no effect on syt uptake (NS).

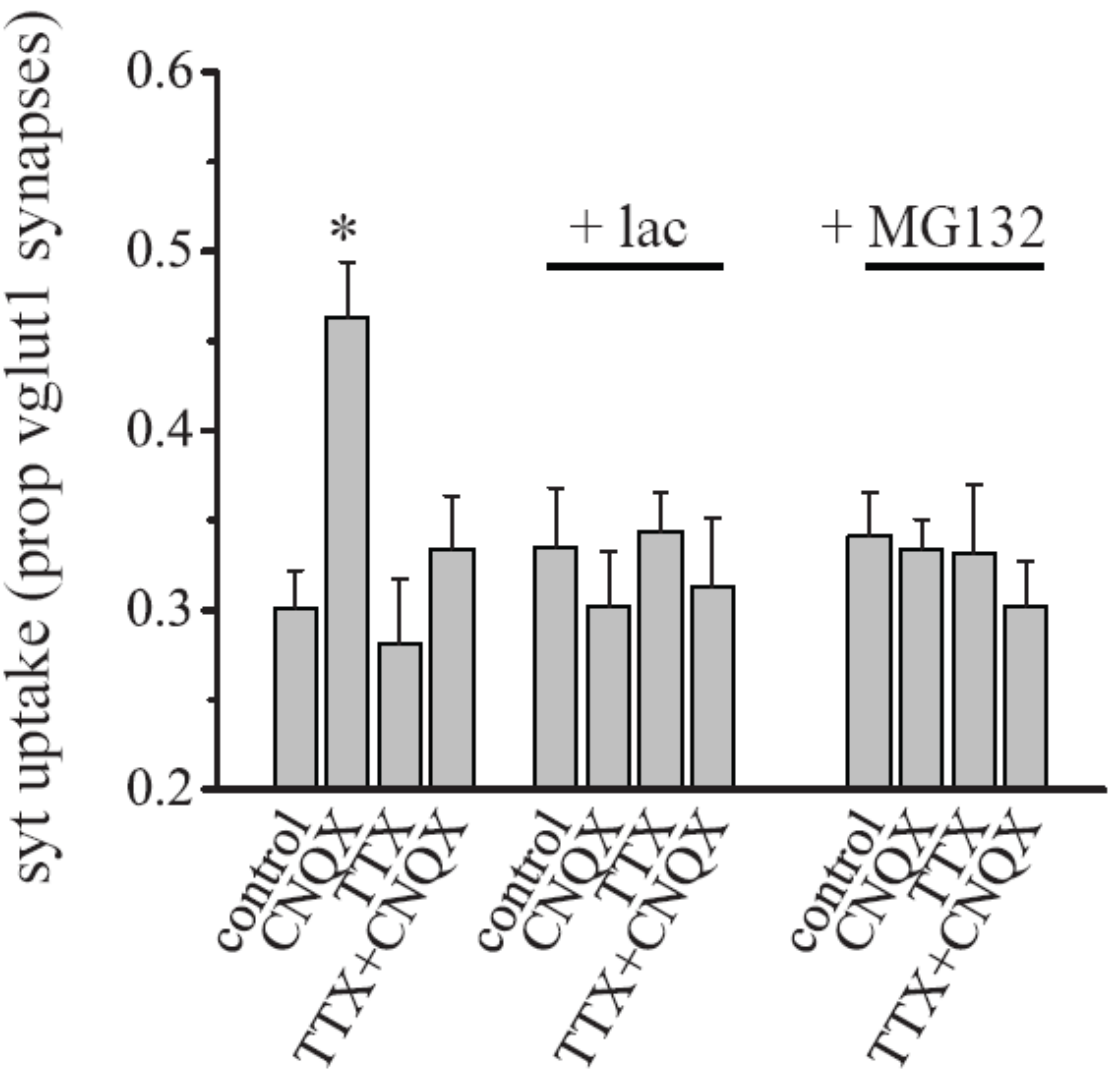
syt uptake (prop vglut1 synapses)
0.6
0.5
0.4
0.3
0.2
*
+ lac
+ MG132
control
CNQX
TTX
TTX+CNQX
control
CNQX
TTX
TTX+CNQX
control
CNQX
TTX
TTX+CNQX

Figure 4.2

Figure 4.3 Proteasome function is required downstream of retrograde synaptic signaling by BDNF. (A) Representative example traces from cultured hippocampal neurons (≥ 21 DIV) treated with BDNF (250 ng/mL; 2 hr), BDNF + lac (30 min pretreatment; 10 μM) or BDNF + MG132 (30 min pretreatment; 10 μM). (B) Quantification of mEPSC frequency from neurons treated with BDNF, BDNF + lac or BDNF + MG132. Consistent with previous results (Figure 3.8, 9, 10, 11), application of exogenous BDNF increases mEPSC frequency relative to untreated control neurons (* $p < 0.05$) but the BDNF induced enhancement of mEPSC frequency is abolished with co-application of either lac or MG132 (* $p < 0.05$). (C) Representative example images from neurons live labeled with syt primary antibody and subsequently processed for vglut immunofluorescence. Relative to untreated control cells, neurons treated with BDNF had elevated levels of syt uptake yet co-application of lac prevented the BDNF induced increase in presynaptic function. (D) Quantification of syt uptake from cells treated, as indicated for 2 hr BDNF and 30 min pretreatment with proteasome inhibitors lac and MG132. Co-application of either lac or MG132 completely prevented the increase in syt uptake produced by BDNF alone (* $p < 0.05$).

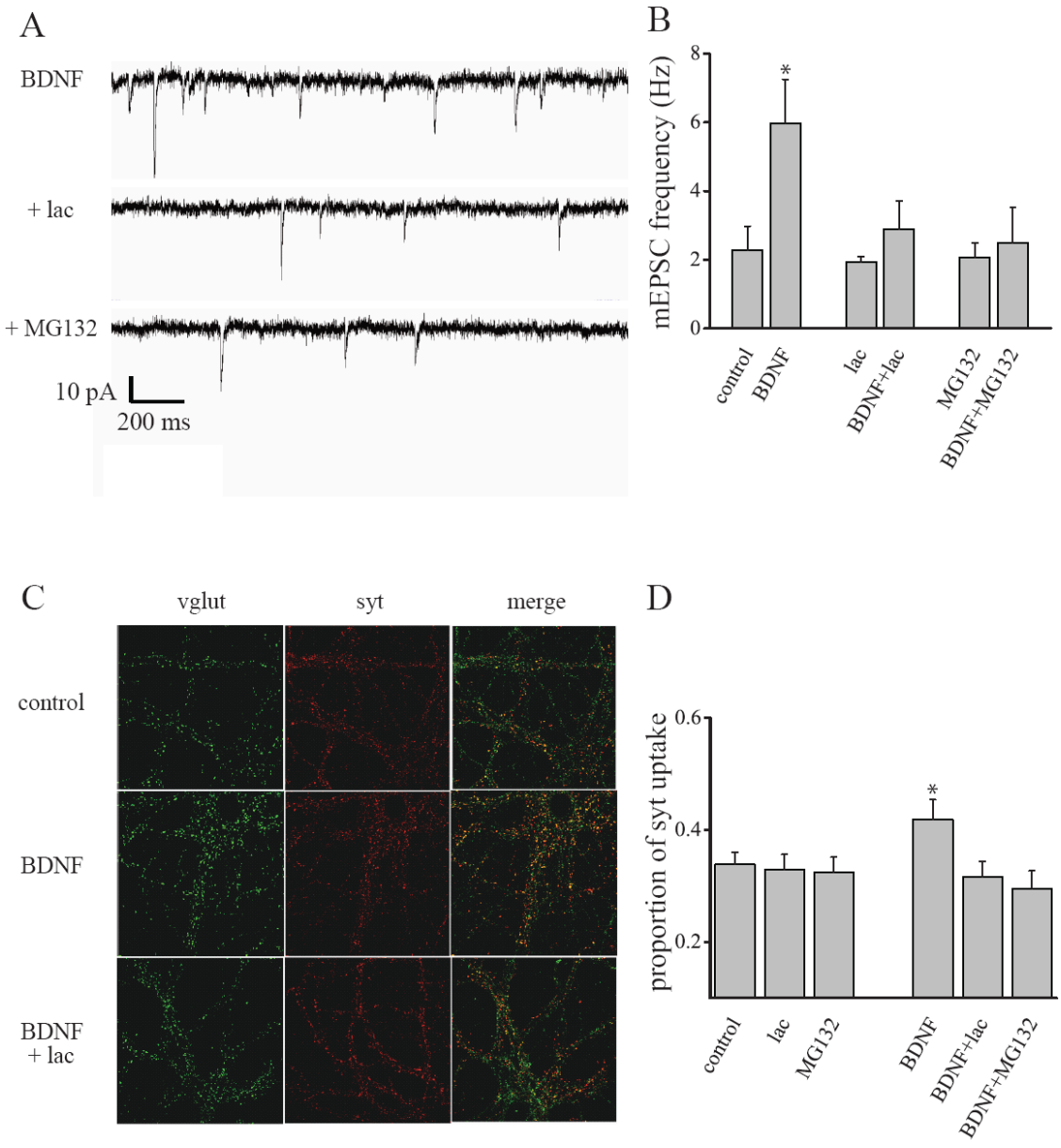
A
BDNF
+ lac
+ MG132
10 pA
200 ms
B
mEPSC frequency (Hz)
8
6
4
2
0
*
control
BDNF
lac
BDNF+lac
MG132
BDNF+MG132
C
vglut
syt
merge
control
BDNF
BDNF
+ lac
D
proportion of syt uptake
0.6
0.4
0.2
*
control
lac
MG132
BDNF
BDNF+lac
BDNF+MG132

Figure 4.3

Figure 4.4 Presynaptic but not postsynaptic polyubiquitination is required for state-dependent increases in presynaptic function. (A) Schematic depicting isolation of postsynaptic knockdown of polyubiquitination. We transfected GFP alongside K48R mutant ubiquitin (ubK48R) and recorded mEPSCs from isolated cells allowing for specific knockdown of postsynaptic proteasome mediated degradation. (B) Representative example image of a pyramidal like neuron, 48 hr post-transfection of GFP and ubK48R. The cells expressing ubK48R have normal morphology and generally, look healthy. (C) Representative example traces from GFP, GFP + CNQX and K48R + CNQX treated neurons. (D) Quantification of mEPSC frequency from GFP alone, GFP + CNQX, ubK48R alone and ubK48R + CNQX treated neurons (* $p < 0.05$). (E) Schematic depicting isolated presynaptic knockdown of proteasome function. Neurons were transfected with synaptophysin-YFP (syp-YFP) alongside ubK48R. Presynaptic terminals were identified as syp-YFP puncta. (F) Representative example image of a neuron transfected with syp-YFP. Fields of view were chosen based off of a process displaying an axon like morphology. (G) Representative example images of axonal processes from syp alone (control), syp + CNQX and ubK48R + CNQX treated neurons. Forty-eight hours post-transfection neurons were live labeled for synaptotagmin. Synaptophysin + CNQX processes exhibit more co-localization between syp and syt puncta relative to syp alone control neurons. The increase in co-localization between syt and syp induced by CNQX is completely abolished the ubK48R + CNQX group. (H) Quantification of syt uptake in syp alone control cells, syp + CNQX and ubK48R + CNQX treated cells. CNQX induces an increase in syt uptake relative to the syp alone control cells that is abolished when the neurons are expressing ubK48R (* $p < 0.05$).

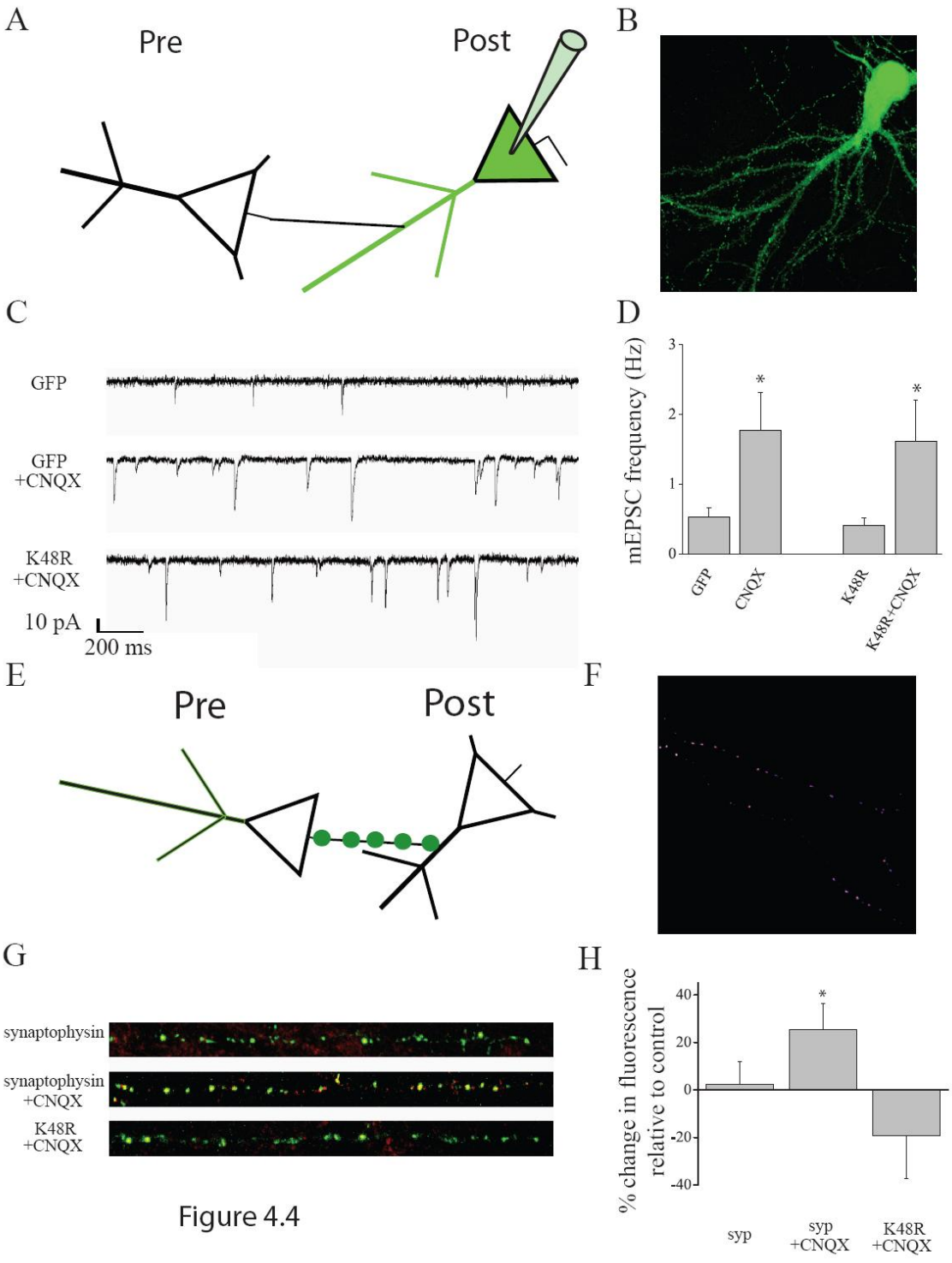
A
Pre
Post
B
C
GFP
GFP
+CNQX
K48R
+CNQX
10 pA
200 ms
D
mEPSC frequency (Hz)
3
2
1
0
*
*
GFP
CNQX
K48R
K48R+CNQX
E
Pre
Post
F
G
synaptophysin
synaptophysin
+CNQX
K48R
+CNQX
H
% change in fluorescence
relative to control
40
20
0
-20
-40
*
syp
syp
+CNQX
K48R
+CNQX

Figure 4.4

Figure 4.5 Activity is required for presynaptic localization of the proteasome. (A) Representative example images of neurons transfected with synaptophysin-YFP and Rtp6-HA using the calcium phosphate method. Red represents pseudocolored synaptophsyin-YFP, green represents HA immunofluorescence and yellow represents co-localization of Rpt6-HA and synaptophysin-YFP at putative presynaptic terminals. Forty-eight hours post-transfection, neurons were treated with CNQX (40μM; 3 hr) with or without TTX (1μM; 5 min pre-treatment) to mimic the induction of state-dependent homeostatic plasticity. Rpt6 expressing neurons treated with CNQX (40μM; 3 hr) did not differ in presynaptic HA expression from untreated control neurons (NS) suggesting that AMPAR activity is not required for the presynaptic localization of the proteasome. Strikingly, however, neurons treated with CNQX+TTX show a profound deficit in the amount of HA staining at synaptophysin-YFP containing puncta suggesting that action potential activity is required for the presynaptic localization of the proteasome. (B) Quantification of the total amount of HA staining at synaptophysin positive puncta plotted as a % change from control (* $p < 0.05$). Together these data suggest that action potential activity may be gating presynaptic state-dependent homeostatic plasticity through activity dependent trafficking of the proteasome to presynaptic terminals.

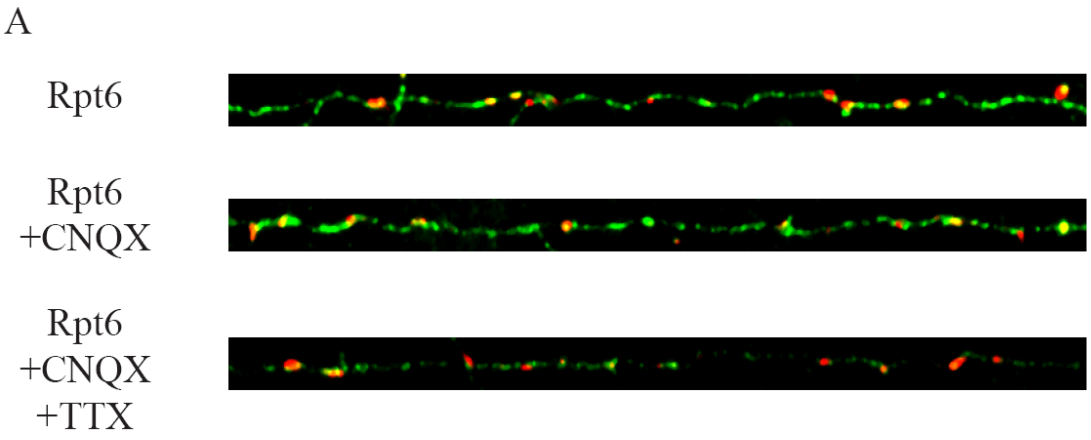
A
Rpt6
Rpt6
+CNQX
Rpt6
+CNQX
+TTX

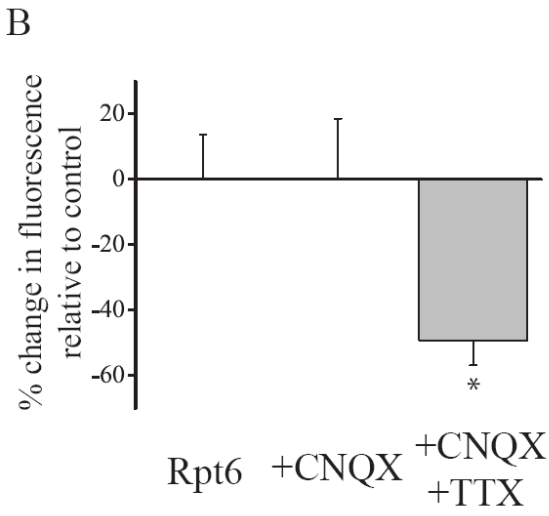
B
% change in fluorescence
relative to control
20
0
-20
-40
-60
*
Rpt6
+CNQX
+CNQX
+TTX

Figure 4.5

Figure 4.6 Phosphorylation of Rpt6 at S120 regulates presynaptic localization of the proteasome. Neurons were transfected with an empty vector prk5 control plasmid or Rpt6 S120-HA to determine if phosphorylation of Rpt6 at S120 is required for presynaptic homeostatic plasticity. (A) Quantification of the proportion of synaptophsyin-YFP (syp-YFP) puncta that contained HA staining. Forty-eight hours post-transfection, neurons were treated with CNQX (40μM; 3hr), fixed, stained and processed for HA immunofluorescence labeling. In response to AMPAR blockade, control (prk5) transfected neurons exhibited an increase in syp-YFP/HA colocalization as compared to the untreated empty vector control group (* $p < 0.05$; Fisher's LSD). In contrast, neurons expressing Rpt6 S120A-HA did not exhibit an increase in syp-YFP/HA co-localization in response to AMPAR blockade suggesting that regulation of Rpt6 phosphorylation is critical for expression of state-dependent homeostatic plasticity. (B) Quantification of the total fluorescence intensity of HA staining from neurons transfected with WT Rpt6-HA, Rpt6 S120A-HA or Rpt6 S120D-HA along with syp-YFP. Phosphorylation of Rpt6 at S120 is required for activity dependent trafficking of the proteasome into dendritic spines (Bingol et al., 2010). We therefore asked if phosphorylation of Rpt6 at S120 could regulate trafficking of the proteasome into presynaptic terminals. Neurons expressing Rpt6 S120A-HA exhibit a decrease in total HA expression at syp positive puncta whereas neurons expression Rpt6 S120D-HA exhibit an increase in the total amount of HA expression at syp positive puncta (* $p < 0.05$; Fisher's LSD) suggesting that phosphorylation state of Rpt6 is alone sufficient to regulate presynaptic localization of the proteasome.

A

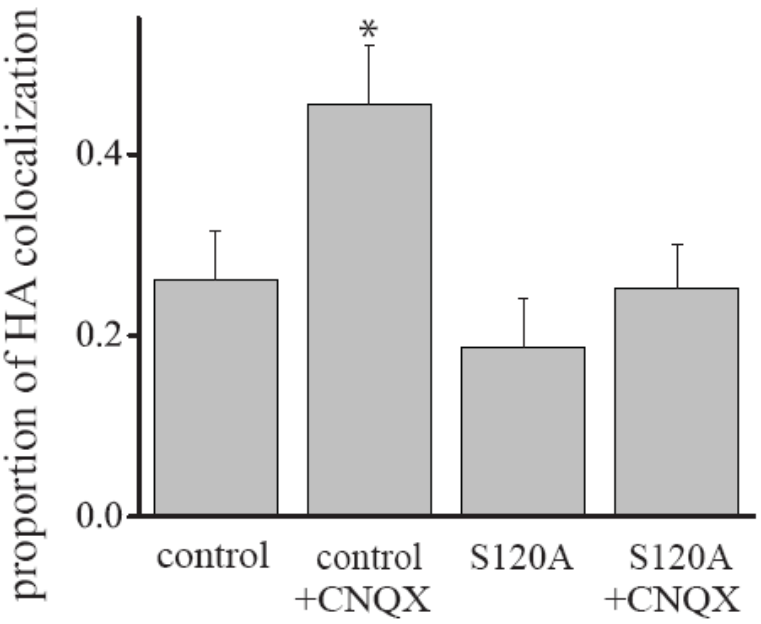
proportion of HA colocalization
0.0
0.2
0.4
*
control
control +CNQX
S120A
S120A +CNQX

B

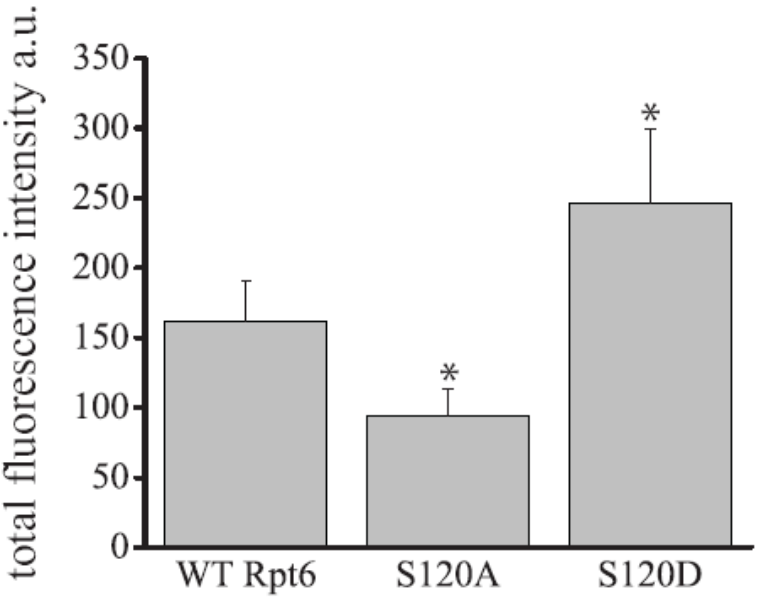
total fluorescence intensity a.u.
0
50
100
150
200
250
300
350
*
*
WT Rpt6
S120A
S120D

Figure 4.6

Figure 4.7 Working model of state-dependent homeostatic plasticity. Blockade of AMPARs homeostatically increases presynaptic release probability through a mechanism that requires retrograde synaptic signaling of BDNF/TrkB (Jakawich et al., 2010 in press). Homeostatic increases in presynaptic function are further gated by presynaptic action potentials and synaptic signaling mediated by high voltage activated Ca^{2+} signaling. Calcium influx likely leads to phosphorylation of Rpt6 at S120 and an activity dependent recruitment of the proteasome into presynaptic terminals.

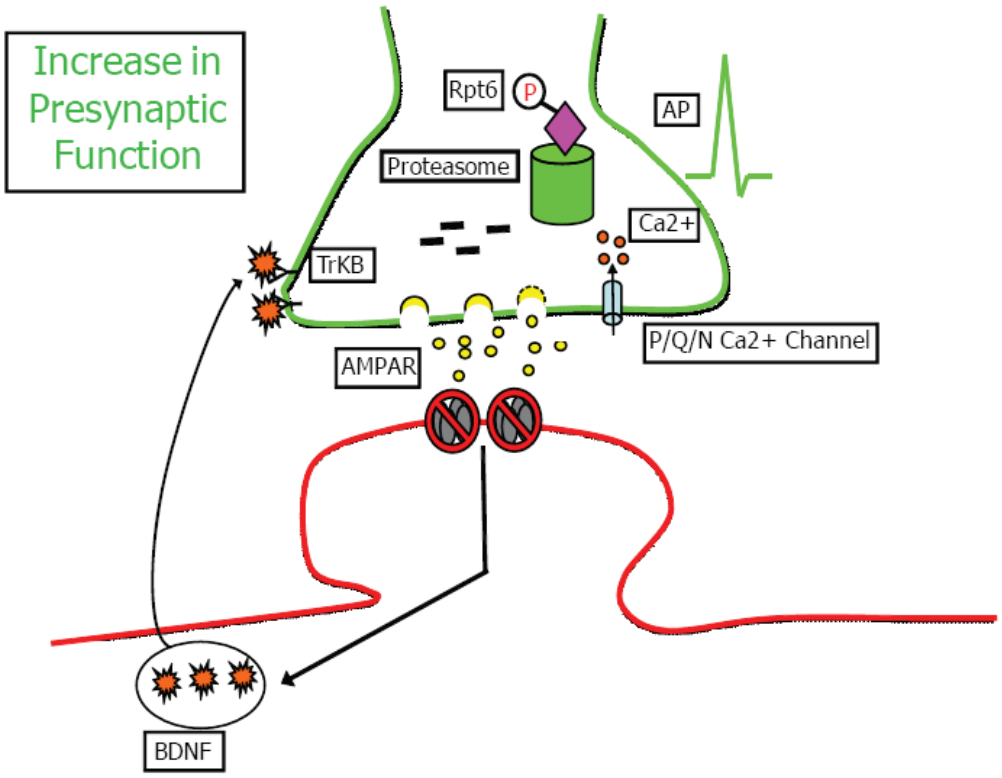
Increase in Presynaptic Function
Rpt6
P
AP
Proteasome
Ca2+
TrKB
P/Q/N Ca2+ Channel
AMPAR
BDNF

Figure 4.7

CHAPTER V

Discussion

Taken together, the experiments summarized above suggest that homeostatic plasticity is a mechanistically complex process that depends upon both intrinsic and synaptic forms of activity. These experiments suggest that homeostatic plasticity requires both protein synthesis and degradation mechanisms that are spatially segregated in the pre- and post- synaptic compartments in order to ensure localized control over synaptic homeostatic response properties. The studies presented above also suggest that presynaptic homeostatic plasticity mechanisms require the interaction between at least two cells (pre- and post- synaptic) whereas postsynaptic homeostatic plasticity mechanisms are able to occur through cell a autonomous mechanism suggesting that presynaptic homeostatic plasticity likely interacts with and or regulates key components of neuron network function. These findings provide an initial understanding to the molecular mechanisms regulate the expression of pre- or post- synaptic forms of homeostatic plasticity as well as rapid or slow forms of homeostatic compensation. Additionally, these studies suggest that homeostatic plasticity mechanisms may depend upon a hierarchical interaction between neuron, intrinsic and synaptic forms of neuron plasticity (Bergquist et al., 2009).

How does the Ubiquitin Proteasome System regulate both synaptic and network driven homeostatic plasticity?

Homeostatic response mechanisms induced by either neuron network quiescence or synaptic inhibition require function of the ubiquitin proteasome system (Figure 2.1 and Figure 4.1). How is the proteasome regulating two mechanistically distinct forms of homeostatic plasticity within the same subset of neurons? One possibility is that network induced forms of homeostatic plasticity may utilize global manipulation of the rate of proteasome degradation whereas synaptically induced homeostatic plasticity may be using a more specific, target based degradation mechanism to directly control synapse function. During slow homeostatic plasticity, proteasome function occludes the induction of homeostatic plasticity (Figure 2.6, 7, 8, 9; Sun and Wolf 2009) suggesting that there may be a temporal overlap in slow homeostatic compensatory mechanisms and proteasome function. During prolonged manipulation of network activity, expression of a stereotyped group of synaptic proteins is regulated in a bidirectional manner (Ehlers, 2003; Jia et al., 2008) suggesting that slow, postsynaptic forms of homeostatic plasticity can be achieved through a programmed set of synaptic conditions that is coordinated by overall changes in proteasome function. Furthermore, long term manipulation of neuron network activity traffics and sequesters the proteasome into dendritic spines (Bingol et al., 2006) and can alter the basal rate of proteasome function as measured by the rate of degradation of a proteasome reporter, paGFPu (Djakovic et al., 2009; Figure 2.4). These observations suggest that prolonged manipulation of neuron network activity may regulate the overall rate of neuronal protein degradation and subsequent function by

exploiting stoichiometric differences in existing protein expression levels. Conversely, presynaptic homeostatic plasticity can be manipulated by the degradation of one, or a few, key presynaptic proteins (Yao et al., 2007; Jiang et al., 2010) suggesting that presynaptic proteasome involvement may rely on a more specific, targeted protein degradation mechanism likely downstream of BDNF/TrkB signaling (Jia et al., 2008; Figure 3.12). Interestingly, exogenous application of BDNF does not alter the overall rate of proteasome activity (Jia et al., 2008) suggesting that presynaptic homeostatic plasticity mechanisms may require BDNF/TrkB signaling to target specific proteins such as Rim1alpha or Munc13/Dunc13 (Aravamudan and Broadie, 2003; Yao et al., 2007; Simsek-Duran and Lonart, 2008; Jiang et al., 2010) for further degradation.

Possible roles for ubiquitin proteasome function beyond proteasomal degradation

Since the discovery of ubiquitin's role in activity dependent protein degradation (Ciechanover et al., 1978), it has become increasingly clear that posttranslational modification of proteins via ubiquitin or ubiquitin-like molecules is critical for protein trafficking/function and endocytosis (Burbea et al., 2002; Juo and Kaplan, 2004). Over a dozen ubiquitin-like molecules have been identified including SUMO, NEDD8, Tmub1/HOPS, ISG-15 and FAT-10 (Kerscher et al., 2006) that can directly regulate neuron function. For instance, SUMO protease mediated cleavage of the plasma membrane leak channel silences the K2P1 channel (Rajan et al., 2005) and Transmembrane and Ubiquitin-Like Domain-Containing Protein 1 (Tmub1/HOPS) conjugation regulates basal synaptic transmission through regulation of GluA2 recycling

to the plasma membrane (Yang et al., 2008). Inhibition of the E1 activating enzyme with a cell permeable pyrazone derivative, PYR-41 increases the total level of sumoylation in cells (Yang et al., 2007) and one of the two mammalian E1 activation enzymes, E1-L2, can activate both ubiquitin and FAT-10 (Chiu et al., 2007). Furthermore, SUMOylation can directly modify the function of several classes of ion channels including Kv1.5 (Benson et al., 2007), Kv2.1 (Dai et al., 2009), kainite receptors (Martin et al., 2007), TRPM4 (Pongs and Kruse, 2009) and the dimeric potassium channel K2P1 (Feliciangeli et al., 2010; Plant et al., 2010). SUMOylation of ion channels thus provides neurons with additional link between the ubiquitin proteasome machinery, post-translation modification and neuron function suggesting that the balance of ubiquitin like protein expression and posttranslational modification is an as yet, unexplored potential consequence of homeostatic regulation of the ubiquitin proteasome system.

How do protein synthesis and protein degradation balance to regulate specific changes in homeostatic plasticity?

Emphasis has recently been placed on the idea of protein homeostasis, or proteostasis, as a critical determinant of normal cellular function (Balch et al., 2008). For example, long term potentiation is impaired in neurons where proteasome function has been disrupted (Chain et al., 1999; Lopez-Salon et al., 2001; Karpova et al., 2006; Dong et al., 2008; Fioravante et al., 2008) but when protein synthesis is blocked in conjunction with protein degradation, normal long term potentiation is restored (Fonseca et al., 2006; Karpova et al., 2006) suggesting that a balance of protein expression is important for

maintenance of long term synaptic plasticity. Here, we describe a series of homeostatic mechanisms that require spatially separated protein synthesis and degradation mechanisms (Figure 2.1, Figure 3.12, and Figure 4.1). If a balance of protein expression is critically important to normal functioning of neurons, why is there spatial segregation between protein synthesis and protein degradation during state-dependent homeostatic plasticity? One reason for the spatial segregation could be that protein synthesis and protein degradation are working to create functional matching between the pre- and post-synaptic components of the synapse. Although technically composed of two cells, the synapse behaves much like a single functional compartment (Davis and Goodman, 1998) suggesting that despite the spatial segregation, both protein synthesis and protein degradation are working together to match pre- and post- synaptic protein expression levels.

Why have both rapid and slow forms of homeostatic plasticity?

It is striking that neurons possess the ability to homeostatically regulate their behavior across a temporal window that ranges from minutes to days. Why is it advantageous to have temporally segregated forms of homeostatic plasticity? One possibility is that having multiple forms of homeostatic plasticity that differ in time course maximizes efficiency of the enduring nature of homeostatic plasticity. Blockade of AMPARs with CNQX or treatment with TTX+APV rapidly increases surface expression of GluA1 (Figure 3.2; Sutton et al., 2006) but not GluA2 (Figure 3.6; Sutton et al., 2006) containing AMPARs. Curiously, however, 24 hr post TTX+APV treatment increased

GluA1 expression has been replaced with an increase in GluA2 suggesting that there is an initial increase in local response mechanisms that require local translation mechanisms and energy expenditure at the synapse but that if the homeostatic responses need to be sustained for a long period of time the requirement for local translation of GluA1 decreases and is replaced with a more stable insertion of GluA2 containing AMPARs at the synapse. Therefore, rapid and slow forms of homeostatic plasticity may be two distinct phases of a single homeostatic plasticity mechanism whereby efficiency of the homeostatic response is mediated by AMPAR subunit composition over time (Sutton et al., 2006). Alternatively, multiple forms of homeostatic plasticity operating over distinct time domains may simply offer neural networks greater versatility in achieving stability despite dynamic changes in network activity.

What is the role of BDNF/TrkB during homeostatic plasticity?

BDNF functions as a synaptic retrograde enhancer of state-dependent function (Figure 3.8). Curiously, co-application of BDNF with TTX completely prevents scaling up of spiking activity that is normally observed with network quiescence alone (Rutherford et al., 1997; Rutherford et al., 1998) suggesting that BDNF/TrkB signaling may be involved in at least two forms of homeostatic plasticity. Although BDNF/TrkB signaling seems to have a clear role in both slow (Rutherford et al., 1997; Rutherford et al., 1998) and rapid (Figure 3.10) forms of homeostatic plasticity, the functional significance of this dual role of BDNF/TrkB signaling remains unclear. Since BDNF/TrkB can both promote (Figure 3.10) and constrain (Rutherford et al., 1997;

Rutherford et al., 1998) homeostatic plasticity, BDNF may be acting as a molecular buffer to keep neuron activity within a set range by driving the appropriate homeostatic alteration in synapse function.

Multiple homeostatic mechanisms exist within a single synapse

Blockade of AMPARs rapidly increases presynaptic and postsynaptic function (Figure 3.1). What advantage is there to simultaneously inducing multiple forms of homeostatic plasticity in a subset of synapses? Given that response properties of neurons depend upon the previous activation history of the neuron (Turrigiano et al., 1994) one purpose could be to encode a unique synaptic memory of homeostatic plasticity. Mathematical modeling of cell signaling pathways suggests "molecular memories" encoded by emergent properties of biochemical interactions arise from variations in input duration and strength (Bhalla et al., 2002) suggesting that the induction of more than one form of homeostatic plasticity could have a more sustainable response than a single form of homeostatic plasticity alone. The ability of local regions of a neuron to encode molecular memories could have implications for further neuron response mechanisms (Turrigiano et al., 1994) especially Hebbian forms of synaptic plasticity.

Local vs. Global homeostatic mechanisms? A role for metaplasticity or hierachichal dominance?

It is becoming increasingly clear that there are several different forms of homeostatic plasticity. However, it is less clear how multiple homeostatic mechanisms may interact to achieve an overall, balanced neuron network. One hypothesis for the integration of homeostatic mechanisms is that a metaplastic-like interaction exists between multiple forms of synaptic plasticity (Thiagarajan et al., 2007); EMJ Venkatesh, AJ Iliff, MA Sutton, unpublished observations)]. For example, induction of Hebbian plasticity constrains the ability of neurons to undergo additional homeostatic plasticity mechanisms (EMJ Venkatesh, AJ Iliff, MA Sutton, unpublished observations) suggesting that prior expression of Hebbian forms of plasticity may alter the magnitude of subsequently induced homeostatic plasticity. In contrast, the data presented here suggest that multiple forms of homeostatic plasticity might interact in a hierarchical, rather than metaplastic, manner (Figure 3.1; Bergquist et al., 2010). Action potential activity gates synaptic compensation through activity dependent localization of protein degradation machinery (Figure 4.5; see also Bingol et al., 2006 and 2010) suggesting that changes in neuron network function, through regulation of the ubiquitin proteasome system, may function to control an all or nothing presynaptic homeostatic response mechanism. Future studies are necessary to more fully understand the manner by which different forms of homeostatic plasticity interact.

Molecular integration of existing theories of homeostatic plasticity

Several molecular mechanisms of homeostatic plasticity have been previously proposed. Do these homeostatic mechanisms represent different facets of one, global

form of homeostatic plasticity? Or, do they each represent a distinct form of activity dependent modification? Our data suggests that rapid (AMPAR blockade) and slow (AP blockade) forms of homeostatic plasticity are indeed molecularly distinct forms of homeostatic compensation. However, crosstalk between described homeostatic plasticity pathways has been described. As little as 20 min of TNFalpha stimulation can increases in RA and GluA2 expression (Cingoliani et al., 2008) suggesting a putative link between 3 different homeostatic plasticity stories that exist in the literature. Furthermore, exogenous RA treatment can both mimic and occlude TTX+APV homeostatic plasticity mechanisms (Aoto et al., 2008; see also Sutton et al., 2006) as well as increase surface expression of TrkB in human neuroblastoma cells (Kaplan et al., 1993) and superior cervical ganglia (Kobayashi et al., 1994) suggesting a mechanisms whereby BDNF and RA could work in tandem to regulate homeostatic modification of presynaptic release probability. Future studies designed with the intent to examine the overlap of existing homeostatic plasticity mechanisms will be required to fully determine if and how much crossover exists between multiple forms of homeostatic plasticity.

Understanding how neurons sense and respond to changes in activity is required for a full understanding of compensatory plasticity

One additional advance key to understanding the molecular identities of homeostatic modification is the identity of the activity sensor. Based on the current understanding of the field, it is likely that there are multiple activity sensors present within neurons that can sense and respond to changes in neuron, synaptic, and intrinsic activity either alone or in combination. Are these activity sensors distinct proteins? Or

are they one protein or a complex of proteins that have the ability to sense and respond to changes in multiple components of neuron function? Sensors must be present that monitor changes in network activity and implement the classical slow synaptic scaling mechanism of compensation that are likely located in the cell soma (Ibata et al., 2008), there must also be synaptic sensors that are capable of locally integrating direct synaptic information on a much more rapid (minutes to hours) timescale. From our studies, it cannot be inferred if one or multiple activity sensors are necessary for homeostatic plasticity but that an activity sensor is likely located both pre- and post- synaptically. One possible candidate activity sensor is CAMKII. Expression of CAMKII T286D, a CAMKII phosphomimetic, increased both EPSC and mEPSC amplitude in cultured visual cortical neurons by increasing quantal content but at the same time decreased the density of synaptic contacts on CAMKII T286D expressing neurons (Pratt et al., 2003). Additionally, inhibition of endogenous CAMKII with an autoinhibitory peptide, decreased mEPSC amplitude while increasing synapse density (Pratt et al., 2003) and CAMKII activity is also necessary for Rpt6 phosphorylation (Djakovic et al., 2009; Bingol et al., 2010) as well as proteasome trafficking into dendritic spines (Bingol et al., 2010). Together these studies suggest a link between changes in synaptic function as well as direct signaling to the ubiquitin proteasome system providing a possible candidate for a homeostatic activity sensor, downstream of synaptic inhibition through AMPAR blockade.

Homeostatic plasticity and disease - cause or effect?

Is homeostatic plasticity the cause or effect of physiological dysfunction? It has been proposed that "homeostatic proteins" may contribute to neurological disorders (Ramocki and Zoghbi, 2008). Although this idea remains highly speculative, the work presented above provides a link between dysregulation of adaptive neuron behavior leading to sustained alterations in synaptic protein expression thought to contribute to the development of Alzheimers disease (Dickman and Davis, 2009), polyglutamine disorders (Ortega et al., 2010) as well as Parkinsons disease (Shimura et al., 2001). In contrast, it has recently been shown that Ltn1 RING-domain-type E3 ubiquitin ligase is necessary for the degradation of aberrant "non-stop proteins" in yeast (Bengtson and Joazeiro, 2010). Yeast expressing Ltn1 are resistant to "non-stop protein" induced stress (Bengtson and Joazeiro 2010) suggesting that homeostatic plasticity, via the ubiquitin proteasome system, may be responsible for regulating homeostatic adaptation during stress. Indeed, immunoproteasomes are upregulated in response to oxidative stress and maintain protein homeostasis in the face of interferon expression in both human and mouse cell lines (Seifert et al., 2010). These findings demonstrate a striking parallel to the necessary involvement of the proteasome in both ER stress mediated augmentation of presynpatic function and state-dependent changes in presynaptic function downstream of AMPAR blockade and suggest that dysregulation of homeostatic plasticity may contribute to neurological disorders. In contrast, disease states have been hypothesized to arise from overly efficient homeostatic plasticity mechanisms. Cocaine treatment occludes the effects of homeostatic synapse-membrane plasticity two days post cocaine withdrawal (Ishikawa et al., 2009) suggesting that addiction is utilizing the same homeostatic mechanisms to aberrantly facilitate neuronal connections in the nucleus accumbens (Sun

and Wolf 2009). These observations suggest that homeostatic plasticity mechanisms may underlie fundamental properties of addiction. Activity suppression-induced homeostatic plasticity also parallels several epilepsy models. Deprivation of visual or aural stimuli can cause interictal spiking (Kellaway, 1989) or an increase in susceptibility to sound-triggered seizures (Pierson and Swann, 1988), respectively. Curiously, activity dependent modulation of network function used to probe homeostatic compensation is also used to probe epileptic function in neuron circuits. Chronic inhibition of neuron network activity with TTX induces chronic focal epilepsy (Galvan et al., 2000) and prolonged epileptiform activity (Niesen and Ge, 1999; Bausch et al., 2006). BDNF expression is greatly enhanced following the induction of seizures (Ernfors et al., 1991; Dugich-Djordjevic et al., 1992) and epileptic phenotypes can be dampened through conditional deletion of TrkB (He et al., 2004) as well as rescued by exogenous expression of BDNF (Paradiso et al., 2009). Given the parallel between described homeostatic plasticity mechanisms and disease models, understanding how homeostatic function differs during disease states will be fundamental to understanding the etiology of neurological disorders.

Difficulties applying homeostatic plasticity mechanisms to behavior

Homeostatic plasticity has been heavily studied over the past decade as a mechanism for maintaining neuron function within a dynamic, yet stable functional range. It is thought that homeostatic plasticity is necessary for behaviorally relevant functions such as learning and memory. Despite recent interest in homeostatic plasticity as a model of neuron stability during learning and memory, it has been difficult to

attribute a specific role for homeostatic plasticity during physiologically relevant functions. One reason why extension of homeostatic theory has been difficult is that experiments designed to test the emergence of homeostatic plasticity have largely been carried out in cultured networks of neurons. Although an excellent tool for dissecting the molecular mechanisms underlying compensation, cultured neurons do not retain the native architecture of brain regions which is important for understanding synapse specific modifications (Kim and Tsien 2008). Additionally, in culture, identification of cell type is largely based on morphology yet specific neuron types are quite heterogeneous with regard to the compliment of proteins that each neuron expresses (Zander et al., 2010) suggesting that future *in vivo* work may reveal an intricate web of synapse specific homeostatic mechanisms that are dependent upon the combined heterogeneity of pre- and post- synaptic functional properties. Furthermore, basal mEPSC and EPSC amplitude and frequency are elevated in cultured networks of neurons when compared to acute preparations (Sutton et al., 2006) suggesting that neurons in cultures may already be "pre-scaled" before experimental manipulation. To that effect, data gathered from populations of cultured neurons may represent a late second or third phase of homeostatic compensation rather than an initial stabilization of neuron function. Together, these caveats illustrate that data garnered from cultured neurons must, in the future, be integrated with studies from acute hippocampal slice as well as *in vivo* studies in awake, behaving animals for a full interpretation of the physiological importance of homeostatic plasticity.

Final thoughts and future directions

Over the last decade, our understanding of homeostatic plasticity has grown exponentially with demonstrations of at least one form of compensatory neuron plasticity across the peripheral as well as the central nervous system. Strikingly, the majority of this work has been descriptive and has centered on demonstrating that many different types of neurons are capable of undergoing adaptive changes in function. Recently, however, a shift has been made to try and elucidate the molecular mechanisms of homeostatic plasticity. From these studies it is becoming increasingly clear, that similar to other forms of neuron plasticity, homeostatic plasticity can be achieved through a host of molecular mechanisms that lead to the overall stabilization of neuron networks. It is certain that further understanding of homeostatic plasticity will contribute a great deal to the overall understanding of healthy neuron network and synaptic function and this basic knowledge of nervous system function will lead to a greater understanding of neurological disorders.

A key future challenge for homeostatic plasticity research is to forge a direct link between *in vitro* models of homeostatic plasticity and models of homeostatic plasticity occurring under physiological conditions *in vivo*. Although there is general agreement that a theoretical need for an adaptive or homeostatic neuron plasticity exists, two major weaknesses have hampered the understanding of homeostatic plasticity *in vivo*: 1) Homeostatic plasticity has largely been studied in dissociated cultures of neuron networks lacking the architecture of intact structures as well as synapse specific information that can influence homeostatic response mechanisms (Kim and Tsien 2008) and, 2) Pharmacological manipulation of activity likely does not fall within the normal

physiological range of activity that neurons generally encounter. Therefore it is critical for the knowledge that has been garnered from the *in vitro* and pharmacological models to move *in vivo* as well into more physiological conditions. Therefore, as homeostatic plasticity seems poised to link many divergent aspects of physiology, the future of the field also lies within the integration of technical advances as well as the continued collaboration between molecular biology, biochemistry, computational biology, electrophysiology and translational research to achieve a full understanding of how and why neurons retain the capacity to regulate stability over time. With the progression of homeostatic plasticity research, we will be able to begin to understand how neurons maintain a stable *millieu interieur* over time.

BIBLIOGRAPHY

Aakalu G, Smith WB, Nguyen N, Jiang CG, Schuman EM (2001) Dynamic visualization of local protein synthesis in hippocampal neurons. Neuron 30:489-502.

Agranoff BW, Klinger PD (1964) Puromycin effect in memory fixation in goldfish. Science 146:952-&.

Agranoff BW, Davis RE, Brink JJ (1965) Memory fixation in goldfish. Proc Natl Acad Sci U S A 54:788-&.

Alvarez A, Munoz JP, Maccioni RB (2001) A cdk5-p35 stable complex is involved in the beta-amyloid-induced deregulation of cdk5 activity in hippocampal neurons. Exp Cell Res 264:266-274.

An JJ, Gharami K, Liao GY, Woo NH, Lau AG, Vanevski F, Torre ER, Jones KR, Feng Y, Lu B, Xu B (2008) Distinct role of long 3 ' UTR BDNF mRNA in spine morphology and synaptic plasticity in hippocampal neurons. Cell 134:175-187.

Anderson HK (1903) Reflex pupil dilatation by way of the cervical sympathetic nerve. J Physiol-London 30:15-24.

Aoto J, Nam CI, Poon MM, Ting P, Chen L (2008) Synaptic Signaling by All-Trans Retinoic Acid in Homeostatic Synaptic Plasticity. Neuron 60:308-320.

Aptowicz CO, Kunkler PE, Kraig RP (2004) Homeostatic plasticity in hippocampal slice cultures involves changes in voltage-gated Na+ channel expression. Brain Res 998:155-163.

Aravamudan B, Broadie K (2003) Synaptic Drosophila UNC-13 is regulated by antagonistic G-protein pathways via a proteasome-dependent degradation mechanism. J Neurobiol 54:417-438.

Aravamudan B, Fergestad T, Davis WS, Rodesch CK, Broadie K (1999) Drosophila Unc-13 is essential for synaptic transmission. Nat Neurosci 2:965-971.

Atasoy D, Ertunc M, Moulder KL, Blackwell J, Chung CH, Su JZ, Kavalali ET (2008) Spontaneous and evoked glutamate release activates two populations of NMDA receptors with limited overlap. J Neurosci 28:10151-10166.

Austin JH, Cullen GE, Hastings AB, McLean FC, Peters JP, Van Slyke DD (1922) Studies of gas and electrolyte equilibria in blood. I. Technique for collection and analysis of blood, and for its saturation with gas mixtures of known composition. J Biol Chem 54:121-147.

Axelsson J, Thesleff S (1959) A study of supersensitivity in denervated mammalian skeletal muscle. J Physiol-London 147:178-193.

Azdad K, Chavez M, Bischop PD, Wetzelaer P, Marescau B, De Deyn PP, Gall D, Schiffmann SN (2009) Homeostatic Plasticity of Striatal Neurons Intrinsic Excitability following Dopamine Depletion. PLoS One 4:12.

Bacci A, Coco S, Pravettoni E, Schenk U, Armano S, Frassoni C, Verderio C, De Camilli P, Matteoli M (2001) Chronic blockade of glutamate receptors enhances presynaptic release and downregulates the interaction between synaptophysin-synaptobrevin-vesicle-associated membrane protein 2. J Neurosci 21:6588-6596.

Balch WE, Morimoto RI, Dillin A, Kelly JW (2008) Adapting proteostasis for disease intervention. Science 319:916-919.

Ballarin M, Ernfors P, Lindefors N, Persson H (1991) Hippocampal damage and kainic acid injection induce a rapid increase in messsenger-RNA for BDNF an NGF in the rat-brain. Exp Neurol 114:35-43.

Barde YA, Edgar D, Thoenen H (1982) Purification of a new neurotrophic factor from mammalian brain. Embo J 1:549-553.

Bartley AF, Huang ZJ, Huber KM, Gibson JR (2008) Differential activity-dependent, homeostatic plasticity of two neocortical inhibitory circuits. J Neurophysiol 100:1983-1994.

Barton AC, Black LE, Sibley DR (1991) Agonist-induced desensitization of D2 dopamine-receptors in human Y-79 retinoblastoma cells. Mol Pharmacol 39:650-658.

Bausch SB, He SJ, Petrova Y, Wang XM, McNamara JO (2006) Plasticity of both excitatory and inhibitory synapses is associated with seizures induced by removal of chronic blockade of activity in cultured hippocampus. J Neurophysiol 96:2151-2167.

Bekinschtein P, Cammarota M, Igaz LM, Bevilaqua LRM, Izquierdo I, Medina JH (2007) Persistence of long-term memory storage requires a late protein synthesis- and BDNF-dependent phase in the hippocampus. Neuron 53:261-277.

Bence NF, Sampat RM, Kopito RR (2001) Impairment of the ubiquitin-proteasome system by protein aggregation. Science 292:1552-1555.

Bence NF, Bennett EJ, Kopito RR (2005) Application and analysis of the GFP(u) family of ubiquitin-proteasome system reporters. In: Ubiquitin and Protein Degradation, Pt B, pp 481-490. San Diego: Elsevier Academic Press Inc.

Bengtson MH, Joazeiro CAP (2010) Role of a ribosome-associated E3 ubiquitin ligase in protein quality control. Nature 467:470-473.

Benson MD, Li QJ, Kieckhafer K, Dudek D, Whorton MR, Sunahara RK, Iniguez-Lluhi JA, Martens JR (2007) SUMO modification regulates inactivation of the voltage-gated potassium channel Kv1.5. Proc Natl Acad Sci U S A 104:1805-1810.

Bergquist S, Dickman DK, Davis GW (2009) A Hierarchy of Cell Intrinsic and Target-Derived Homeostatic Signaling. Neuron 66:220-234.

Beutler B, Greenwald D, Hulmes JD, Chang M, Pan YCE, Mathison J, Ulevitch R, Cerami A (1985) Identity of tumor necrosis factor and the macrophage-secreted factor cachectin. Nature 316:552-554.

Bhalla US, Ram PT, Iyengar R (2002) MAP kinase phosphatase as a locus of flexibility in a mitogen-activated protein kinase signaling network. Science 297:1018-1023.

Bingol B, Schuman EM (2006) Activity-dependent dynamics and sequestration of proteasomes in dendritic spines. Nature 441:1144-1148.

Bingol B, Wang CF, Arnott D, Cheng DM, Peng JM, Sheng M (2010) Autophosphorylated CaMKII alpha Acts as a Scaffold to Recruit Proteasomes to Dendritic Spines. Cell 140:567-578.

Borodinsky LN, Root CM, Cronin JA, Sann SB, Gu XN, Spitzer NC (2004) Activity-dependent homeostatic specification of transmitter expression in embryonic neurons. Nature 429:523-530.

Bradberry CW (2007) Cocaine sensitization and dopamine mediation of cue effects in rodents, monkeys, and humans: areas of agreement, disagreement, and implications for addiction. Psychopharmacology 191:705-717.

Branco T, Staras K, Darcy KJ, Goda Y (2008) Local dendritic activity sets release probability at hippocampal synapses. Neuron 59:475-485.

Brink JJ, Davis RE, Agranoff BW (1966) Effects of puromycin acetoxycycloheximide and actinomycin D on protein synthesis in goldfish brain. J Neurochem 13:889-&.

Brown GL (1937) The action of acetylcholine in denervated mammalian and frog's muscle. The Journal of Physiology London 89.

Brown TH, Wong RKS, Prince DA (1979) Spontaneous miniature synaptic potentials in hippocampal-neurons. Brain Res 177:194-199.

Burbea M, Dreier L, Dittman JS, Grunwald ME, Kaplan JM (2002) Ubiquitin and AP180 regulate the abundance of GLR-1 glutamate receptors at postsynaptic elements in C-elegans. Neuron 35:107-120.

Burrone J, O'Byrne M, Murthy VN (2002) Multiple forms of synaptic plasticity triggered by selective suppression of activity in individual neurons. Nature 420:414-418.

Cai F, Frey JU, Sanna PP, Behnisch T (2010) Protein degradation by the proteasome is required for synaptic tagging and the heterosynaptic stabilization of hippocampal late-phase long-term potentiaion. Neuroscience 169:1520-1526.

Cajal SR (1984) Histologie du Systéme Nerveux de l'Homme et des Vertébres Vol. **2** (transl. Azoulay, L.) (Institute Ramon y Cajal, Madrid, 1955).

Cannon WB (1926) Some general features of endocrine influence on metabolism. Am J Med Sci 171:1-20.

Cannon WB (1929) Organization for physiological homeostasis. Physiol Rev 9:399-431.

Cannon WB, Rosenblueth A (1949) The supersensitivity of denervated structures. A law of denerva-tion: Macmillan Co.

Cao JL, Vialou VF, Lobo MK, Robison AJ, Neve RL, Cooper DC, Nestler EJ, Han MH (2010) Essential role of the cAMP-cAMP response-element binding protein pathway in opiate-induced homeostatic adaptations of locus coeruleus neurons. Proc Natl Acad Sci U S A 107:17011-17016.

Carmignoto G, Pizzorusso T, Tia S, Vicini S (1997) Brain-derived neurotrophic factor and nerve growth factor potentiate excitatory synaptic transmission in the rat visual cortex. J Physiol-London 498:153-164.

Castren E, Zafra F, Thoenen H, Lindholm D (1992) Light regulates expression of brain-derived neurotrophic factor messenger-RNA in rat visual-cortex. Proc Natl Acad Sci U S A 89:9444-9448.

Castren E, Pitkanen M, Sirvio J, Parsadanian A, Lindholm D, Thoenen H, Riekkinen PJ (1993) The induction of LTP increases BDNF and NGF messenger-RNA but decreases NT-3 messenger-RNA in the rat dentate gyrus. Neuroreport 4:895-898.

Chain DG, Casadio A, Schacher S, Hegde AN, Valbrun M, Yamamoto N, Goldberg AL, Bartsch D, Kandel ER, Schwartz JH (1999) Mechanisms for generating the autonomous cAMP-dependent protein kinase required for long-term facilitation in Aplysia. Neuron 22:147-156.

Chen N, Chen X, Wang JH (2008) Homeostasis established by coordination of subcellular compartment plasticity improves spike encoding. J Cell Sci 121:2961-2971.

Chiu YH, Sun Q, Chen ZJJ (2007) E1-L2 activates both ubiquitin and FAT10. Mol Cell 27:1014-1023.

Chub N, O'Donovan MJ (1998) Blockade and recovery of spontaneous rhythmic activity after application of neurotransmitter antagonists to spinal networks of the chick embryo. J Neurosci 18:294-306.

Ciechanover A, Hod Y, Hershko A (1978) Heat-stable polypeptide component of an ATP-dependent proteolytic system from reticulocytes. Biochem Biophys Res Commun 81:1100-1105.

Ciechanover A, Heller H, Katzetzion R, Hershko A (1981) Activation of the heat-stable polypeptide of the ATP-dependent proteolytic system. Proceedings of the National Academy of Sciences of the United States of America-Biological Sciences 78:761-765.

Ciechanover A, Elias S, Heller H, Hershko A (1982) Covalent affinity purification of ubiquitin-activating enzyme. J Biol Chem 257:2537-2542.

Ciechanover A, Heller H, Elias S, Haas AL, Hershko A (1980) ATP-dependent conjugation of reticulocyte proteins with the polypeptide required for protein-degradation. Proceedings of the National Academy of Sciences of the United States of America-Biological Sciences 77:1365-1368.

Cingolani LA, Goda Y (2008) Differential involvement of beta(3) integrin in pre- and postsynaptic forms of adaptation to chronic activity deprivation. Neuron Glia Biol 4:179-187.

Cingolani LA, Thalhammer A, Yu LMY, Catalano M, Ramos T, Colicos MA, Goda Y (2008) Activity-dependent regulation of synaptic AMPA receptor composition and abundance by beta 3 integrins. Neuron 58:749-762.

Claude B (1865) Introduction à l'étude de la Médecine Expérimentale.

Claude B (1878) Lectures on the phenonmenon common to animals and plants. Charles C Thomas.

Cline H (2003) Synaptic plasticity: Importance of proteasome- mediated protein turnover. Curr Biol 13:R514-R516.

Colledge M, Snyder EM, Crozier RA, Soderling JA, Jin YT, Langeberg LK, Lu H, Bear MF, Scott JD (2003) Ubiquitination regulates PSD-95 degradation and AMPA receptor surface expression. Neuron 40:595-607.

Colomo F, Erulkar SD (1968) Miniature synaptic potentials at frog spinal neurones in the presence of tetrodotoxin. J Physiol-London 199:205.

Cuervo AM, Wong ESP, Martinez-Vicente M (2010) Protein Degradation, Aggregation, and Misfolding. Mov Disord 25:S49-S54.

Dai XQ, Kolic J, Marchi P, Sipione S, MacDonald PE (2009) SUMOylation regulates Kv2.1 and modulates pancreatic beta-cell excitability. J Cell Sci 122:775-779.

Dani JA, Heinemann S (1996) Molecular and cellular aspects of nicotine abuse. Neuron 16:905-908.

Davis GW (2006) Homeostatic control of neural activity: From phenomenology to molecular design. Annu Rev Neurosci 29:307-323.

Davis GW, Murphey RK (1993) A role for postsynaptic neurons in determining presynaptic release properties in the cricket CNS - evidence for retrograde control of facilitation. J Neurosci 13:3827-3838.

Davis GW, Goodman CS (1998) Synapse-specific control of synaptic efficacy at the terminals of a single neuron. Nature 392:82-86.

Davis RE, Bright PJ, Agranoff BW (1965) Effect of ECS and puromycin on memory in fish. Journal of Comparative and Physiological Psychology 60:162-&.

Dayer JM, Beutler B, Cerami A (1985) Cachectin tumor necrosis factor stimulates collagenase and prostaglandin-E2 production by human synovial-cells and dermal fibroblasts. J Exp Med 162:2163-2168.

De Gois S, Schafer MKH, Defamie N, Chen C, Ricci A, Weihe E, Varoqui H, Erickson JD (2005) Homeostatic scaling of vesicular glutamate and GABA transporter expression in rat neocortical circuits. J Neurosci 25:7121-7133.

Demartino GN, Moomaw CR, Zagnitko OP, Proske RJ, Chuping M, Afendis SJ, Swaffield JC, Slaughter CA (1994) PA700, An ATP-dependent activator of the 20-S-proteasome, is an ATP-ase containing multiple members of a nucleotide-binding protein family. J Biol Chem 269:20878-20884.

Desai NS, Rutherford LC, Turrigiano GG (1999) Plasticity in the intrinsic excitability of cortical pyramidal neurons. Nat Neurosci 2:515-520.

Desai NS, Cudmore RH, Nelson SB, Turrigiano GG (2002) Critical periods for experience-dependent synaptic scaling in visual cortex. Nat Neurosci 5:783-789.

Dickman DK, Davis GW (2009) The Schizophrenia Susceptibility Gene dysbindin Controls Synaptic Homeostasis. Science 326:1127-1130.

Ding M, Shen K (2008) The role of the ubiquitin proteasome system in synapse remodeling and neurodegenerative diseases. Bioessays 30:1075-1083.

Djakovic SN, Schwarz LA, Barylko B, DeMartino GN, Patrick GN (2009) Regulation of the Proteasome by Neuronal Activity and Calcium/Calmodulin-dependent Protein Kinase II. J Biol Chem 284:26655-26665.

Dong CG, Upadhya SC, Ding L, Smith TK, Hegde AN (2008) Proteasome inhibition enhances the induction and impairs the maintenance of late-phase long-term potentiation. Learn Mem 15:335-347.

Doyle S, Pyndiah S, De Gois S, Erickson JD (2010) Excitation-Transcription Coupling via Calcium/Calmodulin-dependent Protein Kinase/ERK1/2 Signaling Mediates the Coordinate Induction of VGLUT2 and Narp Triggered by a Prolonged Increase in Glutamatergic Synaptic Activity. J Biol Chem 285:14366-14376.

Dugich-Djordjevic MM, Ohsawa F, Okazaki T, Mori N, Day JR, Beck KD, Hefti F (1995) Differential regulation of catalytic and noncatalytic TrkB messenger-RNAs in the rat hippocampus following seizures induced by systemic administration of kainate. Neuroscience 66:861-877.

Echegoyen J, Neu A, Graber KD, Soltesz I (2007) Homeostatic Plasticity Studied Using In Vivo Hippocampal Activity-Blockade: Synaptic Scaling, Intrinsic Plasticity and Age-Dependence. PLoS One 2:9.

Ehlers MD (2003) Activity level controls postsynaptic composition and signaling via the ubiquitin-proteasome system. Nat Neurosci 6:231-242.

Eliot TR (1905) On the action of adrenaline. The Journal of Physiology London 32.

Elliott RC, Inturrisi CE, Black IB, Dreyfus CF (1994) An improved method detects differential NGF and BDNF gene-expression in response to depolarization in cultured hippocampal-neurons. Mol Brain Res 26:81-88.

Ernfors P, Bengzon J, Kokaia Z, Persson H, Linvall O (1991) Increased levels of messenger-RNAs for neurotrophic factors in the brain during kindling epileptogenesis. Neuron 7:165-176.

Evers DM, Matta JA, Hoe HS, Zarkowsky D, Lee SH, Isaac JT, Pak DTS Plk2 attachment to NSF induces homeostatic removal of GluA2 during chronic overexcitation. Nat Neurosci 13:1199-1207.

Feliciangeli S, Tardy MP, Sandoz G, Chatelain FC, Warth R, Barhanin J, Bendahhou S, Lesage F (2010) Potassium Channel Silencing by Constitutive Endocytosis and Intracellular Sequestration. J Biol Chem 285:4798-4805.

Fenteany G, Standaert RF, Lane WS, Choi S, Corey EJ, Schreiber SL (1995) Inhibitino of proteasome activities and subunit-specific amino-terminal threonine modification by lactacystin. Science 268:726-731.

Figurov A, PozzoMiller LD, Olafsson P, Wang T, Lu B (1996) Regulation of synaptic responses to high-frequency stimulation and LTP by neurotrophins in the hippocampus. Nature 381:706-709.

Fioravante D, Liu RY, Byrne JH (2008) The Ubiquitin-Proteasome System Is Necessary for Long-Term Synaptic Depression in Aplysia. J Neurosci 28:10245-10256.

Fonseca R, Vabulas RM, Hartl FU, Bonhoeffer T, Nagerl UV (2006) A balance of protein synthesis and proteasome-dependent degradation determines the maintenance of LTP. Neuron 52:239-245.

Frank CA, Kennedy MJ, Goold CP, Marek KW, Davis GW (2006) Mechanisms underlying the rapid induction and sustained expression of synaptic homeostasis. Neuron 52:663-677.

Frey U, Krug M, Reymann KG, Matthies H (1988) Anisomycin, an inhibitory of protein-synthesis, blocks late phases of LTP phenomena in the hippocampal CA1 region in vitro. Brain Res 452:57-65.

Gainey MA, Hurvitz-Wolff JR, Lambo ME, Turrigiano GG (2009) Synaptic scaling requires the GluR2 subunit of the AMPA receptor. J Neurosci 29:6479-6489.

Galante M, Avossa D, Rosato-Siri M, Ballerini L (2001) Homeostatic plasticity induced by chronic block of AMPA/kainate receptors modulates the generation of rhythmic bursting in rat spinal cord organotypic cultures. Eur J Neurosci 14:903-917.

Galvan CD, Hrachovy RA, Smith KL, Swann JW (2000) Blockade of neuronal activity during hippocampal development produces a chronic focal epilepsy in the rat. J Neurosci 20:2904-2916.

Ganser LR, Dallman JE (2009) Glycinergic synapse development, plasticity, and homeostasis in zebrafish. Front Mol Neurosci 2:30.

Gao M, Sossa K, Song LH, Errington L, Cummings L, Hwang H, Kuhl D, Worley P, Lee HK A Specific Requirement of Arc/Arg3.1 for Visual Experience-Induced Homeostatic Synaptic Plasticity in Mouse Primary Visual Cortex. J Neurosci 30:7168-7178.

Gartner AG, Staiger V (2002) Neurotrophin secretion from hippocampal neurons evoked by long-term-potentiation-inducing electrical stimulation patterns. Proc Natl Acad Sci U S A 99:6386-6391.

Goel A, Lee HK (2007) Persistence of experience-induced homeostatic synaptic plasticity through adulthood in superficial layers of mouse visual cortex. J Neurosci 27:6692-6700.

Gong B, Wang H, Gu S, Heximer SP, Zhuo M (2007) Genetic evidence for the requirement of adenylyl cyclase 1 in synaptic scaling of forebrain cortical neurons. Eur J Neurosci 26:275-288.

Gonzalez-Islas C, Wenner P (2006) Spontaneous network activity in the embryonic spinal cord regulates AMPAergic and GABAergic synaptic strength. Neuron 49:563-575.

Greer PL, Hanayama R, Bloodgood BL, Mardinly AR, Lipton DM, Flavell SW, Kim TK, Griffith EC, Waldon Z, Maehr R, Ploegh HL, Chowdhury S, Worley PF, Steen J,

Greenberg ME (2010) The Angelman Syndrome Protein Ube3A Regulates Synapse Development by Ubiquitinating Arc. Cell 140:704-716.

Gregersen N, Bolund L, Bross P (2005) Protein misfolding, aggregation, and degradation in disease. Mol Biotechnol 31:141-150.

Groth, Lindskog M, Tsien RW (2009) Society for Neuroscience Abstracts.

Guo L, Wang Y (2007) Glutamate stimulates glutamate receptor interacting protein 1 degradation by ubiquitin-proteasome system to regulate surface expression of GluR2. Neuroscience 145:100-109.

Han EB, Stevens CF (2009a) Development regulates a switch between post-and presynaptic strengthening in response to activity deprivation. Proc Natl Acad Sci U S A 106:10817-10822.

Han EB, Stevens CF (2009b) Development regulates a switch between post- and presynaptic strengthening in response to activity deprivation. Proc Natl Acad Sci U S A 106:10817-10822.

Harris EJ, Nicholls JG (1956) The effect of denervation on the rate of entry of potassium into frog muscle. J Physiol-London 131:473-476.

Hartmann K, Bruehl C, Golovko T, Draguhn A (2008) Fast Homeostatic Plasticity of Inhibition via Activity-Dependent Vesicular Filling. PLoS One 3:10.

He XP, Kotloski R, Nef S, Luikart BW, Parada LF, McNamara JO (2004) Conditional deletion of TrkB but not BDNF prevents epileptogenesis in the kindling model. Neuron 43:31-42.

Hebb DO (1949) The organization of behavior

Hegde AN, Goldberg AL, Schwartz JH (1993) Regulatory subunits of cAMP-dependent protein-kinases are degraded after conjugation to ubiquitin - a molecular mechanisms underlying long-term synaptic plasticity. Proc Natl Acad Sci U S A 90:7436-7440.

Hegde AN, Inokuchi K, Pei WZ, Casadio A, Ghirardi M, Chain DG, Martin KC, Kandel ER, Schwartz JH (1997) Ubiquitin C-terminal hydrolase is an immediate-early gene essential for long-term facilitation in Aplysia. Cell 89:115-126.

Henderson Y, Haggard (1918) Respiratory regulation of the CO2 capacity of the blood: I. High levels of CO2 and alkali. The Journal of Biological Chemistry 33:333-344.

Hershko A (2005) The ubiquitin system for protein degradation and some of its roles in the control of the cell division cycle. Cell Death Differ 12:1191-1197.

Hershko A, Tomkins GM (1971) Studies on degradation of tyrosine aminotransferase in hepatoma cells in culture - influence of composition of medium an adenosine triphosphate dependence. J Biol Chem 246:710-&.

Hershko A, Ciechanover A (1992) The ubiquitin proteasome system for prote-degradation. Annu Rev Biochem 61:761-807.

Hershko A, Ciechanover A (1998) The ubiquitin system. Annu Rev Biochem 67:425-479.

Hershko A, Leshinsky E, Ganoth D, Heller H (1984) ATP-dependent degradation of ubiquitin-protein conjugates. Proceedings of the National Academy of Sciences of the United States of America-Biological Sciences 81:1619-1623.

Hershko A, Ciechanover A, Heller H, Haas AL, Rose IA (1980) Proposed role of ATP in protein breakdown - conjugation of proteins with multiple chains of the polypeptide of ATP-dependent proteolysis. Proceedings of the National Academy of Sciences of the United States of America-Biological Sciences 77:1783-1786.

Hofer MM, Barde YA (1988) Brain-derived neurotrophic factor prevents neuronal death in vivo. Nature 331:261-262.

Hoffman L, Rechsteiner M (1994) Activation of the multicatalytic protease - the 11S regulator and 20S ATPase complexes contain distinct 30- kilodalton subunits. J Biol Chem 269:16890-16895.

Hou LF, Antion MD, Hu DY, Spencer CM, Paylor R, Klann E (2006) Dynamic translational and proteasomal regulation of fragile X mental retardation protein controls mGluR-dependent long-term depression. Neuron 51:441-454.

Hou Q, Zhang D, Jarzylo L, Huganir RL, Man HY (2008) Homeostatic regulation of AMPA receptor expression at single hippocampal synapses. Proc Natl Acad Sci U S A 105:775-780.

Hung AY, Sung CC, Brito IL, Sheng M (2010) Degradation of Postsynaptic Scaffold GKAP and Regulation of Dendritic Spine Morphology by the TRIM3 Ubiquitin Ligase in Rat Hippocampal Neurons. PLoS One 5:11.

Huupponen J, Molchanova SM, Taira T, Lauri SE (2007) Susceptibility for homeostatic plasticity is down-regulated in parallel with maturation of the rat hippocampal synaptic circuitry. J Physiol-London 581:505-514.

Ibata K, Sun Q, Turrigiano GG (2008) Rapid synaptic scaling induced by changes in postsynaptic firing. Neuron 57:819-826.

Iijima T, Emi K, Yuzaki M (2009) Activity-Dependent Repression of Cbln1 Expression: Mechanism for Developmental and Homeostatic Regulation of Synapses in the Cerebellum. J Neurosci 29:5425-5434.

Isackson PJ, Huntsman MM, Murray KD, Gall CM (1991) BDNF messenger-RNA expression is increased in adult-rat forebrain after limbic seizures - temporal patterns of induction distinct from NGF. Neuron 6:937-948.

Ishikawa M, Mu P, Moyer JT, Wolf JA, Quock RM, Davies NM, Hu XT, Schluter OM, Dong Y (2009) Homeostatic Synapse-Driven Membrane Plasticity in Nucleus Accumbens Neurons. J Neurosci 29:5820-5831.

Ito HT, Schuman EM (2009) Distance-dependent homeostatic synaptic scaling mediated by a-type potassium channels. Front Cell Neurosci 3:15.

Jackson JH (1884) The Croonian Lectures. The British Medical Journal.

Jensen TP, Buckby LE, Empson RM (2009) Reduced expression of the "fast" calcium transporter PMCA2a during homeostatic plasticity. Mol Cell Neurosci 41:364-372.

Jia JM, Chen Q, Zhou Y, Miao S, Zheng J, Zhang C, Xiong ZQ (2008) Brain-derived neurotrophic factor-tropomyosin-related kinase B signaling contributes to activity-dependent changes in synaptic proteins. J Biol Chem 283:21242-21250.

Jiang XP, Litkowski PE, Taylor AA, Lin Y, Snider BJ, Moulder KL (2010) A Role for the Ubiquitin-Proteasome System in Activity-Dependent Presynaptic Silencing. J Neurosci 30:1798-1809.

Joch M, Ase AR, Chen CXQ, MacDonald PA, Kontogiannea M, Corera AT, Brice A, Seguela P, Fon EA (2007) Parkin-mediated monoubiquitination of the PDZ protein PICK1 regulates the activity of acid-sensing ion channels. Mol Biol Cell 18:3105-3118.

Johnson JE, Barde YA, Schwab M, Thoenen H (1986) Brain-derived neurotrophic factor supports the survival of cultured rat retinal ganglion-cells. J Neurosci 6:3031-3038.

Ju W, Morishita W, Tsui J, Gaietta G, Deerinck TJ, Adams SR, Garner CC, Tsien RY, Ellisman MH, Malenka RC (2004) Activity-dependent regulation of dendritic synthesis and trafficking of AMPA receptors. Nat Neurosci 7:244-253.

Juo P, Kaplan JM (2004) The anaphase-promoting the abundance of GLR-1 complex regulates glutamate receptors in the ventral nerve cord of C-elegans. Curr Biol 14:2057-2062.

Kaneko M, Stellwagen D, Malenka RC, Stryker MP (2008) Tumor necrosis factor-alpha mediates one component of competitive, experience-dependent plasticity in developing visual cortex. Neuron 58:673-680.

Kang HJ, Schuman EM (1996) A requirement for local protein synthesis in neurotrophin-induced hippocampal synaptic plasticity. Science 273:1402-1406.

Kaplan DR, Matsumoto K, Lucarelli E, Thiele CJ (1993) Induction of TrkB by retinoic acid mediates biologic responsiveness to BDNF and differentiation of human neuroblastoma-cells. Neuron 11:321-331.

Karpova A, Mikhaylova M, Thomas U, Knopfel T, Behnisch T (2006) Involvement of protein synthesis and degradation in long-term potentiation of Schaffer collateral CA1 synapses. J Neurosci 26:4949-4955.

Katz B, Miledi R (1963) A study of spontaneous miniature potentials in spinal motorneurones. J Physiol-London 168:389-&.

Kauselmann G, Weiler M, Wulff P, Jessberger S, Konietzko U, Scafidi J, Staubli U, Bereiter-Hahn J, Strebhardt K, Kuhl D (1999) The polo-like protein kinases Fnk and Snk associate with a Ca2+- and integrin-binding protein and are regulated dynamically with synaptic plasticity. Embo J 18:5528-5539.

Kellaway (1989) Introduction to plasticity and sensitive periods. .

Kerscher O, Felberbaum R, Hochstrasser M (2006) Modification of proteins by ubiquitin and ubiquitin-like proteins. Annu Rev Cell Dev Biol 22:159-180.

Kim J, Tsien RW (2008) Synapse-specific adaptations to inactivity in hippocampal circuits achieve homeostatic gain control while dampening network reverberation. Neuron 58:925-937.

Kim J, Alger BE (2010) Reduction in endocannabinoid tone is a homeostatic mechanism for specific inhibitory synapses. Nat Neurosci 13:592-U104.

Kim SH, Ryan TA (2010) CDK5 Serves as a Major Control Point in Neurotransmitter Release. Neuron 67:797-809.

Klein R, Nanduri V, Jing SQ, Lamballe F, Tapley P, Bryant S, Cordoncardo C, Jones KR, Reichardt LF, Barbacid M (1991) The TrKB tyrosine protein-kinase is a receptor for brain-derived neurotrophic factory and neurotrophin-3. Cell 66:395-403.

Kobayashi M, Kurihara K, Matsuoka I (1994) Retinoic acid induces BDNF responsiveness of sympathetic neurons by alteration of TrK neurotrophin receptor expression. FEBS Lett 356:60-65.

Korte M, Carroll P, Wolf E, Brem G, Thoenen H, Bonhoeffer T (1995) Hippocampal long-term potentiation is impaired in mice lacking brain-derived neurotrophic factor. Proc Natl Acad Sci U S A 92:8856-8860.

Lauri SE, Lamsa K, Pavlov I, Riekki R, Johnson BE, Molnar E, Rauvala H, Taira T (2003) Activity blockade increases the number of functional synapses in the hippocampus of newborn rats. Mol Cell Neurosci 22:107-117.

Lee SH, Choi JH, Lee N, Lee HR, Kim JI, Yu NK, Choi SL, Kim H, Kaang BK (2008) Synaptic protein degradation underlies destabilization of retrieved fear memory. Science 319:1253-1256.

Leibrock J, Lottspeich F, Hohn A, Hofer M, Hengerer B, Masiakowski P, Thoenen H, Barde YA (1989) Molecular-cloning and expression of brain-derived neurotrophic factor. Nature 341:149-152.

Lessmann V, Gottmann K, Heumann R (1994) BDNF and NT-4/5 enhance glutamatergic synaptic transmission in cultured hippocampal-neurons. Neuroreport 6:21-25.

Li YX, Xu Y, Ju D, Lester HA, Davidson N, Schuman E (1998) Expression of a dominant negative Trk B receptor, T1, reveals a requirement for presynaptic signaling in BDNF-induced synaptic potentiation in cultured hippocampal neurons. Society for Neuroscience Abstracts 24:800.

Liao DH, Zhang XQ, O'Brien R, Ehlers MD, Huganir RL (1999) Regulation of morphological postsynaptic silent synapses in developing hippocampal neurons. Nat Neurosci 2:37-43.

Lin DH, Sterling H, Wang ZJ, Babilonia E, Yang BF, Dong K, Hebert SC, Giebisch G, Wang WH (2005) ROMK1 channel activity is regulated by monobuquitination. Proc Natl Acad Sci U S A 102:4306-4311.

Lin DH, Yue P, Pan CY, Sun P, Zhang X, Han ZG, Roos M, Caplan M, Giebisch G, Wang WH (2009) POSH Stimulates the Ubiquitination and the Clathrin-independent Endocytosis of ROMK1 Channels. J Biol Chem 284:29614-29624.

Lindefors N, Ernfors P, Falkenberg T, Persson H (1992) Septal cholinergic afferents regulate expression of brain-derived neurotrophic factor and beta-nerve growth-factor messenger-RNA in rat hippocampus. Exp Brain Res 88:78-90.

Lisman J, Schulman H, Cline H (2002) The molecular basis of CaMKII function in synaptic and behavioural memory. Nat Rev Neurosci 3:175-190.

Lissin DV, Gomperts SN, Carroll RC, Christine CW, Kalman D, Kitamura M, Hardy S, Nicoll RA, Malenka RC, von Zastrow M (1998) Activity differentially regulates the surface expression of synaptic AMPA and NMDA glutamate receptors. Proc Natl Acad Sci U S A 95:7097-7102.

Lohof AM, Ip NY, Poo MM (1993) Potentiation of developing neuromuscular synapses by the neurotrophins NT-3 and BDNF. Nature 363:350-353.

Lopez-Salon M, Alonso M, Vianna MRM, Viola H, Souza TME, Izquierdo I, Pasquini JM, Medina JH (2001) The ubiquitin-proteasome cascade is required for mammalian long-term memory formation. Eur J Neurosci 14:1820-1826.

MacLean JN, Zhang Y, Johnson BR, Harris-Warrick RM (2003) Activity-independent homeostasis in rhythmically active neurons. Neuron 37:109-120.

Maffei A, Turrigiano GG (2008) Multiple modes of network homeostasis in visual cortical layer 2/3. J Neurosci 28:4377-4384.

Maffei A, Nelson SB, Turrigiano GG (2004) Selective reconfiguration of layer 4 visual cortical circuitry by visual deprivation. Nat Neurosci 7:1353-1359.

Magby JP, Bi CX, Chen ZY, Lee FS, Plummer MR (2006) Single-cell characterization of retrograde signaling by brain-derived neurotrophic factor. J Neurosci 26:13531-13536.

Maghsoodi B, Poon MM, Nam CI, Aoto J, Ting P, Chen L (2008) Retinoic acid regulates RAR alpha-mediated control of translation in dendritic RNA granules during homeostatic synaptic plasticity. Proc Natl Acad Sci U S A 105:16015-16020.

Mandelstam J (1958) Turnover of protein in growing and non-growing populations of escherichia-coli. Biochem J 69:110-119.

Marder E, Prinz AA (2002) Modeling stability in neuron and network function: the role of activity in homeostasis. Bioessays 24:1145-1154.

Marder E, Goaillard JM (2006) Variability, compensation and homeostasis in neuron and network function. Nat Rev Neurosci 7:563-574.

Martin S, Nishimune A, Mellor JR, Henley JM (2007) SUMOylation regulates kainate-receptor-mediated synaptic transmission. Nature 447:321-U326.

McCurry CL, Shepherd JD, Tropea D, Wang KH, Bear MF, Sur M (2010) Loss of Arc renders the visual cortex impervious to the effects of sensory experience or deprivation. Nat Neurosci 13:450-U469.

McKinney RA, Capogna M, Durr R, Gahwiler BH, Thompson SM (1999) Miniature synaptic events maintain dendritic spines via AMPA receptor activation. Nat Neurosci 2:44-49.

Meltzer SJ, Auer CM (1904) The effect of suprarenal extract upon the pupils of frogs. Am J Physiol 11:449-454.

Messaoudi E, Ying SW, Kanhema T, Croll SD, Bramham CR (2002) Brain-derived neurotrophic factor triggers transcription-dependent, late phase long-term potentiation in vivo. J Neurosci 22:7453-7461.

Miller KD (1996) Synaptic economics: Competition and cooperation in synaptic plasticity. Neuron 17:371-374.

Morimoto S, O-Uchi J, Kawai M, Hoshina T, Kusakari Y, Komukai K, Sasaki H, Hongo K, Kurihara S (2009) Protein kinase A-dependent phosphorylation of ryanodine

receptors increases Ca2+ leak in mouse heart. Biochem Biophys Res Commun 390:87-92.

Moulder KL, Jiang XP, Taylor AA, Olney JW, Mennerick S (2006) Physiological activity depresses synaptic function through an effect on vesicle priming. J Neurosci 26:6618-6626.

Murthy VN, Schikorski T, Stevens CF, Zhu YL (2001) Inactivity produces increases in neurotransmitter release and synapse size. Neuron 32:673-682.

Nelson SB, Turrigiano GG (2008) Strength through diversity. Neuron 60:477-482.

Niesen CE, Ge SD (1999) Chronic epilepsy in developing hippocampal neurons: Electrophysiologic and morphologic features. Dev Neurosci 21:328-338.

O'Brien RJ, Kamboj S, Ehlers MD, Rosen KR, Fischbach GD, Huganir RL (1998) Activity-dependent modulation of synaptic AMPA receptor accumulation. Neuron 21:1067-1078.

Okuda T, Yu LMY, Cingolani LA, Kemler R, Goda Y (2007) beta-Catenin regulates excitatory postsynaptic strength at hippocampal synapses. Proc Natl Acad Sci U S A 104:13479-13484.

Ortega Z, Diaz-Hernandez M, Maynard CJ, Hernandez F, Dantuma NP, Lucas JJ (2010) Acute Polyglutamine Expression in Inducible Mouse Model Unravels Ubiquitin/Proteasome System Impairment and Permanent Recovery Attributable to Aggregate Formation. J Neurosci 30:3675-3688.

Pang PT, Teng HK, Zaitsev E, Woo NT, Sakata K, Zhen SH, Teng KK, Yung WH, Hempstead BL, Lu B (2004) Cleavage of proBDNF by tPA/plasmin is essential for long-term hippocampal plasticity. Science 306:487-491.

Paradis S, Sweeney ST, Davis GW (2001) Homeostatic control of presynaptic release is triggered by postsynaptic membrane depolarization (vol 30, pg 737, 2001). Neuron 31:167-167.

Paradiso B, Marconi P, Zucchini S, Berto E, Binaschi A, Bozac A, Buzzi A, Mazzuferi M, Magri E, Mora GN, Rodi D, Su T, Volpi I, Zanetti L, Marzola A, Manservigi R, Fabene PF, Simonato M (2009) Localized delivery of fibroblast growth factor-2 and brain-derived neurotrophic factor reduces spontaneous seizures in an epilepsy model. Proc Natl Acad Sci U S A 106:7191-7196.

Patrick GN, Bingol B, Weld HA, Schuman EM (2003) Ubiquitin-mediated proteasome activity is required for agonist-induced endocytosis of GluRs. Curr Biol 13:2073-2081.

Patterson GH, Lippincott-Schwartz J (2002) A photoactivatable GFP for selective photolabeling of proteins and cells. Science 297:1873-1877.

Patterson SL, Abel T, Deuel TAS, Martin KC, Rose JC, Kandel ER (1996) Recombinant BDNF rescues deficits in basal synaptic transmission and hippocampal LTP in BDNF knockout mice. Neuron 16:1137-1145.

Pawlak V, Schupp BJ, Single FN, Seeburg PH, Kohr G (2005) Impaired synaptic scaling in mouse hippocampal neurones expressing NMDA receptors with reduced calcium permeability. J Physiol-London 562:771-783.

Pereira DB, Rebola N, Rodrigues RJ, Cunha RA, Carvalho AP, Duarte CB (2006) TrkB receptors modulation of glutamate release is limited to a subset of nerve terminals in the adult rat hippocampus. J Neurosci Res 83:832-844.

Perlman RL (1977) 50 YEARS AGO - HOMEOSTASIS. Trends BiochemSci 2:259-259.

Piedras-Renteria ES, Pyle JL, Diehn M, Glickfeld LL, Harata NC, Cao YQ, Kavalali ET, Brown PO, Tsien RW (2004) Presynaptic homeostasis at CNS nerve terminals compensates for lack of a key Ca2+ entry pathway. Proc Natl Acad Sci U S A 101:3609-3614.

Pierson MG, Swann JW (1988) The sensitive period and optimum dosage for induction of audiogenic-seizure susceptibility by kanamycin in the wistar rat. Hear Res 32:1-10.

Plant LD, Dementieva IS, Kollewe A, Olikara S, Marks JD, Goldstein SAN (2010) One SUMO is sufficient to silence the dimeric potassium channel K2P1. Proc Natl Acad Sci U S A 107:10743-10748.

Plath N et al. (2006) Arc/Arg3.1 is essential for the consolidation of synaptic plasticity and memories. Neuron 52:437-444.

Pongs O, Kruse M (2009) Constituitive SUMOylation of TRPM4 channel associated with cardiac conduction disease. J Physiol Sci 59:66-66.

Poon MM, Chen L (2008) Retinoic acid-gated sequence-specific translational control by RAR alpha. Proc Natl Acad Sci U S A 105:20303-20308.

Pozo K, Goda Y (2010) Unraveling Mechanisms of Homeostatic Synaptic Plasticity. Neuron 66:337-351.

Pozzo-Miller LD, Gottschalk W, Zhang L, McDermott K, Du J, Gopalakrishnan R, Oho C, Sheng ZH, Lu B (1999) Impairments in high-frequency transmission, synaptic vesicle docking, and synaptic protein distribution in the hippocampus of BDNF knockout mice. J Neurosci 19:4972-4983.

Pratt KG, Watt AJ, Griffith LC, Nelson SB, Turrigiano GG (2003) Activity-dependent remodeling of presynaptic inputs by postsynaptic expression of activated CaMKII. Neuron 39:269-281.

Rabinowitch I, Segev I (2008) Two opposing plasticity mechanisms pulling a single synapse. Trends Neurosci 31:377-383.

Rajan S, Plant LD, Rabin ML, Butler MH, Goldstein SAN (2005) Sumoylation silences the plasma membrane leak K+ channel K2P1. Cell 121:37-47.

Ramocki MB, Zoghbi HY (2008) Failure of neuronal homeostasis results in common neuropsychiatric phenotypes. Nature 455:912-918.

Rao A, Craig AM (1997) Activity regulates the synaptic localization of the NMDA receptor in hippocampal neurons. Neuron 19:801-812.

Ravikumar B, Sarkar S, Davies JE, Futter M, Garcia-Arencibia M, Green-Thompson ZW, Jimenez-Sanchez M, Korolchuk VI, Lichtenberg M, Luo SQ, Massey DCO, Menzies FM, Moreau K, Narayanan U, Renna M, Siddiqi FH, Underwood BR, Winslow AR, Rubinsztein DC (2010) Regulation of Mammalian Autophagy in Physiology and Pathophysiology. Physiol Rev 90:1383-1435.

Rich MM, Wenner P (2007) Sensing and expressing homeostatic synaptic plasticity. Trends Neurosci 30:119-125.

Rinetti GV, Schweizer FE (2010) Ubiquitination Acutely Regulates Presynaptic Neurotransmitter Release in Mammalian Neurons. J Neurosci 30:3157-3166.

Rivera-Arconada I, Lopez-Garcia JA Changes in Membrane Excitability and Potassium Currents in Sensitized Dorsal Horn Neurons of Mice Pups. J Neurosci 30:5376-5383.

Robinson TE, Berridge KC (2003) Addiction. Annu Rev Psychol 54:25-53.

Rogers N, Paine S, Bedford L, Layfield R (2010) Review: The ubiquitin-proteasome system: contributions to cell death or survival in neurodegeneration. Neuropathol Appl Neurobiol 36:113-124.

Rubin DM, Glickman MH, Larsen CN, Dhruvakumar S, Finley D (1998) Active site mutants in the six regulatory particle ATPases reveal multiple roles for ATP in the proteasome. Embo J 17:4909-4919.

Rutherford LC, Nelson SB, Turrigiano GG (1998) BDNF has opposite effects on the quantal amplitude of pyramidal neuron and interneuron excitatory synapses. Neuron 21:521-530.

Rutherford LC, DeWan A, Lauer HM, Turrigiano GG (1997) Brain-derived neurotrophic factor mediates the activity-dependent regulation of inhibition in neocortical cultures. J Neurosci 17:4527-4535.

Saiga T, Fukuda T, Matsumoto M, Tada H, Okano HJ, Okano H, Nakayama KI (2009) Fbxo45 Forms a Novel Ubiquitin Ligase Complex and Is Required for Neuronal Development. Mol Cell Biol 29:3529-3543.

Saliba RS, Gu Z, Yan Z, Moss SJ (2009) Blocking L-type Voltage-gated Ca2+ Channels with Dihydropyridines Reduces gamma-Aminobutyric Acid Type A Receptor Expression and Synaptic Inhibition. J Biol Chem 284:32544-32550.

Saliba RS, Michels G, Jacob TC, Pangalos MN, Moss SJ (2007) Activity-dependent ubiquitination of GABA(A) receptors regulates their accumulation at synaptic sites. J Neurosci 27:13341-13351.

Schinder AF, Berninger B, Poo MM (2000) Postsynaptic target specificity of neurotrophin-induced presynaptic potentiation. Neuron 25:151-163.

Schlesinger DH, Goldstein G (1975) Molecular conservation of 74 amino-acid sequence of ubiquitin between cattle and man. Nature 255:423-424.

Schlesinger DH, Goldstein G, Niall HD (1975) Complete amino-acid sequence of ubiquitin, an adenylate cyclase stimulating polypeptide probably univeral in living cells. Biochemistry 14:2214-2218.

Schoenheimer R (1942) The dynamic state of body constituents.

Schwartz AL, Ciechanover A (2009) Targeting Proteins for Destruction by the Ubiquitin System: Implications for Human Pathobiology. Annu Rev Pharmacol Toxicol 49:73-96.

Seeburg DP, Sheng M (2008) Activity-induced polo-like kinase 2 is required for homeostatic plasticity of hippocampal neurons during epileptiform activity. J Neurosci 28:6583-6591.

Seeburg DP, Feliu-Mojer M, Gaiottino J, Pak DTS, Sheng M (2008) Critical role of CDK5 and Polo-like kinase 2 in homeostatic synaptic plasticity during elevated activity. Neuron 58:571-583.

Segref A, Hoppe T (2009) Think locally: control of ubiquitin-dependent protein degradation in neurons. EMBO Rep 10:44-50.

Seifert U, Bialy LP, Ebstein F, Bech-Otschir D, Voigt A, Schroter F, Prozorovski T, Lange N, Steffen J, Rieger M, Kuckelkorn U, Aktas O, Kloetzel PM, Kruger E (2010) Immunoproteasomes Preserve Protein Homeostasis upon Interferon-Induced Oxidative Stress. Cell 142:613-624.

Shepherd JD, Rumbaugh G, Wu J, Chowdhury S, Plath N, Kuhl D, Huganir RL, Worley PF (2006) Arc/Arg3.1 mediates homeostatic synaptic scaling of AMPA receptors. Neuron 52:475-484.

Shimura H, Schlossmacher MC, Hattori N, Frosch MP, Trockenbacher A, Schneider R, Mizuno Y, Kosik KS, Selkoe DJ (2001) Ubiquitination of a new form of alpha-synuclein by parkin from human brain: Implications for Parkinson's disease. Science 293:263-269.

Simeone FA (1938) Sensitization of the adrenal gland by partial denervation. Am J Physiol 122:186-190.

Simpson MV (1953) The release of labeled amino acids from the proteins of rat liver slices. J Biol Chem 201:143-154.

Simsek-Duran F, Lonart G (2008) The role of RIM1 alpha in BDNF-enhanced glutamate release. Neuropharmacology 55:27-34.

Soppet D, Escandon E, Maragos J, Middlemas DS, Reid SW, Blair J, Burton LE, Stanton BR, Kaplan DR, Hunter T, Nikolics K, Parada LF (1991) The neurotrophic factos brain-derived neurotrophic factor and neurotrophin-3 are ligands for the TrKB tyrosine kinase receptor. Cell 65:895-903.

Speese SD, Trotta N, Rodesch CK, Aravamudan B, Broadie K (2003) The ubiquitin proteasome system acutely regulates presynaptic protein turnover and synaptic efficacy. Curr Biol 13:899-910.

Squinto SP, Stitt TN, Aldrich TH, Davis S, Bianco SM, Radziejewski C, Glass DJ, Masiakowski P, Furth ME, Valenzuela DM, Distefano PS, Yancopoulos GD (1991) TrkB encodes a functional receptor for brain-derived neurotrophic factor and neurotrophin-3 but not nerve growth-factor. Cell 65:885-893.

Stanton, Starvey (1985) Blockade of norepinephrine-induced long-lasting potentiation in the hippocampal denate gyrus by an inhibitor of protein synthesis. Brain Res 361.

Steinmetz CC, Turrigiano GG Tumor Necrosis Factor-alpha Signaling Maintains the Ability of Cortical Synapses to Express Synaptic Scaling. J Neurosci 30:14685-14690.

Stellwagen D, Malenka RC (2006) Synaptic scaling mediated by glial TNF-alpha. Nature 440:1054-1059.

Steward O, Worley PF (2001) Selective targeting of newly synthesized Arc mRNA to active synapses requires NMDA receptor activation. Neuron 30:227-240.

Steward O, Wallace CS, Lyford GL, Worley PF (1998) Synaptic activation causes the mRNA for the IEG Arc to localise selectively near activated postsynaptic sites on dendrites. Neuron 21:741-751.

Sudhof TC (2008) Neuroligins and neurexins link synaptic function to cognitive disease. Nature 455:903-911.

Sun X, Wolf ME (2009) Nucleus accumbens neurons exhibit synaptic scaling that is occluded by repeated dopamine pre-exposure. Eur J Neurosci 30:539-550.

Sutton MA, Wall NR, Aakalu GN, Schuman EM (2004) Regulation of dendritic protein synthesis by miniature synaptic events. Science 304:1979-1983.

Sutton MA, Taylor AM, Ito HT, Pham A, Schuman EM (2007) Postsynaptic decoding of neural activity: eEF2 as a biochemical sensor coupling miniature synaptic transmission to local protein synthesis. Neuron 55:648-661.

Sutton MA, Ito HT, Cressy P, Kempf C, Woo JC, Schuman EM (2006) Miniature neurotransmission stabilizes synaptic function via tonic suppression of local dendritic protein synthesis. Cell 125:785-799.

Swann JW, Le JT, Lam TT, Owens J, Mayer AT (2007) The impact of chronic network hyperexcitability on developing glutamatergic synapses. Eur J Neurosci 26:975-991.

Tai H-C, Besche H, Goldberg AL, Schuman EM (2010) Characterization of the Brain 26S Proteasome and its Interacting Proteins. Front Mol Neurosci 3.

Takei N, Kawamura M, Hara K, Yonezawa K, Nawa H (2001) Brain-derived neurotrophic factor enhances neuronal translation by activating multiple initiation processes - Comparison with the effects of insulin. J Biol Chem 276:42818-42825.

Tanaka JI, Horiike Y, Matsuzaki M, Miyazaki T, Ellis-Davies GCR, Kasai H (2008) Protein synthesis and neurotrophin-dependent structural plasticity of single dendritic spines. Science 319:1683-1687.

Thiagarajan TC, Piedras-Renteria ES, Tsien RW (2002) alpha- and beta CaMKII: Inverse regulation by neuronal activity and opposing effects on synaptic strength. Neuron 36:1103-1114.

Thiagarajan TC, Lindskog M, Tsien RW (2005) Adaptation to synaptic inactivity in hippocampal neurons. Neuron 47:725-737.

Thiagarajan TC, Lindskog M, Malgaroli A, Tsien RW (2007) LTP and adaptation to inactivity: Overlapping mechanisms and implications for metaplasticity. Neuropharmacology 52:156-175.

Tongiorgi E, Righi M, Cattaneo A (1997) Activity-dependent dendritic targeting of BDNF and TrkB mRNAs in hippocampal neurons. J Neurosci 17:9492-9505.

Town T, Zolton J, Shaffner R, Schnell B, Crescentini R, Wu YJ, Zeng J, DelleDonne A, Obregon D, Tan J, Mullan M (2002) p35/Cdk5 pathway mediates soluble amyloid-beta peptide-induced tau phosphorylation in vitro. J Neurosci Res 69:362-372.

Turrigiano G, Abbott LF, Marder E (1994) Activity-dependent changes in the intrinsic-properties of cultured neurons. Science 264:974-977.

Turrigiano GG (2008) The self-tuning neuron: synaptic scaling of excitatory synapses. Cell 135:422-435.

Turrigiano GG, Nelson SB (2004) Homeostatic plasticity in the developing nervous system. Nat Rev Neurosci 5:97-107.

Turrigiano GG, Leslie KR, Desai NS, Rutherford LC, Nelson SB (1998) Activity-dependent scaling of quantal amplitude in neocortical neurons. Nature 391:892-896.

Tyler WJ, Pozzo-Miller LD (2001) BDNF enhances quantal neurotransmitter release and increases the number of docked vesicles at the active zones of hippocampal excitatory synapses. J Neurosci 21:4249-4258.

Watt AJ, van Rossum MC, MacLeod KM, Nelson SB, Turrigiano GG (2000) Activity coregulates quantal AMPA and NMDA currents at neocortical synapses. Neuron 26:659-670.

Wheeler DB, Randall A, Tsien RW (1994) Roles of N-type and Q-type Ca2+ channels in supporting hippocampal synaptic transmission. Science 264:107-111.

Whiting B, Moiseff A, Rubio ME (2009) Cochlear nucleus neurons redistribute synaptic AMPA and glycine receptors in response to monaural conductive hearing loss. Neuroscience 163:1264-1276.

Wierenga CJ, Ibata K, Turrigiano GG (2005) Postsynaptic expression of homeostatic plasticity at neocortical synapses. J Neurosci 25:2895-2905.

Wierenga CJ, Walsh MF, Turrigiano GG (2006) Temporal regulation of the expression locus of homeostatic plasticity. J Neurophysiol 96:2127-2133.

Willeumier K, Pulst SM, Schweizer FE (2006) Proteasome inhibition triggers activity-dependent increase in the size of the recycling vesicle pool in cultured hippocampal neurons. J Neurosci 26:11333-11341.

Wood MA, Kaplan MP, Brensinger CM, Guo WS, Abel T (2005) Ubiquitin C-terminal hydrolase L3 (Uchl3) is involved in working memory. Hippocampus 15:610-621.

Xu BJ, Gottschalk W, Chow A, Wilson RI, Schnell E, Zang KL, Wang DA, Nicoll RA, Lu B, Reichardt LF (2000) The role of brain-derived neurotrophic factor receptors in the mature hippocampus: Modulation of long-term potentiation through a presynaptic mechanism involving TrkB. J Neurosci 20:6888-6897.

Yang HJ, Takagi H, Konishi Y, Ageta H, Ikegami K, Yao I, Sato S, Hatanaka K, Inokuchi K, Seog DH, Setou M (2008) Transmembrane and Ubiquitin-Like Domain-Containing Protein 1 (Tmub1/HOPS) Facilitates Surface Expression of GluR2-Containing AMPA Receptors. PLoS One 3:13.

Yang YL, Kitagaki J, Dai RM, Tsai YC, Lorick KL, Ludwig RL, Pierre SA, Jensen JP, Davydov IV, Oberoi P, Li CCH, Kenten JH, Beutler JA, Vousden KH, Weissman AM (2007) Inhibitors of ubiquitin-activating enzyme (E1), a new class of potential cancer therapeutics. Cancer Res 67:9472-9481.

Yao I, Takagi H, Ageta H, Kahyo T, Sato S, Hatanaka K, Fukuda Y, Chiba T, Morone N, Yuasa S, Inokuchi K, Ohtsuka T, MacGregor GR, Tanaka K, Setou M (2007) SCRAPPER-dependent ubiquitination of active zone protein RIM1 regulates synaptic vesicle release. Cell 130:943-957.

Yi JJ, Ehlers MD (2007) Emerging roles for ubiquitin and protein degradation in neuronal function. Pharmacol Rev 59:14-39.

Yin Y, Edelman GM, Vanderklish PW (2002) The brain-derived neurotrophic factor enhances synthesis of Arc in synaptoneurosomes. Proc Natl Acad Sci U S A 99:2368-2373.

Zafra F, Hengerer B, Leibrock J, Thoenen H, Lindholm D (1990) Activity dependent regulation of BDNF and NGF messenger-RNAs in the rat hippocampus is mediated by non-NMDA glutamate receptors. Embo J 9:3545-3550.

Zander JF, Munster-Wandowski A, Brunk I, Pahner I, Gomez-Lira G, Heinemann U, Gutierrez R, Laube G, Ahnert-Hilger G (2010) Synaptic and Vesicular Coexistence of VGLUT and VGAT in Selected Excitatory and Inhibitory Synapses. J Neurosci 30:7634-7645.

Zhang FX, Hu Y, Huang P, Toleman CA, Paterson AJ, Kudlow JE (2007) Proteasome function is regulated by cyclic AMP-dependent protein kinase through phosphorylation of Rpt6. J Biol Chem 282:22460-22471.

Zhao YL, Hegde AN, Martin KC (2003) The ubiquitin proteasome system functions as an inhibitory constraint on synaptic strengthening. Curr Biol 13:887-898.

Zirrgiebel U, Ohga Y, Carter B, Berninger B, Inagaki N, Thoenen H, Lindholm D (1995) Characterization of TrkB receptor-mediated signaling pathways in rat cerebellar granule neurons - involvement of protein kinase-C in neuronal survival. J Neurochem 65:2241-2250.